

EUROPEAN JOURNAL OF BIOLOGY

Owner

Tansel Ak
Istanbul University, Turkey

Editor in Chief

Sehnaz Bolkent
Istanbul University, Turkey

Deputy Editor in Chief

Fusun Oztay
Istanbul University, Turkey

Editorial Board

Hafiz Ahmed
University of Maryland, USA

Ahmed Asan
Trakya University, Turkey

Ricardo Antunes de Azevedo
Universidade de Sao Paulo, Brazil

Levent Bat
Sinop University, Turkey

Mahmut Caliskan
Istanbul University, Turkey

Carmela Caroppo
Institute for Coastal Marine Environment, Italy

Cihan Demirci
Istanbul University, Turkey

Mustafa Djamgoz
Imperial College, United Kingdom

Editors

Amal Amer
The Ohio State University, USA

Gulriz Baycu Kahyaoglu
Istanbul University, Turkey

Aysegul Mulayim
Istanbul University, Turkey

Jan Zima
Charles University, Czech Republic

Aglika Edrewa
Bulgarian Academy of Science, Bulgaria

Refet Gojak
University of Sarajevo, Bosnia

Ufuk Gunduz
Middle East Technical University, Turkey

Dietmar Keyser
University of Hamburg, Germany

Ayten Kimiran
Istanbul University, Turkey

Domenico Morabito
Université d'Orléans, France

Michael Moustakas
Aristotle University, Greece

Nurdan Ozkucur
Tufts University, USA

Statistical Editor

Ahmet Dirican
Istanbul University, Turkey

Language Editors

Elizabeth Mary Earl
Istanbul University, Turkey

Alan James Newson
Istanbul University, Turkey

Nesrin Ozoren
Bogazici University, Turkey

Majeti Narasimha Vara Prasad
University of Hyderabad, India

Thomas Sawidis
Aristotle University, Greece

Alex Sivan
The Hebrew University of Jerusalem, Israel

Nico M. Van Straalen
Vrije Universiteit, The Netherlands

Ismail Turkan
Ege University, Turkey

Argyro Zenetos
Hellenic Centre for Marine Research, Greece

Coert J. Zuurbier
*Academisch Medisch Centrum Universiteit,
The Netherlands*

Owner on behalf of the Istanbul University Faculty of Science: Tansel Ak – Publication Type: Periodical – Printed by: İlbey Matbaa Kağıt Reklam Org. MÜc. San. Tic. Ltd. Şti. 2.Matbaacılar Sitesi 3NB 3 Topkapı/Zeytinburnu, İstanbul, Turkey www.ilbeymatbaa.com.tr, Sertifika No: 17845 – Printing Date: December 2020

Publisher

Istanbul University Press
İstanbul Üniversitesi Merkez Kampüsü,
34452 Beyazıt, Fatih / İstanbul - Turkey
Phone: +90 (212) 440 00 00



İSTANBUL
UNIVERSITY
P R E S S

Aims and Scope

European Journal of Biology (Eur J Biol) is an international, scientific, open access periodical published in accordance with independent, unbiased, and double-blinded peer-review principles. The journal is the official publication of Istanbul University Faculty of Science and it is published biannually on June and December. The publication language of the journal is English. European Journal of Biology has been previously published as IUFS Journal of Biology. It has been published in continuous publication since 1940.

European Journal of Biology aims to contribute to the literature by publishing manuscripts at the highest scientific level on all fields of biology. The journal publishes original research and review articles, and short communications that are prepared in accordance with the ethical guidelines in all fields of biology and life sciences.

The scope of the journal includes but not limited to; botany, zoology, hydrobiology, animal and plant systematics, ecology, environmental biology, microbiology, radiobiology, molecular biology, biochemistry, genetics, biotechnology, physiology, toxicology, cell biology, cancer biology, neurobiology, developmental biology, stem cell biology, regenerative and reparative biology, nanobiotechnology, system biology, tissue engineering, biomaterials, and omic sciences.

The target audience of the journal includes specialists and professionals working and interested in all disciplines of biology.

The editorial and publication processes of the journal are shaped in accordance with the guidelines of the International Committee of Medical Journal Editors (ICMJE), World Association of Medical Editors (WAME), Council of Science Editors (CSE), Committee on Publication Ethics (COPE), European Association of Science Editors (EASE), and National Information Standards Organization (NISO). The journal is in conformity with the Principles of Transparency and Best Practice in Scholarly Publishing (doaj.org/bestpractice).

European Journal of Biology is currently indexed by Web of Science Zoological Record, CAB Abstracts (CABI), Chemical Abstracts Service (CAS) and TUBITAK-ULAKBIM TR Index.

Processing and publication are free of charge with the journal. No fees are requested from the authors at any point throughout the evaluation and publication process. All manuscripts must be submitted via the online submission system, which is available at dergipark.gov.tr/iufsjb. The journal guidelines, technical information, and the required forms are available on the journal's web page.

All expenses of the journal are covered by the Istanbul University.

Statements or opinions expressed in the manuscripts published in the journal reflect the views of the author(s) and not the opinions of the Istanbul University Faculty of Science, editors, editorial board, and/or publisher; the editors, editorial board, and publisher disclaim any responsibility or liability for such materials.

All published content is available online, free of charge at dergipark.gov.tr/iufsjb. Printed copies of the journal are distributed free of charge.



Editor in Chief: Prof. Sehnaz BOLKENT

Address: Istanbul University, Faculty of Science, Department of Biology, 34134 Vezneciler, Fatih, Istanbul, TURKEY

Phone: +90 212 4555700 (Ext. 15079)

Fax: +90 212 5280527

E-mail: sbolkent@istanbul.edu.tr

Instructions to Authors

European Journal of Biology (Eur J Biol) is an international, scientific, open access periodical published in accordance with independent, unbiased, and double-blinded peer-review principles. The journal is the official publication of Istanbul University Faculty of Science and it is published biannually on June and December. The publication language of the journal is English. European Journal of Biology has been previously published as IUFS Journal of Biology. It has been published in continuous publication since 1940.

European Journal of Biology aims to contribute to the literature by publishing manuscripts at the highest scientific level on all fields of biology. The journal publishes original research and review articles, and short communications that are prepared in accordance with the ethical guidelines in all fields of biology and life sciences.

The scope of the journal includes but not limited to; botany, zoology, hydrobiology, animal and plant systematics, ecology, environmental biology, microbiology, radiobiology, molecular biology, biochemistry, genetics, biotechnology, physiology, toxicology, cell biology, cancer biology, neurobiology, developmental biology, stem cell biology, regenerative and reparative biology, nanobiotechnology, system biology, tissue engineering, biomaterials, and omic sciences.

The editorial and publication processes of the journal are shaped in accordance with the guidelines of the International Council of Medical Journal Editors (ICMJE), the World Association of Medical Editors (WAME), the Council of Science Editors (CSE), the Committee on Publication Ethics (COPE), the European Association of Science Editors (EASE), and National Information Standards Organization (NISO). The journal conforms to the Principles of Transparency and Best Practice in Scholarly Publishing (doaj.org/bestpractice).

Originality, high scientific quality, and citation potential are the most important criteria for a manuscript to be accepted for publication. Manuscripts submitted for evaluation should not have been previously presented or already published in an electronic or printed medium. Manuscripts that have been presented in a meeting should be submitted with detailed information on the organization, including the name, date, and location of the organization.

Manuscripts submitted to European Journal of Biology will go through a double-blind peer-review process. Each submission will be reviewed by at least three external, independent peer reviewers who are experts in their fields in order to ensure an unbiased evaluation process. The editorial board will invite an external and independent editor to manage the evaluation processes of manuscripts submitted by editors or by the editorial board members of the journal. The Editor in Chief is the final authority in the decision-making process for all submissions.

An approval of research protocols by the Ethics Committee in accordance with international agreements (World Medical Association Declaration of Helsinki "Ethical Principles for Medi-

cal Research Involving Human Subjects," amended in October 2013, www.wma.net) is required for experimental, clinical, and drug studies. If required, ethics committee reports or an equivalent official document will be requested from the authors.

For manuscripts concerning experimental research on humans, a statement should be included that shows the written informed consent of patients and volunteers was obtained following a detailed explanation of the procedures that they may undergo. Information on patient consent, the name of the ethics committee, and the ethics committee approval number should also be stated in the Materials and Methods section of the manuscript. It is the authors' responsibility to carefully protect the patients' anonymity. For photographs that may reveal the identity of the patients, signed releases of the patient or of their legal representative should be enclosed.

European Journal of Biology requires experimental research studies on vertebrates or any regulated invertebrates to comply with relevant institutional, national and/or international guidelines. The journal supports the principles of Basel Declaration (basel-declaration.org) and the guidelines published by International Council for Laboratory Animal Science (ICLAS) (iclas.org). Authors are advised to clearly state their compliance with relevant guidelines.

European Journal of Biology advises authors to comply with IUCN Policy Statement on Research Involving Species at Risk of Extinction and the Convention on the Trade in Endangered Species of Wild IUCN Policy Statement on Research Involving Species at Risk of Extinction and the Convention on the Trade in Endangered Species of Wild Fauna and Flora.

All submissions are screened by a similarity detection software (iThenticate by CrossCheck).

In the event of alleged or suspected research misconduct, e.g., plagiarism, citation manipulation, and data falsification/fabrication, the Editorial Board will follow and act in accordance with COPE guidelines.

Each individual listed as an author should fulfil the authorship criteria recommended by the International Committee of Medical Journal Editors (ICMJE - www.icmje.org). The ICMJE recommends that authorship be based on the following 4 criteria:

- 1 Substantial contributions to the conception or design of the work; or the acquisition, analysis, or interpretation of data for the work; AND
- 2 Drafting the work or revising it critically for important intellectual content; AND
- 3 Final approval of the version to be published; AND
- 4 Agreement to be accountable for all aspects of the work in ensuring that questions related to the accuracy or integrity of any part of the work are appropriately investigated and resolved.

In addition to being accountable for the parts of the work he/she has done, an author should be able to identify which co-authors are responsible for specific other parts of the work. In addition, authors should have confidence in the integrity of the contributions of their co-authors.

All those designated as authors should meet all four criteria for authorship, and all who meet the four criteria should be identified as authors. Those who do not meet all four criteria should be acknowledged in the title page of the manuscript.

European Journal of Biology requires corresponding authors to submit a signed and scanned version of the authorship contribution form (available for download through the journal's web page) during the initial submission process in order to act appropriately on authorship rights and to prevent ghost or honorary authorship. If the editorial board suspects a case of "gift authorship," the submission will be rejected without further review. As part of the submission of the manuscript, the corresponding author should also send a short statement declaring that he/she accepts to undertake all the responsibility for authorship during the submission and review stages of the manuscript.

European Journal of Biology requires and encourages the authors and the individuals involved in the evaluation process of submitted manuscripts to disclose any existing or potential conflicts of interests, including financial, consultant, and institutional, that might lead to potential bias or a conflict of interest. Any financial grants or other supports received for a submitted study from individuals or institutions should be disclosed to the Editorial Board. To disclose a potential conflict of interest, the ICMJE Potential Conflict of Interest Disclosure Form should be filled and submitted by all contributing authors. Cases of a potential conflict of interest of the editors, authors, or reviewers are resolved by the journal's Editorial Board within the scope of COPE and ICMJE guidelines.

The Editorial Board of the journal handles all appeal and complaint cases within the scope of COPE guidelines. In such cases, authors should get in direct contact with the editorial office regarding their appeals and complaints. When needed, an ombudsperson may be assigned to resolve cases that cannot be resolved internally. The Editor in Chief is the final authority in the decision-making process for all appeals and complaints.

When submitting a manuscript to European Journal of Biology, authors accept to assign the copyright of their manuscript to Istanbul University Faculty of Science. If rejected for publication, the copyright of the manuscript will be assigned back to the authors. European Journal of Biology requires each submission to be accompanied by a Copyright Transfer Form (available for download at the journal's web page). When using previously published content, including figures, tables, or any other material in both print and electronic formats, authors must obtain permission from the copyright holder. Legal, financial and criminal liabilities in this regard belong to the author(s).

Statements or opinions expressed in the manuscripts published in European Journal of Biology reflect the views of the author(s) and not the opinions of the editors, the editorial board, or the publisher; the editors, the editorial board, and the publisher disclaim any responsibility or liability for such materials. The final responsibility in regard to the published content rests with the authors.

MANUSCRIPT SUBMISSION

European Journal of Biology endorses ICMJE-Recommendations for the Conduct, Reporting, Editing, and Publication of Scholarly Work in Medical Journals (updated in December 2015 - <http://www.icmje.org/icmje-recommendations.pdf>). Authors are required to prepare manuscripts in accordance with the CONSORT guidelines for randomized research studies, STROBE guidelines for observational original research studies, STARD guidelines for studies on diagnostic accuracy, PRISMA guidelines for systematic reviews and meta-analysis, ARRIVE guidelines for experimental animal studies, TREND guidelines for non-randomized public behaviour, and COREQ guidelines for qualitative research.

Manuscripts can only be submitted through the journal's online manuscript submission and evaluation system, available at the journal's web page. Manuscripts submitted via any other medium will not be evaluated.

Manuscripts submitted to the journal will first go through a technical evaluation process where the editorial office staff will ensure that the manuscript has been prepared and submitted in accordance with the journal's guidelines. Submissions that do not conform to the journal's guidelines will be returned to the submitting author with technical correction requests.

During the initial submission, authors are required to submit the following:

- Copyright Transfer Form,
- Author Contributions Form, and

ICMJE Potential Conflict of Interest Disclosure Form (should be filled in by all contributing authors). These forms are available for download at the journal's web page.

Preparation of the Manuscript

Title page: A separate title page should be submitted with all submissions and this page should include:

- The full title of the manuscript as well as a short title (running head) of no more than 50 characters,
- Name(s), affiliations, and highest academic degree(s) of the author(s),
- Grant information and detailed information on the other sources of support,
- Name, address, telephone (including the mobile phone number) and fax numbers, and email address of the corresponding author,
- Acknowledgment of the individuals who contributed to the preparation of the manuscript but who do not fulfil the authorship criteria.

Abstract: Abstract with subheadings should be written as structured abstract in submitted papers except for Review Articles and Letters to the Editor. Please check Table 1 below for word count specifications (250 words).

Keywords: Each submission must be accompanied by a minimum of three to a maximum of six keywords for subject indexing at the end of the abstract. The keywords should be listed in full without abbreviations.

Manuscript Types

Original Articles: This is the most important type of article since it provides new information based on original research. A structured abstract is required with original articles and it should include the following subheadings: Objective, Materials and Methods, Results and Conclusion. The main text of original articles should be structured with Introduction, Materials and Methods, Results, Discussion, and Conclusion subheadings. Please check Table 1 for the limitations of Original Articles.

Statistical analysis to support conclusions is usually necessary. Statistical analyses must be conducted in accordance with international statistical reporting standards. Information on statistical analyses should be provided with a separate subheading under the Materials and Methods section and the statistical software that was used during the process must be specified.

Units should be prepared in accordance with the International System of Units (SI).

Short Communications: Short communication is for a concise, but independent report representing a significant contribution to Biology. Short communication is not intended to publish preliminary results. But if these results are of exceptional interest and are particularly topical and relevant will be considered for publication.

Short Communications should include an abstract and should be structured with the following subheadings: "Introduction", "Materials and Methods", "Results and Discussion".

Editorial Comments: Editorial comments aim to provide a brief critical commentary by reviewers with expertise or with high reputation in the topic of the research article published in the journal. Authors are selected and invited by the journal to provide such comments. Abstract, Keywords, and Tables, Figures, Images, and other media are not included.

Review Articles: Reviews prepared by authors who have extensive knowledge on a particular field and whose scientific background has been translated into a high volume of publications with a high citation potential are welcomed. These authors may even be invited by the journal. Reviews should describe, discuss, and evaluate the current level of knowledge of a topic in clinical practice and should guide future studies. The main text should contain Introduction, Experimental and Clinical Research Consequences, and Conclusion sections. Please check Table 1 for the limitations for Review Articles.

Letters to the Editor: This type of manuscript discusses important parts, overlooked aspects, or lacking parts of a previously published article. Articles on subjects within the scope of the journal that might attract the readers' attention, particularly educative cases, may also be submitted in the form of a "Letter to the Editor." Readers can also present their comments on the published manuscripts in the form of a "Letter to the Editor." Abstract, Keywords, and Tables, Figures, Images, and other media should not be included. The text should be unstructured. The manuscript that is being commented on must be properly cited within this manuscript.

Tables

Tables should be included in the main document, presented after the reference list, and they should be numbered consecutively in the order they are referred to within the main text. A descriptive title must be placed above the tables. Abbreviations used in the tables should be defined below the tables by footnotes (even if they are defined within the main text). Tables should be created using the "insert table" command of the word processing software and they should be arranged clearly to provide easy reading. Data presented in the tables should not be a repetition of the data presented within the main text but should be supporting the main text.

Figures and Figure Legends

Figures, graphics, and photographs should be submitted as separate files (in TIFF or JPEG format) through the submission system. The files should not be embedded in a Word document or the main document. When there are figure subunits, the subunits should not be merged to form a single image. Each subunit should be submitted separately through the submission system. Images should not be labeled (a, b, c, etc.) to indicate figure sub-

Table 1. Limitations for each manuscript type

Type of manuscript	Word limit	Abstract word limit	Reference limit	Table limit	Figure limit
Original Article	4500	250 (Structured)	No limit	6	Maximum 10
Short Communication	2500	200	30	3	4
Review Article	5500	250	No limit	5	6
Letter to the Editor	500	No abstract	5	No tables	No media

nits. Thick and thin arrows, arrowheads, stars, asterisks, and similar marks can be used on the images to support figure legends. Like the rest of the submission, the figures too should be blind. Any information within the images that may indicate an individual or institution should be blinded. The minimum resolution of each submitted figure should be 300 DPI. To prevent delays in the evaluation process, all submitted figures should be clear in resolution and large in size (minimum dimensions: 100 × 100 mm). Figure legends should be listed at the end of the main document.

All acronyms and abbreviations used in the manuscript should be defined at first use, both in the abstract and in the main text. The abbreviation should be provided in parentheses following the definition.

When a drug, chemical, product, hardware, or software program is mentioned within the main text, product information, including the name of the product, the producer of the product, and city and the country of the company (including the state if in USA), should be provided in parentheses in the following format: "Discovery St PET/CT scanner (General Electric, Milwaukee, WI, USA)"

All references, tables, and figures should be referred to within the main text, and they should be numbered consecutively in the order they are referred to within the main text.

Limitations, drawbacks, and the shortcomings of original articles should be mentioned in the Discussion section before the conclusion paragraph.

References

While citing publications, preference should be given to the latest, most up-to-date publications. If an ahead-of-print publication is cited, the DOI number should be provided. Authors are responsible for the accuracy of references. Journal titles should be abbreviated in accordance with the journal abbreviations in Index Medicus/ MEDLINE/PubMed. When there are six or fewer authors, all authors should be listed. If there are seven or more authors, the first six authors should be listed followed by "et al." In the main text of the manuscript, references should be cited using Arabic numbers in parentheses. The reference styles for different types of publications are presented in the following examples.

Journal Article: Rankovic A, Rancic N, Jovanovic M, Ivanović M, Gajović O, Lazić Z, et al. Impact of imaging diagnostics on the budget – Are we spending too much? *Vojnosanit Pregl* 2013; 70: 709-11.

Book Section: Suh KN, Keystone JS. Malaria and babesiosis. Gorbach SL, Barlett JG, Blacklow NR, editors. *Infectious Diseases*. Philadelphia: Lippincott Williams; 2004.p.2290-308.

Books with a Single Author: Sweetman SC. *Martindale the Complete Drug Reference*. 34th ed. London: Pharmaceutical Press; 2005.

Editor(s) as Author: Huizing EH, de Groot JAM, editors. *Functional reconstructive nasal surgery*. Stuttgart-New York: Thieme; 2003.

Conference Proceedings: Bengissson S, Sothemin BG. Enforcement of data protection, privacy and security in medical informatics. In: Lun KC, Degoulet P, Piemme TE, Rienhoff O, editors.

MEDINFO 92. Proceedings of the 7th World Congress on Medical Informatics; 1992 Sept 6-10; Geneva, Switzerland. Amsterdam: North-Holland; 1992. pp.1561-5.

Scientific or Technical Report: Cusick M, Chew EY, Hoogwerf B, Agrón E, Wu L, Lindley A, et al. Early Treatment Diabetic Retinopathy Study Research Group. Risk factors for renal replacement therapy in the Early Treatment Diabetic Retinopathy Study (ETDRS), *Kidney Int*: 2004. Report No: 26.

Thesis: Yılmaz B. Ankara Üniversitesindeki Öğrencilerin Beslenme Durumları, Fiziksel Aktiviteleri ve Beden Kitle İndeksleri Kan Lipidleri Arasındaki İlişkiler. H.Ü. Sağlık Bilimleri Enstitüsü, Doktora Tezi. 2007.

Epub Ahead of Print Articles: Cai L, Yeh BM, Westphalen AC, Roberts JP, Wang ZJ. Adult living donor liver imaging. *Diagn Interv Radiol*. 2016 Feb 24. doi: 10.5152/dir.2016.15323. [Epub ahead of print].

Manuscripts Published in Electronic Format: Morse SS. Factors in the emergence of infectious diseases. *Emerg Infect Dis* (serial online) 1995 Jan-Mar (cited 1996 June 5): 1(1): (24 screens). Available from: URL: [http:// www.cdc.gov/ncidod/EID/cid.htm](http://www.cdc.gov/ncidod/EID/cid.htm).

REVISIONS

When submitting a revised version of a paper, the author must submit a detailed "Response to the reviewers" that states point by point how each issue raised by the reviewers has been covered and where it can be found (each reviewer's comment, followed by the author's reply and line numbers where the changes have been made) as well as an annotated copy of the main document. Revised manuscripts must be submitted within 30 days from the date of the decision letter. If the revised version of the manuscript is not submitted within the allocated time, the revision option may be cancelled. If the submitting author(s) believe that additional time is required, they should request this extension before the initial 30-day period is over.

Accepted manuscripts are copy-edited for grammar, punctuation, and format. Once the publication process of a manuscript is completed, it is published online on the journal's webpage as an ahead-of-print publication before it is included in its scheduled issue. A PDF proof of the accepted manuscript is sent to the corresponding author and their publication approval is requested within 2 days of their receipt of the proof.

Editor in Chief: Prof. Sehnaz BOLKENT

Address: Istanbul University, Faculty of Science, Department of Biology, 34134 Vezneciler, Fatih, Istanbul, TURKEY

Phone: +90 212 4555700 (Ext. 15079)

Fax: +90 212 5280527

E-mail: sbolkent@istanbul.edu.tr

Contents

Research Articles

- 67 Colchicine Quantification in Salt Stress Treated Culture of *Colchicum luteum* Baker by High Pressure Liquid Chromatography**
Mehpara Maqsood, Mir Khusrau, Zahoor Ahmad Kaloo, Tareq Ahmad Wani, Abdul Mujib
- 75 Somatic Missense Mutations of Histone Variant H3.3 in Central Nervous System Cancers**
Burcu Biterge Sut
- 83 Expression of *blaA* and *blaB* and Susceptibility to Penicillins and Cephalosporins in *Yersinia enterocolitica* from Different Foods**
Fatma Ozdemir, Seza Arslan, Hafize Gizem Erturk
- 89 Proteomic Analysis of the Protective Effect of Sodium Nitroprusside on Leaves of Barley Stressed by Salinity**
Mustafa Yildiz, Melike Celik, Hakan Terzi
- 98 Antioxidant, Cytotoxic, and Enzyme Inhibitory Activities of *Agropyron repens* and *Crataegus monogyna* Species**
Ebru Deveci, Gulsen Tel Cayan, Serdar Karakurt, Mehmet Emin Duru
- 106 Diversity and New Records of Polychaetes (Annelida) in the Sinop Peninsula, Turkey (Southern Black Sea)**
Mulkibar Ciftcioglu, Guley Kurt, Sevgi Kus
- 115 The Effect of Olaparib and Bortezomib Combination Treatment on Ovarian Cancer Cell Lines**
Caglar Berkel, Burak Kucuk, Merve Usta, Esra Yilmaz, Ercan Cacan
- 124 Effects of *Nigella sativa* on Plasma Oxidative Stress, and Some Apoptotic Protein Markers in Cerebrum and Hippocampus in Pentylene-tetrazol-Induced Kindling Rats**
Savas Ustunova, Ismail Meral, Abdurrahim Kocyigit, Aysu Kilic, Oyku Zeybek, Mehmet Uyuklu, Sedat Meydan
- 132 Numerical Taxonomic Analysis on Some *Lepidium* L. taxa (Brassicaceae) from Turkey**
Mehmet Bona
- 144 The Role of *Aspergillus parasiticus* NRRL:3386 Strain on Petroleum Biodegradation and Biosorption Processes**
Sezen Bilen Ozyurek, Nermin Hande Avcioglu
- 151 Evaluation of *In Vitro* Wound Healing Activity of Thymoquinone**
Murat Pekmez, Nihan Sultan Milat
- 157 Profile of Apoptotic Proteins after Curcumin Treatment by Antibody Array in H69AR Lung Cancer Cells**
Süleyman İlhan

Colchicine Quantification in Salt Stress Treated Culture of *Colchicum luteum* Baker by High Pressure Liquid Chromatography

Mehpara Maqsood¹ , Mir Khusrau², Zahoor Ahmad Kaloo³ , Tareq Ahmad Wani³ ,
Abdul Mujib⁴ 

¹Government College for Women, M.A. Road, Srinagar, Jammu & Kashmir

²Government Degree College (Boys), Anantnag, Jammu & Kashmir

³University of Kashmir, Department of Botany, Hazratbal, Srinagar, Jammu & Kashmir

⁴Department of Botany, Jamia Hamdard, New Delhi, India

ORCID IDs of the authors: M.M. 0000-0002-0966-2946; Z.A.K. 0000-0002-1968-476X; T.A.W. 0000-0002-1530-7027; A.M. 0000-0002-4104-6887

Please cite this article as: Maqsood M, Khusrau M, Kaloo ZA, Wani TA, Mujib A. Colchicine Quantification in Salt Stress Treated Culture of *Colchicum luteum* Baker by High Pressure Liquid Chromatography. Eur J Biol 2020; 79(2): 67-74.
DOI: 10.26650/EurJBiol.2020.0013

ABSTRACT

Objective: The aim of the present work was to develop a protocol for season independent propagation of *Colchicum luteum* and enrichment of colchicine yield under salt stress.

Materials and Methods: *C. luteum* was collected from Kashmir, India and was cultured *in vitro*. The callus was exposed to different NaCl (salt) treatments and the yield of colchicine was quantified by high pressure liquid chromatography (HPLC).

Results: Different explants viz. seeds, leaves, anthers and corm were used and the callus was only induced from corm segments. The callus induction and proliferation were best achieved on Murashige and Skoog medium supplemented with 2.0 mg L⁻¹ 2, 4-D + 4.0 mg L⁻¹ BAP. Direct and indirect plant regeneration from corm was observed in 2.0 mg L⁻¹ BAP + 2.0 mg L⁻¹ NAA added medium. The addition of adjuvants like activated charcoal and citric acid was noted to be less efficient for improving callus growth. Induced callus was elicited with different NaCl concentrations (T₀ = without NaCl, T₁ = 25, T₂ = 50, T₃ = 75, and T₄ = 100 mM). The yield of colchicine was quantified by HPLC at periodic intervals (2, 4, and 6 weeks). All the used levels improved colchicine yield, but the content was maximum at T₃ (871.4 ng mg⁻¹ DWB). This is the first report of callus induction and plant regeneration from corm and the quantification of colchicine under salt stress in *C. luteum*.

Conclusion: Sodium chloride is thus a potential inducer and elicitor in improving colchicine yield in *C. luteum*.

Keywords: *Colchicum luteum*, exudates, regeneration, colchicine, *in vitro* cultures, stress

INTRODUCTION

Colchicum luteum Baker is rare to Jammu and Kashmir and belongs to the family Colchicaceae (1). It is commonly known as "Suranjan" or "Hirantutiya" and in Kashmir the plant is known as "Vir keom". The plant is popularly found on the edges of sub alpine forests and in open meadows in the temperate western Himalayas extending from Kashmir to Chamba at

altitudes of between 700 and 2800 m. The plant bears conical-shaped corm with a middle groove, running longitudinally along its flat side, rapier (elongated and pointed) leaves, short scape and bright yellow flowers. The corms are wrapped with a dark brown thin cover, flattened on one side while the other side is rounded. Leaves are fewer in number and are approximately 15-30 cm in length and 0.8-1.5 cm broad. The alkaloid colchicine is extracted from *C. luteum* (2), and is used for



Corresponding Author: Abdul Mujib

E-mail: amujib3@yahoo.co.in

Submitted: 08.04.2020 • **Revision Requested:** 03.06.2020 • **Last Revision Received:** 26.06.2020 •

Accepted: 26.09.2020 • **Published Online:** 13.12.2020

© Copyright 2020 by The Istanbul University Faculty of Science • Available online at <http://ejb.istanbul.edu.tr> • DOI: 10.26650/EurJBiol.2020.0013

the treatment of various diseases like Behçet's syndrome (3) and gout - also known as "rich man's disease". *C. luteum* possesses anti cancerous activity due to colchicine and demecolcine (4). The corms of *C. luteum* are antinociceptive and anti inflammatory (5).

Seed propagation of *C. luteum* is rather difficult because of its hard coat, low germination rate and long juvenile stage of about five years (6). Because of these difficulties in seed based propagation, young corms could be used as a good alternative source of different *Colchicum* species (7). Colchicine is used widely in plant improvement programmes and because of its other medicinal applications there arises an urgent need to conserve plant sources *in vitro* and *ex situ*. *In vitro* micro propagation provides a sensible technique for the conservation of rare and endangered plants (8).

The objective of the present work was to design a method for propagation of *C. luteum* and to enrich colchicine levels in cultivated tissues under NaCl elicitation/stress. To our best knowledge there is no report on callus culture from corm sections in *C. luteum*. The effect of salt stress in regulating the colchicine yield was also described.

MATERIALS AND METHODS

Collection of Plant Material

Colchicum luteum Baker plants (10 accessions each) were collected from different locations viz., Sonmarg, Gulmarg, Awantipora, Ferozpur, Apharwat and Kralisangri of Kashmir province. The plants were very similar apart for one or two morphological attributes (corm, perianth). Plant material was authenticated and the herbarium of the same was submitted to the Centre for Biodiversity and Taxonomy, University of Kashmir, bearing voucher no. 2212-KASH.

Surface Sterilization of Explants

Different explants viz. leaves, corms, perianth, filaments, anthers and seeds were used during the present study. The explants were kept under running tap water for 30-45 min, the corms however, required more time (45-60 min). Later these explants were kept in labolene and tween for a further 15 min. The explants were sterilized with double distilled water to remove the traces of detergents and dipped in 70% ethanol for 5 min, followed by washing with double distilled water multiple times to remove the traces of ethanol. Afterwards, these explants (other than corms) were surface sterilized in 4% sodium hypochlorite (10 min) while the corms were dipped in 0.1% mercuric chloride (HgCl_2) for 20 min and washed 3-4 times by using autoclaved double distilled water under a laminar hood. The surface disinfected explants were inoculated in Murashige and Skoog (MS) (9) medium fortified with different plant growth regulators (PGRs). In some cases, citric acid and activated charcoal were used as adjuvants to analyze their influence on callus initiation and other *in vitro* morphogenesis process.

Callus Induction, Proliferation and Regeneration

MS medium was used for the initiation of cultures. Before inoculation, the incised corm sections were first put into

autoclaved water for 15 min to leach out alkaloids or other materials that would otherwise interfere with growth. After inoculation, the cultures were placed in an incubation room and were exposed to 16 h of photoperiodism. The MS medium used for the establishment of culture was supplemented with different PGRs. The different concentrations and combinations of PGRs were 0.5 mg L⁻¹ 2, 4-D, 0.5 mg L⁻¹ NAA, 0.5 mg L⁻¹ BAP, 0.5 mg L⁻¹ 2, 4-D + 0.5 mg L⁻¹ BAP, 1.0 mg L⁻¹ 2, 4-D + 1.0 mg L⁻¹ BAP, 0.5 mg L⁻¹ 2, 4-D + 0.5 mg L⁻¹ NAA and 1.0 mg L⁻¹ 2, 4-D + 1.0 mg L⁻¹ NAA. To initiate and proliferate callus at higher rate, other physico-chemical parameters tried were the effect of red light and the effect of GA₃ (0.25, 0.50 and 1.0 mg L⁻¹).

Scanning Electron Microscopy (SEM)

For SEM, callus with somatic embryos were collected from sub cultured medium. The tissue was fixed in 3% gluteraldehyde, washed with a 0.05 M potassium phosphate buffer (pH 7.0) and then dehydrated using ethanol. The sample was dried in a High Vacuum Evaporator (Hitachi-HUS 5GB). After gold plating, the sample was observed under a Scanning Electron Microscope (Hitachi S-3000).

Stress Treatment

Sodium chloride (NaCl) was added to the MS medium and dissolved properly prior to pH maintenance. The callus was then exposed with different concentrations of sodium chloride. The various concentrations used were T₁= 25 mM, T₂= 50 mM, T₃= 75 mM and T₄= 100 mM NaCl and a control (T₀= 0 mM) was also kept for comparison.

HPLC

Extraction

The collected callus material was dried at room temperature for 1-2 weeks. The dried samples were ground using a pestle and mortar. Powder samples weighing 0.5 g were placed in a 50 ml conical flask containing 10 ml of Petroleum Ether, frequently shaken for 1 h, this process repeated, and finally the mixture was filtered using Watmann's filter paper. The solid residues were dried in a vacuum, 10 ml of dichloromethane was added and then shaken regularly for 45 min. Then, 0.5 ml of 12.5% ammonium hydroxide was added followed by 15 min constant shaking. The cocktail was kept undisturbed for 30 min and the calli residues and the supernatant were preserved after filtration. About 10 ml of HPLC grade dichloromethane was used to wash the calli residues and was later filtered. The filtrates were collected and the organic phase was allowed to evaporate to dryness in a vacuum at room temperature and then dissolved in 10 ml of ethanol (70%). The mixture was filtered using filter paper and then transferred to 2.0 ml Eppendorf tubes. A few biochemical tests were carried out to confirm the presence of colchicine. An alcoholic solution of colchicine is red in colour when treated with ferric chloride (FeCl_3) and yellow in colour when treated with mineral acids.

Instrumentation

The analysis of the colchicine was done by using HPLC system called WATERS (Milford, USA) having Waters PDA 2998 series

photodiode array detector set at wavelength range 190-800 nm. The column from the Waters Spherisorb® C18 bonded with 5 µm (4.6 x 250 mm) accompanied with EMPOWER-2 software was utilized for collection and processing of chromatographic data. Ultrasonic cleaner (Steryl medi-equip systems) and water purification system ELIX 03 (MILLIPORE, USA) was also used.

Sample Preparation

Stock solution of colchicine (marker) of concentration 1 mg/ml was used. Other samples were dissolved in methanol and stored at a low temperature (4°C) until used. Different dilutions of stock solution with methanol were used to obtain 100 µg/ml so as to get standard curve.

Optimization of Chromatographic Conditions

Separation of compounds by HPLC is largely governed by the type of mobile phase used and organic modifiers. Different compositions, combinations, flow rate of organic solvents and other chromatographic parameters were used to standardize the protocol for optimization. The mobile phase combination of H₂O: MeOH: Formic acid in the ratio of 50: 50:0.1 with isocratic elution at flow rate of 1.0 ml/min was used and found to be the optimum combination. For colchicine, best resolution and sensitivity was obtained at 352 nm. The chromatogram of sharp and symmetric peak of retention time 3.82 min was obtained under optimized conditions.

Validation of Optimized Method

After optimizing the chromatographic method, it was validated according to ICH guidelines for linearity, sensitivity, precision and recovery studies were carried out (ICH Guidelines, 1994; IC Guidelines, 1996).

Calibration Curve (Linearity)

The calibration curve linearity was drawn by using six different concentrations of colchicine (in triplicate) and the calibration curve was plotted in 1-100 µg/ml of colchicine range. The curve was plotted by replicate analysis at all concentration levels and the linear relationship was established using the least square method with Microsoft® Excel program.

Precision

Intra-day and inter-day precision for the developed method were calculated as percent relative standard deviation (% RSD). For intra-day precision, the experiments were repeated three times a day while for inter-day, three different days were considered. The concentration values for both intra-day and inter-day precision were calculated six times respectively and % RSD was similarly computed.

Detection and Quantification Limits (LOD and LOQ)

Limits of detection and quantification were calculated by method based on standard deviation (σ) and slope (S) of calibration plot using formula $LOD = 3.3\sigma/S$ and $LOQ = 10\sigma/S$.

RESULTS

Different explants viz. corms, leaves, perianths, filaments, anthers and seeds of *C. luteum* plants from different geographical locations were tested in MS medium. Callus initiation was only achieved from corm explant (Figure 1a) irrespective of source regions. Seeds showed no response even after physical scarification (rubbing with sand paper) as the seeds possess a hard seed coat. The leaf and anther were also noted to be non responsive. Anthers turned black after a week of inoculation, perianth showed slight puffiness at the base of attachment after two weeks of inoculation and filaments showed bulging after two weeks of incubation. Anther, perianth and leaf all failed to produce callus in tested media conditions.

Different concentrations and combinations of PGRs were tried for callus production. In the first sets of experiments, 2, 4-D alone and in combination with BAP was used. From Table 1, it is apparent that the low auxin and high cytokinin concentrations / ratios were more efficient in inducing callus and for further growth (Figure 1b). Of all the combinations tested, 2.0 mg L⁻¹ 2, 4-D + 4.0 mg L⁻¹ BAP proved to have a good effect on callusing frequency. BAP alone had no effect on callus initiation. The induced callus initiated

Table 1. Callus induction (%) from corm in *C. luteum*, MS medium was amended with below mentioned PGRs.

PGR (mg L ⁻¹)	Callus induction (%)		
	2 weeks	4 weeks	6 weeks
0.25 2,4-D	15.0±2.88 ^a	18.33±1.66 ^a	21.66±4.40 ^b
0.50 2,4-D	18.33±1.66 ^a	20.00±5.00 ^b	41.66±1.66 ^d
1.0 2,4-D	35.00±2.88 ^c	41.66±3.33 ^d	43.33±1.66 ^d
1.0 2,4-D + 2.0 BAP	21.66±1.66 ^b	23.33±1.66 ^b	26.66±1.66 ^b
2.0 2,4-D + 4.0 BAP	53.33±3.33 ^e	61.66±1.66 ^f	76.66±1.66 ^f
3.0 2,4-D + 6.0 BAP	28.33±4.40 ^b	31.66±1.66 ^c	35.00±2.88 ^c
LSD at 5%	0.01	0.00	0.002

Values are means ± standard errors of 3 replicates. Within each column, values are followed by the same alphabet are not significantly different at $p \leq 0.05$ level according to LSD.

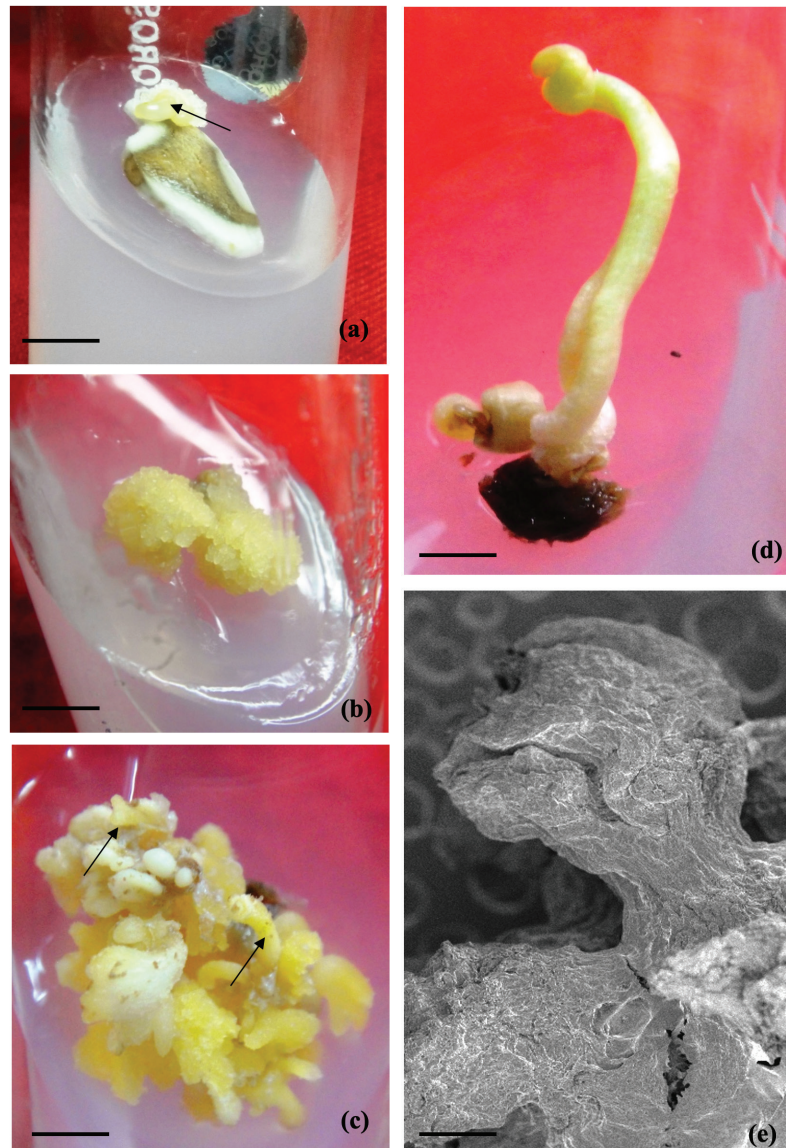


Figure 1. Callus induction, embryogenesis and plant regeneration in *C. luteum* (a) initiation of callus from corm explant (arrow) (b) callus proliferation (c) somatic embryos (arrows) (d) direct shoot regeneration and (e) SEM of somatic embryo. (Bar 1a-1d =2 mm; bar 1f = 300 μ m).

from corm explant was yellowish, soft and exudated slimy viscous secretions. For a higher rate of callus initiation and proliferation, other methods using explant with GA₃ and exposing the explant in red light (by providing a red transparent cover to the vial) was noted ineffective. Callus biomass growth/proliferation was observed in different PGR combinations and concentrations but the rate of growth was highest (0.65 mg) in the 2.0 mg L⁻¹ 2, 4-D + 4.0 mg L⁻¹ BAP (Figure 2) added medium. The initial amount of callus placed in the MS medium was 0.15 mg and the biomass increase was monitored after 2, 4 and 6 weeks of culture. In order to adsorb phenolic exudates, various strategies like the addition of citric acid and activated charcoal were used as adjuvants. These adjuvants were added to the medium to

see the influence of their effect on callusing and on growth by reducing callus browning, however, the response was noted to be non-promotive (Tables 2 and 3).

On sub culturing the callus on the same medium, the corm-callus transformed into embryogenic callus, which was distinctly different from non embryogenic tissue. Although the number of somatic embryos varied, on average 6-8 different stages of embryos (Figure 1c) were noticed per callus mass of about 200-300 mg. The number of embryos increased with each subculture. Moreover, the young corm-bud directly regenerated into shoots (Figure 1d) on MS medium. The embryo bearing callus was subjected to SEM studies to know more about the embryo details which revealed globular

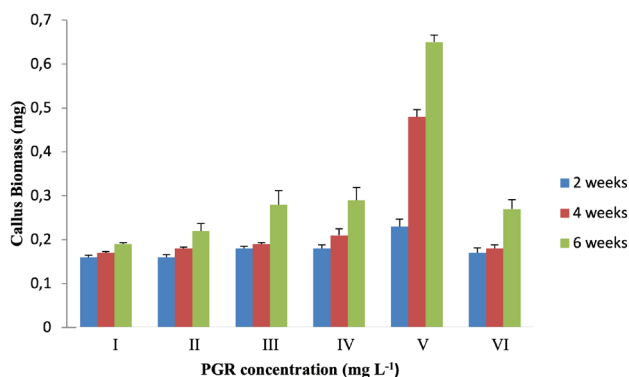


Figure 2. Callus biomass growth (mg) in different concentrations and combinations of PGR. (I = 0.25 2, 4-D; II = 0.50 2, 4-D; III = 1.0 2, 4-D; IV = 1.0 2, 4-D + 2.0 BAP; V = 2.0 2, 4-D + 4.0 BAP; VI = 3.0 2, 4-D + 6.0 BAP)

embryos with stalk present on the surface of the callus (Figure 1e). The embryo developed on embryogenic callus on shoot regeneration medium produced shoots (Table 4); the combination of 4.0 mg L⁻¹ BAP + 2.0 mg L⁻¹ NAA was noted to be the most efficient treatment for shoot development. For direct shoot regeneration, 2.0 mg L⁻¹ BAP + 2.0 mg L⁻¹ NAA supplemented medium was observed to be very effective (Table 5). All other treatments also showed some direct shoot regeneration ability with variable efficiency (33.33- 40.66% after 6th weeks of culture).

The process of elicitation is an important technique to improve secondary metabolites in culture. Elicitors are molecules which activate plant defense mechanism and in turn improve alkaloid yield. In the present study, NaCl was used as an abiotic (salt) stress and the yield of colchicine was quantified in embryogenic

Table 2. Effect of adjuvants on callus induction percentage, MS medium was supplemented with 2.0 mg L⁻¹ 2, 4-D + 4.0 mg L⁻¹ BAP

Adjuvants	Callus induction (%)		
	2 weeks	4 weeks	6 weeks
Control (without adjuvant)	53.33±1.66 ^c	61.66±1.66 ^c	76.66±1.66 ^c
Citric acid (10 g L ⁻¹)	41.66±1.66 ^a	45.00±2.88 ^a	48.33±4.40 ^a
Activated charcoal (1.0 g L ⁻¹)	45.00±2.88 ^b	45.00±2.88 ^b	51.66±3.33 ^b
LSD at 5%	0.021	0.005	0.011

Values are means ± standard errors of 3 replicates. Within each column, values are followed by the same alphabet are not significantly different at $p \leq 0.05$ level according to LSD.

Table 3. Effect of adjuvants on callus biomass, MS was supplemented with 2.0 mg L⁻¹ 2, 4-D + 4.0 mg L⁻¹ BAP (initial weight = 0.15 mg)

Adjuvants	Callus proliferation (mg)		
	2 weeks	4 weeks	6 weeks
Control (without adjuvants)	0.20±0.02 ^b	0.30±0.02 ^b	0.58±0.01 ^d
Citric acid	0.18±0.005 ^a	0.22±0.01 ^b	0.32±0.01 ^c
Activated charcoal	0.19±0.005 ^a	0.21±0.008 ^b	0.23±0.006 ^b
LSD at 5%	0.60	0.04	0.00

Values are means ± standard errors of 3 replicates. Within each column, values are followed by the same alphabet are not significantly different at $p \leq 0.05$ level according to LSD.

Table 4. Effect of BAP and NAA at below concentrations on shoot development ability from embryogenic callus in *C. luteum*.

PGR (mg L ⁻¹)	Shoot development rate (%)		
	2 weeks	4 weeks	6 weeks
2.0 BAP+1.0 NAA	36.66±1.66 ^a	43.33±1.66 ^b	46.66±1.66 ^b
4.0 BAP+2.0 NAA	53.33±2.88 ^c	60.00±2.88 ^d	70.00±2.88 ^d
6.0 BAP+3.0 NAA	38.33±4.40 ^a	41.66±3.33 ^b	46.66±3.33 ^b
LSD at 5%	0.01	0.006	0.001

Values are means ± standard errors of at least 3 replicates. Within each column, values are followed by the same alphabet are not significantly different at $p \leq 0.05$ level according to LSD.

Table 5. Shoots directly regenerated from corm explants in *C. luteum*, MS medium was amended with below PGR combinations and concentrations.

PGR (mg L ⁻¹)	Direct regeneration rate (%)		
	2 weeks	4 weeks	6 weeks
1.0 2,4-D+1.0 BAP	26.66±4.40 ^a	30.00±2.88 ^b	36.66±4.40 ^b
2.0 2,4-D+2.0 BAP	23.33±3.33 ^a	30.00±2.88 ^b	35.00±2.88 ^b
3.0 2,4-D+3.0 BAP	28.33±1.66 ^a	35.00±3.33 ^b	40.66±2.88 ^b
1.0 BAP+1.0 NAA	25.00±2.88 ^a	28.33±1.66 ^a	33.33±3.33 ^b
2.0 BAP+2.0 NAA	55.00±2.88 ^d	61.66±1.66 ^e	71.66±1.66 ^f
3.0 BAP+3.0 NAA	31.66±1.66 ^b	36.66±1.66 ^b	40.00±2.88 ^b
LSD at 5%	0.00	0.00	0.01

Values are means ± standard errors of 3 replicates. Within each column, values are followed by the same alphabet are not significantly different at $p \leq 0.05$ level according to LSD.

cultures as these tissues were more differentiated and supposed to synthesize alkaloids much than the undifferentiated, non-embryogenic callus. The HPLC chromatograms of standard and treated culture are presented in Figure 3 and Figure 4. Almost all the concentrations of NaCl improved colchicine in tissues, but the content was at its maximum in T₃ (133.6 ng mg⁻¹ DWB), followed by T₄ (106.6 ng mg⁻¹ DWB) after 6th weeks of culture.

As expected, the minimum level of colchicine was detected in T₀ i.e. NaCl-free culture (Table 6). Results clearly indicate that the colchicine level improved with an increase in NaCl concentration, but at higher doses, the colchicine accumulation declined.

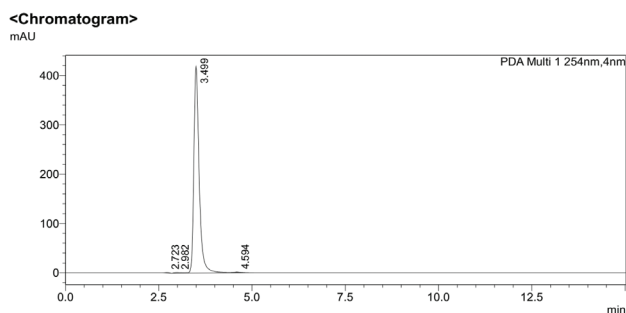
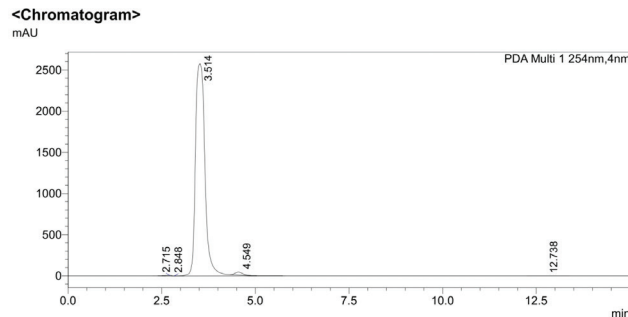


Figure 3. Chromatogram showing standard peak of colchicine.

Figure 4. Chromatogram peak showing maximum yield of colchicine in salt treated cultures at T₃ (T₃ = 75 mM) in *C. luteum*.**Table 6.** Effect of different concentrations of NaCl (salt) on colchicine content (ng mg⁻¹ DWB) in *C. luteum* after regular interval of time (2 weeks, 4 weeks and 6 weeks)

NaCl	Colchicine content (ng mg ⁻¹ DWB)		
	After 2 weeks	After 4 weeks	After 6 weeks
T ₀	47.00±3.2 ^b	55.00±6.0 ^c	66.66±5.2 ^c
T ₁	79.66±5.2 ^c	85.33±4.0 ^b	98.33±6.3 ^c
T ₂	73.33±3.3 ^b	87.33±6.1 ^c	98.66±8.4 ^d
T ₃	102.3±6.5 ^c	112.0±5.6 ^c	133.6±13.5 ^f
T ₄	88.00±6.6 ^c	101.0±7.9 ^d	106.6±7.2 ^c
LSD at 5%	0.00	0.001	0.004

Values are means ± standard errors of 3 replicates. Within each column, values are followed by the same alphabet are not significantly different at $p \leq 0.05$ level according to LSD. (T₀= without NaCl, T₁ = 25mM, T₂ = 50mM, T₃ = 75mM and T₄ = 100 mM NaCl).

DISCUSSION

In this present investigation, the impact of NaCl was studied on colchicine yield in *in vitro* raised tissues in *C. luteum*. Seeds are the primary source of explants, but here in this present study, the seeds did not germinate, even after stratification. Morteza et al. (10) reported similar response of no seed germination with stratification; hot temperature treatment, however, improved seed germination potentiality in *C. kotschyi*. As an alternative, other plant parts viz. leaves, corms, perianth, filaments and anthers were used for inducing callus and the corm was noted to be responsive only in producing callus. In another species of *Colchicum* (*C. hierosolymitanum*), callus was successfully induced from embryonic axis of seeds inoculated on 0.45 μM 2, 4-D supplemented medium (11). This explant-specific response is not new and has been noted in a large number of investigated cases (12). This differential callus forming ability may be due to the presence or absence of an endogenous level of PGRs and other physiological gradient in diverse explants (13). The callus was established in 2, 4-D added medium alone and in combination with BAP. The addition of PGRs particularly the auxin, was noted to be very promotive in producing callus in a number of studied plant materials (14,15). With a few exceptions of brown callus, the callus was mostly pale yellow, moderately hard, compact and slimy in nature. The browning may have been due to exudates present in corm which leached out into the medium (11). This result is very similar to previous findings on *Origanum vulgare* L. where phenolic browning appeared after two weeks of callus incubation (16). Shweta et al. (17) reported that the addition of citric acid (10.0 mg L^{-1}) in medium efficiently minimized the effect of phenolic exudation in *C. luteum*. In our present study, citric acid amendment had no significant effect on *Colchicum* cultures. The callus however, grew well and produced good amount of biomass (fresh weight) on increased concentration of BA ($9 \mu\text{M}$) and 2, 4-D ($0.45 \mu\text{M}$) in other investigated study and the observation (11) is similar and coincides with our present investigation.

The induced callus on sub culturing on the same 2,4-D containing medium transformed into embryogenic callus, distinctly different from non-embryogenic tissues on which a variable number of embryos were differentiated indirectly. No embryo was developed on the medium supplemented with NAA under light or dark conditions, a few embryos were, however, obtained on PGR-free medium. This indirect formation of embryo on callus was noted in several economically important plants (18). The influence of 2, 4-D/auxins on induction of callus and later on embryo formation was reported in several investigated cases (19,15). Nidal et al. (11) noted that the presence of 2, 4-D alone or in combination with BA was very effective in inducing callus and promoting somatic embryo numbers in *C. hierosolymitanum* culture. In this present study, we observed embryogenic callus on 2, 4-D and BAP added medium, confirmed by SEM studies. Scanning electron microscopic study has been widely used for the establishment and confirmation of somatic embryo mediated plant regeneration in a number of plant systems (20,21). The auxin's molecular role in inducing callus/embryo

is not known fully but several lines of research suggested that auxins upregulate genes under stress situations in acquiring embryogenic competence (22,23). Induced embryos matured and germinated into plants on a BAP added medium. The embryo germination/maturation is a key step in embryo-mediated propagation in which the addition of BAP or with NAA supplementation in medium facilitated plantlet production from embryos in other systems is used (24). The dormant corm bud was inoculated for shoot formation and within one or two weeks, outgrowths appeared as a first indicator of bud, which later turned into shoot primordia and grew moderately in the same BAP + NAA amended medium. Similar direct shoot primordia formation and their growth were noted in BAP, and with NAA added MS medium in many plants (25).

The present investigation was also conducted to see the impact of NaCl on colchicine yield in *in vitro* raised embryogenic tissues. The yield of colchicine was noted high in NaCl amended medium especially at T3. A similar enriched level of phyto-compounds following elicitation was reported in several investigated plant materials (26-28). The current study also revealed that the influence is dependent on NaCl concentration, the high to moderate level (75 mM) was more responsive in promoting colchicine compared to low NaCl levels (25 mM and 50 mM) and control. Earlier, in a similar approach Al-Fayyad et al. (29) quantified colchicine yield in corms (0.052%), flowers (0.025%) and leaves (0.013%) in *Colchicum hierosolymitanum* by using different NPK fertilizer levels. In this species (*C. hierosolymitanum*), the maximum yield of colchicine was also noted in callus added to 30 mM NH_4 and 0.1 M of sucrose (30). Sivakumar et al. (31) described the importance of bio-rhizomes, rhizome specific genes/gene which over expressed in rhizomes for the biomanufacture of colchicine as root, callus and cell suspension of *G. superba* and various species of *Colchicum* yielded poor level of colchicine. It is believed that the synthesis of colchicine and colchicoside, a related secondary metabolite are often controlled by various external factors; our results thus indicate that NaCl could be a good inducer in improving colchicine yield, therefore of huge practical applications. The synthesis of alkaloid has been noted to be more in differentiated embryogenic tissue and at the onset of somatic embryo formation (marked by the appearance of procambial tissue and rudiments of transport systems like vascular elements), the synthesis of alkaloids begins, this indicates that the yield content of alkaloid is directly related with embryogenesis (32). How and why synthesis is variable in different plant parts is still not known, some future experiments dealing with genes participating colchicine biosynthesis may help in unraveling the fact.

CONCLUSION

For callus induction, corm pieces proved to be the suitable explant, which produced callus on 0.5 mg L^{-1} 2, 4-D and 0.5 mg L^{-1} BAP added MS medium. In *C. luteum*, the combination of low auxin and high cytokinin concentration are necessary compared to the auxin alone. The growth of callus at the beginning is, however, slow. The induced callus transformed

into embryogenic tissue and later produced somatic embryos. The recent study suggests sodium chloride is a potential inducer in improving colchicine yield in *C. luteum*.

Peer-review: Externally peer-reviewed.

Author Contributions: Conception/Design of study: M.M., Z.A.K.; Data Acquisition: M.M., M.K., T.A.W.; Data Analysis/ Interpretation: M.M., M.K., A.M.; Drafting Manuscript: M.M., M.K., Z.A.K., A.M.; Critical Revision of Manuscript: M.M., Z.A.K., A.M.; Final Approval and Accountability: M.M., M.K., Z.A.K., A.M., T.A.W.; Supervision: M.M., Z.A.K., A.M.

Conflict of Interest: The authors declare that they have no conflicts of interest to disclose.

Financial Disclosure: There are no funders to report for this submission.

REFERENCES

- Kumar GP, Kumar R, Chaurasia OP, Singh SB. Current status and potential prospects of medicinal plant sector in trans-Himalayan Ladakh. *J Med Plants Res* 2011; 5: 2929-40.
- Bashir A. Antioxidant activity and phenolic compounds from *Colchicum luteum* Baker (Liliaceae). *Afr J Biotechnol* 2010; 9: 5762-6.
- Wechsler B. Colchicine and Behcet's disease: An efficiency enfinreconnue! (Behcet's disease and colchicines: An efficacious treatment finally recognized. *J Med Int* 2002; 23: 355-6.
- Sakarkar DM, Deshmukh VN. Ethno pharmacological review of traditional medicinal plants for anticancer activity. *Int J Pharm Tech Research* 2011; 3: 298-308.
- Azmat A, Ahmed KZ, Tariq B. Antinociceptive effects of poly herbal oil extract. *Pak J Pharmacy* 2006; 23: 1-7.
- Al-Fayyad M. Study of morphological characteristics, colchicine content and genetic variation of two wild *Colchicum* species in Jordan. Ph.D. Thesis, University of Jordan, Amman, Jordan. 2001.
- Inchem. *Colchicum autumnale* L. Accessed on line at website: <http://www.inchem.org/documents/ims/plant/im142.htm>. 2006; PP: 1-33.
- Naz R, Anis M. Acceleration of adventitious shoots by interaction between exogenous hormone and adenine sulphate in *Althaea officinalis* L. *Appl Biochem Biotechnol* 2012; 168:1239-55.
- Murashige T, Skoog F. A revised medium for rapid growth and bioassay with tobacco tissue cultures. *Physiol Plant* 1962; 15: 473-97.
- Morteza AN, Hossein A, Shamsali R, Mahmoud S, Yahya S, Navid VM. Warm stratification and chemical treatments overcome the dormancy and promotes germination of *Colchicum kotschyi* Boiss seeds under *in vitro* condition. *Not Sci Biol* 2011; 3: 104-7.
- Nidal QD, Rida AS, Ibrahim MM, Feras A, Tamara SA. Callus Culture and Somatic Embryogenesis in Wild *Colchicum hierosolymitanum* Feib. *Jordan J Agricultural Sciences* 2012; 8: 536-56.
- Ling APK, Tan KP, Hussein S. Comparative effects of plant growth regulators on leaf and stem explants of *Labisia pumila* var. *alata*. *J Zhejiang Univ Sci B* 2013; 14: 621-31.
- Ghosh S, Sengupta S, Pal A. Abscisic acid, one of the key determinants of *in vitro* shoot differentiation from cotyledons of *Vigna radiate*. *Amer J Pl Sci* 2014; 5: 704 -13.
- Su YH, Zhao XY, Liu YB, Zhang CL, O'Neill SD, Zhang X. Auxin-induced *WUS* expression is essential for embryonic stem cell renewal during somatic embryogenesis in *Arabidopsis*. *Plant J* 2009; 59: 448-60.
- Fehér A. Somatic embryogenesis - Stress-induced remodeling of plant cell fate. *Biochim Biophys Acta* 2015; 1849(4): 385-402.
- Arafeh RM, Shibli RA, Al-Mahmoud M, Shatnawi MA. Callusing, cell suspension culture and secondary metabolites production in Persian Oregano (*Origanum vulgare* L.) and Arabian Oregano (*O. syriacum* L.). *Jordan J Agri Sci* 2006; 2: 274-82.
- Shweta S, Madhuparna B, Haider ZA. Conservation of *Colchicum luteum* Baker through micropropagation. *J Research (BAU)* 2013; 25: 96-100.
- Gao F, Yong Y, Dai C. Effects of endophytic fungal elicitor on two kinds of terpenoids production and physiological indexes in *Euphorbia pekinensis* suspension cells. *J Med Plants Res* 2011; 5: 4418- 25.
- Yang JL, Seong ES, Kim MJ, Ghimire BK, Kang WH, Yu CY, et al. Direct somatic embryogenesis from pericycle cells of broccoli (*Brassica oleracea* L. var. *italica*) root explants. *Plant Cell Tiss Org Cult* 2010; 100: 49-58.
- Aslam J, Mujib A, Sharma MP. Somatic embryogenesis in *Catharanthus roseus*: a scanning electron microscopic study. *Not Sci Biol* 2015; 6 (2): 167-72.
- Wang HC, Chen JT, Chang WC. Morphogenetic routes of long-term embryogenic callus culture of *Areca catechu*. *Biol Plant* 2010; 54:1-5.
- Gliwicka M, Nowak K, Balazadeh S, Mueller-Roeber B, Gaj MD. Extensive modulation of the transcription factor transcriptome during somatic embryogenesis in *Arabidopsis thaliana*. *PLoS ONE* 2013; 8: e69261. doi: 10.1371/journal.pone.0069261.
- Bai B, Su YH, Yuan J, Zhang XS. Induction of somatic embryos in *Arabidopsis* requires local *YUCCA* expression mediated by the down-regulation of ethylene biosynthesis. *Mol Plant* 2013; 6: 1247-60.
- Mujib A, Ali M, Dipti T, Zafar N. Embryogenesis in ornamental monocots: Plant growth regulators as signaling element. In: Mujib, A., (ed). *Somatic embryogenesis in ornamentals and its applications*, Springer 2016 pp: 187-201.
- Ashraf MF. Effect of cytokinin types, concentrations and their interactions on *in vitro* shoot regeneration of *Chlorophytum borivilianum* Sant. & Fernandez. *Electronic J Biotech* 2014; 7: 275-9.
- Ramakrishna A, Ravishankar GA. Influence of abiotic stress signals on secondary metabolites in plants. *Plant Signal Behav* 2011; 6: 1720-31.
- Ribkahwati Purnobasuki H, Isnaeni Utami ESW. Quantity essential oil from rose callus leaf (*Rosa hybrid* L. variety *Hybride tea purple*): Results of light elicitation. *J Chem Pharma Res* 2015; 7: 496-9.
- Samar F, Mujib A, Tonk D. NaCl amendment improves vinblastine and vincristine synthesis in *Catharanthus roseus*: a case of stress signalling as evidenced by antioxidant enzymes activities. *Plant Cell Tissue Org Cult* 2015; 121: 445-58.
- Al-Fayyad M, Alali F, Alkofali A, Tell A. Determination of colchicine content in *Colchicum hierosolymitanum* and *Colchicum tunicatum* under cultivation. *Nat Prod Let* 2002; 16: 395-400.
- Daradkeh NQ, Shibli RA, Makhadmeh IM, Alali F, Al-Qudah TS. Cell suspension and *in vitro* production of colchicine in wild colchicum hierosolymitanum Feib. *TOPROJ* (2012); 3: 52-9. 10.2174/1876326X01203020052.
- Sivakumar G, Alba K, Phillips GC. Biorhizome: A Biosynthetic Platform for Colchicine Biomanufacturing. *Front Plant Sci* 2017; 8: 1137.
- Tatiana YG, Valeria PG, Dmitry VB, Galina KT, Victor PB. Tempo-spatial pattern of stepharine accumulation in *Stephania glabra* morphogenic tissues. *Int J Mol Sci* 2019; 20: 808, doi:10.3390/ijms20040808.

Somatic Missense Mutations of Histone Variant H3.3 in Central Nervous System Cancers

Burcu Biterge Sut¹ 

¹Niğde Ömer Halisdemir University, Faculty of Medicine, Department of Medical Biology, Niğde, Turkey

ORCID IDs of the authors: B.B.S. 0000-0001-5756-5756

Please cite this article as: Biterge Sut B. Somatic Missense Mutations of Histone Variant H3.3 in Central Nervous System Cancers. Eur J Biol 2020; 79(2): 75-82. DOI: 10.26650/EurJBiol.2020.0019

ABSTRACT

Objective: Histone variants are important modulators of chromatin functions. Studies have pointed out that epigenetic factors are often dysregulated in carcinogenesis. Although some cancer-associated mutations of the histone variant H3.3 have been identified previously, a complete list of H3.3 mutations and their potential effects is yet to be uncovered. Therefore, this study aims to identify the missense mutations of the histone variant H3.3 in central nervous system (CNS) cancers and to computationally predict their functional consequences on pathogenicity, protein stability and structure.

Materials and Methods: A complete set of human H3.3 mutations was acquired from the COSMIC v90 database and missense mutations were selected. The potential effects of these mutations were assessed using PredictSNP2 and FATHMM-XF. Structural outcomes were predicted using MUpro and HOPE servers.

Results: We identified 45 unique missense H3.3 substitutions in several tissues including CNS. PredictSNP2 and FATHMM-XF predicted 17 and 42 mutations as deleterious respectively, most of which caused decreased protein stability. Amino acid alterations in CNS cancers were predicted to cause alterations of the 3D structure.

Conclusion: Histone variants play significant roles in epigenetic regulation and are often mutated in cancers. Our results showed that H3.3 mutations detected in CNS cancers could affect the genomic distribution of post-translational modifications and histone variants, hence dramatically alter the gene expression profile and contribute to carcinogenesis.

Keywords: Epigenetics, histone variant H3.3, mutation analysis, cancer

INTRODUCTION

Epigenetic regulation is a phenomenon that modulates cellular processes such as proliferation, progression through the cell cycle, transcriptional memory, and DNA damage repair via regulating accessibility of DNA through chromatin condensation (1). The genetic material of eukaryotic organisms exists within the cell as a complex macromolecule called chromatin, consisting of DNA and histone proteins. The packaging of DNA into chromatin dictates differential gene expression patterns which are crucial for the proper functioning of the cell. Perturbations in these processes, as well as transcriptional regulation mechanisms are often associated with complex diseases such as cancer. These regulatory mechanisms are orchestrated by DNA meth-

ylation, RNA interference, post-translational histone modifications and incorporation of histone variants into chromatin. Histones are small, basic proteins encoded by several copies of histone genes located within the major histone locus. Canonical histones, namely H2A, H2B, H3 and H4 are strictly synthesized during the S-phase and deposited onto the chromatin in a replication-dependent manner. Histone variants, however, are expressed throughout the cell cycle and incorporated into chromatin in a context-dependent manner (2). Canonical histones and their corresponding variants differ in their amino acid sequence, which affects interactions between histone proteins within the same nucleosome and results in alterations in transcriptional activity. The most commonly studied histone variants



Corresponding Author: Burcu Biterge Sut

E-mail: bbitergesut@ohu.edu.tr

Submitted: 30.04.2020 • **Revision Requested:** 05.05.2020 • **Last Revision Received:** 09.06.2020 •

Accepted: 18.06.2020 • **Published Online:** 23.07.2020

© Copyright 2020 by The Istanbul University Faculty of Science • Available online at <http://ejb.istanbul.edu.tr> • DOI: 10.26650/EurJBiol.2020.0019

are centromere specific H3 variant CENP-A (3); DNA damage site specific H2A.X (4); H2A.Z and H3.3 variants that are commonly found at active transcription sites (5); and macroH2A which is associated with transcriptional repression (6).

Tumors of the brain and the spinal cord, which collectively comprise the central nervous system (CNS), are amongst the most heterogeneous cancer types. The World Health Organization classifies CNS cancers into more than 120 subtypes based on molecular and histopathological characteristics (7). CNS tumors often originate from different cell types, such as astrocytes, glias and meninges. Gliomas and meningiomas are the major subtypes of brain tumors in adults and are rarely seen (8). On the contrary, CNS cancers are the most common solid tumor type in children between the ages of 0-14 (9), 30% of which is constituted by medulloblastomas (10). Gliomas are graded at four levels depending on the severity, aggressiveness and curability of the disease. Medulloblastoma is the common name for a group of malignant embryonic tumor subtypes that originate from the primitive neuronal cells within the posterior cranial fossa (11). Although the etiology of CNS cancers remains unknown to date, several genetic factors have been associated with increased risk. For instance, a recent study indicated the significant contribution of germline mutations and a genetic disposition to pediatric medulloblastoma (12). Similarly, the mutational status of TP53, BRAF, FGFR1, IDH and TERT as well as the copy number variations of EGFR, CDKN2A/B, PTEN, PDGFRA are often linked with tumor pathogenesis in the CNS (13,14). These genetic variations also serve as powerful molecular tools for cancer subtype characterization.

Studies have shown that several epigenetic factors, including histone variants, are mutated or their activities are dysregulated during cancer pathogenesis. Although previous studies have identified some cancer-associated mutations of the histone variant H3.3 in chondroblastoma, pediatric sarcoma, giant cell tumor of bone, glioma and medulloblastoma (15-17), a complete list of H3.3 mutations and their potential effects is yet to be uncovered. Therefore, this paper aims to identify H3.3 mutations in CNS cancers and to predict their functional consequences on pathogenicity, protein stability and structure using computational approaches.

MATERIALS AND METHODS

Retrieval of Somatic Mutations from COSMIC Database

Somatic mutations of the H3F3A gene (COSMIC gene ID: COSG55679) encoding human H3.3 were downloaded from the Catalogue of Somatic Mutations in Cancer (COSMIC) database v90 (<https://cancer.sanger.ac.uk/cosmic>).

Identification of Deleterious Mutations

The functional consequences and the pathogenicity scores of the H3.3 mutations were predicted using PredictSNP2 (<https://loschmidt.chemi.muni.cz/predictsnp2/>) (18) and FATHMM-XF (<http://fathmm.biocompute.org.uk/fathmm-xf/index.html>) (19) in reference to genome assembly GRCh38/hg38.

Protein Stability Prediction

The effect of the missense mutations on the stability of the protein was analyzed via MUpro using H3.3 amino acid sequence retrieved from UniProt (ID: P84243), which is based on machine learning methods (<http://mupro.proteomics.ics.uci.edu/>) (20). The tool provides 84.2% accuracy.

Determination of 3D Structural Changes

The structural effects of the nonsynonymous H3.3 mutations, which were commonly encountered in CNS cancers were predicted via HOPE server using H3.3 amino acid sequence retrieved from UniProt (ID: P84243) (<https://www3.cmbi.umcn.nl/hope>) (21).

In silico Evaluation of H3.3 Conservation

The amino acid sequences of histone H3.3 for *Homo sapiens* (P84243-1), *Mus musculus* (P84244-1), *Rattus norvegicus* (P84245-1), *Gallus gallus* (P84247-1), *Xenopus laevis* (Q6PI79-1), *Danio rerio* (Q6PI20-1), *Saccharomyces cerevisiae* (P10651-1) and *Arabidopsis thaliana* (P59169-1) were retrieved from UniProt. In silico evaluation of protein similarity was performed using Clustal Omega (<https://www.ebi.ac.uk/Tools/msa/clustalo/>) (22). Histone domain structure was determined in accordance with Luger et al. (23).

RESULTS

Identification of H3.3 Mutations

COSMIC database analysis over 1012 unique samples showed that 94.2% of all somatic H3.3 mutations were missense substitutions (n=953), most of which were caused by A>T nucleotide change. Furthermore, 2 nonsense substitutions, 8 synonymous substitutions, 2 frameshift deletions, 1 inframe insertion, 1 inframe deletion and 2 uncharacterized mutations were detected. The missense mutations were detected in various tissue types including but not limited to breast, cervix, prostate, upper aerodigestive tract, bone and central nervous system tissues. Table 1 shows a complete list of 45 nonsynonymous mutations identified in H3.3. Proteins often undergo N-terminal methionine cleavage by methionine aminopeptidase (MAP), which removes the first methionine coded by the start codon (24). Therefore, the starting methionine is not always present in the mature protein. We realized that the locations of the amino acid substitutions identified by the COSMIC database analysis differ from the mature protein by one amino acid, since the COSMIC database did not take the methionine removal into account. The amino acid changes before (detected by COSMIC) and after MAP cleavage are shown in Table 1. For coherence with other studies in the literature, our further analyses were based on the locations of amino acid substitutions after N-terminal methionine cleavage.

Prediction of Pathogenicity and Protein Stability

The potential effects of somatic H3.3 mutations on carcinogenesis were predicted using two methods. PredictSNP2 calculates an *expected accuracy* value, which is the consensus classifier for prediction of the effects of nucleotide variants based on 5 different nucleotide-based prediction tools (CADD, DANN, FATHMM, FunSeq2 and GWAVA). PredictSNP2 analysis revealed that 17

Table 1. Computational predictions of pathogenicity and protein stability for the H3.3 mutations.

CDS mutation	AA mutation (COSMIC)	AA mutation (MAP cleavage)	PredictSNP2 Analysis		FATHMM-XF Analysis	MUpuro Analysis	
			Pathogenicity prediction	Expected accuracy	Pathogenicity score	Stability prediction	Confidence score
c.7C>T	p.R3C	p.R2C	Neutral	65%	0.580	Decrease	-0.639
c.14A>T	p.K5M	p.K4M	Neutral	63%	0.860	Increase	0.133
c.17A>C	p.Q6P	p.Q5P	Neutral	63%	0.941	Decrease	-0.469
c.18G>C	p.Q6H	p.Q5H	Neutral	67%	0.436	Decrease	-0.481
c.25C>G	p.R9G	p.R8G	Neutral	63%	0.913	Decrease	-1.865
c.25C>T	p.R9C	p.R8C	Neutral	63%	0.879	Decrease	-0.853
c.26G>A	p.R9H	p.R8H	Neutral	63%	0.873	Decrease	-1.566
c.34A>G	p.T12A	p.T11A	Neutral	65%	0.839	Decrease	-1.544
c.37G>A	p.G13S	p.G12S	Neutral	63%	0.882	Decrease	-1.347
c.60A>C	p.Q20H	p.Q19H	Neutral	89%	0.323	Decrease	-0.804
c.67A>C	p.T23P	p.T22P	Deleterious	82%	0.940	Decrease	-1.642
c.76G>T	p.A26S	p.A25S	Neutral	65%	0.878	Decrease	-1.333
c.82A>G	p.K28E	p.K27E	Neutral	63%	0.874	Decrease	-0.218
c.83A>T	p.K28M	p.K27M	Deleterious	82%	0.874	Decrease	-1.566
c.84G>T	p.K28N	p.K27N	Neutral	63%	0.559	Decrease	-0.414
c.86G>C	p.S29T	p.S28T	Neutral	63%	0.863	Decrease	-0.496
c.98C>T	p.T33I	p.T32I	Neutral	63%	0.856	Decrease	-0.256
c.103G>T	p.G35W	p.G34W	Deleterious	82%	0.920	Decrease	-0.756
c.103G>A/C	p.G35R	p.G34R	Deleterious	87%	0.912	Decrease	-0.739
c.104G>T	p.G35V	p.G34V	Deleterious	87%	0.917	Decrease	-0.746
c.110A>T	p.K37M	p.K36M	Neutral	63%	0.851	Increase	0.315
c.111G>T	p.K37N	p.K36N	Neutral	65%	0.687	Decrease	-0.176
c.118C>A	p.H40N	p.H39N	Deleterious	87%	0.890	Increase	0.148
c.136A>G	p.T46A	p.T45A	Neutral	63%	0.855	Decrease	-0.494
c.139G>A	p.V47M	p.V46M	Neutral	63%	0.888	Decrease	-0.013
c.143C>A	p.A48E	p.A47E	Neutral	63%	0.889	Decrease	-0.334
c.148C>T	p.R50C	p.R49C	Deleterious	87%	0.647	Decrease	-0.127
c.149G>A	p.R50H	p.R49H	Neutral	65%	0.892	Decrease	-0.768
c.160C>T	p.R54C	p.R53C	Deleterious	82%	0.910	Decrease	-1.181
c.168G>T	p.Q56H	p.Q55H	Deleterious	82%	0.577	Decrease	-1.236
c.190C>T	p.R64C	p.R63C	Neutral	67%	0.909	Decrease	-1.283
c.218G>A	p.R73Q	p.R72Q	Deleterious	82%	0.869	Decrease	-0.505
c.244G>A	p.D82N	p.D81N	Deleterious	87%	0.878	Decrease	-0.620
c.245A>T	p.D82V	p.D81V	Deleterious	87%	0.881	Decrease	-0.105
c.262G>T	p.A88S	p.A87S	Deleterious	82%	0.636	Decrease	-0.748
c.268A>G	p.I90V	p.I89V	Neutral	65%	0.480	Decrease	-0.920
c.295G>A	p.A99T	p.A98T	Neutral	67%	0.836	Decrease	-1.258
c.299A>G	p.Y100C	p.Y99C	Neutral	63%	0.906	Decrease	-1.230
c.317A>T	p.E106V	p.E105V	Neutral	63%	0.918	Decrease	-0.412
c.344C>G	p.A115G	p.A114G	Deleterious	82%	0.924	Decrease	-1.305
c.371A>G	p.D124G	p.D123G	Deleterious	82%	0.913	Decrease	-1.351
c.378G>T	p.Q126H	p.Q125H	Deleterious	87%	0.792	Decrease	-1.024
c.385C>T	p.R129C	p.R128C	Neutral	65%	0.926	Decrease	-0.823
c.386G>A	p.R129H	p.R128H	Neutral	63%	0.912	Decrease	-1.120
c.389G>A	p.R130H	p.R129H	Deleterious	82%	0.915	Decrease	-1.542

Distribution of H3.3 mutations across tissues

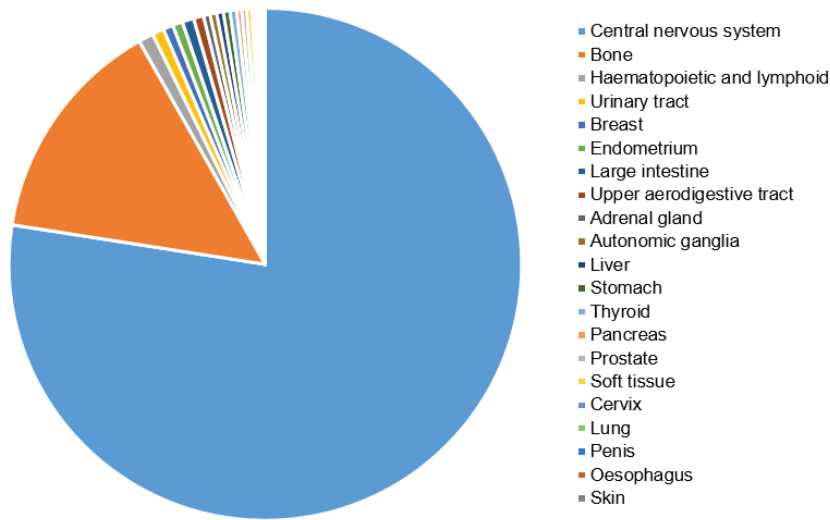


Figure 1. Distribution of the somatic missense mutations of histone variant H3.3 across tissue types. The majority of the mutations are detected in central nervous system (77%) and bone (14%).

out of 45 nucleotide substitutions were deleterious mutations with more than 82% expected accuracy. Higher percentage values indicate higher confidence; hence, G34R/V, H39N, R49C and D81N/V substitutions had the most confident pathogenicity prediction percentages (87%).

A second analysis was performed using FATHMM-XF, which produces *p*-values (*pathogenicity scores*) between 0-1 and predicts mutations with *p*>0.5 as pathogenic/deleterious. FATHMM-XF analysis yielded 42 mutations predicted to be deleterious.

Lastly, the effect of H3.3 mutations on the overall protein stability was predicted using the MUpro tool, which calculates a *confidence score*, the prediction of the value of energy change ($\Delta\Delta G$), using a machine learning approach, namely the Support Vector Machine. Values <0 indicate decreased protein

stability, while values >0 suggest increased protein stability, showing that most of the mutations caused decreased protein stability with varying confidence scores. Amino acid substitutions with the lowest confidence scores, which are R8G, R8H, T11A, K27M and R129H, are predicted to result in a greater decrease in protein stability.

H3.3 Mutations in CNS

Among the analyzed set of unique H3.3 missense mutations, the majority were identified in CNS (77%) and bone (14%) (Figure 1). Therefore, we selected the ones that originated from the CNS as the primary site for further analysis. H3.3 mutations in the CNS namely p.R2C, p.R8H, p.K27M, p.G34R, p.G34R, p.G34W and p.G34V, were mainly derived from brain, cerebral hemisphere, temporal lobe and frontal lobe, while they were also detected to a

Table 2: Somatic missense mutations of histone variant H3.3 in central nervous system (CNS) cancers.

AA mutation	CDS mutation	Primary tissue	Tissue subtype	Histology
p.R2C	c.7C>T	CNS	Brain	Glioma
p.R8H	c.26G>A	CNS	Brain	Glioma, primitive neuroectodermal tumour-medulloblastoma
p.K27M	c.83A>T	CNS	Brain, cerebral hemisphere, thalamus, temporal lobe, spinal cord, posterior fossa, brainstem	Glioma, primitive neuroectodermal tumour-medulloblastoma
p.G34R	c.103G>A	CNS	Brain, cerebral hemisphere, occipital lobe, frontal lobe, parietal lobe, temporal lobe	Glioma, primitive neuroectodermal tumour-medulloblastoma
p.G34R	c.103G>C	CNS	Basal ganglia, cerebral hemisphere, temporal lobe	Glioma, primitive neuroectodermal tumour-medulloblastoma
p.G34W	c.103G>T	CNS	Frontal lobe	Glioma
p.G34V	c.104G>T	CNS	Brain, frontal lobe	Glioma

ration of significantly different side chains into the protein. The amino acid sequence alignment of histone H3.3 from human, mouse, rat, chicken, frog, zebra fish, yeast and plant tissues indicated significant conservation across species (Figure 3). All mutant residues given in Figure 2 were located within the highly conserved N-terminal tail of histone H3.3, which is an important domain for interaction with other molecules.

DISCUSSION

Histone H3 has three main variants; while H3.1 and H3.2 are classified as the canonical histone H3, H3.3 is the so called "replacement variant" which gets synthesized and incorporated into the chromatin throughout the cell cycle (25). Although the amino acid sequence of H3.3 differs only slightly from the canonical H3, most of these variant residues lie within structurally important domains that affect its interaction with other histones in the nucleosome and histone chaperones (26). Therefore, nucleosomes containing H3.3 usually confer an open chromatin conformation and are found at active or poised transcription sites that are enriched in tri-methylations of histone H3 at lysine 4 and 27 (27,28). Genes encoding epigenetic factors such as histones, their modifiers and chaperones, as well as chromatin remodeling enzymes are often mutated in cancer and are linked with tumorigenesis (29,30). Studies that have previously identified H3.3 mutations in various cancers mostly focused on the amino acid substitutions at K27, G34 and K36. Mutations in K27 were mainly found in diffuse intrinsic pontine glioma (DIPG), a subtype of pediatric glioma, and were associated with poor prognosis (15-17). G34 substitutions were found in pediatric gliomas located in cerebral hemispheres and giant cell tumors of the bones in young adults (15,31,32). K36 mutations were identified in chondroblastomas and pediatric sarcomas (17,33). In this paper, we identified the whole set of H3.3 mutations in addition those previously identified and characterized their physical and functional properties. Our *in-silico* analyses showed that most missense mutations of H3.3 were pathogenic/deleterious and resulted in decreased protein stability.

Among all the somatic missense mutations of histone variant H3.3 retrieved from the COSMIC database across different tissues, the majority were found in the central nervous system cancers. These mutations can potentially act through two mechanisms: either by affecting histone PTMs or altering interactions between histones and their chaperones. Most of these mutation hotspots are functionally critical as they can be post-translationally modified, which is a crucial mechanism for epigenetic regulation of transcriptional activity. H3K27me3 is a repressive histone modification located in transcriptionally inactive genes and compact chromatin loci (34,35). Substitution of lysine at position 27 to methionine abolishes this function and results in decreased H3K27me3 levels since methionine cannot be methylated. In line with this, it was previously reported that patients with p.K27M substitutions exhibit globally reduced H3K27me3 levels (36). H3K36me3 is found in actively transcribed gene bodies and missense mutations resulting in p.K36M/N cause reduced H3K36me3 levels (26). Glycine is not directly modified,

but it is an amino acid that provides flexibility to the protein, which could be required for its proper functioning; thus, its mutation could result in disrupting this function. Furthermore, due to its proximity to K36, it is suggested that G34 substitutions could affect the function of H3K36me3 (32). In addition to these previously identified mutations, histone H3 can be methylated at arginine 2 and 8 by PRMT6 and PRMT5, respectively (37,38). Both of these post-transcriptional modifications are considered as repressive marks (37-40). Substitutions of arginines at positions 2 and 8 would prevent these methylations to take place and alter the transcriptional profile. Therefore, p.R2C and p.R8H could be as important as K27M and G34R/V/W in CNS tumorigenesis, although they are observed less frequently.

We also showed that all H3.3 mutations detected in CNS cancers introduced structural changes into the protein in varying degrees, which might be affecting its interactions with other proteins, such as histone chaperones. Histones are composed of N- and/or C-terminal tails and three α -helices connected by two loops, which is called the "histone fold motif" (41). This structure is highly conserved and is significant for interacting with both chromatin modulators and the DNA itself. For instance, histone tails that protrude from the nucleosome often interact with the DNA and contribute to the higher-order chromatin formation (42). Furthermore, histone variant H3.3 is deposited onto chromatin by two main histone chaperon complexes, namely HIRA and DAXX/ATRX (43); and disruption of these interactions would drastically change both the genomic distribution of histone variants and the transcriptional activity. Interestingly, patients with H3.3 mutations are reported to have frequent co-occurring mutations in DAXX and ATRX (44, 45). Almost all patients with mutated H3.3 and DAXX/ATRX also exhibit activation of a mechanism called "alternate lengthening of telomeres", which is a hallmark of cancer (44).

CONCLUSION

Incorporation of histone variant H3.3 into chromatin, as well as its somatic missense mutations dramatically alter the epigenomic landscape and the gene expression profile of a cell. Previous studies suggested that distinct gene expression patterns (45), transcriptome and interactome profiles (46) are established between tumors carrying different H3.3 mutations. Therefore, H3.3 mutations in CNS cancers are considered both as disruptors of the expression of genes required for brain function and as drivers of tumorigenesis (44,46). In conclusion, histone variants play significant roles in epigenetic regulation. Therefore, mutations in histone variant genes often contribute to carcinogenesis. A better understanding of these cancer-related mutations and their potential effects is useful for future studies.

Peer-review: Externally peer-reviewed.

Author Contributions: Conception/Design of study: B.B.S.; Data Acquisition: B.B.S.; Data Analysis/Interpretation: B.B.S.; Drafting Manuscript: B.B.S.; Critical Revision of Manuscript: B.B.S.

Conflict of Interest: The authors declare that they have no conflicts of interest to disclose.

Financial Disclosure: There are no funders to report for this submission.

REFERENCES

1. Kouzarides T. Chromatin modifications and their function. *Cell* 2007; 6(4): 693-705.
2. Albig W, Doenecke D. The human histone gene cluster at the D6S105 locus. *Hum Genet* 1997; 101: 284-94.
3. Yoda K, Ando S, Morishita S, Houmura K, Hashimoto K, Takeyasu K, et al. Human centromere protein A (CENP-A) can replace histone H3 in nucleosome reconstitution in vitro. *Proc Natl Acad Sci USA* 2000; 97: 7266-71.
4. Rogakou EP, Boon C, Redon C, Bonner WM. Megabase chromatin domains involved in DNA double-strand breaks in vivo. *J Cell Biol* 1999; 146: 905-16.
5. Thakar A, Gupta P, Ishibashi T, Finn R, Silva-Moreno B, Uchiyama S, et al. H2A.Z and H3.3 histone variants affect nucleosome structure: biochemical and biophysical studies. *Biochemistry* 2009; 48(46): 10852-7.
6. Chakravarthy S, Gundimella SK, Caron C, Perche PY, Pehrson JR, Khochbin S, et al. Structural characterization of the histone variant macroH2A. *Mol Cell Biol* 2005; 25: 7616-24.
7. Louis DN, Perry A, Reifenberger G, von Deimling A, Figarella-Branger D, Cavenee WK, et al. The 2016 World Health Organization classification of tumors of the central nervous system: a summary. *Acta Neuropathol* 2016; 131(6): 803-20. doi: 10.1007/s00401-016-1545-1.
8. McNeill KA. Epidemiology of brain tumors. *Neurol Clin* 2016; 34(4): 981-98. <http://dx.doi.org/10.1016/j.ncl.2016.06.014>.
9. Ostrom QT, de Blank PM, Kruchko C, Petersen CM, Liao P, Finlay JL, et al. Alex's Lemonade Stand Foundation infant and childhood primary brain and central nervous system tumors diagnosed in the United States in 2007-2011. *Neuro Oncol* 2015; 16(Suppl 10): x1-36.
10. Ajeawung NF, Wang HY, Gould P, Kamnasaran D. Advances in molecular targets for the treatment of medulloblastomas. *Clin Invest Med* 2012; 35(5): E246.
11. Coluccia D, Figuereido C, Isik S, Smith C, Rutka JT. Medulloblastoma: tumor biology and relevance to treatment and prognosis paradigm. *Curr Neurol Neurosci Rep* 2016; 16(5): 43. doi: 10.1007/s11910-016-0644-7.
12. Waszak SM, Northcott PA, Buchhalter I, Robinson GW, Sutter C, Groebner S, et al. Spectrum and prevalence of genetic predisposition in medulloblastoma: a retrospective genetic study and prospective validation in a clinical trial cohort. *Lancet Oncol* 2018; 19(6): 785-98. doi: 10.1016/S1470-2045(18)30242-0.
13. Park SH, Won J, Kim SI, Lee Y, Park CK, Kim SK, et al. Molecular testing of brain tumor. *J Pathol Transl Med* 2017; 51(3): 205-23. doi:10.4132/jptm.2017.03.08.
14. Aldape K, Zadeh G, Mansouri S, Reifenberger G, von Deimling A. Glioblastoma: pathology, molecular mechanisms and markers. *Acta Neuropathol* 2015; 129: 829-48.
15. Khuong-Quang DA, Buczkowicz P, Rakopoulos P, Liu XY, Fontebasso AM, Bouffet E et al. K27M mutation in histone H3.3 defines clinically and biologically distinct subgroups of pediatric diffuse intrinsic pontine gliomas. *Acta Neuropathol* 2012; 124(3): 439-47. doi:10.1007/s00401-012-0998-0.
16. Wan YCE, Liu J, Chan KM. Histone H3 mutations in cancer. *Curr Pharmacol Rep* 2018; 4(4): 292-300. doi: 10.1007/s40495-018-0141-6.
17. Weinberg DN, Allis CD, Lu C. Oncogenic mechanisms of histone H3 mutations. *Cold Spring Harb Perspect Med* 2017; 3: 7(1). pii: a026443. doi: 10.1101/cshperspect.a026443.
18. Bendl J, Musil M, Štourač J, Zendulka J, Damborský J, Brezovský J. PredictSNP2: a unified platform for accurately evaluating SNP effects by exploiting the different characteristics of variants in distinct genomic regions. *PLoS Comput Biol* 2016; 12(5): e1004962. doi: 10.1371/journal.pcbi.1004962.
19. Rogers MF, Shihab HA, Mort M, Cooper DN, Gaunt TR, Campbell C. FATHMM-XF: accurate prediction of pathogenic point mutations via extended features. *Bioinformatics* 2018; 34(3): 511-3. doi: 10.1093/bioinformatics/btx536.
20. Cheng J, Randall A, Baldi P. Prediction of protein stability changes for single-site mutations using support vector machines. *Proteins* 2006; 62(4): 1125-32.
21. Venselaar H, Te Beek TA, Kuipers RK, Hekkelman ML, Vriend G. Protein structure analysis of mutations causing inheritable diseases. An e-Science approach with life scientist friendly interfaces. *BMC Bioinformatics* 2010; 11: 548. doi: 10.1186/1471-2105-11-548.
22. Sievers F, Wilm A, Dineen D, Gibson TJ, Karplus K, Li W, et al. Fast, scalable generation of high-quality protein multiple sequence alignments using Clustal Omega. *Mol Syst Biol* 2011; 7: 539. doi: 10.1038/msb.2011.75.
23. Luger K, Mäder AW, Richmond RK, Sargent DF, Richmond TJ. Crystal structure of the nucleosome core particle at 2.8 Å resolution. *Nature* 1997; 389(6648): 251-60. doi: 10.1038/38444.
24. Frottin F, Martinez A, Peynot P, Mitra S, Holz RC, Giglione C, et al. The proteomics of N-terminal methionine cleavage. *Mol Cell Proteomics* 2006; 5(12): 2336-49.
25. Hake SB, Garcia BA, Duncan EM, Kauer M, Dellaire G, Shabanowitz J, et al. Expression patterns and post-translational modifications associated with mammalian histone H3 variants. *J Biol Chem* 2006; 281(1): 559-68.
26. Lan F, Shi Y. Histone H3.3 and cancer: a potential reader connection. *Proc Natl Acad Sci USA* 2015; 112(22): 6814-9. doi: 10.1073/pnas.1418996111.
27. Chen P, Zhao J, Wang Y, Wang M, Long H, Liang D, et al. H3.3 actively marks enhancers and primes gene transcription via opening higher-ordered chromatin. *Genes Dev* 2013; 27(19): 2109-24.
28. Delbarre E, Jacobsen BM, Reiner AH, Sørensen AL, Küntziger T, Collas P. Chromatin environment of histone variant H3.3 revealed by quantitative imaging and genome-scale chromatin and DNA immunoprecipitation. *Mol Biol Cell* 2010; 21(11): 1872-84. doi: 10.1091/mbc.E09-09-0839.
29. Dawson MA, Kouzarides T. Cancer epigenetics: from mechanism to therapy. *Cell* 2012; 150(1): 12-27. doi: 10.1016/j.cell.2012.06.013.
30. Suvà ML, Riggi N, Bernstein BE. Epigenetic reprogramming in cancer. *Science* 2013; 339(6127): 1567-70. doi: 10.1126/science.1230184.
31. Sturm D, Witt H, Hovestadt V, Khuong-Quang DA, Jones DT, Konermann C, et al. Hotspot mutations in H3F3A and IDH1 define distinct epigenetic and biological subgroups of glioblastoma. *Cancer Cell* 2012; 22(4): 425-37. doi: 10.1016/j.ccr.2012.08.024.
32. Kallappagoudar S, Yadav RK, Lowe BR, Partridge JF. Histone H3 mutations—a special role for H3.3 in tumorigenesis? *Chromosoma* 2015; 124(2): 177-89. doi: 10.1007/s00412-015-0510-4.
33. Behjati S, Tarpey PS, Presneau N, Scheipl S, Pillay N, Van Loo P, et al. Distinct H3F3A and H3F3B driver mutations define chondroblastoma and giant cell tumor of bone. *Nat Genet* 2013; 45(12): 1479-82. doi: 10.1038/ng.2814.
34. Cao R, Zhang Y. The functions of E(Z)/EZH2-mediated methylation of lysine 27 in histone H3. *Curr Opin Genet Dev* 2004; 14(2): 155-64.

35. Black JC, Van Rechem C, Whetstone JR. Histone lysine methylation dynamics: establishment, regulation, and biological impact. *Mol Cell* 2012; 48(4): 491-507. doi: 10.1016/j.molcel.2012.11.006.
36. Bender S, Tang Y, Lindroth AM, Hovestadt V, Jones DT, Kool M, et al. Reduced H3K27me3 and DNA hypomethylation are major drivers of gene expression in K27M mutant pediatric high-grade gliomas. *Cancer Cell* 2013; 24(5): 660-72. doi: 10.1016/j.ccr.2013.10.006.
37. Guccione E, Bassi C, Casadio F, Martinato F, Cesaroni M, Schuchlantz H, et al. Methylation of histone H3R2 by PRMT6 and H3K4 by an MLL complex are mutually exclusive. *Nature* 2007; 449: 933-7.
38. Pal S, Vishwanath SN, Erdjument-Bromage H, Tempst P, Sif S. Human SWI/SNF-associated PRMT5 methylates histone H3 arginine 8 and negatively regulates expression of ST7 and NM23 tumor suppressor genes. *Mol Cell Biol* 2004; 24: 9630-45.
39. Hyllus D, Stein C, Schnabel K, Schiltz E, Imhof A, Dou Y, et al. PRMT6-mediated methylation of R2 in histone H3 antagonizes H3 K4 trimethylation. *Genes Dev* 2007; 21: 3369-80.
40. Wang L, Pal S, Sif S. Protein arginine methyltransferase 5 suppresses the transcription of the RB family of tumor suppressors in leukemia and lymphoma cells. *Mol Cell Biol* 2008; 28: 6262-77.
41. Arents G, Moudrianakis EN. The histone fold: a ubiquitous architectural motif utilized in DNA compaction and protein dimerization. *Proc Natl Acad Sci USA* 1995; 92(24): 11170-4. doi: 10.1073/pnas.92.24.11170.
42. Iwasaki S, Iwasaki W, Takahashi M, Sakamoto A, Watanabe C, Shichino Y, et al. The translation inhibitor rocaglamide targets a bimolecular cavity between eIF4A and polypurine RNA. *Mol Cell* 2019; 73(4): 738-748.e9. doi: 10.1016/j.molcel.2018.11.026.
43. Goldberg AD, Banaszynski LA, Noh KM, Lewis PW, Elsaesser SJ, Stadler S, et al. Distinct factors control histone variant H3.3 localization at specific genomic regions. *Cell* 2010; 140(5): 678-91. doi: 10.1016/j.cell.2010.01.003.
44. Yuen BT, Knoepfler PS. Histone H3.3 mutations: a variant path to cancer. *Cancer Cell* 2013; 24(5): 567-74. doi: 10.1016/j.ccr.2013.09.015.
45. Schwartzenruber J, Korshunov A, Liu XY, Jones DT, Pfaff E, Jacob K, et al. Driver mutations in histone H3.3 and chromatin remodelling genes in paediatric glioblastoma. *Nature* 2012; 482(7384): 226-31. doi: 10.1038/nature10833.
46. Lim J, Park JH, Baude A, Fellenberg J, Zustin J, Haller F, et al. Transcriptome and protein interaction profiling in cancer cells with mutations in histone H3.3. *Sci Data* 2018; 5: 180283. doi: 10.1038/sdata.2018.283.

Expression of *blaA* and *blaB* and Susceptibility to Penicillins and Cephalosporins in *Yersinia enterocolitica* from Different Foods

Fatma Ozdemir¹ , Seza Arslan¹ , Hafize Gizem Erturk¹ 

¹Bolu Abant İzzet Baysal University, Faculty of Arts and Sciences, Department of Biology, Bolu, Turkey

ORCID IDs of the authors: F.O. 0000-0002-4804-936X; S.A. 0000-0002-2478-6875; H.G.E. 0000-0001-8151-5185

Please cite this article as: Ozdemir F, Arslan S, Erturk HG. Expression of *blaA* and *blaB* and Susceptibility to Penicillins and Cephalosporins in *Yersinia enterocolitica* from Different Foods. Eur J Biol 2020; 79(2): 83-88. DOI: 10.26650/EurJBiol.2020.0021

ABSTRACT

Objective: *Yersinia enterocolitica* which is an important foodborne pathogen causing illness in humans is an extremely heterogeneous species consisting of different subtypes. It has the intrinsic resistance to β -lactam antibiotics because of the production of β -lactamases, BlaA and BlaB. *Y. enterocolitica* exhibits variable susceptibilities to β -lactams.

Materials and Methods: The expression of the *blaA* and *blaB* genes by polymerase chain reaction, and the susceptibility to some β -lactams including penicillins and cephalosporins using the broth microdilution and disk diffusion methods were determined. A total of 18 *Y. enterocolitica* isolates were examined.

Results: Overall, 33.3% of these isolates carried the *blaA* and *blaB* genes, all of which were recovered from chicken meat. The wide range of MIC for ampicillin (≤ 2 -128 $\mu\text{g/mL}$) and ceftazidime (≤ 0.0625 -2 $\mu\text{g/mL}$) was also observed. Of the *Y. enterocolitica* isolates, 55.6% were resistant to ampicillin (≥ 32 $\mu\text{g/mL}$) while the remaining isolates (44.4%) were susceptible to ampicillin (≤ 8 $\mu\text{g/mL}$). All isolates were susceptible to ceftazidime at the concentration tested. According to the disk diffusion test, 55.6% and 33.3% of the isolates were resistant to ticarcillin and cefoxitin, respectively. No resistance to piperacillin and ceftriaxone was found.

Conclusion: The results showed that the presence of the *blaA* and *blaB* genes and intrinsic resistance against penicillins and cephalosporins were variable among *Y. enterocolitica* food isolates. Furthermore, the *blaA* and *blaB* genes were expressed in most of the resistant isolates to β -lactams, which may indicate the contribution of the genes to the drug resistance.

Keywords: *Yersinia enterocolitica*, *blaA*, *blaB*, β -lactams, antimicrobial susceptibility, food

INTRODUCTION

Yersinia enterocolitica is a Gram-negative, rod-shaped, nonlactose-fermenting and facultative anaerobic bacterium from the *Enterobacteriaceae*. This organism is an extremely heterogeneous species consisting of different subtypes that the subtypes have differences in geographic distribution, habitat and virulence characteristics (1-3).

Y. enterocolitica has been widely found in various sources; water, food, sewage, animal and human (1). Many previous studies reported that foods including

ground beef, chicken meat, cheese, and raw milk were frequently contaminated with *Y. enterocolitica* (4-8). *Y. enterocolitica* as a foodborne pathogen is transmitted to human via consumption of contaminated food and leads to yersiniosis, the most common form of gastroenteritis (1,9). It also causes some extraintestinal diseases such as urinary tract and respiratory tract infection, erythema nodosum, osteoarticular infection, and axillary abscesses. Severe infections including septicemia, pneumonia, meningitis, and endocarditis can often result in death in immunocompromised patients (1,3).



Corresponding Author: Fatma Özdemir

E-mail: ozkardes_f@ibu.edu.tr

Submitted: 08.05.2020 • **Revision Requested:** 30.06.2020 • **Last Revision Received:** 02.07.2020 •

Accepted: 09.07.2020 • **Published Online:** 13.12.2020

© Copyright 2020 by The Istanbul University Faculty of Science • Available online at <http://ejb.ibu.edu.tr> • DOI: 10.26650/EurJBiol.2020.0021

Resistance to β -lactams is the most common and important mechanism in the *Enterobacteriaceae*. *Y. enterocolitica* is generally resistant to β -lactam antimicrobials such as penicillin, ampicillin and first generation cephalosporins (10-13). β -lactam resistance in *Y. enterocolitica*, which was first reported in 1975, is due to two chromosomally encoded β -lactamases, BlaA and BlaB (14). BlaA is a penicillinase-type β -lactamase which is produced constitutively while BlaB is an inducible class C cephalosporinase (15,16). The expression of these β -lactamases is quite variable among different species and the strain (17). Previous studies indicated that in *Y. enterocolitica* strains which are extremely heterogeneous, differences in the susceptibility to β -lactams are mainly due to differences in the expression of β -lactamases. Different *Y. enterocolitica* subtypes exhibit variability in the level and spectrum of resistance (18-21).

Therefore, this study aims to investigate the expression of the genes *blaA* and *blaB* and determine the susceptibility to β -lactam antimicrobials including penicillins and cephalosporins using the disk diffusion and broth microdilution methods in the *Y. enterocolitica* isolates from different foods.

MATERIALS AND METHODS

Bacterial Isolates

The 18 *Y. enterocolitica* isolates obtained from various foods were used. The isolates were identified using phenotypic methods and polymerase chain reaction (PCR) amplification of the *Y. enterocolitica* 16S rRNA-specific gene (22,23). These isolates belonging to biovar 1A were recovered from chicken meat containing breast and leg parts (n=10), open white cheeses (n=3), ground beef (n=3) and raw milk (n=2). All *Y. enterocolitica* isolates were kept individually at -20°C in Brain Heart Infusion Broth (BHI, Merck, Darmstadt, Germany) containing 20% glycerol. To activate the cultures, a 400 μ l of glycerol stock was inoculated into 5 mL BHI Broth and incubated for 18-24 h at 28°C. The resulting culture was streaked on Nutrient Agar (Merck) to obtain individual colonies.

DNA Extraction

Genomic DNA of the *Y. enterocolitica* isolates was extracted using hexadecyltrimethylammonium bromide-method (CTAB) according to Ausubel et al. (24). The isolates in 5 mL BHI Broth (Merck) were incubated at 28°C for 18 h. Then 1.5 mL of the culture was transferred to an Eppendorf tube and centrifuged. Then pellet was suspended in 567 μ l TE buffer (10mM Tris, 1mM EDTA), 30 μ l SDS (10%) and 3 μ l proteinase K (20 mg/mL) (1h at 37°C). After addition of 100 μ l NaCl (5M), 80 μ l cetyltrimethyl ammonium bromide was added and incubated (65°C/10 min). Equal volume chloroform/isoamyl alcohol (24:1) solution was added and centrifuged. The supernatant was transferred to a new centrifuge tube and equal volume phenol/chloroform/isoamyl alcohol (25:24:1) solution was added. After centrifugation, the DNA pellet was precipitated with isopropanol and washed with 70% ethanol. Finally, the DNA was dissolved in 100 μ l TE buffer.

Determination of the *blaA* and *blaB* Genes

The *blaA* and *blaB* genes were investigated by PCR in all 18 *Y. enterocolitica* biovar 1A isolates from food. The *blaA* primer se-

quences were A9-f (5'-GAG ATT CAG GAA TGA AGC ACT CTT CG-3') and A10-r (5'-TCA GGA TAT TTG CGA CAA AAT TAT-3'), which were predicted to yield an 896 bp product (2). The *blaB* primer sequences were blaB5 (5'-CCC ACT TTA TAC CTT GGC ACA AA-3') and blaB3 (5'-GAA CAT ATC TCC TGC CTG GAA AT-3'), which were predicted to yield an 827 bp product (18). All reactions were carried out with the T100 thermal cycler (Bio-Rad, Hercules, USA). PCR mixture (50 μ L) contained 5 μ l of 10 \times PCR buffer (Vivantis Technologies, Selangor DE, Malaysia), 4 mM MgCl₂ (Vivantis), 0.2 mM dNTP mix (Thermo Fisher Scientific, Waltham, Massachusetts, USA), 0.4 μ M (each) primers (Biomers, Ulm, Germany), 1.5 U of Taq DNA polymerase (Vivantis), 5 μ l of 50 ng of template DNA and 35.7 μ l nuclease free water (AppliChem, Darmstadt, Germany). PCR reaction conditions included an initial denaturation (94°C, 5 min), 30 cycles of denaturation (94°C, 1 min), annealing (56°C, 1 min), extension (72°C, 1 min) followed by final extension (72°C, 8 min). The products were analyzed by electrophoresis (Bio-Rad) in a 1% agarose gel and photographed using a UV transilluminator (DNR Minilumi Bio-imaging Systems Ltd., Jerusalem, Israel). *Y. enterocolitica* ATCC 23715 was used as a control in this study.

Minimum Inhibitory Concentration (MIC) by Broth Microdilution

Broth microdilution method which is used to determine the minimum inhibitory concentration (MIC) offers the possibility to quantify resistance by actual concentrations of a particular agent and might yield reliable results (25,26). In this study, susceptibility to ampicillin and ceftazidime against *Y. enterocolitica* isolates was evaluated by the broth microdilution MIC according to the CLSI guidelines (27). Antimicrobial powder of ampicillin and ceftazidime (Sigma, St. Louis, Missouri, USA) was stored as recommended in the manufacturer's instructions. Stock solutions of ampicillin and ceftazidime were prepared considering the potency of each antimicrobial agent. All stock solutions of antimicrobials were dispensed into aliquots and kept frozen at -20°C. The stock solutions of ampicillin and ceftazidime were diluted in sterile distilled water to obtain 512 μ g/mL and 32 μ g/mL concentrations, respectively. At the end of each day, stock solutions used were discarded and never refrozen. The MICs were determined by the microdilution method in 96-well plates (TPP, Switzerland). Firstly, *Y. enterocolitica* isolates were cultured overnight on Nutrient Agar plates. Several colonies were taken and suspended into Mueller Hinton broth (MH, Merck) to adjust the bacterial turbidity to 0.5 McFarland standard (about 10⁸ CFU/mL). Serial dilutions of antimicrobials were prepared in sterile MH broth in 96-well plates. The adjusted inoculum suspension was first diluted 1:150 in MH broth, and 50 μ l was transferred to each well (5 \times 10⁴ CFU/well) of the microplate. For each test, a sterility control well (only MH broth) and a growth control well (containing MH broth with bacterial culture, no antimicrobial) were included. The microtiter plates were incubated for 18 h at 35°C. MIC experiments were carried out in triplicates. Bacterial growth was measured by optical density (ELISA reader, Thermo Electron Corporation, Vantaa, Finland). The MIC value for each *Y. enterocolitica* isolate was defined as the lowest concentration of antimicrobial which completely prevents the growth of a microorganism (27). According to CLSI, ampicillin MIC breakpoints for *Y. enterocolitica* are \leq 8 μ g/mL for

susceptible, 16 $\mu\text{g/mL}$ for intermediate, and $\geq 32 \mu\text{g/mL}$ for resistant. The breakpoints of ceftazidime are $\leq 4 \mu\text{g/mL}$, (susceptible), 8 $\mu\text{g/mL}$ (intermediate), and $\geq 16 \mu\text{g/mL}$ (resistant). Reference strains for the antimicrobial susceptibility test were *Escherichia coli* ATCC 25922 and *Y. enterocolitica* ATCC 23715.

Standard Disk Diffusion Method

All *Y. enterocolitica* isolates were examined for susceptibility to some antimicrobials belonging to the penicillin group and the cephalosporin group by the disk diffusion method (27). The antimicrobial agents tested were ticarcillin (75 μg), piperacillin (100 μg), cefoxitin (30 μg) and ceftriaxone (30 μg) (Oxoid, Basingstoke, UK). Cell suspensions adjusted to 0.5 McFarland standards were spread on Mueller Hinton Agar (Merck). The antimicrobial disks were applied on the agar surface. All plates were incubated for 24 h at 30°C. The zones of growth inhibition were evaluated as susceptible, intermediate or resistant (27).

RESULTS

In the present study, the existence of the *blaA* and *blaB* genes was examined in the 18 *Y. enterocolitica* isolates belonging to biovar 1A using PCR. Out of the 18 *Y. enterocolitica* isolates, 33.3% were found to be positive for both the *blaA* and *blaB* genes (Table 1). These positive isolates were only isolated from chicken meat. However, 66.7% of the isolates from different foods including open white cheese, ground beef, and raw milk were not found to be positive for both *blaA* and *blaB* gene (Table 1). Furthermore, Figure 1 shows the agarose gel electrophoresis image of the *blaA* and *blaB* genes in the *Y. enterocolitica* isolates.

In this study, the MIC values of the ampicillin and ceftazidime by the broth microdilution method were determined in all *Y. enterocolitica* isolates (Table 1). Ampicillin resistance was detected in 55.6% of the isolates. Antimicrobial susceptibility to ampicillin varied ranged from 2-128 $\mu\text{g/mL}$. The MIC₅₀ and MIC₉₀ were 32 $\mu\text{g/mL}$ and 128 $\mu\text{g/mL}$, respectively. Ampicillin resistance was observed in 80% of the chicken isolates. None of the isolates originated from ground beef were resistant to ampicillin. All isolates

were sensitive to ceftazidime (MIC $\leq 4 \mu\text{g/mL}$). For ceftazidime, the MIC₅₀ and MIC₉₀ were 0.25 $\mu\text{g/mL}$ and 1 $\mu\text{g/mL}$, respectively.

Susceptibilities of the isolates to some β -lactam antimicrobials belonging to the penicillin and cephalosporin group by the disk diffusion method are given in Table 1. Resistance to ticarcillin was detected in 55.6% of the isolates. On the contrary, none of the isolates were resistant to piperacillin. All isolates (100%) were found to be sensitive to ceftriaxone while 33.3% were found to be resistant to cefoxitin. All cefoxitin resistant isolates carried both *blaA* and *blaB* genes. In addition, ampicillin resistant isolates were also resistant to ticarcillin.

DISCUSSION

Y. enterocolitica is transmitted through consumption of contaminated food or water and mainly cause of gastrointestinal infections. Most *Y. enterocolitica* strains are β -lactamase producers which harbor chromosomal genes *blaA* and *blaB* encoding BlaA and BlaB, respectively (1). In the present study, these genes were detected in 33.3% of the *Y. enterocolitica* biovar 1A isolates. Numerous studies reported the presence of the genes associated with β -lactamase production of *Y. enterocolitica* (19,28,29). In India, all biovar 1A strains of *Y. enterocolitica* carried genes *blaA* and *blaB* (30). In a study, *Y. enterocolitica* biovar 1A strains isolated from different countries were found to be positive for both *blaA* and *blaB* genes (2). Sharma et al. (16) reported that all *Y. enterocolitica* biovar 1A strains from different sources also harbored both *blaA* and *blaB* genes. In Poland, in a study conducted by Kot et al. (29), the presence of the *blaA* and *blaB* genes of *Y. enterocolitica*, isolated from the feces of children suffering from diarrhea, was 90.5% and 57.1%, respectively. They indicated that the *blaA* gene was detected in all strains of biovar 4 and 2, while found the *blaB* gene in some strains of biovar 2 and biovar 4. On the other hand, in their study, biovar 1A strains did not carry both the genes. It was documented in the study of Ye et al. (28) that the *blaA* and *blaB* were found to be positive of 97% and 100% of the *Y. enterocolitica* biotype 1A isolates from retail foods in China, respectively. In Germany, all *Y. enterocolitica* biovars 2, 4 and 5 strains had the *blaA* and *blaB* genes (18). Stock et al. (19) observed that all biovar 1A, 1B and 3 strains carried the *blaB*. The *blaA* was found in some biovar 1B and 3 strains, but not in biovar 1A strains. These studies of Stock et al. (18,19) suggested that expression of β -lactamase genes, *blaA* and *blaB*, varied with the biovar. Furthermore, variable expression and activities of *blaA* and *blaB* genes might have an effect on the level and spectrum of β -lactam resistance (18,30). Strain variations have been shown to be depending on the different subtypes and geographical origin of the isolates (2,18,31-33).

In this study, more than half of the isolates (55.6%) were positive for ampicillin resistance, but all isolates were sensitive to ceftazidime. Many studies have been performed to determine the levels of resistance to ampicillin and ceftazidime in *Y. enterocolitica* strains from different sources (8,34). *Y. enterocolitica* strains from retail poultry and swine feces presented 100% resistance to ampicillin and 100% susceptibility to ceftazidime

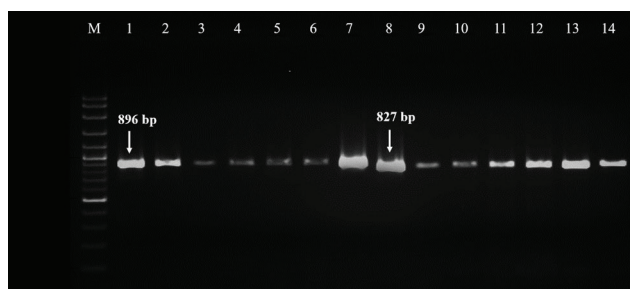


Figure 1. Agarose gel electrophoresis of PCR-amplified *blaA* and *blaB* gene products from the *Y. enterocolitica* isolates. Lane M: 100 bp DNA Ladder. Lane 1: *Y. enterocolitica* ATCC 23715 positive control for *blaA* (896 bp). Lanes 2-7: *blaA* of the chicken meat isolates in this study. Lane 8: *Y. enterocolitica* ATCC 23715 positive control for *blaB* (827 bp). Lanes 9-14: *blaB* of the chicken meat isolates in this study.

Table 1. Presence of β -lactamase genes and susceptibility profiles to penicillins and cephalosporins of 18 *Y. enterocolitica* isolates from food.

Isolate	Origin	PCR analysis			Ampicillin MIC			Ceftazidime MIC			Disk Diffusion		
		<i>blaA</i>	<i>blaB</i>	MIC ^c /Interpretation	MIC ₅₀	MIC ₉₀	MIC ^d /Interpretation	MIC ₅₀	MIC ₉₀	TIC	PRL	FOX	CRO
T1	Chicken meat	+ ^a	+	32/R			0.5/S			R	S	R	S
T2	Chicken meat	+	+	32/R			1/S			R	S	R	S
T3	Chicken meat	+	+	64/R			2/S			R	I	R	S
T4	Chicken meat	- ^b	-	64/R			0.25/S			R	S	S	S
T5	Chicken meat	+	+	32/R			0.25/S			R	S	R	S
T6	Chicken meat	+	+	128/R			1/S			R	I	R	S
T7	Chicken meat	-	-	128/R			0.25/S			R	S	S	S
T8	Chicken meat	-	-	8/S			0.25/S			S	S	S	S
T9	Chicken meat	+	+	32/R	32	128	0.25/S	0.25	1	R	I	R	S
T10	Chicken meat	-	-	2/S			0.0625/S			S	S	S	S
K1	Ground beef	-	-	4/S			0.25/S			S	S	S	S
K2	Ground beef	-	-	4/S			0.25/S			S	S	S	S
K3	Ground beef	-	-	4/S			0.25/S			S	S	S	S
M1	Open white cheese	-	-	128/R			1/S			R	I	S	S
M2	Open white cheese	-	-	2/S			0.5/S			S	S	S	S
M3	Open white cheese	-	-	4/S			0.0625/S			S	S	S	S
S1	Raw milk	-	-	8/S			0.25/S			S	S	S	S
S2	Raw milk	-	-	128/R			0.25/S			R	S	S	S

MIC: Minimum inhibitory concentrations were recorded in the unit of $\mu\text{g/mL}$; R: Resistant, I: Intermediate, Susceptible: S, TIC: Ticarcillin, PRL: Piperacillin, FOX: Cefoxitin, CRO: Ceftriaxone; ^aPositive for the gene; ^bNegative for the gene; ^cMIC breakpoints for ampicillin; Susceptible, ≤ 8 ; Intermediate, 16; Resistant, $\geq 32 \mu\text{g/mL}$; ^dMIC breakpoints for ceftazidime; Susceptible, ≤ 4 ; Intermediate, 8; Resistant, $\geq 16 \mu\text{g/mL}$.

by the broth microdilution method (34). Similarly, MIC results for ceftazidime in *Y. enterocolitica* from swine and pork products showed that all strains were categorized as susceptible (35). All *Y. enterocolitica* from the pork production chain (8) and from fruits and vegetables (36) were resistant to ampicillin. In some studies, the resistance to ampicillin was detected in 92% of the isolates from different samples including human and nonhuman and 87.2% of *Y. enterocolitica* clinical isolates (37,38). In a study conducted by Weiner (39), ampicillin MICs were ≥ 32 $\mu\text{g/mL}$ (resistant) in all *Y. enterocolitica* isolates from animals.

In this study, *Y. enterocolitica* isolates were resistant to ticarcillin (55.6%) and cefoxitin (33.3%) whereas resistance to piperacillin and ceftriaxone was not observed. Resistance to ticarcillin in *Y. enterocolitica* strains was detected in Brazil at the level of 94%, in Canada at the level of 90% and in Poland at the level of 76.2% (10,29,40). However, Ye et al. (41) reported that all *Y. enterocolitica* strains from retail frozen foods were sensitive to ticarcillin. In previous studies, the rates of susceptibility to piperacillin were 100% (10,35). Susceptibility against cefoxitin (62%) and ceftriaxone (100%) was found by Kwaga et al. (35), similar to our ceftriaxone results. Similarly, Baumgartner et al. (42) in Switzerland indicated that no strains of *Y. enterocolitica* from human patients, pigs and retail pork were resistant to ceftriaxone. In contrast to our results, the *Y. enterocolitica* strains isolated from clinical and non-clinical sources in Brazil were not positive for cefoxitin resistance (40).

β -lactamases, BlaA and BlaB that offer ampicillin and first-generation cephalosporin resistance in *Y. enterocolitica* have been reported in previous studies (13,36,37,43). In this study, the positive isolates for *blaA* and *blaB* genes were ampicillin resistant and ceftazidime susceptible according to MIC values. However, some ampicillin resistant isolates on the basis of MIC breakpoints did not carry the β -lactamase genes. In contrast to our study, Peng et al. (34) reported that all *Y. enterocolitica* isolates carried the *blaA* and *blaB* were also resistant to ampicillin and susceptible to ceftazidime by the broth microdilution method. On the other hand, some studies showed that some ampicillin sensitive *Y. enterocolitica* strains carried the *blaA* and *blaB* genes. Most ceftazidime sensitive strains also were positive for these genes. Although there is some correlation between MIC results and β -lactamase induction, it may not possible to predict the expression of BlaA and BlaB enzymes from MIC results (18,28).

CONCLUSION

In this study, both *blaA* and *blaB* genes which confer resistance to β -lactam antimicrobials were detected in *Y. enterocolitica* biovar 1A isolates from foods, particularly in chicken meat isolates. More than half of the isolates were resistant to ampicillin whereas all isolates were sensitive to ceftazidime. The isolates carried both the *blaA* and *blaB* genes were resistant to ampicillin, ticarcillin and cefoxitin. Consequently, the results of this study demonstrated that the presence of the *blaA* and *blaB* genes and intrinsic resistance against penicillins and cephalosporins were variable among *Y. enterocolitica* food isolates. Furthermore, the *blaA* and *blaB* genes were expressed in most of the resistant iso-

lates to β -lactams, which may indicate the contribution of the genes to the drug resistance.

Peer-review: Externally peer-reviewed.

Author Contributions: Conception/Design of study: F.Ö., S.A.; Data Acquisition: F.Ö., S.A., H.G.E.; Data Analysis/Interpretation: F.Ö., S.A.; Drafting Manuscript: F.Ö., S.A., H.G.E.; Critical Revision of Manuscript: F.Ö., S.A., H.G.E.; Final Approval and Accountability: F.Ö., S.A., H.G.E.; Technical or Material Support: F.Ö., S.A.; Supervision: S.A.

Conflict of Interest: The authors declare that they have no conflicts of interest to disclose.

Financial Disclosure: There are no funders to report for this submission.

REFERENCES

1. Carniel E, Autenrieth I, Cornelis G, Fukushima H, Guinet F, Isberg R, et al. *Y. enterocolitica* and *Y. pseudotuberculosis*. Dworkin M, Falkow S, Rosenberg E, Schleifer, KH, Stackebrandt E, editors. The Prokaryotes. New York, NY: Springer; 2006.p.270-398.
2. Sharma S, Mittal S, Mallik S, Virdi JS. Molecular characterization of β -lactamase genes *blaA* and *blaB* of *Yersinia enterocolitica* biovar 1A. FEMS Microbiol Lett 2006; 257: 319-27.
3. Bhunia AK. Foodborne Microbial Pathogens: Mechanisms and Pathogenesis. New York, NY: Springer; 2008.
4. Logue CM, Sheridan JJ, Wauters G, McDowell DA, Blair IS. *Yersinia* spp. and numbers, with particular reference to *Y. enterocolitica* bio/serotypes, occurring on Irish meat and meat products, and the influence of alkali treatment on their isolation. Int J Food Microbiol 1996; 33: 257-74.
5. Capita R, Calleja CA, Prieto M, Fernandez MDCG, Moreno B. Incidence and pathogenicity of *Yersinia* spp. isolates from poultry in Spain. Food Microbiol 2002; 19: 295-301.
6. Soltan-Dallal MM, Tabarraie A, MoezArdalan K. Comparison of four methods for isolation of *Yersinia enterocolitica* from raw and pasteurized milk from northern Iran. Int J Food Microbiol 2004; 94: 87-91.
7. Van Damme I, Berkvens D, Botteldoorn N, Dierick K, Wits J, Pochet B, et al. Evaluation of the ISO 10273:2003 method for the isolation of human pathogenic *Yersinia enterocolitica* from pig carcasses and minced meat. Food Microbiol 2013; 36: 170-5.
8. Martins BTF, Botelho CV, Silva DAL, Lanna FGPA, Grossi JL, Campos-Galvao MEM, et al. *Yersinia enterocolitica* in a Brazilian pork production chain: Tracking of contamination routes, virulence and antimicrobial resistance. Int J Food Microbiol 2018; 276: 5-9.
9. Ray B. Fundamental Food Microbiology. 3rd ed. Boca Raton, Florida: CRC Press; 2004.
10. Preston MA, Brown S, Borczyk AA, Riley G, Krishnan C. Antimicrobial susceptibility of pathogenic *Yersinia enterocolitica* isolated in Canada from 1972 to 1990. Antimicrob Agents Chemother 1994; 38: 2121-4.
11. Crowe M, Ashford K, Ispahani P. Clinical features and antibiotic treatment of septic arthritis and osteomyelitis due to *Yersinia enterocolitica*. J Med Microbiol 1996; 45: 302-9.
12. Stock I. Natural susceptibility of *Yersinia enterocolitica*-like species to β -lactam antibiotics. Rev Med Microbiol 2004; 15: 81-92.
13. Fabrega A, Vila J. *Yersinia enterocolitica*: pathogenesis, virulence and antimicrobial resistance. Enferm Infecc Microbiol Clin 2012; 30: 24-32.

14. Cornelis G, Abraham EP. β -lactamases from *Yersinia enterocolitica*. J Gen Microbiol 1975; 87: 273-84.
15. Pham JN, Bell SM, Lanzarone JYM. A study of the β -lactamases of 100 clinical isolates of *Yersinia enterocolitica*. J Antimicrob Chemother 1991; 28: 19-24.
16. Sharma S, Ramnani P, Viridi JS. Detection and assay of β -lactamases in clinical and non-clinical strains of *Yersinia enterocolitica* biovar 1A. J Antimicrob Chemother 2004; 54: 401-5.
17. Livermore DM. β -Lactamases in laboratory and clinical resistance. Clin Microbiol 1995; 8: 557-84.
18. Stock I, Heisig P, Wiedemann B. Expression of β -lactamases in *Yersinia enterocolitica* strains of biovars 2, 4 and 5. J Med Microbiol 1999; 48: 1023-7.
19. Stock I, Heisig P, Wiedemann B. β -lactamase expression in *Yersinia enterocolitica* biovars 1A, 1B, and 3. J Med Microbiol 2000; 49: 403-8.
20. Bent ZW, Young GM. Contribution of BlaA and BlaB β -lactamases to antibiotic susceptibility of *Yersinia enterocolitica* Biovar 1B. Antimicrob Agents Chemother 2010; 54: 4000-2.
21. Singhal N, Srivastava A, Kumar M, Viridi JS. Structural variabilities in β -lactamase (blaA) of different biovars of *Yersinia enterocolitica*: implications for β -lactam antibiotic and β -lactamase inhibitor susceptibilities. PloS One 2015; 10(4): e0123564.
22. Neubauer H, Hensel A, Aleksic S, Meyer H. Identification of *Yersinia enterocolitica* within the genus *Yersinia*. Syst Appl Microbiol 2000; 23: 58-62.
23. Bottone EJ, Bercovier H, Mollaret HH. Genus XLI. *Yersinia*. Garrity GM, Brenner DJ, Krieg NR, Staley JT, editors. Bergey's manual of systematic bacteriology. New York, NY: Springer; 2005. p. 838-48.
24. Ausubel FM, Kingston RE, Brent R, Moore DD, Seidman J, Smith JA, et al. editors. Current protocols in molecular biology. New York, NY: Greene Publishing Associates & Wiley Interscience; 1991.
25. Meyer C, Stolle A, Fredriksson-Ahomaa M. Comparison of broth microdilution and disk diffusion test for antimicrobial resistance testing in *Yersinia enterocolitica* 4/O:3 strains. Microb Drug Resist 2011; 17: 479-84.
26. International Standard. Susceptibility testing of infectious agents and evaluation of performance of antimicrobial susceptibility test devices-Part 1: Broth micro-dilution reference method for testing the in vitro activity of antimicrobial agents against rapidly growing aerobic bacteria involved in infectious diseases. Geneva, Switzerland; ISO 20776-1: 2019.
27. Clinical and Laboratory Standards Institute (CLSI), Performance standards for Antimicrobial Susceptibility Testing; Twenty-sixth Edition, in, Wayne, PA, USA, 2016.
28. Ye Q, Wu Q, Hu H, Zhang J, Huang H. Prevalence and characterization of *Yersinia enterocolitica* isolated from retail foods in China. Food Control 2016; 61: 20-7.
29. Kot B, Piechota M, Jakubiak K. Virulence genes and antibiotic resistance of *Yersinia enterocolitica* strains isolated from children. EJBR 2017; 7: 366-73.
30. Singhal N, Kumar M, Viridi JS. Molecular analysis of β -Lactamase genes to understand their differential expression in strains of *Yersinia enterocolitica* biotype 1A. Sci Rep 2014; 4:5270.
31. Pham JN, Bell SM, Martin L, Carniel E. The β -lactamases and β -lactam antibiotic susceptibility of *Yersinia enterocolitica*. J Antimicrob Chemother 2000; 46: 951-7.
32. Mittal S, Mallik S, Sharma S, Viridi JS. Characteristics of β -lactamases and their genes (*blaA* and *blaB*) in *Yersinia intermedia* and *Y. frederiksenii*. BMC Microbiol 2007; 7:25.
33. Fabrega A, Balleste-Delpierre C, Vila J. Antimicrobial resistance in *Yersinia enterocolitica*. Chen C-Y, Yan X, Jackson CR, editors. Antimicrobial Resistance and Food Safety; 2015.p.77-104.
34. Peng Z, Zou M, Li M, Liu D, Guan W, Hao Q, et al. Prevalence, antimicrobial resistance and phylogenetic characterization of *Yersinia enterocolitica* in retail poultry meat and swine feces in parts of China. Food Control 2018; 93: 121-8.
35. Kwaga J, Iversen JO. In vitro antimicrobial susceptibilities of *Yersinia enterocolitica* and related species isolated from slaughtered pigs and pork products. Antimicrob Agents Chemother 1990; 34: 2423-5.
36. Verbikova V, Borilova G, Babak V, Moravkova M. Prevalence, characterization and antimicrobial susceptibility of *Yersinia enterocolitica* and other *Yersinia* species found in fruits and vegetables from the European Union. Food Control 2018; 85: 161-7.
37. Bonke R, Wacheck S, Stuber E, Meyer C, Martlbauer E, Fredriksson-Ahomaa M. Antimicrobial susceptibility and distribution of β -lactamase A (*blaA*) and β -lactamase B (*blaB*) genes in enteropathogenic *Yersinia* species. Microb Drug Resist 2011; 17: 575-81.
38. Abdel-Haq NM, Papadopol R, Asmar BI, Brown WJ. Antibiotic susceptibilities of *Yersinia enterocolitica* recovered from children over a 12-year period. Int J Antimicrob Agents 2006; 27: 449-52.
39. Weiner M. ERIC-based differentiation and antimicrobial susceptibility of *Yersinia enterocolitica* O:9 isolated from animals serologically positive and negative for brucellosis. Bull Vet Inst Pulawy 2013; 57: 493-8.
40. Frazao MR, Andrade LN, Darini ALC, Falcao JP. Antimicrobial resistance and plasmid replicons in *Yersinia enterocolitica* strains isolated in Brazil in 30 years. Braz J Infect Dis 2017; 21: 477-80.
41. Ye Q, Wu Q, Hu H, Zhang J, Huang H. Prevalence, antimicrobial resistance and genetic diversity of *Yersinia enterocolitica* isolated from retail frozen foods in China. FEMS Microbiol Lett 2015; 362: 1-7.
42. Baumgartner A, Kuffer M, Suter D, Jemni T, Rohner P. Antimicrobial resistance of *Yersinia enterocolitica* strains from human patients, pigs and retail pork in Switzerland. Int J Food Microbiol 2007; 115: 110-4.
43. Bonardi S, Bassi L, Brindani F, D'Incau M, Barco L, Carra E, et al. Prevalence, characterization and antimicrobial susceptibility of *Salmonella enterica* and *Yersinia enterocolitica* in pigs at slaughter in Italy. Int J Food Microbiol 2013; 163: 248-57.

Proteomic Analysis of the Protective Effect of Sodium Nitroprusside on Leaves of Barley Stressed by Salinity

Mustafa Yildiz¹ , Melike Celik¹ , Hakan Terzi¹ 

¹Afyon Kocatepe University, Faculty of Science and Literature, Department of Molecular Biology and Genetics, Afyonkarahisar, Turkey

ORCID IDs of the authors: M.Y. 0000-0002-6819-9891; M.C. 0000-0002-5364-5596; H.T. 0000-0003-4817-1100

Please cite this article as: Yildiz M, Celik M, Terzi H. Proteomic Analysis of the Protective Effect of Sodium Nitroprusside on Leaves of Barley Stressed by Salinity. Eur J Biol 2020; 79(2): 89-97. DOI: 10.26650/EurJBiol.2020.0026

ABSTRACT

Objective: The salinization of agricultural soils poses a serious challenge across the world. Although recent studies have shown that exogenous sodium nitroprusside (SNP) application can alleviate the harmful effects of salinity, the roles of SNP in the regulation of proteomic changes remain poorly understood.

Materials and Methods: To unravel the protective roles of exogenous SNP in alleviating salt-induced damage in barley (*Hordeum vulgare* L.), proteomic analysis was carried out on the leaves of seedlings exposed to 100 mM NaCl stress following 200 µM SNP pre-treatment.

Results: Our results indicated that SNP pre-treatment restored the seedling growth reduced by salinity stress. Comparing 2-DE gels from the treatments showed that 24 proteins were differentially accumulated under SNP and/or NaCl stress treatments. Among them, 15 proteins were identified by matrix-assisted laser desorption ionization time-of-flight mass spectrometry. Gene ontology analysis demonstrated that several pathways were regulated by SNP and/or NaCl treatments, including photosynthesis, protein metabolism, stress defense, and energy metabolism. Exogenous SNP increased the expression levels of 20 kDa chaperonin, proteasome subunit beta type-2, 2-Cys peroxiredoxin BAS1, ferredoxin-NADP reductase, thiazole biosynthetic enzyme 1-1, S-adenosylmethionine synthetase 3, and elongation factor Tu proteins in the leaves of barley seedlings under NaCl stress.

Conclusion: Our results indicate that SNP pre-treatment may induce salinity tolerance through regulation of photosynthesis, activation of stress defence, degradation of damaged proteins, and the promoting of the synthesis of polyamines, proline, and GABA.

Keywords: Barley, nitric oxide, salinity stress, sodium nitroprusside, proteomics

INTRODUCTION

Plants are faced with a range of environmental constraints which can frequently cause significant reductions in growth and development. Of these, salinity is regarded as one of the most important environmental constraints that depress plant growth by inducing water deficiency and ion toxicity. It has been estimated that approximately 6% of the world's total land area is exposed to salinity (1,2). Since high soil salinity leads to a decline in crop productivity, improving salinity tolerance of agricultural plants has become an urgent priority. One of the ways to increase the adaptation of

plants to salt stress is exogenous applications of various chemicals such as phytohormones, antioxidants, signal molecules, and trace elements (3,4). Among those, nitric oxide (NO) has significant and diversified functions in mitigation of salt-induced adverse effects (5).

Nitric oxide is a gaseous free radical, and it regulates several physiological processes such as seed germination and seedling growth (6). Numerous studies have examined the ameliorative effects of exogenous sodium nitroprusside (SNP; NO donor) on salt-induced metal toxicity in plants (4,7). Different mechanisms have been suggested for NO-mediated salt tolerance. Yadu et al. (8)



Corresponding Author: Mustafa Yildiz

E-mail: mustafa_yildizus@yahoo.com

Submitted: 18.06.2020 • **Revision Requested:** 10.08.2020 • **Last Revision Received:** 10.08.2020 •

Accepted: 26.09.2020 • **Published Online:** 13.12.2020

© Copyright 2020 by The Istanbul University Faculty of Science • Available online at <http://ejb.istanbul.edu.tr> • DOI: 10.26650/EurJBiol.2020.0026

and Ahmad et al. (4) have demonstrated that NO improved the salinity tolerance of pea and tomato seedlings by enhancing the antioxidant capacity and synthesis of flavonoid, glycine betaine, and proline. Exogenous application of SNP has also been shown to improve photosynthetic capacity by protecting pigments, enhancing quantum-yield of photosystem II, and increasing stomatal conductance and RuBisCO activity (9,10).

Although the ameliorative effects of exogenous NO under salinity stress have been comprehensively studied, there have also been several attempts to unravel the molecular basis of NO-induced salinity tolerance (11,12). It has been suggested that exogenous NO helped maize seedlings to overcome salinity stress by enhancing the expression of G-protein-associated proteins and activating antioxidant system (11). Another previous study showed that exogenous NO up-regulated the abundance proteins functioning in energy metabolism, photosynthesis and stress response in mangrove plant *Avicennia marina* leaves under salinity stress (12). Since a few studies have examined the protective roles of NO at proteome levels, we used a 2-DE based proteomic analysis to identify protein alterations in response to salt stress and NO in barley leaves.

MATERIALS AND METHODS

Plant Material and Treatments

Seeds of barley (*Hordeum vulgare* L. cv. Tarm-92) were obtained from Ankara Field Crops Central Research Institute. After surface sterilization of the seeds in 1% NaOCl solution, the seeds were washed 5 times with sterile distilled water. The sterilized seeds were germinated in a controlled climate cabin (23°C, dark, 60% humidity) for 48 h. The uniformly germinated seedlings were placed into perforated tubes with 3 seedlings per tube. Five tubes were placed in a pot containing 0.5 L of modified Hoagland nutrient solution (pH 6.0). The seedlings were grown for 3 d under relative humidity of 60%, 14 h photoperiod (250 $\mu\text{mol}\cdot\text{m}^{-2}\cdot\text{s}^{-1}$), and constant temperature of 25 °C in the growth chamber. For SNP pre-treatment, 200 μM NO donor SNP was applied along with the nutrient solution for 48 h. After pre-treatment, salinity stress was induced using a nutrient solution supplemented with 100 μM NaCl. The treatments of SNP and NaCl were as follows: (1) control; 0 mM NaCl, (2) SNP; 200 μM SNP, (3) NaCl; 100 μM NaCl, and (4) SNP+NaCl; 200 μM SNP + 100 μM NaCl. Experiments were arranged in a randomized complete block design. After seven days of NaCl treatment, the seedlings were separated into roots and shoots, and the fresh weight (FW) was weighed. Dry weights (DW) of root and shoot tissues were determined after drying at 80 °C for 2 d.

Protein Extraction and Two-Dimensional Gel Electrophoresis

The total proteins from fresh barley leaves were extracted using the phenol extraction protocol described by Ahsan et al. (13). One gram of mixed root tissues was ground with liquid nitrogen, and fine powders were transferred into the extraction solution (0.5 M Tris-HCl (pH 8.3), 2% β -mercaptoethanol, 2% NP-40, 0.7 M sucrose, 20 μM MgCl₂, and 1 μM phenylmethyl sulfonyl fluoride), and fractionated with Tris-buffered (pH 8.0) phenol. After centrifugation, phenol phase was mixed with methanol containing ammonium acetate to precipitate the proteins. The Bradford assay was used to

quantify protein concentration by dissolving air-dried pellets in a lysis buffer containing 7 M urea, 2 M thiourea, 40 μM DL-dithiothreitol (DTT), 0.2% biolytes (pH 3–10), and 4% CHAPS (14).

For separation of proteins via 2-DE, IPG strips (pH 4–7, Bio-Rad) were used. Dry IPG strips were passively rehydrated with 300 μL of rehydration buffer containing 80 μg proteins. Isoelectric focusing of the rehydrated strips was performed on the Proteans i12™ IEF System for 80 kVh. For the reduction and alkylation of the sulfhydryl groups, the strips were equilibrated with buffer A (0.05 M Tris-HCl pH 8.8, 6 M urea, 20% glycerol, 2% SDS, and 1% DTT), and then with buffer B (2.5% iodoacetamide instead of DTT). Second dimension electrophoresis was carried out on 12.5% SDS-PAGE gels using a Protean II XL Cell System (Bio-Rad). The preparative gels containing 500 μg proteins were stained with a modified method of colloidal Coomassie brilliant blue (15), and analytical gels were silver-stained (16).

Image Analysis and Matrix-Assisted Laser Desorption Ionization Time-of-Flight Mass Spectrometry (MALDI-TOF/TOF MS)

Images of the triplicate silver-stained gels were obtained using the ChemiDoc™ MP System and they were evaluated with PDQuest 8.01 (Bio-Rad). Before spot matching, spot detection and background subtraction were performed. The volume of each protein spot was normalized on the basis of total density of gels. The student's t-test with a significance level of 95% was performed to evaluate the significant changes in spots among treatments ($p < 0.05$). A protein showing a more than 1.5-fold increase in abundance in at least one treatment was considered as a differentially expressed protein.

Trypsin digestion was carried out using a commercial kit (ThermoFisher Scientific). A solution of digested peptides was purified using ZipTip C₁₈ pipette tips (Millipore), mixed with the matrix solution (α -cyano-hydroxy cinnamic acid), and then spotted onto a MALDI plate. Peptide mass spectra were obtained using an AB Sciex TOF/TOF 5800 mass spectrometer.

The obtained MS/MS spectra were used to search the Swiss-Prot database with the MASCOT search engine (<http://www.matrix-science.com>). The search criteria were as follows: Taxonomy, Viridiplantae (green plants); database, Swiss-Prot; Enzyme, Trypsin; Mass accuracy, 50 ppm; Peptide MS tolerance, ± 0.4 Da; Variable modifications, Oxidation of methionine; Fixed modification, Carbamidomethylation of cysteine; and allowance of one missed cleavage. The differentially expressed proteins were classified on the basis of functions according to the database at <http://www.uniprot.org/uniprot>. To explore the relationships in the protein-protein interaction (PPI) network, proteins identified in the current study were analysed by STRING 11.0 (17). BiNGO was used to estimate biological processes and molecular functions (18).

Statistical Analysis

All experiments with triplicate were performed twice. Statistical analyses were performed by analysis of variance (ANOVA) using SPSS 22.0 software. Means from physiological analyses were statistically analysed with Duncan's multiple range test (DMRT).

RESULTS

Effect of SNP on Barley Growth under NaCl Stress

The effect of 200 μ M SNP pre-treatment and 100 μ M NaCl stress on growth of barley seedlings in this study is given in Table 1. NaCl stress resulted in significant reductions in both shoot and root fresh and dry weights compared to the control ($p < 0.05$). However, SNP pre-treatment completely restored the growth parameters except for shoot fresh weight. Additionally, SNP pre-treatment resulted in an increase in all growth parameters compared to the control (Table 1).

Table 1. The effects of SNP pre-treatment and NaCl stress on fresh (FW) and dry weights (DW) of barley seedlings

Treatments	Shoot	Shoot	Root	Root
	FW	DW	FW	DW
mg.seedling ⁻¹				
Control	647 \pm 26 ^b	63.7 \pm 1.2 ^a	223 \pm 8.6 ^b	14.0 \pm 0.4 ^b
SNP	737 \pm 25 ^a	68.2 \pm 2.4 ^a	249 \pm 13.9 ^a	16.3 \pm 0.2 ^a
NaCl	409 \pm 36 ^d	49.4 \pm 2.6 ^b	160 \pm 15.3 ^c	12.4 \pm 0.8 ^c
SNP + NaCl	542 \pm 21 ^c	64.0 \pm 4.9 ^a	233 \pm 6.4 ^{ab}	16.4 \pm 1.0 ^a

* Different letters (a-d) within the same column indicate significant differences between treatments at $P < 0.05$, according to DMRT. Each value is the average of six replicates, in which 10 seedlings are sampled per replicates. Standard error (\pm SE).

Effect of SNP on NaCl-Induced Proteome Alterations

In this study, proteome profiles of proteins extracted from leaf tissues of barley seedlings from control, SNP, NaCl and SNP+NaCl treatments were obtained using the 2-DE (IEF/SDS-PAGE) analysis (Figure 1). In the 2-DE gel profiles, changes in the expression of proteins were analysed using the PDQuest software. According to image analysis, 24 protein spots which showed at least a 1.5-fold difference in expression level were determined in the leaf tissue. Among them, 15 proteins were successfully identified by MALDI-TOF/TOF analysis and Swiss-Prot database searching (Table 2).

The identified proteins were grouped into various categories according to the biological functions such as photosynthesis, stress defence, energy metabolism, protein metabolism, and primary metabolism (Table 2). In the present study, 6 proteins (spots 1, 2, 3, 4, 10 and 12) associated with photosynthesis were differently accumulated in SNP and/or NaCl treatments compared to the control (Figure 1, Table 2). The expression level of the RuBisCO small subunit (RBCS, spot 1) increased in NaCl treatment, while it decreased to control level in SNP+NaCl application. The expression levels of another RuBisCO small subunit (spot 2) and cytochrome b6-f complex iron-sulphur subunit (spot 3) were down-regulated in SNP+NaCl treatment. Additionally, the expression levels of RuBisCO large subunit (RBCL, spot 4) and RuBisCO activase A (RCA, spot 12) proteins were down-regulated by NaCl treatment, while SNP pre-treatment removed this inhibition. Additionally, the expression level of the ferredoxin-NADP reductase (FNR, spot 10) protein was up-regulated by SNP and SNP+NaCl treatments (Table 2).

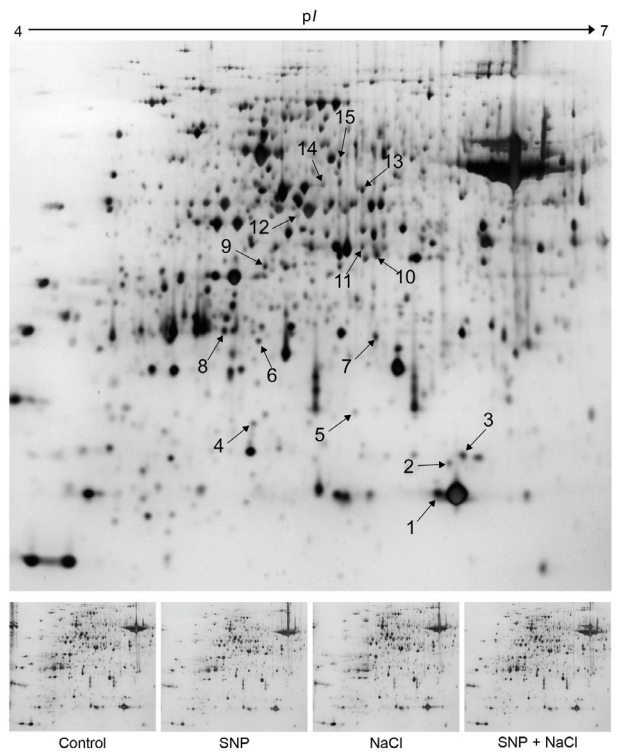


Figure 1. Two-dimensional (2-D) electrophoretic profiles of proteins extracted from leaf tissues of barley seedlings exposed to control, SNP, NaCl, and SNP + NaCl treatments. Total proteins (80 μ g) were loaded on 17 cm IPG strips (pH 4-7), and SDS-PAGE was performed on 12% gel. Proteins were visualised by silver staining. Arrow indicates the differentially accumulated proteins (Table 2).

Four proteins (spots 5, 6, 7, and 14) related to protein synthesis and metabolisms were differentially expressed in SNP and/or NaCl treatments (Figure 1, Table 2). The expression level of the eukaryotic translation initiation factor 5A-3 (ELF5A-3, spot 5) protein was down-regulated by SNP and NaCl treatments while it decreased to the control level in SNP+NaCl treatment. Proteasome subunit beta type-2 (spot 7) protein was up-regulated by SNP+NaCl treatment. Additionally, 20 kDa chaperonin (CPN20, spot 6) and elongation factor Tu (EFTU, spot 14) proteins increased gradually (Table 2).

The expression level of the 2-Cys peroxylodoxin BAS1 (BAS, spot 8) protein was up-regulated by SNP+NaCl treatment. However, the abundance of thiazole biosynthetic enzyme 1-1 (THI1, spot 9) was up-regulated by SNP and SNP+NaCl treatments (Table 2). A glycolysis related protein fructose-bisphosphate aldolase (FBA, spot 11) was increased by NaCl treatment, while SNP pre-treatment removed this increase. S-adenosylmethionine synthetase 3 (SAMS, spot 13) protein was increased by SNP and SNP+NaCl treatments. Finally, the abundance of glutamate decarboxylase (GAD, spot 15) protein, which plays a role in the synthesis of gamma-aminobutyric acid (GABA), increased in all applications compared to control (Table 2).

Table 2. Proteins identified by MALDI-TOF/TOF mass spectrometry in leaf tissues of barley seedlings exposed to SNP pre-treatment and/or NaCl stress.

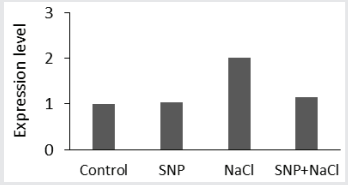
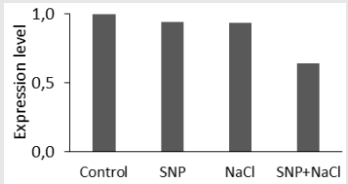
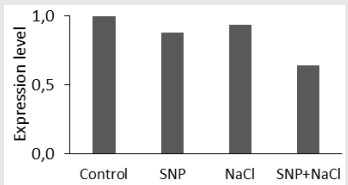
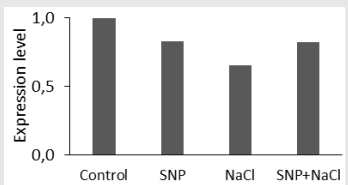
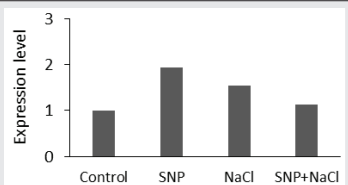
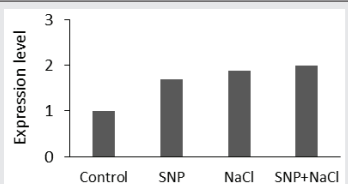
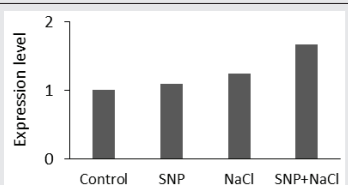
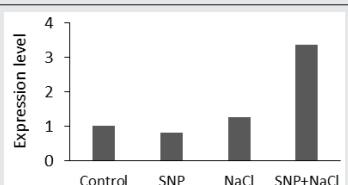
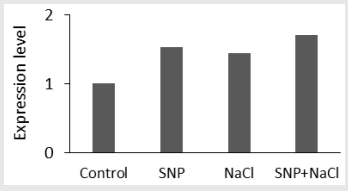
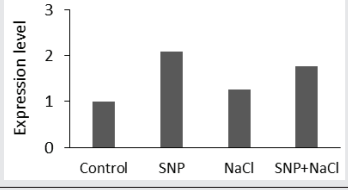
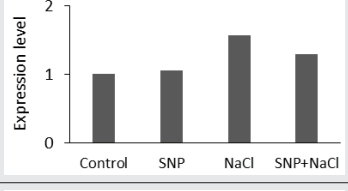
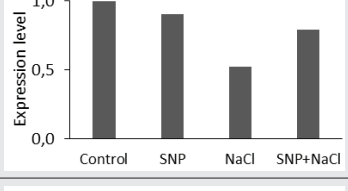
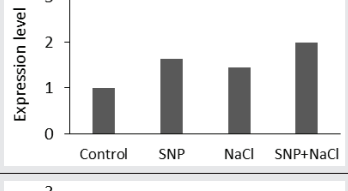
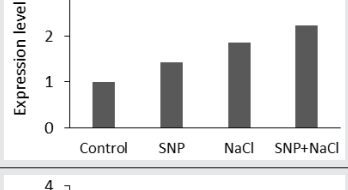
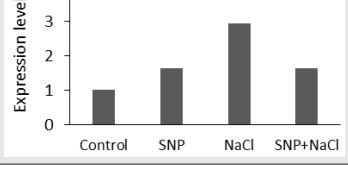
Spot	Accession number	Protein	Score	MW/pI	Seq. cover.	MP	Expression level
1	RBS_HORVU	Ribulose biphosphate carboxylase small chain	293	19.4/8.98	55%	22	
2	RBS_HORVU	Ribulose biphosphate carboxylase small chain	52	19.4/8.98	27%	8	
3	UCRIA_WHEAT	Cytochrome b6-f complex iron-sulfur subunit	264	23.7/8.47	57%	15	
4	RBL_HORVU	Ribulose biphosphate carboxylase large chain	316	53.0/6.22	13%	14	
5	IF5A3_ARATH	Eukaryotic translation initiation factor 5A-3	60	17.2/5.56	32%	7	
6	CH10C_ARATH	20 kDa chaperonin	47	26.8/8.86	11%	4	
7	PSB2_ORYSJ	Proteasome subunit beta type-2	63	23.5/5.42	16%	5	
8	BAS1_HORVU	2-Cys peroxiredoxin BAS1	83	23.3/5.48	23%	13	

Table 2. Continued.

Spot	Accession number	Protein	Score	MW/pI	Seq. cover.	MP	Expression level
9	THI41_MAIZE	Thiazole biosynthetic enzyme 1-1	260	37.1/5.22	24%	17	
10	FENR1_PEA	Ferredoxin--NADP reductase	203	40.2/8.56	31%	19	
11	ALFC_ORYSJ	Fructose-bisphosphate aldolase, chloroplastic	146	41.9/6.38	16%	11	
12	RCAA_HORVU	Ribulose bisphosphate carboxylase/oxygenase activase A	246	51.0/8.04	29%	26	
13	METK3_HORVU	S-adenosylmethionine synthetase 3	160	42.7/5.51	33%	17	
14	EFTU_PEA	Elongation factor Tu	209	53.0/6.62	12%	8	
15	DCE_SOLLC	Glutamate decarboxylase	92	56.7/5.97	9%	8	

Based on STRING analysis, protein-protein interactions of identified proteins are shown in Figure 2a. RCA, FNR, FBA and BAS proteins were found to be important interaction points, suggesting that photosynthesis, energy metabolism and stress defence are very important for response to NaCl stress and exogenous SNP. Differently expressed proteins

were analysed using BiNGO to obtain statistically under- and over-represented categories of molecular functions and biological pathways related to NaCl stress and exogenous SNP (Figure 2b). NaCl stress and exogenous SNP promoted predominantly stress-responsive proteins and less photosynthesis-related proteins.

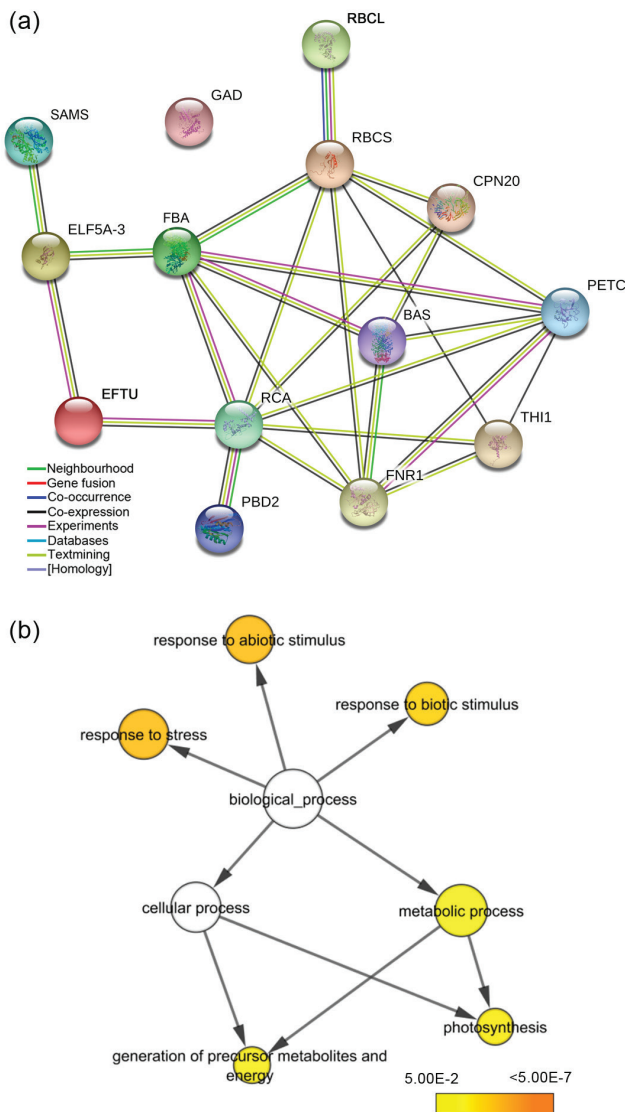


Figure 2. a) Protein-protein interactions were created using the STRING system (<http://string.embl.de>). Lines of different colours indicate different evidence types for the association of the proteins. b) The molecular function networks generated by BiNGO. The size of the node is proportional to the number of molecules within this group, and the colour of the node represents the significance of enrichment.

DISCUSSION

Nitric oxide has been reported to be a signalling molecule that alleviates the reduction in growth of plants under diversified biotic and abiotic stresses (4,19,20). In our study, SNP pre-treatment alleviated the detrimental effects of NaCl stress on seedling growth. These results have also been shown in many plant species exposed to NaCl stress (4,7,8). It has been reported that NO can loosen the cell wall, affect the phospholipid layer, increase membrane fluidity, and promote plant growth by increasing cell expansion (21). Dong et al. (22) re-

ported that NO increases stem and root elongation by improving cytoplasmic viscosity and increasing the osmotic pressure under high salinity. However, it has been demonstrated that NO-mediated induction of salt tolerance is associated with increased activities of antioxidant enzymes and the accumulation of osmoprotectants (4,8). Additionally, NO has been shown to interact with salicylic acid and hydrogen peroxide to mediate the elimination of oxidative damage in many stress conditions (23). Overall, SNP-induced salt tolerance in barley seedlings may be associated with a high accumulation of important osmotic protective compounds or promoting the antioxidant defence system.

High soil salinity limits the productivity of agricultural crops in arid and semi-arid regions. Thus, understanding the molecular basis of salt stress tolerance in plants is useful for the development of plant species that can tolerate salt stress. In the present study, the effects of SNP and/or NaCl stress on leaf tissues of barley seedlings were evaluated using a proteomic approach. The differential regulation of salt-responsive proteins by SNP pre-treatment stress is discussed below.

It is well-known that salinity stress can severely inhibit the photosynthetic pathway (24). The decrease in photosynthetic activity under salt stress conditions is directly related to the expression levels of proteins associated with photosynthesis. It has been reported that the decrease in the photosynthetic activity reduces the ability of plants to overcome stress (3). In our study, proteomic analysis showed that 6 photosynthetic proteins involved in CO₂ fixation and light reactions were expressed differently in NaCl stress and/or SNP treatments (Table 2). The abundance of RBCL and RCA proteins decreased in salt stress conditions, but this decrease was restored by SNP pre-treatment. Additionally, salt stress caused an approximately 2-fold increase in the expression level of the RBCS protein compared to the control. RCA has been shown to play a significant role in maintaining assimilation at low CO₂ levels caused by salt stress (25). FNR plays a role in photosynthetic electron flow from reduced ferredoxin to NADP⁺ and is required for CO₂ fixation in plants (26). Additionally, ferredoxin has been reported to play a role in different biological pathways including phenolic biosynthesis, nitrogen fixation, biogenesis of iron-sulphur clusters, and detoxification of xenobiotics (27). However, overexpression of the chloroplastic FNR enzyme in agricultural plants has been reported to increase oxidative stress tolerance (28). In our study, the expression level of FNR protein was increased by SNP and SNP+NaCl treatments. As a result, a higher activity of photosynthetic enzymes after SNP treatments could provide a better photosynthetic activity and improve salt tolerance of barley seedlings.

Salt stress can seriously affect protein synthesis and cause ER stress by disrupting protein folding (29). In our study, the abundance of chloroplastic EFTU protein increased in NaCl, and its expression further increased in SNP+NaCl treatment. Previous research has shown that EFTU plays a significant role in the high temperature tolerance of *Brassica campestris* plants (30). SNP-induced up-regulation of EFTU protein under salt stress

conditions may repair the damaged photosynthetic proteins in chloroplasts by increasing protein biosynthesis under salt stress. However, the expression level of molecular chaperone CPN20 protein was up-regulated by SNP pre-treatment in NaCl-stressed seedlings. Chaperonins help protein folding and assembling and function in protecting and repairing proteins under stress conditions (31). Additionally, the abundance of the proteasome subunit beta type-2 protein was up-regulated by SNP+NaCl treatment. This protein has been reported to play a role in ubiquitin-mediated protein degradation (32). This result suggests that NO can alleviate salt stress-induced damage by increasing the degradation of misfolded or damaged proteins. As a result, an SNP-induced increase in these proteins can lead to a general improvement in cellular processes during stress conditions.

The over-production of reactive oxygen species is a well-documented indirect effect of salinity stress (33). In our study, the abundance of BAS and THI1 protein was increased by SNP+NaCl treatment. It has been reported that a thiol specific antioxidant BAS is localized to chloroplasts and it has antioxidant and chaperone activity during photosynthesis and plant development (34). THI1 is an important enzyme functioning in the thiamine biosynthesis pathway and participates in stress tolerance mechanisms in yeast, bacteria, and *Arabidopsis thaliana* by repairing DNA damage (35,36). Additionally, thiamine has been shown to alleviate the effects of oxidative stress in plants during environmental stresses (37). SNP-induced up-regulation of BAS and THI1 proteins may alleviate NaCl-induced oxidative stress in barley leaves by reducing oxidative stress and maintaining DNA stability.

Regulation of energy metabolism is one of the important strategies for overcoming salinity stress (38). In our study, the level of expression of the glycolysis-related FBA protein was up-regulated by salt stress. FBA catalyses the reversible separation of fructose-1,6-bisphosphate into glyceraldehyde 3-phosphate and dihydroxyacetone phosphate. Yin et al. (39) found that FBA is important in maintaining the physiological functions of *B. napus* leaves under biotic stress conditions. However, overexpression of the *Sesuvium portulacastrum* FBA gene (*SpFBA*) in *E. coli* bacteria enhanced salinity tolerance (40). It suggests that increased glycolysis activity may be a possible plant strategy to overcome salt stress.

S-adenosylmethionine synthase (SAMS) catalyse the biosynthesis of SAM from methionine and ATP, and SAM functions as the precursor of phytohormones such as polyamines and ethylene (41). Transgenic experiments have proven that SAM contributes to stress tolerance by increasing accumulation of polyamines (41,42). However, it has been stated that the abundance of SAMS protein was higher in salt-tolerant barley than in salt-sensitive barley (43). In our study, SNP pre-treatment resulted in an increase in the abundance of SAMS protein in both control and salt stress conditions. It can be suggested that an increased abundance of SAMS may increase salt tolerance by promoting polyamine biosynthesis.

Glutamate decarboxylase (GAD) is a Ca²⁺-dependent calmodulin-binding protein that catalyses the synthesis of amino-gamma-aminobutyric acid (GABA). GABA plays a role in various biological pathways including cytosolic pH regulation, nitrogen metabolism, and carbon flow to the TCA cycle (44). Renault et al. (45) reported that GABA accumulation was associated with GAD activity in Arabidopsis plants under salinity stress. Additionally, exogenous GABA application has been reported to increase salt tolerance by increasing antioxidant capacity and photosynthetic activity, ensuring osmotic adjustment and regulating water use efficiency (46). The increased GAD activity has been shown to be associated with the rapid accumulation of proline which increases salt tolerance in sesame (47). In our study, the expression level of GAD protein increased approximately 3-fold in NaCl application, and 1.6-fold in SNP+NaCl applications. This result suggested that the accumulation of GAD protein may contribute to salt tolerance of barley seedlings.

CONCLUSION

SNP application significantly increased biomass and helped maintain the growth of barley seedlings under salt stress. In our study, proteins that have a role in important biological functions and are differentially expressed in response to SNP application and/or NaCl stress in barley seedlings were identified by MALDI-TOF/TOF mass spectrometry. It can be argued that these proteins, which are mostly up-regulated, affect plant metabolism in order to overcome the negative effects of salinity stress. Exogenous SNP increased the expression levels of CPN20, BAS, FNR, THI1, SAMS, EFTU, and proteasome subunit beta type-2, proteins in the leaves of barley seedlings under NaCl stress. SNP has contributed greatly to the increase of salt tolerance by regulating photosynthesis, protein metabolism and defense systems. These findings will allow for a better understanding of SNP-induced salt tolerance mechanisms in barley plants.

Peer-review: Externally peer-reviewed.

Author Contributions: Conception/Design of study: MY, HT; Data Acquisition: MY, HT, MÇ; Data Analysis/Interpretation: MY, HT, MÇ; Final Approval and Accountability: MY, HT; Drafting Manuscript: MY, HT; Critical Revision of Manuscript: MY, HT; Technical or Material Support: MY, HT, MÇ.

Conflict of Interest: The authors declare that they have no conflicts of interest to disclose.

Financial Disclosure: The support of Afyon Kocatepe University Research Fund (Project No. 18.FEN.BIL.01) to this research is thankfully acknowledged.

Acknowledgement: The authors gratefully acknowledge the Medicinal Genetics Laboratory of Afyonkarahisar Health Sciences University and the DEKART Proteomics Laboratory of Kocaeli University for their technical help. The authors also wish to thank Afyon Kocatepe University's Foreign Language Support Unit for language editing.

REFERENCES

- Munns R, Tester M. Mechanisms of salinity tolerance. *Ann Rev Plant Biol* 2008; 59: 651–81.
- Setia R, Gottschalk P, Smith P, Marschner P, Baldock J, Setia D et al., Soil salinity decreases global soil organic carbon stocks. *Sci Total Environ* 2013; 465: 267–72.
- Soundararajan P, Manivannan A, Ko CH, Muneer S, Jeong BR. Leaf physiological and proteomic analysis to elucidate silicon induced adaptive response under salt stress in *rosa hybrida* 'rock fire.' *Int J Mol Sci* 2017; 18(8): 1768.
- Ahmad P, Abass AM, Nasser AM, Wijaya L, Alam P, Ashraf M. Mitigation of sodium chloride toxicity in *Solanum lycopersicum* L. by supplementation of jasmonic acid and nitric oxide. *J Plant Interact* 2018; 13(1): 64–72.
- Hasanuzzaman M, Oku H, Nahar K, Bhuyan MHMB, Al Mahmud J, Baluska F et al., Nitric oxide-induced salt stress tolerance in plants: ROS metabolism, signaling, and molecular interactions. *Plant Biotechnol Rep* 2018; 12(2): 77–92.
- Fancy NN, Bahlmann AK, Loake GJ. Nitric oxide function in plant abiotic stress. *Plant Cell Environ* 2017; 40(4): 462–72.
- Ali Q, Daud MK, Haider MZ, Ali S, Rizwan M, Aslam N et al., Seed priming by sodium nitroprusside improves salt tolerance in wheat (*Triticum aestivum* L.) by enhancing physiological and biochemical parameters. *Plant Physiol Biochem* 2017; 119: 50–8.
- Yadu S, Dewangan TL, Chandrakar V, Keshavkant S. Imperative roles of salicylic acid and nitric oxide in improving salinity tolerance in *Pisum sativum* L. *Physiol Mol Biol Plants* 2017; 23(1): 43–58.
- Wu XX, Zhu XH, Chen JL, Yang SJ, Ding HD, Zha DS. Nitric oxide alleviates adverse salt-induced effects by improving the photosynthetic performance and increasing the anti-oxidant capacity of eggplant (*Solanum melongena* L.). *J Hort Sci Biotech* 2015; 88(3): 352–60.
- Fatma M, Khan NA. Nitric oxide protects photosynthetic capacity inhibition by salinity in Indian mustard. *J Funct Environ Bot* 2014; 4: 106–16.
- Bai X, Yang L, Yang Y, Ahmad P, Yang Y, Hu X. Deciphering the protective role of nitric oxide against salt stress at the physiological and proteomic levels in maize. *J Proteome Res* 2011; 10: 4349–64.
- Shen Z, Chen J, Ghoto K, Hu W, Gao G, Luo M et al., Proteomic analysis on mangrove plant *Avicennia marina* leaves reveals nitric oxide enhances the salt tolerance by up-regulating photosynthetic and energy metabolic protein expression. *Tree Physiol* 2018; 38(11): 1605–22.
- Ahsan N, Lee DG, Alam I, Kim PJ, Lee JJ, Ahn YO et al., Comparative proteomic study of arsenic-induced differentially expressed proteins in rice roots reveals glutathione plays a central role during As stress. *Proteomics* 2008; 8: 3561–76.
- Bradford MM. A rapid and sensitive method for the quantification of microgram quantities of protein utilizing the principle of protein dye binding. *Anal Biochem* 1976; 72: 248–54.
- Candiano G, Bruschi M, Musante L, Santucci L, Ghiggeri GM, Carnemolla B et al., Blue silver: a very sensitive colloidal Coomassie G-250 staining for proteome analysis. *Electrophoresis* 2004; 25: 1327–33.
- Sinha P, Poland J, Schnölzer M, Rabilloud T. A new silver staining apparatus and procedure for matrix-assisted laser desorption/ionization-time of flight analysis of proteins after two-dimensional electrophoresis. *Proteomics* 2001; 1: 835–40.
- Szklarczyk D, Franceschini A, Kuhn M, Simonovic M, Roth A, Minguez P et al., The STRING database in 2011: functional interaction networks of proteins, globally integrated and scored. *Nucleic Acids Res* 2011; 39: 561–8.
- Maere S, Heymans K, Kuiper M. BiNGO: a Cytoscape plugin to assess overrepresentation of Gene Ontology categories in biological networks. *Bioinformatics* 2005; 21: 3448–9.
- Terrón-Camero LC, Peláez-Vico MÁ, Del-Val C, Sandalio LM, Romero-Puertas MC. Role of nitric oxide in plant responses to heavy metal stress: exogenous application versus endogenous production. *J Exp Bot* 2019; 70(17): 4477–88.
- Tripathi DK, Singh S, Singh S, Srivastava PK, Singh VP, Singh S et al., Nitric oxide alleviates silver nanoparticles (AgNps)-induced phytotoxicity in *Pisum sativum* seedlings. *Plant Physiol Biochem* 2017; 110: 167–77.
- Leshem YY, Haramaty E. Plant aging: the emission of NO and ethylene and effect of NO-releasing compounds on growth of pea (*Pisum sativum*) foliage. *J Plant Physiol* 1996; 148: 258–63.
- Dong YJ, Jinc SS, Liu S, Xu LL, Kong J. Effects of exogenous nitric oxide on growth of cotton seedlings under NaCl stress. *J Soil Sci Plant Nutr* 2014; 14: 1–13.
- Mostofa MG, Fujita M, Tran LSP. Nitric oxide mediates hydrogen peroxide- and salicylic acid-induced salt tolerance in rice (*Oryza sativa* L.) seedlings. *Plant Growth Regul* 2015; 77: 265–77.
- Chaves MM, Flexas J, Pinheiro C. Photosynthesis under drought and salt stress: regulation mechanisms from whole plant to cell. *Ann Bot* 2009; 103(4): 551–60.
- de Abreu CE, Araujo Gdos S, Monteiro-Moreira AC, Costa JH, Leite Hde B, Moreno FB et al., Proteomic analysis of salt stress and recovery in leaves of *Vigna unguiculata* cultivars differing in salt tolerance. *Plant Cell Rep* 2014; 33(8): 1289–306.
- Fukuyama K. Structure and function of plant type ferredoxins. *Photosynth Res* 2004; 81:289–301.
- Musumeci MA, Ceccarelli A, Catalano-Dupuy DL. The plant-type ferredoxin-NADP⁺ reductases. Najafpour M, editor. *Advances in Photosynthesis-Fundamental Aspects*; InTech: Rijeka, Croatia; 2012; pp. 539–62.
- Rodríguez RE, Lodeyro A, Poli HO, Zurbriggen M, Peisker M, Palatnik JF et al., Transgenic tobacco plants overexpressing chloroplastic ferredoxin-NADP(H) reductase display normal rates of photosynthesis and increased tolerance to oxidative stress. *Plant Physiol* 2007; 143(2): 639–49.
- Wang M, Xu Q, Yuan M. The unfolded protein response induced by salt stress in *Arabidopsis*. *Method Enzymol* 2011; 489: 319–28.
- Peng HT, Li YX, Zhang CW, Li Y, Hou XL. Chloroplast elongation factor BcEF-Tu responds to turnip mosaic virus infection and heat stress in non-heading Chinese cabbage. *Biol Plant* 2014; 58(3): 561–6.
- Roy S, Mishra M, Dhankher OP, Singla-Pareek SL, Pareek A. Molecular Chaperones: Key players of abiotic stress response in plants. Rajpal V, Sehgal D, Kumar A, Raina S, editors. *Genetic Enhancement of Crops for Tolerance to Abiotic Stress: Mechanisms and Approaches*, Vol. I. Sustainable Development and Biodiversity, vol 20. Springer.2019.
- Cui F, Liu L, Zhao Q, Zhang Z, Li Q, Lin Q et al., *Arabidopsis* ubiquitin conjugase UBC32 is an ERAD component that functions in brassinosteroid-mediated salt stress tolerance. *Plant Cell* 2012; 24: 233–44.
- Hossain MS, Dietz KJ. Tuning of redox regulatory mechanisms, reactive oxygen species and redox homeostasis under salinity stress. *Front Plant Sci* 2016; 7: 548.
- Kim SY, Jang HH, Lee JR, Sung NR, Bin Lee H, Lee DH et al., Oligomerization and chaperone activity of a plant 2-Cys peroxiredoxin in response to oxidative stress. *Plant Sci* 2009; 177(3): 227–32.
- Machado CR, de Oliveira RL, Boiteux S, Prækelt UM, Meacock PA, Menck CF. Thi1, a thiamine biosynthetic gene in *Arabidopsis thaliana*, complements bacterial defects in DNA repair. *Plant Mol Biol* 1996; 31(3): 585–93.

36. Ribeiro DT, Farias LP, de Almeida JD, Kashiwabara PM, Ribeiro AF, Silva-Filho MC et al., Functional characterization of the thi1 promoter region from *Arabidopsis thaliana*. J Exp Bot 2005; 56(417): 1797–804.
37. Rapala-Kozik M, Wolak N, Kujda M, Banas AK. The upregulation of thiamine (vitamin B1) biosynthesis in *Arabidopsis thaliana* seedlings under salt and osmotic stress conditions is mediated by abscisic acid at the early stages of this stress response. BMC Plant Biol 2012; 12: 2.
38. Zhang H, Han B, Wang T, Chen S, Li H, Zhang Y et al., Mechanisms of plant salt response: insights from proteomics. J Proteome Res 2012; 11: 49–67.
39. Yin H, Li S, Zhao X, Bai X, Du Y. Isolation and characterization of an oilseed rape SKP1 gene BnSKP1 involved on defence in *Brassica napus*. J Biotechnol 2008; 136: S227.
40. Fan W, Zhang ZL, Zhang YL. Cloning and molecular characterization of fructose-1,6-bisphosphate aldolase gene regulated by high-salinity and drought in *Sesuvium portulacastrum*. Plant Cell Rep 2009; 28: 975–84.
41. Gong B, Li X, VandenLangenberg KM, Wen D, Sun S, Wei M et al., Overexpression of S-adenosyl-L-methionine synthetase increased tomato tolerance to alkali stress through polyamine metabolism. Plant Biotechnol J 2014; 12: 694–708.
42. Qi YC, Wang FF, Hui Z, Liu WQ. Overexpression of *Suaeda salsa* S-adenosylmethionine synthetase gene promotes salt tolerance in transgenic tobacco. Acta Physiol Plant 2010; 32: 263–9.
43. Witzel K, Weidner A, Surabhi GK, Börner A, Mock H. Salt stress-induced alterations in the root proteome of barley genotypes with contrasting response towards salinity. J Exp Bot 2009; 60:3545–57.
44. Gut H, Dominici P, Pilati S, Astegno A, Petoukhov MV, Svergun DI et al., A common structural basis for pH- and calmodulin-mediated regulation in plant glutamate decarboxylase. J Mol Biol 2009; 392: 334–51.
45. Renault H, Roussel V, El Amrani A, Arzel M, Renault D, Bouchereau A et al., The *Arabidopsis* pop2-1 mutant reveals the involvement of GABA transaminase in salt stress tolerance. BMC Plant Biol 2010; 10: 20.
46. Li Z, Cheng B, Zeng W, Zhang X, Peng Y. Proteomic and metabolomic profilings reveal crucial functions of γ -aminobutyric acid in regulating ionic, water, and metabolic homeostasis in creeping bentgrass under salt stress. J Proteome Res 2020; 19: 769–80.
47. Zhang Y, Wei M, Liu A, Zhou R, Li D, Dossa K et al., Comparative proteomic analysis of two sesame genotypes with contrasting salinity tolerance in response to salt stress. J Proteomics 2019; 201: 73–83.

Antioxidant, Cytotoxic, and Enzyme Inhibitory Activities of *Agropyron repens* and *Crataegus monogyna* Species

Ebru Deveci¹ , Gulsen Tel Cayan² , Serdar Karakurt³ , Mehmet Emin Duru⁴ 

¹Konya Technical University, Department of Chemistry and Chemical Processing Technologies, Konya, Turkey

²Muğla Sıtkı Koçman University, Department of Chemistry and Chemical Processing Technologies, Muğla, Turkey

³Selçuk University, Faculty of Science, Department of Biochemistry, Konya, Turkey

⁴Muğla Sıtkı Koçman University, Faculty of Science, Department of Chemistry, Muğla, Turkey

ORCID IDs of the authors: E.D. 0000-0002-2597-9898; G.T.Ç. 0000-0002-1916-7391; S.K. 0000-0002-4449-6103; M.E.D. 0000-0001-7252-4880

Please cite this article as: Deveci E, Tel Cayan G, Karakurt S, Duru ME. Antioxidant, Cytotoxic, and Enzyme Inhibitory Activities of *Agropyron repens* and *Crataegus monogyna* Species. Eur J Biol 2020; 79(2): 98-105. DOI: 10.26650/EurJBiol.2020.0077

ABSTRACT

Objective: The aim of this study was to investigate antioxidant, enzyme inhibitory and cytotoxic activities of *Agropyron repens* and *Crataegus monogyna* methanol extracts with total phenolic and flavonoid contents.

Materials and Methods: Total phenolic and flavonoid contents of *A. repens* and *C. monogyna* methanol extracts were measured according to Folin Ciocalteu and aluminum nitrate methods, respectively. Antioxidant and enzyme inhibitory activities of the methanol extracts were tested spectrophotometrically. Also, cytotoxic activities of the methanol extracts against DLD-1 and CCD-18Co were investigated by using Alamar Blue assay.

Results: *C. monogyna* methanol extract with the highest total phenolic and flavonoid contents (68.13±0.34 µg GAEs/mg extract and 36.91±0.17 µg QEs/mg extract, respectively) had the best antioxidant activity in β-carotene-linoleic acid (IC₅₀: 32.72±0.15 µg/mL), CUPRAC (A_{0.50}: 282.69±0.25 µg/mL), DPPH[•] (IC₅₀: 71.69±0.85 µg/mL), and ABTS^{•+} (IC₅₀: 40.43±0.55 µg/mL) assays. *A. repens* methanol extract showed the highest effect against AChE (18.73±0.47 %), BChE (37.59±1.07 %), urease (89.18±0.84%), α-glucosidase (6.71±0.23 %), whereas *C. monogyna* methanol extract showed the highest effect against tyrosinase (30.52±1.00%) and α-amylase (37.24±0.06 %). Also, *A. repens* (IC₅₀: 57.38 µg/mL) and *C. monogyna* (IC₅₀: 54.04 µg/mL) methanol extracts showed close cytotoxic activity on DLD-1.

Conclusion: Antioxidant, cytotoxic, and enzyme inhibitory activities of *A. repens* and *C. monogyna* methanol extracts were investigated with total phenolic and flavonoid contents in this study. The results obtained with this study strengthen the potential of the studied plants as a new source for the discovery of antioxidant, cytotoxic, and enzyme inhibitor agents.

Keywords: *Agropyron repens*, *Crataegus monogyna*, antioxidant activity, cytotoxic activity, enzyme inhibitory activity

INTRODUCTION

Pharmacologically, medicinal plants have always been at the forefront of almost all civilizations. Medicinal plants are used to treat diseases and prevent possible epidemics, and additionally to flavor and to preserve foods. Also, medicinal plants are considered as rich sources of traditional medicines, and most synthetic medicines are produced from these plants. Secondary metabolites produced by plants are generally respon-

sible for the biological properties of plant species used worldwide (1,2). Compounds such as alkaloids, tannins, flavonoids, and phenolics found in plants are therapeutic for human health (3,4).

Agropyron species is a member of Poaceae. *Agropyron repens* (Quack grass) is known as 'Ayrik otu' in Turkey. It is often used in folk medicine as a diuretic in prostate disease, urinary infections, as well as calming of spasms and pain in the urinary tract (5). *A. repens* has been reported



Corresponding Author: Ebru Deveci

E-mail: edevcei@ktun.edu.tr

Submitted: 27.10.2020 • **Revision Requested:** 19.11.2020 • **Last Revision Received:** 23.11.2020 •

Accepted: 25.11.2020 • **Published Online:** 13.12.2020

© Copyright 2020 by The Istanbul University Faculty of Science • Available online at <http://ejb.istanbul.edu.tr> • DOI: 10.26650/EurJBiol.2020.0077

to be used in Bulgarian traditional medicine as antitussive, anti-inflammatory, and diuretic; in Kosovo traditional medicine as antirheumatic and antianemic; in Turkey traditional medicine to treat treatment of kidney stones and gastrointestinal diseases (6-8). *A. repens* was previously determined to contain phenol compounds, carbohydrates, pectins, saponins and to have anti-inflammatory, antiadhesive, and diuretic effects (9-11).

Crataegus species is a member of Rosaceae and widely grown in Europe, America, and Asia. The genus *Crataegus* consists of 200 species around the world and represented by 21 species in Turkey. *Crataegus* (Hawthorn) is known as 'Aliç' in Turkey (12). *Crataegus* (hawthorn) species are widely used in folk medicine in the therapy of diseases such as congestive heart failure, angina, hypertension, arrhythmia. *Crataegus* species have been reported to be used in traditional Chinese medicine to remove blood stasis, improve circulation, treat diarrhea, indigestion, hyperlipidemia, hypertension and abdominal pain; in European traditional medicine in the therapy of heart problems in associated with their antiatherosclerotic, cardiotoxic, antispasmodic, and hypotensive properties; in Turkey traditional medicine as a diuretic agent for the treatment of intestinal disorders (13). It has been reported that *Crataegus* species indicated immunostimulant, radical scavenging, antiviral, anti-lipoperoxidant, antimicrobial, anti-inflammatory, antihyperlipidemic, hepatoprotective, gastroprotective, and hypoglycemic activities in relation to containing phenolic compounds, proanthocyanins, triterpenoids, and flavonoid glycosides (12,14).

Investigating the effects of medicinal plants on health is important for the discovery or design of new drugs, and studies in this area have been increasing in recent years. Therefore, the aim of this study is to investigate the antioxidant, cytotoxic, and enzyme inhibitory activities of *A. repens* and *Crataegus monogyna* methanol extracts with total phenolic and flavonoid contents.

MATERIALS AND METHODS

Plant Materials

A. repens and *C. monogyna* were collected from Konya, Turkey in 2017. The plant species were identified by Dr. Ergün Kaya at Muğla Sıtkı Koçman University, Muğla, Turkey. The voucher specimen has been deposited at Plant Molecular Genetics and Biotechnology Laboratory, Department of Molecular Biology and Genetics, Muğla Sıtkı Koçman University with voucher no EK.1688 (for *A. repens*) and EK.1687 (for *C. monogyna*).

Extraction

The aerial parts of *A. repens* and *C. monogyna* were extracted with methanol at room temperature for 24 h and four times. Solvent was evaporated under vacuum by an evaporator to obtain the methanol extracts. All extracts were stored at +4°C until analysis.

Instruments

Antioxidant and enzyme inhibitory tests were measured by using a 96-well microplate reader, SpectraMax 340PC384 (Molecular Devices, Silicon Valley, California, USA). Softmax PRO v5.2 software (Molecular Devices, Silicon Valley) was used to

calculate and measure the bioactivity data. A 96-well microplate reader (MultiskanGo, Thermo Scientific Co., MA, USA) was used to analyze cytotoxic activity studies. Cytotoxic activity results were measured and calculated by using GraphPad Prism (GraphPad Software v5.0, USA).

Total Phenolic and Flavonoid Contents

The phenolic contents of extracts were tested based on the method reported by Slinkard and Singleton (15). Results were given as a microgram of gallic equivalents (GAEs) using the following equation that was obtained from standard gallic acid graph:

$$\text{Absorbance} = 0.0104[\text{gallic acid } (\mu\text{g})] - 0.0263 \quad (r^2, 0.9974)$$

Total flavonoid contents of extracts were measured by using the aluminum nitrate method (16). Results were given as microgram quercetin equivalents (QEs) using the following equation that was obtained from standard quercetin acid graph:

$$\text{Absorbance} = 0.0158[\text{quercetin } (\mu\text{g})] - 0.0306 \quad (r^2, 0.9993)$$

Antioxidant Activity

β -carotene-linoleic acid, metal chelating, cupric reducing antioxidant capacity (CUPRAC), 1,1-diphenyl-2-picrylhydrazyl free radical (DPPH), and (3-ethylbenzothiazoline-6-sulfonic acid) diammonium salt cation radical (ABTS⁺) scavenging assays were performed for measurement of antioxidant activities of the extracts (17). The graph of the inhibition percentage (%) versus the concentration ($\mu\text{g}/\text{mL}$) was used to calculate the IC₅₀ values of the extracts. The graph of the absorbance versus the concentration ($\mu\text{g}/\text{mL}$) was used to calculate 0.50 absorbance (A_{0.5}) values of the extracts. The antioxidant activity results were stated as 50 % inhibition concentration (IC₅₀) for β -carotene-linoleic acid, ABTS and DPPH scavenging, inhibition percentage (%) at 400 $\mu\text{g}/\text{mL}$ concentration for metal chelating assay and A_{0.50} which corresponds to the concentration producing 0.500 absorbance for CUPRAC assay.

Enzyme Inhibitory Activity

Acetylcholinesterase (AChE), butyrylcholinesterase (BChE), urease, and tyrosinase inhibitory activities of the extracts were carried out as reported in our previous study (18). α -Amylase and α -glucosidase inhibitory activities were screened according to the method previously reported by Deveci et al. (19). Galantamine, Kojic acid, Thiourea and Acarbose were used as standards. The enzyme inhibitory activity results were stated as IC₅₀ and inhibition percentages (%).

Cell Culture

DLD-1 (colorectal cancer), and CCD-18Co (human colon fibroblast cell line) were cultivated in RPMI-1640 and EMEM growth mediums (ATCC, Virginia, USA), respectively and incubated with 1% penicillin/streptomycin, 10% fetal bovine serum (FBS), 2 mM L-glutamine (Sigma, St. Louis, Missouri, USA) in 5% CO₂ at 37°C and 90-95 % humidity.

Cell Viability Assay

1x10⁴ cells were put into 96-well plate with growth medium and incubated in 5% CO₂ at 37°C for 24h until attached to the

bottom. Then, different concentrations (between 1 µg/mL and 1000 µg/mL) of the extracts were added to each well. Viability and proliferation of the cells were tested according to the previously described Alamar Blue assay (20). The results were measured by using 96-well microplate reader at 570 nm and 610 nm. The sigmoidal plot of the inhibition rate (%) versus the log concentration (µg/mL) was used to calculate the IC₅₀ values of the extracts.

Statistical Analysis

Antioxidant, cytotoxic, and enzyme inhibitory activity results were the average of three parallel sample measurements. The data were registered as the mean ± S.E.M.

RESULTS

Total Phenolic and Flavonoid Contents

Total phenolic and flavonoid contents of *A. repens* and *C. monogyna* methanol extracts were measured according to

Folin Ciocalteu and aluminum nitrate methods, respectively. Total phenolic contents of *A. repens* and *C. monogyna* methanol extracts were calculated as 24.57±0.22 and 68.13±0.34 µg GAEs/mg extract. Total flavonoid contents of *A. repens* and *C. monogyna* methanol extracts were recorded as 9.31±0.41 and 36.91±0.17 µg QEs/mg extract (Table 1).

Antioxidant Activity

Antioxidants have different mechanisms of action, so more than one method is need to be used to test antioxidant properties. Therefore, antioxidant activities of *A. repens* and *C. monogyna* methanol extracts were screened by using five different assays, namely, β-carotene-linoleic acid, metal chelating, CUPRAC, scavenging of ABTS cation radical and DPPH free radical assays and results are summarized in Table 2.

β-carotene-linoleic acid method is an important test system that demonstrates the ability of antioxidant compounds to inhibit linoleic acid oxidation. The degree of the bleaching caused

Table 1. Total phenolic and flavonoid contents of the extracts^a.

	Total phenolic content (µg GAEs/mg extract) ^b	Total flavonoid contents (µg QEs/mg extract) ^c
<i>A. repens</i> methanol	24.57±0.22	9.31±0.41
<i>C. monogyna</i> methanol	68.13±0.34	36.91±0.17

^a Values represent the means ± SEM of three parallel sample measurements (n=3) analyzed 3 times. T test was used to determine significant differences between means, *p* values <0.05 were regarded as significant.
^b Values expressed are means ± S.E.M. of three parallel measurements (*p*<0.05).
^b GAEs, gallic acid equivalents.
^c QEs, quercetin equivalents.

Table 2. Antioxidant activities of the extracts.

Extracts	Antioxidant Activity				
	β-carotene-linoleic acid assay	DPPH [•] assay	ABTS ^{•+} assay	CUPRAC assay	Metal chelating assay
	IC ₅₀ (µg/mL) ^a	IC ₅₀ (µg/mL) ^a	IC ₅₀ (µg/mL) ^a	A _{0.50} (µg/mL) ^b	Inhibition (%) ^c
<i>A. repens</i> methanol	77.62±0.09	>400	127.78±0.99	>400	13.09±0.99
<i>C. monogyna</i> methanol	32.72±0.15	71.69±0.85	40.43±0.55	282.69±0.25	NA ^e
α-Tocopherol ^d	2.10±0.08	37.18±0.41	38.51±0.54	66.72±0.81	NT ^f
BHA ^d	1.34±0.04	19.80±0.36	11.82±0.09	24.40±0.69	NT ^f
EDTA ^d	NT ^f	NT ^f	NT ^f	NT ^f	95.20±0.13

^a: IC₅₀ values represent the means ± SEM of three parallel measurements (n=3) analyzed 3 times. T test was used to determine significant differences between means, *p* values <0.05 were regarded as significant.

^b: A_{0.50} values represent the means ± SEM of three parallel measurements (*p*<0.05).

^c: Inhibition % of 400 µg/mL concentration of the extracts.

^d: Standards

^e: NA: Not active.

^f: NT: Not tested.

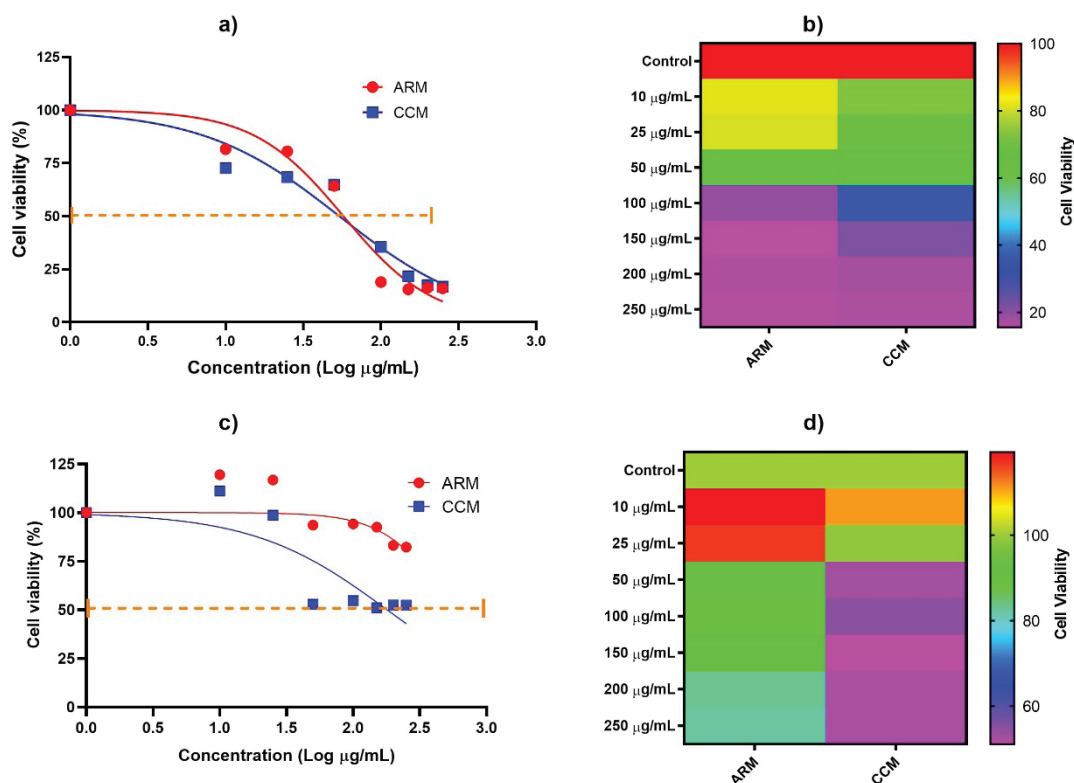


Figure 1. Cytotoxic effects of *A. repens* and *C. monogyna* methanol extracts on DLD-1 and CCD-18Co a) IC_{50} values on DLD-1 b) Heat Map analyses of dose-dependent inhibition against DLD-1 cells. Cell viability decreased from red to pink color c) IC_{50} values on CCD-18Co d) Heat Map analyses of dose-dependent inhibition against CCD-18Co. Cell viability decreased from green to pink color. ARM: *A. repens* methanol extract, CMM: *C. monogyna* methanol extract.

by lipid peroxyl radicals formed in the method in the color of β -carotene is inhibited by antioxidant compounds are tested. IC_{50} values of *A. repens* and *C. monogyna* methanol extracts were found as 77.62 ± 0.09 and 32.72 ± 0.15 $\mu\text{g/mL}$ in the β -carotene-linoleic acid assay.

ABTS⁺ and DPPH[•] radicals are the most widely used radicals in determining of radical scavenging activities. As it is seen in Table 2, the best scavenging activities on ABTS⁺ (IC_{50} : 40.43 ± 0.55 $\mu\text{g/mL}$) and DPPH[•] (IC_{50} : 71.69 ± 0.85 $\mu\text{g/mL}$) radicals were observed in *C. monogyna* methanol extract. Also, *C. monogyna* methanol extract indicated near-standard activity in ABTS⁺ assay.

The reducing power is an important indicator to evaluate antioxidant activity and the electron donation capabilities of the methanol extracts were determined by using the CUPRAC method. When compared to the standards, both methanol extracts showed low cupric reducing power.

Transition metals accumulate in the body at high rates, contributing to oxidative damage and thus causing various abnormalities. Therefore, metal chelating activity is of great importance in explaining of antioxidant activity. When *A. repens* methanol extract exhibited low metal chelating activity with an inhibition

Table 3. Cytotoxic activities of the extracts.

	DLD-1	CCD-18Co
Extracts	IC_{50} ($\mu\text{g/mL}$)	IC_{50} ($\mu\text{g/mL}$)
<i>A. repens</i> methanol	57.38	543.30
<i>C. monogyna</i> methanol	54.04	179.60

value of 13.09 ± 0.99 % at 400 $\mu\text{g/mL}$ concentration, *C. monogyna* methanol extract showed no activity.

Cytotoxic Activity

Cytotoxic activities of *A. repens* and *C. monogyna* methanol extracts were tested on DLD-1 (colorectal cancer) and CCD-18Co (human colon fibroblast cell line) according to Alamar Blue assay. Figure 1 represents the cytotoxic effects of the methanol extracts on DLD-1 and CCD-18Co. Table 3 shows the calculated IC_{50} values of the methanol extracts. As seen in Figure 1a and 1c, the methanol extracts inhibited the viability of DLD-1 and CCD-18Co dose-dependently. *A. repens* (IC_{50} : 57.38 $\mu\text{g/mL}$) and *C. monogyna* (IC_{50} : 54.04 $\mu\text{g/mL}$) methanol extracts showed similar cytotoxic activity on DLD-1.

Table 4. Enzyme inhibitory activities of the extracts^a.

Extracts	AChE		BChE		Tyrosinase		Urease		α-Amylase		α-Glucosidase	
	Inhibition (%) ^b	IC ₅₀ (µg/mL)	Inhibition (%) ^b	IC ₅₀ (µg/mL)	Inhibition (%) ^b	IC ₅₀ (µg/mL)	Inhibition (%) ^b	IC ₅₀ (µg/mL)	Inhibition (%) ^c	IC ₅₀ (µg/mL)	Inhibition (%) ^d	IC ₅₀ (µg/mL)
<i>A. repens</i> methanol	18.73±0.47	>200	37.59±1.07	>200	NA ^g	>200	89.18±0.84	24.85±0.08	33.39±0.92	>500	6.71±0.23	>500
<i>C. monogyna</i> methanol	10.92±0.66	>200	22.43±0.60	>200	30.52±1.00	>200	NA ^g	>200	37.24±0.06	>500	4.76±0.48	>500
<i>Galantamine</i> ^e	80.41±0.98	4.31±0.03	82.23±0.37	12.29±0.06	NT ^f	NT ^f						
<i>Kojic acid</i> ^e	NT ^f	NT ^f	NT ^f	NT ^f	83.6±0.20	144.91±0.19	NT ^f	NT ^f	NT ^f	NT ^f	NT ^f	NT ^f
<i>Thiourea</i> ^e	NT ^f	NT ^f	NT ^f	NT ^f	NT ^f	NT ^f	78.93±0.18	7.87±0.18	NT ^f	NT ^f	NT ^f	NT ^f
<i>Acarbose</i> ^e	NT ^f	NT ^f	NT ^f	NT ^f	NT ^f	NT ^f	NT ^f	NT ^f	94.01±0.09	21.63±0.01	31.95±0.62	378.66±0.14

^a Values represent the means ± SEM of three parallel sample measurements (n=3) analyzed 3 times. T test was used to determine significant differences between means. p values <0.05 were regarded as significant.
^b Inhibition % of 200 µg/mL concentration of the plant extracts. ^c Inhibition % of 500 µg/mL concentration of the plant extracts.
^d Inhibition % of 250 µg/mL concentration of the plant extracts. ^e Standards. ^f NT^f: not tested. ^g NA: not active. AChE: Acetylcholinesterase, BChE: Butyrylcholinesterase.

Enzyme Inhibitory Activity

Cholinesterase inhibitory activities of *A. repens* and *C. monogyna* methanol extracts were screened according to the Ellman method and the results are given in Table 4. *A. repens* displayed the best inhibitory activity against AChE (18.73±0.47 %) and BChE (37.59±1.07 %) at 200 µg/mL concentration.

Dopachrome method was used to test tyrosinase inhibitory activities of *A. repens* and *C. monogyna* methanol extracts. As it is given in Table 4, *C. monogyna* methanol extract showed low inhibitory activity against tyrosinase while *A. repens* methanol extract exhibited no activity.

Indophenol method was used for the measurement of urease inhibitory activity of *A. repens* and *C. monogyna* methanol extracts and results are summarized in Table 4. *A. repens* methanol extract (89.18±0.84 %) was found as better urease inhibitor by comparison with thiourea (78.93±0.18 %) at 200 µg/mL concentration.

Antidiabetic activities of *A. repens* and *C. monogyna* methanol extracts on α-amylase and α-glucosidase were determined. As it presented in Table 4, the highest α-amylase inhibitory activity was found in *C. monogyna* methanol extract (37.24±0.06 % at 500 µg/mL concentration) while the best α-glucosidase inhibitory activity was observed in *A. repens* methanol extract (6.71±0.23 % at 250 µg/mL concentration).

DISCUSSION

Medicinal plants, besides being used as taste, color, aroma and preservatives in foods for centuries, are excellent sources of natural antioxidants, and their bioactive compounds, especially phenolic substances, have the potential to reduce the risk of degenerative diseases such as diabetes, obesity, cardiovascular diseases and cancer (21). Antioxidant, cytotoxic, and enzyme inhibitory activities of *A. repens* and *C. monogyna* methanol extracts were investigated with total phenolic and flavonoid contents in this current study.

Phenolic compounds are one of the largest and most common secondary metabolite groups in the plant world with more than 8000 identified phenolic structures (22) Phenolic compounds can be found in all organs of plants and are involved in many functions, from skeletal components of different tissues to pigmentation (23). Phenolic compounds have diverse biological functions such as inhibition of lipid peroxidation, antioxidant and antimicrobial activities, inhibition of carcinogenesis, direct constrictive action on capillaries (24). Flavonoids are an essential group of naturally occurring phenolic compounds found in all vascular plants. It was well documented that flavonoids had antioxidant, cardioprotective, antidiabetic, anti-inflammatory, anti-allergic, antiviral, and anticancer effects (25). Plant phenolics and flavonoids have received greater attention since they have various biological properties. The highest amounts of total phenolic and flavonoid contents were found in *C. monogyna* methanol extract. Öztürk and Tunçel (26) reported the total phenolic contents of the methanol, ethyl acetate,

aqueous, and infusion extracts of *C. monogyna* in the range of 108.65 and 343.54 mg GAE/g extract. In a different study, total phenolic (361.39±3.78-398.48±0.98 mg GAE/g extract) and flavonoid (13.69±0.51-23.87±2.74 mg QE/g extract) contents of *C. orientalis*, *C. monogyna*, *C. pontica*, *C. turcicus*, *C. rhipidophylla* were investigated (12). Cosmulescu et al. found contents of 203.01±9.56 mg GAE/100 g FW phenolics and 147.98±7.29 mg QE/100 g FW flavonoids in the methanol extract of *C. monogyna* (27). Total phenolic content of *A. repens* methanol extract was calculated as 743 GAE mg/100 g extract by Dogan et al. (28).

Oxidative stress plays an important role in the development and initiation of many diseases, comprising autoimmune diseases, inflammation, Parkinson's and neurodegenerative diseases, aging, cataracts, arteriosclerosis, and cancer (29). Studies have proven that oxidative damage is effective in the development of age-related and chronic diseases, and dietary antioxidant supplementation counteracts it and reduces the risk of disease (30). Antioxidants are substances that delay or prevent oxidation of an oxidizable substrate at low concentrations (31). In this study, antioxidant activities of *A. repens* and *C. monogyna* methanol extracts were screened by using five different assays and *C. monogyna* methanol extract was recorded to have the highest antioxidant activity in all activity assays excluding metal chelating assay. The highest antioxidant activity could be connected with the highest level of total phenolic and flavonoid contents. Many previous studies have proved that there is a positive relationship between the levels of total phenolic and flavonoid contents and antioxidant activity (12,18). There are studies on the antioxidant properties of *A. repens* and *C. monogyna* species in the literature. Scavenging activity of DPPH was found as 0.32±0.01 mmol Trolox/100 g FW in *C. monogyna* methanol extract (27). Antioxidant activity of the water, 80% ethanol: water and ethanol extracts of *C. monogyna* were studied by Nunes et al. (32). When 80 % ethanol: water extract exhibited the highest activity in total antioxidant activity (243.31±9.61 AAE/g dw), reducing power (177.86±7.54 mg TE/g dw), ferric reducing antioxidant power (225.52±10.91 mg TE/g dw) assays, the water extract (61.56±4.00 µg sample/mL) in DPPH radical scavenging assay. Rocchetti et al. reported the decoction, infusion, and methanolic extracts of leaves and twig of *C. tanacetifolia*, *C. szovitsii*, *C. orientalis* by using phosphomolybdenum (1.18±0.06-3.45±0.09 mmol TE/g), ABTS (81.35±5.28-515.54±6.29 mg TE/g), DPPH (74.20±1.26-393.69±0.48 mg TE/g), CUPRAC (200.51±2.71-708.09±13.35 mg TE/g), FRAP (97.84±1.10-399.02±2.03 mg TE/g) and metal chelating (11.90±1.68-48.95±1.01 mg EDTAE/g) assays (33). In a different report, antioxidant properties of 50% ethanol, 70% methanol, and water extracts of *C. monogyna* were tested according to DPPH and FRAP assays. 50% ethanol extract was found to have the highest activity in DPPH and FRAP assays with the value of 1955.9±2.8 and 1989.8±1.1 mM Trolox/g, respectively (34). In the research of Ferysiuk et al., water, aqueous ethanol (50:50) and ethanol extracts of *A. repens* scavenged 1.77±0.41, 2.92±0.18, 4.42±0.3 % of DPPH[•] and 1.23±0.17, 4.85±0.22, 3.6±0.15 % of ABTS^{•+}, respectively (5).

Colorectal cancer ranks 3rd after lung and breast cancer deaths in women, and lung and prostate cancer deaths in men. Considering the etiology of colorectal cancer, it is basically the genetic change process of the epithelial cells in the colon mucosa. The factors that trigger colon cancer include susceptibility to mutagenic effects, red meat consumption, bile acids, and insufficient intake of vitamins and minerals (35). Although the main treatment is surgery, recurrences occur in most of the patients within the first 3 years after surgery with only surgical treatment (36). Many different treatment modalities are used in cancer treatment to reduce mortality and increase survival. These can be listed as surgery, radiotherapy, chemotherapy, hormone therapy and new treatment methods, immunotherapy, signal transduction system inhibitors, gene therapy, and angiogenesis inhibitors. Chemotherapy is a form of treatment aimed mainly at killing cancer cells. However, the effectiveness of current chemotherapy agents in different cancer types is limited (37,38). For cancer treatment, many drugs, and new treatment methods have been developed in recent years, and studies to obtain new, natural and side effects free drugs from plants have gained importance. *A. repens* and *C. monogyna* methanol extracts showed close cytotoxic activity on DLD-1. There are only two reports on the literature related with cytotoxic activity of *Crataegus* species. The % inhibition values of HCT116 (colorectal cancer) by *Crataegus* L. polysaccharide extract were reported as in a range from 20% to 80% between 125 and 1000 µg/mL concentrations (39). Ganie et al. revealed that *C. songarica* methanol, ethanol and ethyl acetate extracts inhibited ~ 80%, 85%, 75% of SW480 (colorectal cancer) at 80 µg/mL concentration (40).

In Alzheimer's disease (AD), the acetylcholine level decreases with the loss of neurons and axons. For this reason, increasing the acetylcholine level is important in the therapy of AD. Acetylcholine level can be increased by suppressing cholinesterase enzymes that break down acetylcholine. AChE and BChE are enzymes that are encoded by different genes but differ from each other, especially due to their substrate selectivity and differences in some catalytic mechanisms. Studies have reported that increases in acetylcholine levels due to cholinesterase inhibition may improve unconsciousness in the early stages of AD (41,42). Tyrosinase is an important enzyme in hyperpigmentation problems such as skin spots caused by excessive melanin synthesis in the body and such as psoriasis and vitiligo caused by insufficient melanin synthesis. Agents that inhibit this enzyme can be used in the treatment of hyperpigmentation problems (43,44). Urease is an enzyme catalyse the hydrolysis of urea to ammonia and bicarbonate. Inhibition of urease is especially important in the treatment of urinary and gastrointestinal tract infections. Urease inhibitors are very important for *Helicobacter pylori*, an anaerobic bacterium that has recently caused stomach reflux, ulcers and gastritis. In fact, urease activity has an essential role in buffering the acidic pH in the stomach, in food intake, and in enhancing the ability of *H. pylori* to colonize the gastric epithelium. Urease inhibition is very important for the treatment of diseases associated with *H. pylori* (45,46). Diabetes mellitus, characterized by insulin

deficiency or ineffectiveness, is a lifelong metabolic disease. In type 2 diabetes, the level of sugar in the blood increases due to both insufficient insulin secretion and decreased insulin sensitivity (47). One of the treatment methods to reduce blood sugar is to delay the passage of glucose into the blood by inhibiting the activity of carbohydrate digestive enzymes such as α -glucosidase and α -amylase in the digestive system, or to allow them to pass into the blood regularly (48). According to obtained results, *A. repens* methanol extract displayed the highest effect against AChE, BChE, urease, α -glucosidase enzymes whereas *C. monogyna* methanol extract showed the highest effect against tyrosinase and α -amylase enzymes. Previously, tyrosinase inhibition values of *C. monogyna* and *C. oxyacantha* were reported as ~40% and ~50%, respectively (49). α -Amylase (IC_{50} : 10.71 \pm 0.11 mg/mL), α -glucosidase (IC_{50} : 10.72 \pm 0.43 mg/mL), AChE (IC_{50} : 69.59 \pm 1.12 mg/mL) and BChE (IC_{50} : 132.70 \pm 2.12 mg/mL) inhibitory activities of *Crataegus* L. methanol:water extract were investigated by Nowicka and Wojdylo (50). The decoction, infusion and methanolic extracts of twig and leaves of *C. tanacetifolia*, *C. szovitsii*, *C. orientalis* were tested for their inhibitory activities against AChE (3.62 \pm 0.25-4.33 \pm 0.05 mg GALAE/g), BChE (1.43 \pm 0.05-5.21 \pm 0.07 mg GALAE/g), tyrosinase (9.80 \pm 2.39-128.78 \pm 0.94 mg KAE/g), α -amylase (0.11 \pm 0.01-0.66 \pm 0.02 mmol ACAE/g) and α -glucosidase (3.01 \pm 0.11-33.57 \pm 0.02 mmol ACAE/g) (27). This study can be assumed as the first investigation on AChE, BChE, α -amylase, α -glucosidase, and urease inhibitory activities of *A. repens* and *C. monogyna* methanol extracts.

CONCLUSION

Antioxidant, cytotoxic, and enzyme inhibitory activities of *A. repens* and *C. monogyna* methanol extracts were investigated with total phenolic and flavonoid contents in this current study. It was determined that *C. monogyna* methanol extract with the highest total phenolic and flavonoid contents had the best antioxidant activity in all studied assays except metal chelating assay. When the extracts showed moderate enzyme inhibitory activities, *A. repens* methanol extract showed superior inhibitory activity against urease enzyme. Also, *A. repens* and *C. monogyna* methanol extracts showed close cytotoxic activity on DLD-1. This study can be considered as the first investigation on cytotoxic and enzyme inhibitory activities of *A. repens* and *C. monogyna* species. It is thought that this study will further contribute to the biological values of these plants, which are used for different purposes in folk medicines.

Peer-review: Externally peer-reviewed.

Authors Contributions: Concept: E.D., G.T.C.; Design: E.D., G.T.C., S.K.; Supervision: E.D. G.T.C.; Materials: E.D., G.T.C., M.E.D., S.K.; Data Collection and/or Processing: E.D., G.T.C., S.K.; Analysis and/or Interpretation: E.D., G.T.C., S.K., M.E.D.; Literature Search: E.D., G.T.C.; Writing: E.D., G.T.C.; Critical Reviews: E.D., G.T.C., S.K., M.E.D.

Conflict of Interest: The authors declare that they have no conflicts of interest to disclose.

Financial Disclosure: There are no funders to report for this submission.

Acknowledgements: Authors would like to thank Dr. Ergün Kaya (Faculty of Science, Department of Molecular Biology and Genetics, Muğla Sıtkı Koçman University) for the identification of the plant samples.

REFERENCES

1. Dar RA, Shah Nawaz M, Qazi PH. General overview of medicinal plants: A review. *J Phytopharmacol* 2017; 6: 349-51.
2. Top R, Erden Y, Tekin S. The investigation of antioxidant and anticancer effects of some importance medical plants. *BEU J Sci* 2019; 8(2): 435-42.
3. Ginwala R, Bhavsar R, Chigbu DI, Jain P, Khan ZK. Potential role of flavonoids in treating chronic inflammatory diseases with a special focus on the anti-inflammatory activity of apigenin. *Antioxidants* 2019; 8(2): e35.
4. Rawat D, Shrivastava S, Naik RA, Chhonker SK, Mehrotra A, Koiri RK. An overview of natural plant products in the treatment of hepatocellular carcinoma. *Anticancer Agents Med Chem* 2018; 18(3): 1838-59.
5. Ferysiuk K, Wójciak KM. The spectrophotometric analysis of antioxidant properties of selected herbs in vision-pro™ uv-vis. *Appl Comput Sci* 2019; 15: 49-62.
6. Leporatti ML, Ivancheva S. Preliminary comparative analysis of medicinal plants used in the traditional medicine of Bulgaria and Italy. *J Ethnopharmacol* 2003; 87:123-42.
7. Mustafa B, Hajdari A, Krasniqi F, Hoxha E, Ademi H, Quave CL, et al. Medical ethnobotany of the Albanian Alps in Kosovo. *J Ethnobiol Ethnomed* 2012; 8:6.
8. Sargın SA, Akçicek E, Selvi S. An ethnobotanical study of medicinal plants used by the local people of Alaşehir (Manisa) in Turkey. *J Ethnopharmacol* 2013; 150:860-74.
9. Grases F, Ramis M, Costa-Bauza A, March JG. Effect of *Herniaria hirsuta* and *Agropyron repens* on calcium oxalate urolithiasis risk in rats. *J Ethnopharmacol* 1995; 45: 211-4.
10. Mascolo N, Autore G, Capasso F, Menghini A, Fasulo MP. Biological screening of Italian medicinal plants for anti-inflammatory activity. *Phytother Res* 1987; 1: 28-31.
11. Rafsanjany N, Lechtenberg M, Peterreit F, Hensel A. Antiadhesion as a functional concept for protection against uropathogenic *Escherichia coli*: *In vitro* studies with traditionally used plants with antiadhesive activity against uropathogenic *Escherichia coli*. *J Ethnopharmacol* 2013; 145: 591-7.
12. Bardakci H, Celep E, Gözet T, Kan Y, Kırmızıbekmez H. Phytochemical characterization and antioxidant activities of the fruit extracts of several *Crataegus* taxa. *S Afr J Bot* 2019; 124: 5-13.
13. Edwards JE, Brown PN, Talent N, Dickinson TA, Shipley PR. A review of the chemistry of the genus *Crataegus*. *Phytochemistry* 2012; 79: 5-26.
14. Venskutonis PR. Phytochemical composition and bioactivities of hawthorn (*Crataegus* spp.): a review of recent research advances. *J Food Bioact* 2018; 4: 69-87.
15. Slinkard K, Singleton VL. Total phenol analyses: Automation and comparison with manual methods. *Am J Enol Vitic* 1977; 28: 49-55.
16. Park YK, Koo MH, Ikegaki M, Contado JL. Comparison of the flavonoid aglycone contents of *Apis mellifera* propolis from various regions of Brazil. *Braz Arch Biol Technol* 1997; 40: 97-106.
17. Çayan F, Tel-Çayan G, Deveci E, Öztürk M, Duru ME. Chemical profile, *in vitro* enzyme inhibitory, and antioxidant properties of *Stereum* species (Agaricomycetes) from Turkey. *Int J Med Mushrooms* 2019; 21(11): 1075-87.

18. Deveci E, Tel-Çayan G, Duru ME, Öztürk M. Phytochemical contents, antioxidant effects, and inhibitory activities of key enzymes associated with Alzheimer's disease, ulcer, and skin disorders of *Sideritis albiflora* and *Sideritis leptoclada*. *J Food Biochem* 2019; 43: e13078.
19. Deveci E, Tel Cayan G, Duru ME. *In vitro* antidiabetic activity of seven medicinal plants naturally growing in Turkey. *Eur J Biol* 2020; 79: 23-8.
20. Karakurt S, Adali O. Tannic acid inhibits proliferation, migration, invasion of prostate cancer and modulates drug metabolizing and antioxidant enzymes. *Anticancer Agents Med Chem* 2016; 16(6): 781-9.
21. Patch CS, Sullivan DR, Fenech M. Health benefits of herbs and spices: Cardiovascular disease. *Med J Aust* 2006; 185(4): 7-9.
22. Tsao R. Chemistry and biochemistry of dietary polyphenols. *Nutrients* 2010; 2(12): 1231-46.
23. Ignat I, Volf I, Popa VI. A critical review of methods for characterization of polyphenolic compounds in fruits and vegetables. *Food Chem* 2011; 126: 1821-35.
24. Tanase C, Cosarca S, Muntean DL. A critical review of phenolic compounds extracted from the bark of woody vascular plants and their potential biological activity. *Molecules* 2019; 24(6): 1182.
25. Karak P. Biological activities of flavonoids: an overview. *Int J Pharm Sci Res* 2019; 10(4): 1567-74.
26. Öztürk N, Tunçel M. Assessment of phenolic acid content and *in vitro* antiradical characteristics of hawthorn. *J Med Food* 2011; 14(6): 664-9.
27. Cosmulescu S, Trandafir I, Nour V. Phenolic acids and flavonoids profiles of extracts from edible wild fruits and their antioxidant properties. *Int J Food Prop* 2017; 20(12): 3124-34.
28. Dogan S, Diken ME, Dogan M. Antioxidant, phenolic and protein contents of some medicinal plants. *J Med Plants Res* 2010; 4(23): 2566-73.
29. Lukyanova LD, Storozheva ZI, Proshin AT. Corrective effect of flavonoid containing preparation extralife on the development of Parkinson's syndrome. *Bull Exp Biol Med* 2007; 144: 42-5.
30. Ghasemzadeh A, Ghasemzadeh N. Flavonoids and phenolic acids: Role and biochemical activity in plants and human. *J Med Plants Res* 2011; 5(31): 6697-703.
31. Lucio M, Nunes C, Gaspar D, Ferreira H, Lima JLFC, Reis S. Antioxidant activity of vitamin E and Trolox: understanding of the factors that govern lipid peroxidation studies *in vitro*. *Food Biophys* 2009; 4: 312-20.
32. Nunes R, Pasko P, Tyszka-Czochara M, Szewczyk A, Szlosarczyk M, Carvalho IS. Antibacterial, antioxidant and anti-proliferative properties and zinc content of five south Portugal herbs. *Pharm Biol* 2016; 55(1): 114-23.
33. Rocchetti G, Senizza B, Zengin G, Mahomodally MF, Senkardes I, Lobine D, et al. Untargeted metabolomic profiling of three *Crataegus* species (hawthorn) and their *in vitro* biological activities. *J Sci Food Agric* 2020; 100(5): 1998-2006.
34. Parzhanova AB, Petkova N, Ivanov IG, Ivanova SD. Evaluation of biologically active substance and antioxidant potential of medicinal plants extracts for food and cosmetic purposes. *J Pharm Sci Res* 2018; 10(7): 1804-9.
35. Rostami S. M.Sc Thesis. Investigation of antiproliferative and anti-inflammatory effects of common and endemic species of plants. Department of Biology, Institute of Science, Gazi University, Ankara, Turkey, 2013.
36. Doğan M, Akbulut H. Adjuvant Treatment of Colorectal Cancer. *Türkiye Klinikleri J Med Oncol* 2009; 2(3): 49-57.
37. Dellabona P, Moro M, Crosti MC, Casorati G, Corti A. Vascular attack and immunotherapy: a 'two hits' approach to improve biological treatment of cancer. *Gene Ther* 1999; 6: 153-4.
38. Terrero MN, Li S. Growth factor receptors: targets for gene therapy and immunotherapy for cancer treatment. *Gene Ther Mol Biol* 2004; 8: 175-80.
39. Ma L, Xu GB, Tang X, Zhang C, Zhao W, Wang J, et al. Anti-cancer potential of polysaccharide extracted from hawthorn (*Crataegus*.) on human colon cancer cell line HCT116 via cell cycle arrest and apoptosis. *J Funct Foods* 2020; 64: 103677.
40. Ganie SA, Dar TA, Zargar S, Bhat AH, Dar KB, Masood A, et al. *Crataegus songarica* methanolic extract accelerates enzymatic status in kidney and heart tissue damage in albino rats and its *in vitro* cytotoxic activity. *Pharm Biol* 2015; 54: 1246-54.
41. Howes MJR, Houghton PJ, Perry NSL. Plants with traditional uses and activities, relevant to the management of Alzheimer's disease and other cognitive disorders. *Phytother Res* 2003; 17(1): 1-18.
42. Alkan HÖ, Zengin G, Kaşık G. Antioxidant and *in vitro* some enzyme inhibitory activities of methanolic extract of cultivated *Lentinula edodes*. *J Fungus* 2017; 8(2): 90-8.
43. Chang TM. Tyrosinase and tyrosinase inhibitors. *J Biocatal Bio-transformation* 2012; 1: 2.
44. Gholamhoseinian A, ZohreRazmi Z. Screening the methanolic extracts of some plants for tyrosinase inhibitory activity. *Toxicol Environ Chem* 2012; 94: 310-8.
45. Baltas N, Karaoglu S, Tarakci C, Kolayli S. Effect of propolis in gastric disorders: inhibition studies on the growth of *Helicobacter pylori* and production of its urease. *J Enzyme Inhib Med Chem* 2016; 31(52): 46-50.
46. Baltas N, Yildiz O, Kolayli S. Inhibition properties of propolis extracts to some clinically important enzymes. *J Enzyme Inhib Med Chem* 2016; 31: 52-5.
47. Taslimi P, Gulçin İ. Antidiabetic potential: *in vitro* inhibition effects of some natural phenolic compounds on α -glycosidase and α -amylase enzymes. *J Biochem Mol Toxicol* 2017; 31(10): e21956.
48. Kumar S, Kumar V, Rana M, Kumar D. Enzymes inhibitors from plants: An alternate approach to treat diabetes. *Phcog Commn* 2012; 2(2): 18-33.
49. Natić M, Pavlović A, Bosco FL, Stanisavljević N, Zagorac DD, Akšić MF, et al. Nutraceutical properties and phytochemical characterization of wild Serbian fruits. *Eur Food Res Technol* 2019; 245: 469-78.
50. Nowicka P, Wojdyło A. Anti-hyperglycemic and anticholinergic effects of natural antioxidant contents in edible flowers. *Antioxidants* 2019; 8: 308.

Diversity and New Records of Polychaetes (Annelida) in the Sinop Peninsula, Turkey (Southern Black Sea)

Mulkibar Ciftcioglu¹ , Guley Kurt² , Sevgi Kus³ 

¹Muğla Sıtkı Koçman University, Institute of Natural and Applied Sciences, Muğla, Turkey

²Sinop University, Faculty of Arts and Sciences, Department of Biology, Sinop, Turkey

³Sinop University, Institute of Natural and Applied Sciences, Sinop, Turkey

ORCID IDs of the authors: M.C. 0000-0001-7521-8969; G.K. 0000-0002-9996-4365; S.K. 0000-0002-3336-3444

Please cite this article as: Ciftcioglu M, Kurt G, Kus S. Diversity and New Records of Polychaetes (Annelida) in the Sinop Peninsula, Turkey (Southern Black Sea). Eur J Biol 2020; 79(2): 106-114. DOI: 10.26650/EurJBiol.2020.0024

ABSTRACT

Objective: This study determines the diversity of annelid polychaete species distributed around the coast of Sinop and to identify possible spatial and temporal variations of the Polychaeta community.

Materials and Methods: Benthic material was collected from 8 stations using Van Veen grab between October 2013 and July 2014 on the soft bottom of Sinop Peninsula.

Results: A total of 90 species belonging to 30 families were identified. Among them, *Galathowenia cf. oculata*, *Rhodine loveni* Malmgren, 1865, *Paradoneis armata* Glémarec, 1966, *Paralacydonia paradoxa* Fauvel, 1913 and *Syllis cf. amica* are new records for the Black Sea fauna and *Glycera tridactyla* Schmarda, 1861 is new for the Turkish coast of the Black Sea. *Prionospio (Minuspio) maciolekae* Dagli and Çinar, 2011, *Micronephthys longicornis* (Perejaslvtseva, 1891) and *Protodorvillea kefersteini* (McIntosh, 1869) were the most frequent and dominant species in the study area. The highest mean number of species (29 species) was found in spring at station G2; the lowest mean number of species (4 species) was determined at station G3 in winter. The highest mean density value (9470 ind. m⁻²) was determined at G2 station in summer; the lowest mean density value (357 ind. m⁻²) was calculated in autumn at station G5.

Conclusion: The Polychaeta diversity on the soft bottom of the Sinop Peninsula was analyzed and four species were newly recorded for the Black Sea fauna and one for the Turkish Black Sea fauna.

Keywords: Polychaeta, benthos, community, diversity, density

INTRODUCTION

Annelid polychaetes are the most diverse benthic invertebrates and they densely occur on the sea-floor. Although most of the polychaetes live in a marine environment, fresh and brackish water forms are also known. Up to date, more than 12,000 species of Polychaeta have been reported in the world oceans (1); from them, more than 1,100 species have been reported in the Mediterranean Sea (2). Nowadays, a total of 711 species have been reported on the coast of Turkey with 459 species in the Levantine Sea, 559 species in the Aegean Sea, 398 species in the Sea of Marmara, and 187 in the Black Sea (3-7).

Sinop Peninsula is located on the Black Sea with a salinity of about 18‰. The Black Sea is one of the largest semi-closed seas in the world with an area of approximately 4.2x10⁵ km², an average depth of 2,212 m, and a water volume of 534,000 km³ (8). Due to the high rate of hydrogen sulphide (H₂S), most of the Black Sea basin (~ 87%) shows anoxic properties (8, 9). Anoxic conditions affect the vertical distribution of organisms at depths below 70-200 meters. The hydrographic regime is characterized by high salinity in the deep waters of the Mediterranean origin, which is covered by the low salinity surface waters of the river.



Corresponding Author: Guley Kurt

E-mail: gkurt@sinop.edu.tr

Submitted: 29.06.2020 • **Revision Requested:** 18.08.2020 • **Last Revision Received:** 05.10.2020 •

Accepted: 07.10.2020 • **Published Online:** 13.12.2020

© Copyright 2020 by The Istanbul University Faculty of Science • Available online at <http://ejb.istanbul.edu.tr> • DOI: 10.26650/EurJBiol.2020.0024

The structure of the Black Sea ecosystem differs from the Mediterranean because of less diversity and dominant groups of species. However, productivity, total biomass and abundance values of the Black Sea are higher than those of the Mediterranean Sea (5, 9).

There are only a few investigations on polychaete diversity from the Black Sea (10-16). All the studies that addressed the Turkish Black Sea have focused on the pyrophosphoric region, (17-24) and some others on the Anatolian coasts (5-7, 25-28).

Hence, the aims of this study are to assess diversity of polychaetes in the soft bottoms of the Sinop Peninsula and to determine temporal and spatial variations in the community of polychaetes.

MATERIALS AND METHODS

Samplings were conducted between October 2013 and July 2014 to identify diversity and seasonal changes of polychaete species along the coast of Sinop. Benthic samples were collected seasonally from soft substratum using a Van Veen grab at 8 stations, each with 3 replicates (Figure 1; Table 1). The material was sieved on board by using a 0.5 mm mesh sieve, and seawater for dilution. The organisms were fixed with 4% formaldehyde and placed in containing plastic bags. In the laboratory, the fixed material was washed off with tap water using a 0.5 mm mesh and sorted into major taxonomic groups using a light and stereomicroscope and each sample was preserved into tubes containing 70% ethanol. Polychaetes were determined at species level, although those undetermined were kept at genus level, and the numbers of individuals were counted. The material was deposited in the Hydrobiology Laboratory of the Biology Department of Sinop University, Turkey.

The following biotic indices were used to assess the structure of polychaete communities in the research area: Dominance Index of Bellan-Santini (29), Shannon-Wiener's diversity index (H'), Pielou's evenness index (J') and, Soyer's frequency index (30). All were performed by using PRIMER 5 and STATISTICA 7.0.



Figure 1. Sampling stations at Sinop Peninsula, Turkey (Black Sea).

The identified species were also classified according to the ecological groups mentioned by Çinar et al. (31). The first ecological group includes sensitive and insensitive species (GI and GII), the second ecological group includes tolerant species (GIII), and the third ecological group includes first and second order opportunistic species (GIV and GV) (31).

Table 1. Coordinates, depth, and sediment type of sampling stations at Sinop Peninsula.

Station	Coordinates	Depth (m)	Sediment type
G1	42° 02 ' 030 " N 35° 15 ' 060 " E	14	Mud and shell fragments
G2	42° 01 ' 329 " N 35° 18 ' 371 " E	15	Mud and shell fragments
G3	42° 02 ' 166 " N 35° 21 ' 077 " E	20	Fine sand
G4	42° 03 ' 804 " N 35° 19 ' 353 " E	21	Fine sand
G5	42° 09 ' 936 " N 34° 94 ' 968 " E	14	Silt
G6	42° 08 ' 497 " N 35° 02 ' 176 " E	20	Fine sand, mud and shell fragments
G7	42° 06 ' 300 " N 35° 04 ' 548 " E	20	Sand, Fine sand and Mud
G8	42° 03 ' 121 " N 35° 15 ' 344 " E	14	Sand

RESULTS

A total of 90 species belonging to 30 families and 63 genera were determined in the study area (Table 2). *Galathowenia cf. oculata*, *Rhodine loveni* Malmgren 1865, *Paradoneis armata* Glémarec, 1966, *Paralacydonia paradoxa* Fauvel, 1913 and *Syllis cf. amica* were new records for the Black Sea fauna and *Glycera tridactyla* Schmarada, 1861 was a new record for the Turkish coast of the Black Sea.

According to frequency index values, 40 species were distributed as constant ($50 < F \leq 100$), 15 as common ($25 < F \leq 50$), and 35 species as rare ($0 < F \leq 25$) (Table 2). Among them, *Micronephthys longicornis*, *Prionospio maciolekae*, *Spio decoratus*, *Heteromastus filiformis* and *Melinna palmata* were found at all stations (100%). Syllidae (13 species) was the most diverse family in the area, followed by Spionidae (8 species), Paraonidae (8 species) and Nereididae (7 species). According to the number of individuals, the most dominant families were identified as Spionidae, Nephtyidae and Dorvilleidae, and these families were found during all sampling periods. The most dominant species were *P. maciolekae*, *M. longicornis*, *P. kefersteini*, *H. filiformis* and *S. decoratus*.

Table 2. List of species collected during the study and their maximum densities (ind. m⁻²) per station (A: autumn, W: winter, Sp: spring, S: summer, F: Frequency values (%)).

Species	G1	G2	G3	G4	G5	G6	G7	G8	F
Ampharetidae									
<i>Melinna palmata</i> Grube, 1870	80/Sp	100/S	290/Sp	510/Sp	440/S	330/W	1120/W	300/S	100
Capitellidae									
<i>Capitella cf. capitata</i>	60/W	-	10/Sp	10/S	20/S	30/Sp	140/Sp	20/Sp-S	87.5
<i>Capitomastus minima</i> (Langerhans, 1881)	-	-	150/Sp	-	-	120/Sp	10/W-S	250/W	50
<i>Heteromastus filiformis</i> (Claparède, 1864)	950/Sp	730/Sp	10/A-Sp	390/W	50/Sp	870/W	340/W	50/Sp	100
<i>Mediomastus sp.</i>	-	-	10/Sp	-	-	-	60/S	-	25
<i>Notomastus latericeus</i> Sars, 1851	690/Sp	570/S	10/Sp	190/W	60/Sp	110/W	80/Sp-W	-	87.5
<i>Notomastus sp.</i>	130/A	20/S	-	10/A	-	-	10/S	-	50
Cirratulidae									
<i>Chaetozone sp.</i>	10/Sp	-	-	10/A	-	-	-	-	25
<i>Cirriformia tentaculata</i> (Montagu, 1808)	-	-	-	10/A	-	-	-	-	12.5
Dorvilleidae									
<i>Dorvillea rubrovittata</i> (Grube, 1855)	10/Sp	130/W	-	-	-	-	-	-	25
<i>Protodorvillea kefersteini</i> (McIntosh, 1869)	570/Sp	940/Sp	540/Sp	1810/A	-	4150/A	2310/Sp	-	75
<i>Schistomeringos rudolphi</i> (Delle Chiaje, 1828)	500/A	310/Sp	10/S	50/W	-	150/A	10/A	-	
Eunicidae									
<i>Eunice vittata</i> (delle Chiaje, 1828)	90/W	70/S	-	20/A	-	-	-	-	37.5
<i>Lysidice ninetta</i> Audouin-Milne Edwards, 1833	-	10/Sp-W	-	-	-	-	-	-	12.5
Glyceridae									
<i>Glycera alba</i> Grube, 1840	-	-	-	30/A	40/A	10/A	20/A	-	50
<i>Glycera tessellata</i> Grube, 1863	-	-	-	40/W	50/W	-	-	-	25
** <i>Glycera tridactyla</i> Schmarda, 1861	10/Sp	10/Sp-W	-	10/S	50/Sp	30/Sp	10/Sp-S	10/W	87.5
<i>Glycera sp.</i>	-	20/S	-	10/A	80/S	10/Sp	10/W-S	10/W-S	75
Hesionidae									
<i>Microphthalmus sp.</i>	20/Sp	-	60/Sp	100/A	-	90/W	90/Sp-S	10/Sp	75
Lacydoniidae									
* <i>Paralacydonia paradoxa</i> Fauvel, 1913	-	10/S	-	-	-	-	10/Sp	-	25
Lumbrineridae									
<i>Lumbrineris sp.</i>	-	10/S	-	-	-	-	-	-	12.5

Tablo 2 (Continued)									
Magelonidae									
<i>Magelona mirabilis</i> (Johnston, 1865)	-	10/Sp-W	30/Sp-W	170/S	310/Sp-W	20/Sp-W-S	100/Sp-W	90/Sp-W	87.5
Maldanidae									
<i>Leiochone leiopygos</i> (Grube, 1860)	10/Sp-W	-	10/Sp	100/Sp	110/Sp	120/W	60/Sp	10/Sp-S	87.5
* <i>Rhodine loveni</i> Malmgren, 1865	-	40/Sp	-	70/A	30/S	-	70/S	-	50
Nephtyidae									
<i>Micronephthys longicornis</i> (Perejaslvtseva, 1891)	4290/W	2570 /Sp	260/Sp	3830/W	310/Sp	1470/W	1430/A	530/W	100
<i>Nephtys hombergii</i> Savigny in Lamarck, 1818	-	-	-	10/A	20/Sp	10/W	10/A-S	20/W	62.5
<i>Nephtys</i> sp.	-	-	20/W	40/W	200/W	90/W	20/W	130/Sp	75
Nereididae									
<i>Ceratonereis</i> sp.	-	50/S	-	-	-	-	-	-	12.5
<i>Eunereis longissima</i> (Johnston, 1840)	20/W	10/Sp	-	-	-	-	-	-	25
<i>Nereis</i> cf. <i>zonata</i>	20/A-Sp-S	110/S	-	10/S	-	10/Sp	-	-	50
<i>Perinereis cultrifera</i> (Grube, 1840)	170/W	180/A	-	70/W	-	30/W	10/Sp-W	-	62.5
<i>Platynereis dumerilii</i> (Audouin-Milne Edwards, 1833)	90/A	80/W	-	30/A	-	10/A	40/A	-	62.5
<i>Websterinereis glauca</i> (Claparède, 1870)	-	10/A	-	-	-	-	-	-	12.5
<i>Nereididae</i> (sp.)	60/W	120/S	210/S	10/A-S	-	-	10/A-W	-	62.5
Opheliidae									
<i>Polyopthalmus pictus</i> (Dujardin, 1839)	-	-	-	-	-	10/A	10/W-Sp	-	25
Orbiniidae									
<i>Phylo foetida</i> (Claparède, 1868)	-	-	-	10/A-W-S	50/Sp	-	-	-	25
Oweniidae									
* <i>Galathowenia</i> cf. <i>oculata</i>		540/Sp	10/S	-	-	10/A	40/W	-	50
Paraonidae									
<i>Aricidea (Acmira) catherinae</i> Laubier, 1967	50/A	20/A-S	-	450/A	20/Sp	200/A	80/Sp	70/Sp	87.5
<i>Aricidea (Strelzovia) claudiae</i> Laubier, 1967	650/S	80/W	20/Sp	50/S	-	10/Sp	-	10/Sp	75
<i>Aricidea (Aricidea) pseudoarticulata</i> Hobson, 1972	-	-	-	-	10/A	-	20/A	-	25
<i>Aricidea (Acmira) simonae</i> Laubier & Ramos, 1974	-	-	-	10/W	-	-	-	10/Sp	25

Tablo 2 (Continued)									
<i>Aricidea</i> sp.	10/W	-	-	-	-	-	10/S	-	25
<i>*Paradoneis armata</i> Glémarec, 1966	-	-	-	-	80/Sp	10/Sp	-	-	25
<i>Paradoneis lyra</i> (Southern, 1914)	-	-	-	-	50/A	-	-	-	12.5
<i>Paradoneis</i> sp.	-	-	-	-	10/S	-	-	-	12.5
Pectinariidae									
<i>Lagis koreni</i> Malmgren, 1866	70/Sp	80/Sp	-	20/W	-	20/A	10/A-W	-	62.5
Pholoidae									
<i>Pholoe inornata</i> Johnston, 1839	170/Sp-W	320/A	30/Sp	450/A	-	150/Sp	530/A	-	75
Phyllodocidae									
<i>Eumida</i> cf. <i>sanguinea</i>	70/W	160/W	10/Sp	20/A-W	-	40/A	20/A-Sp	20/W	87.5
<i>Mysta picta</i> (Quatrefages, 1866)	20/Sp	30/Sp-W	10/S	20/W	-	60/W	40/Sp	10/Sp	87.5
<i>Nereiphylla rubiginosa</i> (Saint-Joseph, 1888)	10/Sp	30/Sp	-	20/A-W	-	50/Sp	10/W	-	62.5
<i>Phyllodoce (Anaitides) rosea</i> (McIntosh, 1877)	-	20/Sp	-	-	10/S	-	10/W	-	37.5
<i>Phyllodoce</i> sp.	-	-	-	10/Sp	-	10/Sp-S	10/A	-	37.5
<i>Pterocirrus macroceros</i> (Grube, 1860)	-	20/Sp-S	-	30/A	-	10/Sp	10/S	-	50
Pilargidae									
<i>Sigambra tentaculata</i> (Treadwell, 1941)	610/A	1110/W	10/Sp	40/A	-	270/A	360/A	-	75
<i>Sigambra</i> sp.	-	20/W	-	-	-	-	-	-	12.5
Pisionidae									
<i>Pisione remota</i> (Southern, 1914)	-	-	10/S	-	-	-	-	-	12.5
Polygordiidae									
<i>Polygordius lacteus</i> Schneider, 1868	-	-	-	-	-	-	30/Sp	-	12.5
Polynoidea									
<i>Harmothoe imbricata</i> (Linnaeus, 1767)	40/W	30/A-W	-	40/W	-	20/W	10/A	-	75
<i>Harmothoe</i> sp.	150/Sp	240/Sp-S	20/Sp	130/W	-	40/W	80/Sp	10/Sp	87.5
<i>Malmgrenia liliana</i> (Pettibone, 1993)	20/Sp	-	10/S	-	-	-	-	-	25
<i>Malmgreniella</i> sp.	10/W	20/A	-	-	-	-	-	-	25
Serpulidae									
<i>Pileolaria militaris</i> Claparède, 1870	210/Sp	1170/S	-	290/W	-	-	10/Sp	-	50

Tablo 2 (Continued)									
<i>Spirobranchus triqueter</i> (Linnaeus, 1758)	100/S	290/W	10/S	230/W	-	30/W	-	-	62.5
<i>Vermiliopsis striaticeps</i> (Grube, 1862)	-	10/A	-	-	-	-	-	-	12.5
Spionidae									
<i>Aonides paucibranchiata</i> Southern, 1914	-	350/Sp	1820/S	1040/Sp	20/S	130/A	1200/Sp	-	75
<i>Aonides</i> sp.	10/S	-	-	-	-	-	-	-	12.5
<i>Prionospio (Minuspio) maciolekae</i> Dagli & Çinar, 2011	4400/Sp	5080/Sp	460/Sp	6790/W	50/A	7480/A	3140/A	30/Sp-W	100
<i>Prionospio</i> sp.	30/W	60/S	20/S	20/W	10/A	-	20/Sp	10/W	87.5
<i>Pygospio elegans</i> Claparède, 1863	-	-	20/Sp	10/Sp	20/Sp	-	10/A	10/Sp-W	62.5
<i>Pseudopolydora</i> sp.	-	-	10/S	-	-	-	-	-	12.5
<i>Spio decoratus</i> Bobretzky, 1870	30/Sp	110/Sp	390/S	500/S	780/S	530/A	700/S	470/S	100
<i>Spio</i> cf. <i>filicornis</i>	-	-	10/A	-	-	-	-	-	12.5
Syllidae									
<i>Exogone naidina</i> Örsted, 1845	870/Sp	470/Sp	40/Sp	30/W	-	30/Sp	30/Sp	50/Sp	87.5
<i>Myrianida</i> sp.	10/Sp	20/Sp	-	-	-	-	-	-	25
<i>Pionosyllis</i> sp.	-	-	-	-	-	10/Sp	-	-	12.5
<i>Salvatoria</i> cf. <i>dolichopoda</i>	130/Sp	80/Sp	-	-	-	10/Sp	-	-	37.5
<i>Salvatoria clavata</i> (Claparède, 1863)	290/W	40/Sp	60/Sp	20/W	-	100/W	-	-	62.5
<i>Salvatoria</i> sp.	-	10/W	-	-	-	-	-	-	12.5
<i>Sphaerosyllis taylori</i> Perkins, 1981	150/W	-	10/S	10/Sp	-	-	10/A	10/S	62.5
<i>Sphaerosyllis thomasi</i> San Martín, 1984	-	-	-	10/A	-	-	30/Sp	-	25
* <i>Syllis</i> cf. <i>amica</i>	10/W	30/W	10/A	20/A	-	-	-	-	50
<i>Syllis gracilis</i> Grube, 1840	-	40/S	-	-	-	-	-	-	12.5
<i>Syllis krohnii</i> Ehlers, 1864	20/A	-	-	10/A-W	-	-	10/A	-	37.5
<i>Syllis</i> sp.	10/A	20/S	20/A	10/S	-	40/A	-	10/S	75
<i>Trypanosyllis zebra</i> (Grube, 1860)	-	10/A-W	-	-	-	-	-	-	12.5
Terebellidae									
<i>Polycirrus jubatus</i> Bobretzky, 1868	40/W	40/W	10/Sp	80/W	-	-	40/Sp	-	62.5
<i>Polycirrus</i> sp.	20/W	30/S	-	70/S	-	10/A	10/A	-	62.5
<i>Terebella</i> cf. <i>lapidaria</i>	10/A	30/Sp	-	-	-	-	60/A	-	37.5
Terebellidae (sp.)	30/A	-	-	-	-	-	-	-	12.5
Trichobranchidae									
<i>Terebellides stroemii</i> Sars, 1835	170/Sp	700/Sp	10/Sp	60/W	-	10/A-Sp-W	50/A	-	75

*New records for the Black Sea, ** New records for the Turkish coast of the Black Sea

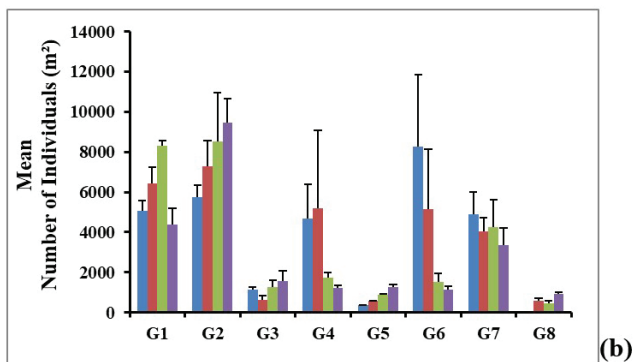
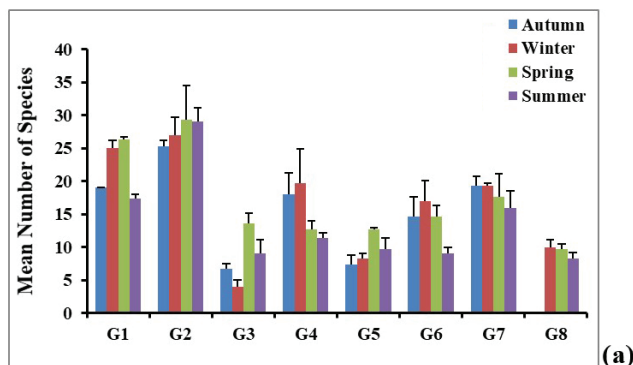


Figure 2. Seasonal distribution of the mean number of species (a) and individuals (m^2) (b).

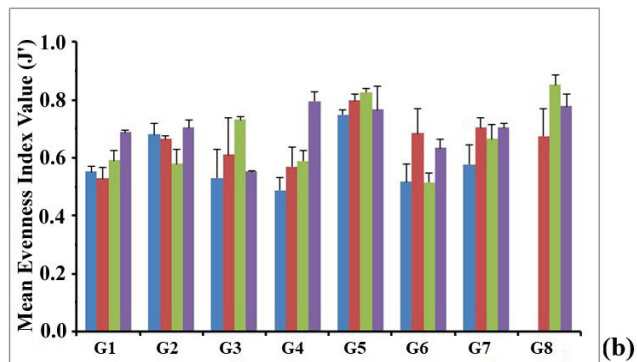
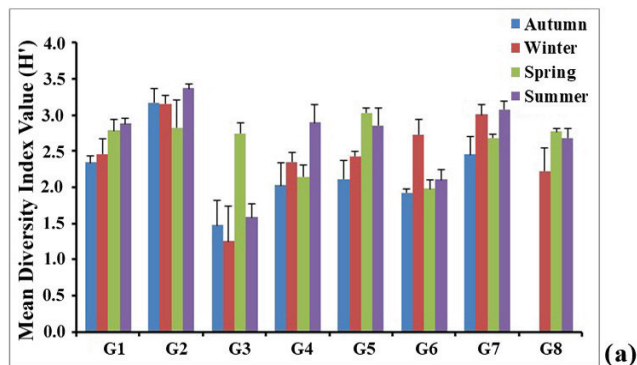


Figure 3. Seasonal distribution of the mean diversity (H') (a) and evenness (J') (b) index values.

Among dominant and constant species, *Prionospio maciolekae* was a sensitive species (G1), *Micronephthys longicornis*, *Protodorvillea kefersteini* and *Spio decoratus* were tolerant species (GIII), and *Heteromastus filiformis* (GV) was a first-order opportunistic species according to the five ecological groups.

The highest mean number of species for all seasons was determined at station G2 (Figure 2a). There was no significant difference between the stations in terms of the average number of individuals; the highest values were determined at G2 in all seasons just except G6 in autumn (Figure 2b). *Prionospio maciolekae*, *Micronephthys longicornis* and *Protodorvillea kefersteini* were the most dominant species in all seasons. The maximum density values for dominant species were *P. maciolekae* with $6,790 \text{ ind. m}^{-2}$ in winter; *M. longicornis* with $4,290 \text{ ind. m}^{-2}$ in winter; *P. kefersteini* with $4,150 \text{ ind. m}^{-2}$ in autumn.

The highest mean H' value was determined in summer ($H'=3.37$) at station G2; whereas the lowest mean value was found at station G3 in winter ($H'=1.25$) (Figure 3a). The highest mean evenness index value was calculated in spring at station G8 ($J'=0.85$); and the lowest mean value was found at station G4 ($J'=0.48$) in autumn (Figure 3b).

DISCUSSION

The first detailed study on Polychaeta species of soft substratum around the Sinop Peninsula (southern Black Sea) was carried out by Kurt Sahin et al. (5). The present study was per-

formed in the same area, but with different and deeper stations that represent both sides of the peninsula. Kurt-Sahin and colleagues reported *M. longicornis*, *P. kefersteini*, *P. maciolekae*, *H. filiformis* and *S. decoratus* as dominant and constant species. We also found these species as dominant and constant in the area. This is probably related to the sediment structure of the area.

Benthic communities were examined in five ecological groups according to their sensitivity to environmental factors. Of the dominant and constant species determined in the present study, *Prionospio maciolekae* was a sensitive species, *Micronephthys longicornis*, *Protodorvillea kefersteini* and *Spio decoratus* were tolerant species, and *Heteromastus filiformis* was a first-order opportunistic species. There were no dense populations of species identified as opportunistic in the research area. According to previous studies conducted on the Black Sea coast (32); (5, 6, 10, 28, 33) and the current research, they are typical species in soft bottoms of the Black Sea.

In the current study, station G2 was represented with the highest value in all seasons in terms of mean number of species (Figure 2a). This is probably related to the sediment structure of station G2. The biotope consists of mud and shell fragments, whose may provide different habitats allowing settlement of diverse species. Station G1 followed station G2 in terms of the number of species in all seasons (Figure 2a). The highest number of species (67 species) was presented in spring and the lowest number of species (62 species) was found in summer and winter (Figure 2a). Considering the average number of individ-

uals, there is significant difference between the seasons (Figure 2b). As a result of the analysis, it was determined that the average number of individuals was the highest at station G2 in three seasons (maximum density 9,740 ind.m⁻² in summer) and the highest density was calculated at station G6 (2,470 ind.m⁻² in autumn) (Figure 2b).

Syllidae, with 13 species, was the most diverse family in the area, followed by Spionidae, Nereididae and Paraonidae. Kurt Sahin and Çinar (4) stated that most of the species in the Black Sea dwell in soft bottoms. They reported Syllidae and Spionidae (32 and 31 species, respectively) as the most dominant families by means of number of species, followed by Phyllodocidae and Nereididae. Kurt Sahin *et al.*, (5) reported the most dominant families in the Sinop Peninsula as Syllidae (12 species), Spionidae (8 species) and Paraonidae (7 species).

Spionidae, Nephtyidae and Dorvilleidae were the families with the highest number of individuals and the best representative species were *Prionospio maciolekae*, *Micronephthys longicornis* and *Protodorvillea kefersteini*. Kurt Sahin *et al.*, (5) reported that *P. kefersteini* has the highest population density (15,125 ind. m⁻²) in winter, whereas *M. longicornis* (10,425 ind.m⁻²) in summer. In the present study, the highest population density belonged to *P. maciolekae* (7,480 ind.m⁻²) at station G6 in the autumn period. Subsequently, *M. longicornis* (4,290 ind.m⁻²) had the highest density at station G1 in winter, and *P. kefersteini* (4,150 ind.m⁻²) at station G6 in autumn.

The highest diversity index value (H'=3.37) was found in summer and the lowest (H'=1.25) in winter (Figure 3a). The highest evenness index value was calculated as J'=0.85 in spring and the lowest as J'=0.48 in autumn (Figure 3b). Kurt Sahin *et al.*, (5) recorded the highest mean diversity index value (H'=3.05) in summer and the lowest (H'=0.3) in autumn, and the authors stated that high values were generally seen in summer in the Sinop Peninsula. In the present study, mean evenness index values were high in summer (J'= 0.88) and the lowest in winter (J'=0.2).

Polychaete of the soft bottom Turkish coasts of the Mediterranean Sea, the Aegean Sea, and the Sea of Marmara has been well studied, but in the Black Sea, the studies are limited. The first research conducted on Polychaeta biodiversity of Sinop Peninsula was carried out by Cinar and Gönülğür-Demirci (25) that reported 55 polychaete species associated with algae and mussel beds. Gozler *et al.*, (27), reported 9 nereidid species associated with *Cystoseira barbata* and *Mytilaster lineatus* facies. Sezgin *et al.*, (34) reported 50 polychaete species in the Anatolian coasts of the Black Sea. Polychaetes from other Black Sea coasts are relatively well known compared with those from Turkey (5). Soft bottom Polychaeta fauna of the Black Sea has been studied in Bulgaria (10), Crimea (12), Romania (13, 15, 16), and the Ukraine (14).

Kurt Sahin *et al.*, (5) reported 76 species from the Sinop Peninsula and Kurt Sahin *et al.*, (6) reported 58 species from the İğneada coast. Finally, Kurt Sahin *et al.*, (7) reported 4 new records for the

Black Sea coast of Turkey and 4 new species for the fauna of the Black Sea.

It is well known that the distribution of soft substratum polychaetes depends on depth, seasonal variables, and sediment structure (35-37). Gambi and Giangrande (38) and Mackie *et al.*, (36) reported that both density and diversity of benthic communities were affected as depth increased. However, it is not possible to make a comparison because there is no significant difference.

CONCLUSION

The present study shows the current status of the soft substratum polychaetes along the Sinop Peninsula and provides new records for the Black Sea and the Turkish Black Sea coast.

Peer-review: Externally peer-reviewed.

Author Contributions: Conception/Design of study: G.K., M.Ç., Data Acquisition: G.K., M.Ç, S.K.; Data Analysis/Interpretation: G.K., M.Ç, S.K.; Drafting Manuscript: G.K., M.Ç, S.K.; Critical Revision of Manuscript: G.K.; Final Approval and Accountability: G.K.; Technical or Material Support: G.K.; Supervision: G.K.

Conflict of Interest: The authors declare that they have no conflicts of interest to disclose.

Financial Disclosure: There are no funders to report for this submission.

REFERENCES

1. Appeltans W, Ahyong ST, Anderson G, Angel MV, Artois T, Bailly N *et al.* The magnitude of global marine species diversity. *Curr Biol* 2012; 22: 2189-202.
2. Coll M, Piroddi C, Steenbeek J, Kaschner K, Lasram FBR, Aguzzi J *et al.* The biodiversity of the Mediterranean Sea: Estimates, patterns and threats. *Plos One* 2010; 5: 11842.
3. Çinar ME, Daglı E, Kurt Sahin G. Check-list of Annelida from the Coasts of Turkey. *Turk J Zool* 2014; 38: 734-64.
4. Kurt Sahin G, Çinar ME. A check-list of polychaete species (Annelida: Polychaeta) from the Black Sea. *J Black Sea Medit Envir* 2012; 18: 10-48.
5. Kurt Sahin G, Daglı E, Sezgin M. Spatial and temporal variations of soft bottom polychaetes of Sinop Peninsula (southern Black Sea) with new records, *Turk J Zool* 2017a; 41 (1): 89-101.
6. Kurt-Sahin G, Sezgin M, Ünlüer F, Öztürk B, Cavdar E, Daglı E. Macrozoobenthic community structure of İğneada region in Turkey (the southwestern Black Sea). *Oceanol Hydrobiol St* 2017b; 46: 340-9.
7. Kurt-Sahin G, Çinar ME, Daglı E. New records of polychaetes (Annelida) from the Black Sea. *Cah Biol Mar* 2019; 60: 153-65.
8. Zaitsev YuP, Alexandrov BG, Berlinsky NA, Zenetos A. Europe's biodiversity -biogeographical regions and seas: The Black Sea an oxygen-poor sea. Environmental issue report Published by EEA (European Environment Agency) Copenhagen 2002.
9. Zaitsev YuP, Alexandrov BG. Black Sea biological diversity – Ukraine. *Black Sea Environmental Series, 7, United Nations Publishing, 1998.*
10. Marinov T. Fauna of Bulgaria. In: *BristleWorms (Polychaeta)*. Vol. 6. *Bulgar- skata Akademijana Naukite, Sofia, 1977.*

11. Kiseleva MI. Benthos of the Soft Bottoms of the Black Sea. Naukova Dumka, Kiev, 1981.
12. Revkov NK, Boltacheva NA, Nikolaenko TV, Kolesnikova EA. Zoo-benthos Biodiversity over the Soft Bottom in the Crimean coastal zone of the Black Sea. *Mar Biol* 2002; 42: 561-71.
13. Gomoiu MT, Secieru D, Paraschiv G, Opreanu P, Puschiada D. Some remarks on the ecological state of benthic populations recorded during the IAEA'98 Black Sea cruise of "Prof. Vodyanitsky" R/V. *Geoecomarina* 2004; 9: 12-20.
14. Losovskaya GV. Species and Ecological Diversity and Polychaeta Taxocen in the Northwestern Part of the Black Sea. *Hydrobiol J* 2005; 41: 3-8.
15. Surugiu V. Inventory of inshore polychaetes from the Romanian coast (Black Sea). *Medit Mar Sci* 2005; 6, 51-73.
16. Paraschiv GM, Samargiu MD, Sava D. Ecological Study of Vagile Fauna Distribution from the Black Sea Shallow Water at Vama Veche. *Agroprint Timisoara* 2007; 499-506.
17. Jakubova LI. Features of the biology of Prebosphoric sector of the Black Sea. *Trudy Sevastopol'skoj, Biologicheskoi Stantsii*, 1948; 6: 274-85.
18. Marinov T. Sur la faune de Polychètes des amas de moules de la mer Noire. *Compt Acad Bulg Sci* 1959; 12 : 443-6.
19. Dimitrescu E. Contributions à la connaissance des Polychètes de la Mer Noire, spécialement des eaux prébosphoriques. *Trav Mus Natl Hist Nat Grigore Antipa* 1960; 2: 69-85.
20. Dimitrescu E. Nouvelle contribution à l'étude des Polychètes de la Mer Noire. *Trav Mus Natl Hist Nat Grigore Antipa* 1962; 3: 61-8.
21. Rullier F. Les annélides polychètes du Bosphore, de la Mer de Marmara et de la Mer Noire, en relation avec celles de la Méditerranée. *Rapp Com Int Mer Médit* 1963; 17: 161-260.
22. Caspers H. La macrofaune benthique du Bosphore et les problèmes de l'infiltration des éléments Méditerranées dans la mer Noire. *Rapp Com Int Mer Médit* 1968; 19: 107-15.
23. Gillet P, Unsal M. Résultats de la campagne océanographique de "Bilim": annélides polychètes de la Mer de Marmara, du Bosphore et des régions prébosphoriques de la Mer Noire. *Mésogée* 2000; 58: 85-91.
24. Uysal A, Yuksek A, Okus E, Yilmaz N. Benthic community structure of the Bosphorus and surrounding area. *Water Sci Tech* 2002; 46: 37-44.
25. Çınar ME, Gönülğür-Demirci G. Polychaete assemblage on shallow-water benthic habitats along the Sinop Peninsula (Black Sea, Turkey). *Cah Biol Mar* 2005; 46: 253-63.
26. Agirbas E, Gozler AM, Sahin C, Hacimurtazaoglu N. Doğu Karadeniz'de Dağılım Gösteren Ulva fasiesinin Poliket Faunası. *J Fish Sci* 2008; 2: 427-31.
27. Gozler AM, Agirbas E, Sahin C. Spatial and temporal distribution of Nereidae (Polychaeta: Annelida) along the coast of Turkish eastern Black Sea in the upper-infralittoral zone. *J Anim Vet Adv* 2009; 8: 229-34.
28. Kus S, Kurt-Sahin G. Temporal Changes in the Polychaeta (Annelida) Community Associated with Cystoseira Beds of Sinop Peninsula (Southern Black Sea). *Turk J Fish Aquat Sc* 2016; 16: 61-8.
29. Bellan-Santini D. Contribution à l'étude des peuplements infralittoraux sur substrat rocheux (Etude qualitative et quantitative de la franch Superiere). *Travaux Station Marine d'Endoume*, 1969; 63(47): 9-294.
30. Soyer T. Bionomie benthique du plateau continental de la cote catalana Française, III: Les peuplements de Copepodes Harpacticoides (Crustacea). *Vie Milieu* 1970; 21: 377-511.
31. Çınar ME, Bakir K, Öztürk B, Katagan T, Dagli E, Açık S et al. TUBI (Turkish Benthic Index): A new biotic index for assessing impacts of organic pollution on benthic communities. *J Black Sea Medit Env* 2015; 21: 135-68.
32. Dimitrescu E. Polychètes marins de la zone littorale Roumaine (1 à 20 m de profondeur). *Trav Mus Natl Hist Nat Grigore Antipa* 1963; 4: 181-92.
33. Surugiu V. Polychaete Research in the Black Sea. *Rom J Aqua Ecol* 2011; 1: 101-22.
34. Sezgin M, Kirkim F, Dagli E, Dogan A, Unluoglu A, Katagan T et al. Sublittoral soft-bottom zoobenthic communities and diversity of southern coast of the Black Sea (Turkey). *Rapp Comm Int Mer Medit* 2010; 39: 662.
35. Tom M, Galil B. The macrobenthic associations of Haifa Bay, Mediterranean coast of Israel. *P.S.Z.N.I.: Mar Ecol* 1991; 12: 75-86.
36. Mackie ASY, Parmiter C, Tong LKY. Distribution and diversity of Polychaeta in the southern Irish Sea. *Bull Mar Sci* 1997; 60: 467-81.
37. San Martín G, Parapar J, García FJ, Redondo MS. Quantitative analysis of soft bottoms infaunal macrobenthic polychaetes from South Shetland Islands (Antarctica). *Bull Mar Sci* 2000; 67: 83-102.
38. Gambi, MC, Giangrande, A. Distribution of soft-bottom polychaetes in two coastal areas of the Tyrrhenian Sea (Italy): structural analysis. *Estuar Coast Shelf Sci* 1986; 23: 847-62.

The Effect of Olaparib and Bortezomib Combination Treatment on Ovarian Cancer Cell Lines

Caglar Berkel¹ , Burak Kucuk¹ , Merve Usta¹ , Esra Yilmaz² , Ercan Cacan¹ 

¹Tokat Gaziosmanpasa University, Department of Molecular Biology and Genetics, Tokat, Turkey

²Tokat Gaziosmanpasa University, Department of Biology, Tokat, Turkey

ORCID IDs of the authors: C.B. 0000-0003-4787-5157; B.K. 0000-0002-9325-2359; M.U. 0000-0002-5086-6270; E.Y. 0000-0002-9922-8341; E.C. 0000-0002-3487-9493

Please cite this article as: Berkel C, Kucuk B, Usta M, Yilmaz E, Cacan E. The Effect of Olaparib and Bortezomib Combination Treatment on Ovarian Cancer Cell Lines. Eur J Biol 2020; 79(2): 115-123. DOI: 10.26650/EurJBiol.2020.0035

ABSTRACT

Objective: Ovarian cancer (OC) is the deadliest gynecologic malignancy and has a poor survival rate due to late diagnosis and chemoresistance development. In the standard treatment of OC, platinum-based chemotherapeutics are used. However, following several rounds of chemotherapy, these drugs' efficacy eventually becomes limited due to the development of chemoresistance in most patients who previously responded to this treatment. Therefore, overcoming chemoresistance in the treatment of OC is of high importance. In this study, we investigated the effect of combinatorial inhibition of poly(ADP-ribose) polymerase (PARP) and proteasome by olaparib and bortezomib on chemosensitive and chemoresistant OC cell lines.

Materials and Methods: We used sulphorhodamine B assay to screen cell viability following drug treatments alone or in combination, and used the cytotoxicity data to model the effect of drugs on cell death in R programming environment. In addition to olaparib and bortezomib, we performed cytotoxicity screenings where we applied cisplatin to OC cells. We also carried out flow cytometry analysis to quantify apoptotic cells following treatments.

Results: We showed that combination treatment was more effective on chemosensitive OC cell lines when cisplatin was not used. In the presence of cisplatin, olaparib and bortezomib combination treatment resulted in higher cytotoxicity in chemoresistant OC lines compared to chemosensitive OC cell lines. Combinatorial inhibition of PARP and proteasome led to a higher number of apoptotic cells in OV2008 chemosensitive cell line compared to drugs alone.

Conclusion: Our data shows that olaparib and bortezomib combination treatment might show promise *in vivo* in the treatment of OC. Also, the efficacy of this combination treatment might be dependent on OC cells' chemosensitivity profiles.

Keywords: Ovarian cancer, olaparib, bortezomib, chemoresistance, proteasome

INTRODUCTION

Ovarian cancer is the most lethal gynecologic malignancy, with an overall 5-year survival rate of less than 25% and with approximately 30,000 new cases and over 18,000 deaths worldwide each year (1). Cisplatin is used for the standard treatment of ovarian cancer as a first-line chemotherapeutic agent, but its efficacy in the clinic is limited due to resistance development (2). Most patients, initially responding to cisplatin treatment, are ultimately diagnosed with a relapse of chemoresistant disease within two years, leading to therapeutic failure

(3,4). Olaparib, a poly (ADP-ribose) polymerase (PARP) inhibitor (PARPi), is approved as a maintenance treatment for platinum-sensitive relapsed ovarian cancer, regardless of its *BRCA1/2* mutation status (5). PARP proteins have the ability to catalyze the transfer of ADP-ribose to its target proteins and have crucial functions in many cellular processes including transcription, replication, recombination, modulation of chromatin structure and, most importantly in this case, DNA repair and DNA damage response (6). However, PARP inhibition with olaparib treatment might result in PARPi resistance and possible mechanisms are currently being investigated (7).



Corresponding Author: Ercan Cacan

E-mail: ercan.cacan@gop.edu.tr

Submitted: 07.09.2020 • **Revision Requested:** 10.09.2020 • **Last Revision Received:** 25.10.2020 •

Accepted: 29.10.2020 • **Published Online:** 13.12.2020

© Copyright 2020 by The Istanbul University Faculty of Science • Available online at <http://ejb.istanbul.edu.tr> • DOI: 10.26650/EurJBiol.2020.0035

Bortezomib, a first-in-class proteasome inhibitor, is used for the treatment of adults with multiple myeloma (MM) or mantle cell lymphoma. However, its administration does not show significant therapeutic efficacy in solid tumors, including ovarian cancer (8). Inhibition of proteasome function with bortezomib leads to an accumulation of damaged proteins, resulting in the activation of caspase cascade and ultimately cell death (9). Although it is not effective in ovarian cancer as a single agent, the combination of bortezomib with olaparib may result in an increased cytotoxicity as well as a decrease of PARPi resistance. To our knowledge, to date, no previous study has reported the effect of combinatorial inhibition of proteasome and PARP with the combination of bortezomib and olaparib on ovarian cancer cell viability *in vitro*.

In the current study, we investigated the effect of bortezomib and olaparib combination treatment on chemoresistant and chemosensitive ovarian cancer cell lines in the presence or absence of cisplatin. We modeled the cell viability responses of four different ovarian cancer cell lines (namely, OV2008, C13, A2780 and A2780-AD) following PARP and proteasome inhibition in combination using olaparib and bortezomib, respectively and analyzed each drugs' contribution to drug combination effect on cell viability. This is the first study analyzing the combined effect of these two antineoplastic agents in ovarian cancer *in vitro*, considering their chemosensitivity profiles. We believe that the preliminary data presented in the current *in vitro* study will guide further research to study this particular drug combination in more advanced experimental models of ovarian cancer including *in vivo* animal models. We also provided our experimental data as tables to contribute to open cancer research data to make it possible for other cancer researchers to completely reproduce the analysis we performed.

MATERIALS AND METHODS

Cell Culture and Reagents

Human ovarian cancer cell lines (OV2008, C13, A2780 and A2780-AD) were generously provided by Dr. Shelly B. Hooks, University of Georgia. These cells were maintained in RPMI-1640 medium (Sigma-Aldrich) supplemented with 10% fetal bovine serum, 5 mM L-glutamine and 5 mM pen/strep, in humidified 5% CO₂ incubator at 37°C. Chemoresistant cell lines C13 and A2780-AD were continuously grown with 3 µM cisplatin. The cell lines have the following characteristics: OV2008 (66y, serous histotype, sequence variation: heterozygous for *PIK3CA* p.Glu545Lys (c.1633G>A)) (10), A2780 (age unspecified, endometrioid histotype, sequence variations: *ATM* p.Pro604Ser (c.1810C>T), *PTEN* p.Lys128_Arg130del (c.383_391del9)) (11,12). All cell lines used in the present study are epithelial ovarian cancer cell lines (serous and endometrioid subtypes).

Chemotherapeutic Agents

Cisplatin was purchased from Kocak Pharma (Istanbul, Turkey). Bortezomib was purchased from LC Laboratories (Woburn, MA, USA). Olaparib was purchased from Sigma-Aldrich (St. Louis, MO, USA). Bortezomib and olaparib were dissolved in dimethyl

sulfoxide (DMSO, ultra-pure grade, Amresco, VWR) and DMSO controls were included in the assays. The bortezomib stock solution was kept at -20°C and the olaparib stock solution was kept at 4°C. Cisplatin was diluted in phosphate-buffered saline (PBS) and was kept at room temperature (RT) in the dark. Extensive free-thaw cycles were avoided in the storage of drugs. Olaparib concentrations used on ovarian cancer cell lines were in the 0-20 µM range, and bortezomib concentrations used were in 0-20 nM range. Only one concentration of cisplatin was used (10 µM) in triple combination treatments in the present study. The drug concentrations used in combination treatments were determined based on minimum effective drug concentrations on cell viability (i.e. 10 µM for olaparib and 10 nM for bortezomib).

Cell Viability Assay

The viability of cells after drug treatment were determined by sulphorhodamine B (SRB) colorimetric assay as previously described (13,14). Briefly, cells were seeded in 96-well flat-bottom plates in 200 µl media as 10,000 cells per well and allowed to adhere overnight. The cells were incubated with bortezomib and/or olaparib for 24 h and then, cisplatin was added, and the cells were further incubated for an additional 48 h. Following the fixation of cells to bottom of the plate with TCA (trichloroacetic acid) solution, 200 µl SRB dye solution in 1% acetic acid was added to each well and the plates were incubated for 30 minutes using an orbital shaker. Then, washing steps were performed with 1% acetic acid four times and the plates were left to dry at a 50°C incubator. At the final step of SRB assay, following solubilization of dye with Tris-base solution, spectrophotometric reading (Multiskan Go, Thermo Scientific) was performed to measure absorbances at 492 nm. Sulphorhodamine B dye was purchased from Sigma-Aldrich (St. Louis, MO, USA). All experiments were repeated at least three times (with n≥3 in each experiment).

Flow Cytometry

PE Annexin V Apoptosis Detection Kit was used to determine the effects of bortezomib and olaparib on apoptosis and necrosis in chemosensitive and chemoresistant ovarian cancer cells. The cells were plated in 12-well culture dishes and treated with bortezomib and olaparib considering the dose and time points determined in the previous cytotoxicity analyses. Following the drug incubation period, the assay was followed according to the manufacturer's instructions. Briefly, cells were harvested and washed twice with ice-cold PBS, and then resuspended in a 1X binding buffer. 5 µl of PE Annexin V and/or 7-AAD (7-aminoactinomycin D) were added and incubated for 15 minutes at room temperature. The cells were then analyzed within 1 hour by flow cytometry (Attune Acoustic Focusing Cytometer, Applied Biosystems). Living cells were negative for Annexin V or 7-AAD, while early apoptotic cells were positive for Annexin V. Necrotic cells were counted as positive for 7-AAD, while apoptotic cells were positive for both Annexin V and 7-AAD.

Statistical Analysis and Data Visualization

The data visualization and analysis were performed in R statistical programming language / environment (15-17). The follow-

ing R packages were used in this study: tidyverse (a collection of R packages) (18), readxl (19), plot3D (20), magick (21), gridExtra (22), ggpubr (23) and rmarkdown (24,25). The data in this study were derived from at least three independent biological repeats. lm function of base R was used to fit linear models using percent cell viability values (as response) and drug concentrations (as terms). Model coefficients were analyzed in order to identify the drugs' contributions to the combinatorial effect on cell viability. More detail can be found in the figure legends. Statistical comparisons in boxplots were performed with Student's t-Test using functions from ggpubr R package (23).

RESULTS

Combination of Olaparib and Bortezomib Affects Cell Viability in a Cell Line-Dependent Manner

We first treated four different ovarian cancer cell lines with previously selected concentrations of olaparib and bortezomib to see how combined PARP and proteasome inhibition affects cancer cell viability. We used two chemosensitive and chemoresistant ovarian cancer cell line pairs (OV2008 - C13 and A2780 - A2780-AD; the former being chemosensitive). By using the data obtained following drug treatments, we modeled cell viability (as a response) using olaparib and bortezomib concentrations as predictors. Model coefficients were used to interpret each drugs' contributions to combined cytotoxic effect.

For OV2008 chemosensitive cell line, the model coefficients for bortezomib and olaparib were -1.291658 and -1.723806, respectively (Figure 1, upper row, first plot). This means that both drugs are associated with decreased cell viability when used in combination, although bortezomib contributes slightly to the effect of combination treatment in this chemosensitive ovarian cancer cell line. When we modeled the data for C13 cell line, we saw that increased cytotoxicity in the combination treatment is mostly due to olaparib, and bortezomib treatment results only in a slightly lower cell viability when used in combination with olaparib (model coefficients: -0.6809321 (bortezomib), -1.8865199 (olaparib)) (Figure 1). Therefore, it can be stated that combination of olaparib with bortezomib does not increase cytotoxicity significantly compared to olaparib alone in this chemoresistant ovarian cancer cell line.

The model coefficients were -1.083256 and -2.895892 for bortezomib and olaparib in A2780 chemosensitive cell line, respectively (Figure 1). These results indicate that the contribution of olaparib to the effect of drug combination was almost 3 times higher than that of bortezomib. Therefore, it can be pointed out that bortezomib has a slight effect on cell viability when combined with olaparib in this chemosensitive ovarian cancer cell line. For its chemoresistant subline A2780-AD, the difference in the cytotoxicity of the drugs was more dramatic (model coefficients: -0.5706074 (bortezomib), -3.4457898 (olaparib)) (Figure 1, upper row, last plot). This shows that bortezomib has almost no increasing cytotoxic effect in combination treatment, and single olaparib treatment is already highly cytotoxic itself in this chemoresistant ovarian cancer cell line.

Percent cell viability values for treatments used in modeling are shown in bottom row of Figure 1 with corresponding p values. Percent cell viability values are given in Table 1 in more detail for each drug treatment combination performed in this study to make the analysis more reproducible by other researchers.

The Effect of Olaparib and Bortezomib Combination Treatment on Ovarian Cancer Cell Lines in the Presence of Cisplatin

Next, we investigated how the effect of olaparib and bortezomib combination treatment on ovarian cancer cell lines changes when cells were also treated with cisplatin, a DNA-damaging agent used in the standard treatment of ovarian cancer. When 10 μ M cisplatin was applied following olaparib and/or bortezomib treatment, we observed that the cytotoxicity of bortezomib or olaparib on OV2008 cell line was low since cisplatin alone is highly cytotoxic on this chemosensitive cell line (Model coefficients: -0.70049775 (bortezomib), -0.04669829 (olaparib)) (Figure 2, upper row, first plot). Particularly, olaparib has almost zero effect on cellular viability when combined with cisplatin and bortezomib. When we considered its chemoresistant subline C13, both drugs had very close model coefficients (-0.9430565 (bortezomib), -0.9290382 (olaparib)), indicating that both drugs contribute almost equally to the combination treatment when used in combination with cisplatin (Figure 2). Bortezomib and olaparib decreased cell viability to a higher extent when combined with cisplatin in C13 cell line when compared to the chemosensitive OV2008 cell line.

Similar to the other chemosensitive cell line (OV2008), bortezomib and olaparib showed very slight effects on cell viability of A2780 cell line when combined with cisplatin (Model coefficients: -0.2038118 (bortezomib), -0.5011552 (olaparib)) (Figure 2). This showed that bortezomib and olaparib combination treatment does not increase cytotoxicity caused by cisplatin alone in this cell line. For its chemoresistant subline A2780-AD, the drugs' effect on cellular viability was higher (Model coefficients: -0.8512043 (bortezomib), -1.2631613 (olaparib)), indicating that combination treatment might increase cytotoxicity of cisplatin on this cell line to a certain extent and the contribution of olaparib to combinatorial effect was higher relative to that of bortezomib (Figure 2).

Percent cell viability values for treatments with cisplatin, used in modeling are shown in bottom row of Figure 2 with corresponding p values. Percent cell viability values are given in Table 1 in more detail for each drug treatment combination performed in this study to make the analysis more reproducible by other researchers.

Combination Treatment Results in Increased Cell Death in Chemosensitive Ovarian Cancer Cell Line OV2008

Next, we performed flow cytometry analysis using Annexin V and 7-AAD staining in chemosensitive ovarian cancer cell line OV2008 and its chemoresistant subline C13 following drug treatments. We observed that bortezomib and olaparib combination treatment resulted in an increased number of apoptotic

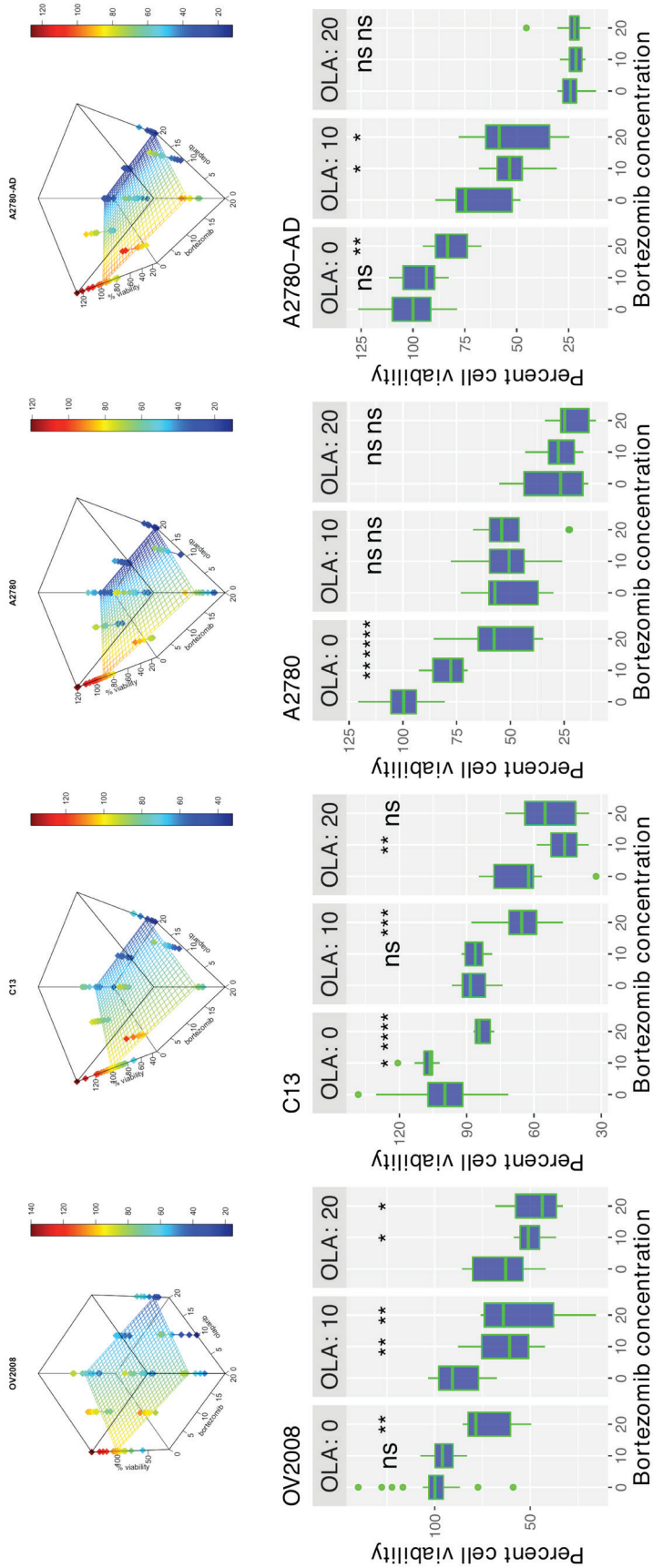


Figure 1. The effect of combination of olaparib with bortezomib on cell viability in a cell line dependent-manner.

Top row: 3D plots showing modeling results on ovarian cancer cell lines following treatment with bortezomib (nM) and olaparib (μM) at indicated concentrations. x axis shows bortezomib concentration, y axis shows OLA concentration and z axis shows % cell viability. Color key shows percent cell viability. Plots were produced using lm (linear model) function in base R and scatter3D function in plot3D R package. Color scale from red to blue indicates decreasing cell viability. In each cell line, the viability of control cells without any treatment (where bortezomib = 0 and OLA = 0) were taken as 100%, other cases were calculated accordingly. Names of cell lines were given at the top of each facet. Cells were incubated with bortezomib and/or OLA for 72 h.

Bottom row: Boxplots showing percent cell viability of ovarian cancer cell lines following the treatment with bortezomib (nM) and OLA (μM) at indicated concentrations. OLA: olaparib. ns: p > 0.05; *, p ≤ 0.05; **, p ≤ 0.01; ***, p ≤ 0.001; ****, p ≤ 0.0001; *****, p ≤ 0.00001.

Table 1. Mean percent cell viability values for each drug combination treatment performed in this study for all cell lines.

"CIS"	"BOR"	"OLA"	"Cell Line"	"Mean Viability"
0	0	0	"A2780"	99.99
0	0	0	"A2780-AD"	99.99
0	0	0	"C13"	99.99
0	0	0	"OV2008"	99.99
0	0	3	"A2780"	72.92
0	0	3	"A2780-AD"	98.33
0	0	3	"C13"	98.09
0	0	3	"OV2008"	99.54
0	0	5	"A2780"	58.75
0	0	5	"A2780-AD"	87.65
0	0	5	"C13"	91.09
0	0	5	"OV2008"	102.56
0	0	10	"A2780"	51.77
0	0	10	"A2780-AD"	68.87
0	0	10	"C13"	86.36
0	0	10	"OV2008"	87.65
0	0	20	"A2780"	29.04
0	0	20	"A2780-AD"	23.28
0	0	20	"C13"	65.43
0	0	20	"OV2008"	64.35
0	0	30	"A2780"	17.3
0	0	30	"A2780-AD"	25.12
0	0	30	"C13"	66.31
0	0	30	"OV2008"	67.69
0	0	40	"A2780"	15.36
0	0	40	"A2780-AD"	24.54
0	5	0	"A2780"	88.56
0	5	0	"A2780-AD"	105.26
0	5	0	"C13"	106.47
0	5	0	"OV2008"	102.74
0	10	0	"A2780"	79.45
0	10	0	"A2780-AD"	96.37
0	10	0	"C13"	108.14
0	10	0	"OV2008"	94.83
0	10	10	"A2780"	50.96
0	10	10	"A2780-AD"	51.93
0	10	10	"C13"	86.34
0	10	10	"OV2008"	63.32
0	10	20	"A2780"	27.63
0	10	20	"A2780-AD"	21.96
0	10	20	"C13"	46.75
0	10	20	"OV2008"	49.46
0	20	0	"A2780"	55.18
0	20	0	"A2780-AD"	81.83
0	20	0	"C13"	82.91
0	20	0	"OV2008"	71.29
0	20	10	"A2780"	49.37
0	20	10	"A2780-AD"	51.32
0	20	10	"C13"	65.36
0	20	10	"OV2008"	54.59
0	20	20	"A2780"	21.46
0	20	20	"A2780-AD"	23.47
0	20	20	"C13"	54.08
0	20	20	"OV2008"	47.26
0	30	0	"A2780"	30.37
0	30	0	"A2780-AD"	38.76

0	30	0	"C13"	80.89
0	30	0	"OV2008"	54.44
0	40	0	"A2780"	27.64
0	40	0	"A2780-AD"	33.78
0	40	0	"C13"	73.43
0	40	0	"OV2008"	47.03
1.5	0	0	"A2780"	86.13
1.5	0	0	"A2780-AD"	97.94
1.5	0	0	"C13"	96.34
1.5	0	0	"OV2008"	94.08
3	0	0	"A2780"	82.6
3	0	0	"A2780-AD"	102.83
3	0	0	"C13"	94.285
3	0	0	"OV2008"	87.56
5	0	0	"A2780"	67.2
5	0	0	"A2780-AD"	85.78
5	0	0	"C13"	96.3
5	0	0	"OV2008"	85.2
10	0	0	"A2780"	61.81
10	0	0	"A2780-AD"	76.76
10	0	0	"C13"	87.23
10	0	0	"OV2008"	33.13
10	0	10	"A2780"	57.57
10	0	10	"A2780-AD"	51.01
10	0	10	"C13"	81.63
10	0	10	"OV2008"	27.57
10	0	20	"C13"	65.77
10	0	20	"OV2008"	25.32
10	10	0	"A2780"	54.93
10	10	0	"A2780-AD"	57.87
10	10	0	"C13"	93.11
10	10	0	"OV2008"	31.9
10	10	10	"A2780"	52.93
10	10	10	"A2780-AD"	50.99
10	10	10	"C13"	77.88
10	10	10	"OV2008"	26.77
10	10	20	"C13"	48.4
10	10	20	"OV2008"	34.18
10	20	0	"A2780"	60.95
10	20	0	"A2780-AD"	49.5
10	20	0	"C13"	53.05
10	20	0	"OV2008"	9.01
10	20	10	"A2780"	51.8
10	20	10	"A2780-AD"	47.18
10	20	10	"C13"	58.95
10	20	10	"OV2008"	10.27
10	20	20	"C13"	65.21
10	20	20	"OV2008"	19.92
20	0	0	"A2780"	51.55
20	0	0	"A2780-AD"	77.24
20	0	0	"C13"	88.26
20	0	0	"OV2008"	24.93
30	0	0	"A2780"	30.8
30	0	0	"A2780-AD"	27.81
30	0	0	"C13"	72.67
30	0	0	"OV2008"	7.19
40	0	0	"A2780"	19.84
40	0	0	"A2780-AD"	23.66
40	0	0	"C13"	67.34
40	0	0	"OV2008"	11.09

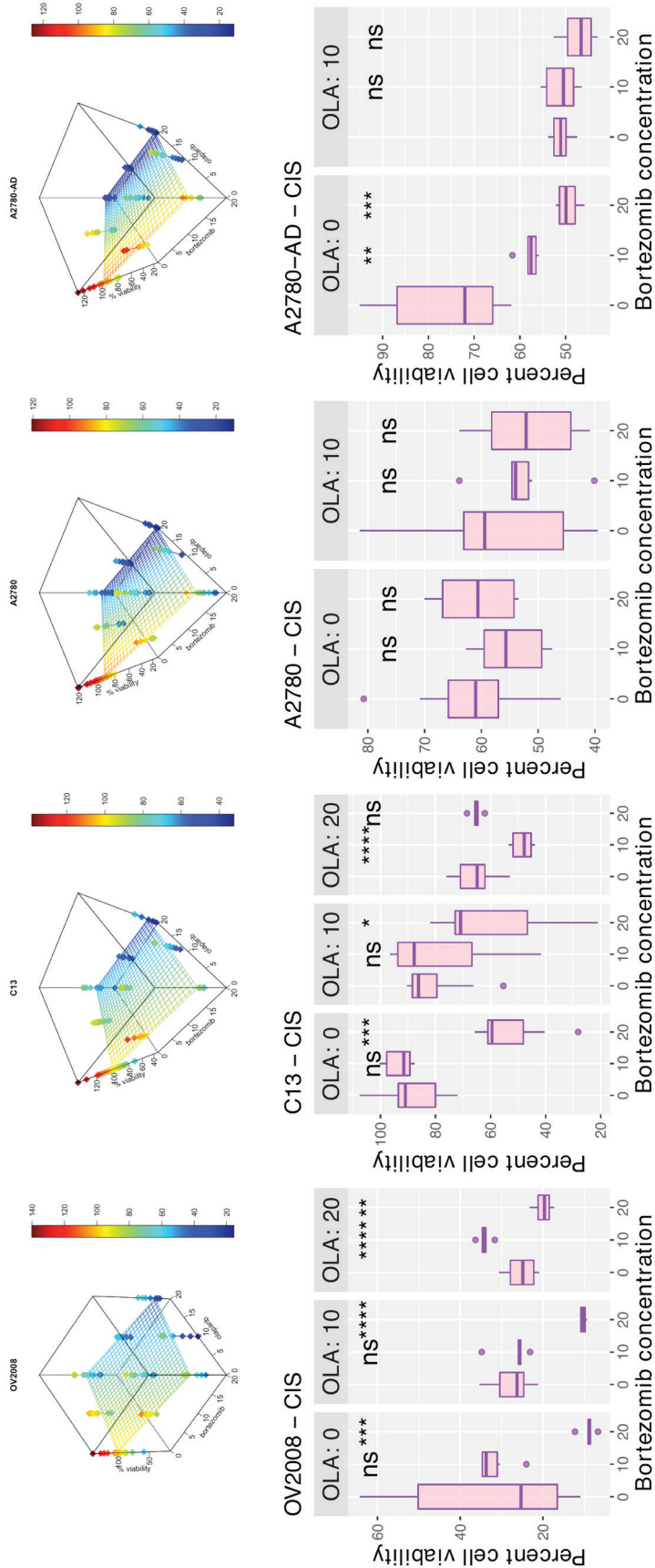
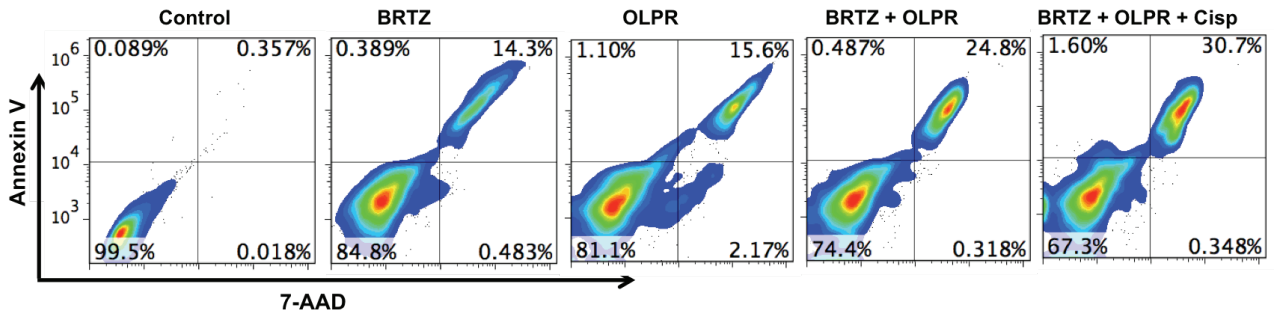


Figure 2. The effect of olaparib and bortezomib combination treatment on ovarian cancer cell lines in the presence of cisplatin. Top row: 3D plots showing modeling results on ovarian cancer cell lines following cisplatin (10 μM) treatment after bortezomib (nM) + olaparib (μM) combination treatment. x axis shows bortezomib concentration, y axis shows OLA concentration and z axis shows % cell viability. Color key shows percent cell viability. Plots were produced using lm (linear model) function in base R and scatter3D function in plot3D R package. Color scale from red to blue indicates decreasing cell viability. In each cell line, the viability of control cells without any treatment (where bortezomib = 0 and OLA = 0) were taken as 100%, other cases were calculated accordingly. Therefore, in this figure, maximum viability shown is less than 100% due to additional cisplatin treatment. Names of cell lines are given at the top of each facet. Cells were incubated with bortezomib and/or OLA for 24 h and then, cisplatin was added, and cells were further incubated for an additional 48 h. Bottom row: Boxplots showing percent cell viability of ovarian cancer cell lines following the treatment with bortezomib (nM) and OLA (μM) at indicated concentrations, when combined with cisplatin. OLA: olaparib. ns: p > 0.05; *: p ≤ 0.05; **: p ≤ 0.01; ***: p ≤ 0.001; ****: p ≤ 0.0001; *****: p ≤ 0.00001.

A) OV2008



B) C13

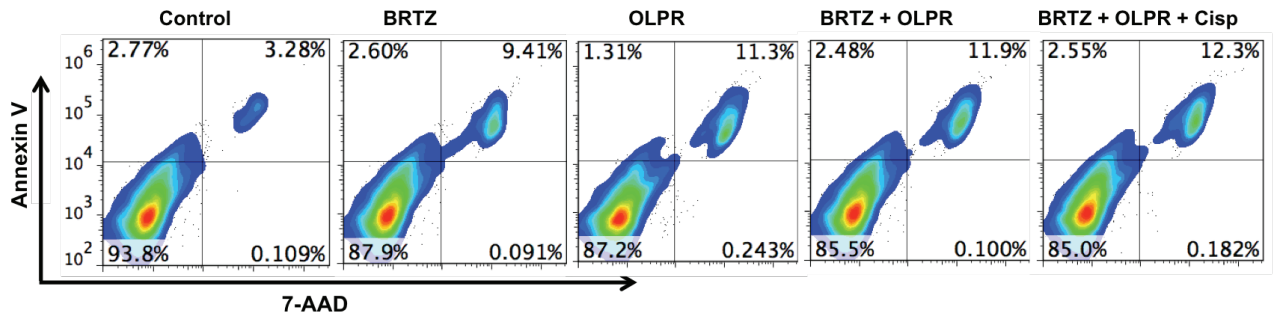


Figure 3. Combination treatment results in increased cell death in chemosensitive ovarian cancer cell line OV2008. Flow cytometry analysis with Annexin V and 7-AAD to study the effect of combination treatment on chemosensitive and chemoresistant ovarian cancer cell lines (OV2008 (A) and C13 (B), respectively). X-axis shows the number of 7-AAD-positive cells and y-axis shows the number of Annexin V-positive cells. Drug treatment conditions are given at the top of each facet. Percentage of cells in each region were given in corresponding corner. Upper right region with high Annexin V and 7-AAD values shows dead cells. BRTZ: bortezomib, OLPR / OLA: olaparib, Cisp: cisplatin.

cells in OV2008 cell line compared to drugs alone (bortezomib only or olaparib only) (Figure 3A). However, in chemoresistant cell line C13, we did not see any significant increase in apoptotic cells relative to drugs alone. Similar to previous experiments, the effect of cisplatin on the chemosensitive cell line OV2008 was higher compared to chemoresistant cell line C13. When we combined cisplatin with bortezomib and olaparib, we observed an increase in cell death in OV2008 cell line compared to bortezomib and olaparib combination treatment. However, this increased cytotoxicity in triple drug treatments might be due to only cisplatin since we did not perform cisplatin only treatments for the flow cytometry experiments. In C13 cell line, the bortezomib and olaparib combination did not further increase cell death relative to drugs alone. The addition of cisplatin did not further increase apoptotic cell death compared to olaparib and bortezomib combination treatment in this chemoresistant cell line (Figure 3).

DISCUSSION

In the current study, we investigated the effect of combinatorial inhibition of PARP and proteasome by olaparib and bortezomib, on the viability of chemosensitive or chemoresistant ovarian cancer cells. Olaparib is currently used in the clinic for a certain

group of ovarian cancer patients including patients with recurrent platinum-sensitive disease with or without a *BRCA* mutation (4). However, bortezomib is not approved for the treatment of ovarian cancer patients (but used in some other cancer types), though multiple studies showed its efficacy when used in combination with other strategies in ovarian cancer (26-28). To our knowledge, there is no report showing the effect of combinatorial inhibition of proteasome and PARP by bortezomib and olaparib, respectively on ovarian cancer cell viability. Since most ovarian cancer patients experience chemoresistance to cisplatin following several rounds of chemotherapy, novel treatment strategies such as in the present study are urgently needed to be investigated and developed in order to increase the survival of ovarian cancer patients (29).

In this study, we observed that combination treatment is mostly effective on chemosensitive ovarian cancer cell lines (OV2008, A2780). However, with chemoresistant cell lines (C13, A2780-AD), the effect of bortezomib is minimal compared to that of olaparib, in combination. Therefore, it can be stated that combination of olaparib with bortezomib might result in higher therapeutic efficacy in chemosensitive ovarian cancer compared to drugs alone. Also, the addition of

bortezomib to olaparib treatment might only lead to a slight increase in cytotoxicity in chemoresistant ovarian cancer cells.

When the bortezomib and olaparib combination treatment is applied with cisplatin, we see that combination treatment does not significantly decrease cell viability in chemosensitive ovarian cancer cell lines, since cisplatin treatment alone is already highly effective itself. In OV2008 chemosensitive cell line, bortezomib might decrease cell viability to a certain extent when applied with cisplatin; however, olaparib treatment does not contribute to cytotoxicity in this case. In A2780 chemosensitive cell line, both bortezomib and olaparib do not significantly affect the cellular viability when combined with cisplatin.

In C13 chemoresistant cell line, both bortezomib and olaparib further decrease cell viability when combined with cisplatin. Similarly, in the other chemoresistant cell line, A2780-AD, both drug treatments might lead to a lower cell viability when used together with cisplatin. Therefore, it can be pointed out that in the presence of cisplatin, combination treatment is mostly effective on chemoresistant cell lines (C13, A2780-AD) when compared to drugs alone.

In flow cytometry data, we observed that bortezomib and olaparib combination treatment leads to increased apoptotic cell death relative to drugs alone in OV2008 chemosensitive cell line. We also saw that the combination of bortezomib and olaparib with cisplatin resulted in increased cell death compared to bortezomib and olaparib combination treatment in this cell line. Considering previous data, this should be mostly due to cisplatin which is already highly effective on chemosensitive ovarian cancer cell lines. Therefore, it can be stated that olaparib and bortezomib combination treatment does not further increase cytotoxicity compared to cisplatin alone in OV2008 chemosensitive cell line; however, olaparib and bortezomib combination increases cell death compared to single agent treatments. This result points to the fact that patients who respond to olaparib treatment but not to cisplatin might benefit from bortezomib + olaparib combination compared to olaparib only treatment. However, for patients who respond to cisplatin treatment, bortezomib + olaparib treatment might not be a preferable clinical option. A more concrete inference based on this data requires *in vivo* experiments performed in mouse models. Considering the cellular and inter-patient heterogeneity in ovarian cancer (most generally in cancer), personalized treatment alternatives should be developed for patients with various chemosensitivity profiles, since chemosensitivity characteristics of cancer cells also influence their response to treatment as also shown in the present study (30-33). In C13 cell line, we saw that combination treatment did not result in increased cell death compared to drugs alone and this is in line with previous experiments. In previous experiments, we saw that in the presence of cisplatin, the effect of bortezomib and olaparib combination treatment was higher in C13 cell line compared to OV2008 cell line; but, in flow cytometry, we saw that cisplatin addition did not increase cell death compared to bortezomib and olaparib treatment.

CONCLUSION

In conclusion, our data shows that combination treatment is particularly effective on chemosensitive ovarian cancer cell lines in the absence of cisplatin. However, when combined with cisplatin, olaparib and bortezomib combination treatment shows its effect especially on chemoresistant ovarian cancer cell lines. As a result, combinatorial inhibition of PARP and proteasome by olaparib and bortezomib can be tested *in vivo* on chemoresistant ovarian cancer which are also treated with cisplatin to overcome cisplatin resistance in these ovarian cancer cell lines. Since the data provided in the current study were obtained using *in vitro* cell line models, *in vivo* studies performed on animal models should be required in the future to make stronger inferences about the effect of combinatorial treatment with bortezomib and olaparib on ovarian cancer.

Peer-review: Externally peer-reviewed.

Author Contributions: Conception/Design of study: B.K., M.U., E.C.; Data Acquisition: C.B., E.Y., E.C.; Data Analysis/Interpretation: C.B., E.C.; Drafting Manuscript: C.B.; Critical Revision of Manuscript: E.C.; Final Approval and Accountability: C.B., E.C.; Supervision: E.C.

Conflict of Interest: The authors declare that they have no conflicts of interest to disclose.

Financial Disclosure: This work was supported by 2209-A program of Scientific and Technological Research Council of Turkey (TUBITAK) (1919B011700125). C.B. is funded by TUBITAK 2211-E graduate student program.

Acknowledgement: Authors declare no conflicts of interest. Authors would like to thank Master's student Muhsine OZEN for her support.

REFERENCES

1. Bray F, Ferlay J, Soerjomataram I, Siegel RL, Torre LA, Jemal A. Global cancer statistics 2018: GLOBOCAN estimates of incidence and mortality worldwide for 36 cancers in 185 countries. *CA Cancer J Clin* 2018; 68(6): 394-424.
2. Berkel C, Cacan E. In silico analysis of DYNLL1 expression in ovarian cancer chemoresistance. *Cell Biol Int* 2020; 44(8): 1598-605.
3. Ali MW, Cacan E, Liu Y, Pierce JY, Creasman WT, Murph MM, Govindarajan R, Eblen ST, Greer SF, Hooks SB. Transcriptional suppression, DNA methylation, and histone deacetylation of the regulator of G-protein signaling 10 (RGS10) gene in ovarian cancer cells. *PLoS One* 2013; 8(3): e60185.
4. Cacan E, Ali MW, Boyd NH, Hooks SB, Greer SF. Inhibition of HDAC1 and DNMT1 modulate RGS10 expression and decrease ovarian cancer chemoresistance. *PLoS One* 2014; 9(1): e87455.
5. European Medicines Agency. Lynparza summary of product characteristics, 2018; Available at: http://ec.europa.eu/health/documents/community-register/2018/20180508140545/anx_140545_en.pdf.
6. Morales J, Li L, Fattah FJ, Dong Y, Bey EA, Patel M, et al. Review of poly (ADP-ribose) polymerase (PARP) mechanisms of action and rationale for targeting in cancer and other diseases. *Crit Rev Eukaryot Gene Expr* 2014; 24(1): 15-28.

7. Vescarelli E, Gerini G, Megiorni F, Anastasiadou E, Pontecorvi P, Solito L, et al. MiR-200c sensitizes Olaparib-resistant ovarian cancer cells by targeting Neuropilin 1. *J Exp Clin Cancer Res* 2020; 39(1): 3.
8. Wang L, Shi C, Wright FA, Guo D, Wang X, Wang D, et al. Multifunctional telodendrimer nanocarriers restore synergy of bortezomib and doxorubicin in ovarian cancer treatment. *Cancer Res* 2017; 77(12): 3293-305.
9. Cacan E, Spring AM, Kumari A, Greer SF, Garnett-Benson C. Combination treatment with sublethal ionizing radiation and the proteasome inhibitor, bortezomib, enhances death-receptor mediated apoptosis and anti-tumor immune attack. *Int J Mol Sci* 2015; 16(12): 30405-21.
10. Takenaka M, Saito M, Iwakawa R, Yanaiharu N, Saito M, Kato M, et al. Profiling of actionable gene alterations in ovarian cancer by targeted deep sequencing. *Int J Oncol* 2015; 46(6): 2389-98.
11. Anglesio MS, Wiegand KC, Melnyk N, Chow C, Salamanca C, Prentice LM, et al. Type-specific cell line models for type-specific ovarian cancer research. *PLoS One* 2013; 8(9): e72162.
12. Beaufort CM, Helmijr JC, Piskorz AM, Hoogstraat M, Ruigrok-Ritstier K, Besselink N, et al. Ovarian cancer cell line panel (OCCP): clinical importance of in vitro morphological subtypes. *PLoS One* 2014; 9(9): e103988.
13. Vichai V, Kirtikara K. Sulforhodamine B colorimetric assay for cytotoxicity screening. *Nat Protoc* 2006; 1(3): 1112-6.
14. Skehan P, Storeng R, Scudiero D, Monks A, McMahon J, Vistica D, et al. New colorimetric cytotoxicity assay for anticancer-drug screening. *J Natl Cancer Inst* 1990; 82(13): 1107-112.
15. R Core Team. R: A language and environment for statistical computing. R Foundation for Statistical Computing, 2018; Vienna, Austria. URL <https://www.R-project.org/>.
16. Golemund G, Wickham H. R for data science, 2016; 1st edition. California: O'Reilly.
17. Holmes S, Huber W. Modern statistics for modern biology, 2019; 1st edition. Cambridge: Cambridge University Press.
18. Wickham H. tidyverse: Easily Install and Load the 'Tidyverse'. R package version, 2017, 1.2.1. <https://CRAN.R-project.org/package=tidyverse>
19. Wickham H and Bryan J. readxl: Read Excel Files. R package version 1.3.1, 2019. <https://CRAN.R-project.org/package=readxl>
20. Soetaert K. plot3D: Plotting Multi-Dimensional Data. R package version 1.3, 2019. <https://CRAN.R-project.org/package=plot3D>
21. Ooms J. magick: Advanced graphics and image-processing in R. R package version 2.4.0, 2020. <https://CRAN.R-project.org/package=magick>
22. Auguie B. gridExtra: Miscellaneous functions for "Grid" graphics. R package version 2.3, 2017. <https://CRAN.R-project.org/package=gridExtra>
23. Kassambara A. ggpubr: 'ggplot2' Based Publication Ready Plots. R package version 0.4.0, 2020. <https://CRAN.R-project.org/package=ggpubr>
24. Xie Y, Allaire JJ, Golemund G. R Markdown: The Definitive Guide. Chapman and Hall/CRC, 2018. ISBN 9781138359338. URL <https://bookdown.org/yihui/rmarkdown>.
25. Xie Y, Dervieux C, Riederer E. R Markdown Cookbook. Chapman and Hall/CRC, 2020. ISBN 9780367563837. URL <https://bookdown.org/yihui/rmarkdown-cookbook>.
26. He YJ, Meghani K, Caron MC, Yang C, Ronato DA, Bian J, et al. DYNLL1 binds to MRE11 to limit DNA end resection in BRCA1-deficient cells. *Nature* 2018; 563(7732): 522-6.
27. Janyst K, Janyst M, Siernicka M, Lasek W. Synergistic antitumor effects of histone deacetylase inhibitor scriptaid and bortezomib against ovarian cancer cells. *Oncol Rep* 2018; 39(4): 1999-2005.
28. Wang L, Shi C, Wright FA, Guo D, Wang X, Wang D, et al. Multifunctional telodendrimer nanocarriers restore synergy of bortezomib and doxorubicin in ovarian cancer treatment. *Cancer Res* 2017; 77(12): 3293-305.
29. Berkel C, Cacan E. GAB2 and GAB3 are expressed in a tumor stage-, grade- and histotype-dependent manner and are associated with shorter progression-free survival in ovarian cancer. *J Cell Commun Signal* 2020; 10.1007/s12079-020-00582-3.
30. Berkel C, Cacan E. Single-cell epigenomics in cancer research. *Biomed J Sci&Tech Res* 2019; 21(3).
31. Kroeger PT, Jr, & Drapkin R. Pathogenesis and heterogeneity of ovarian cancer. *Curr Opin Obstet Gynecol* 2017; 29(1): 26-34.
32. Winterhoff BJ, Maile M, Mitra AK, Sebe A, Bazzaro M, Geller MA, et al. Single cell sequencing reveals heterogeneity within ovarian cancer epithelium and cancer associated stromal cells. *Gynecol Oncol* 2017; 144(3): 598-606.
33. Shih AJ, Menzin A, Whyte J, Lovecchio J, Liew A, Khalili H, et al. Identification of grade and origin specific cell populations in serous epithelial ovarian cancer by single cell RNA-seq. *PLoS One* 2018; 13(11): e0206785.

Effects of *Nigella sativa* on Plasma Oxidative Stress, and Some Apoptotic Protein Markers in Cerebrum and Hippocampus in Pentylentetrazol-Induced Kindling Rats

Savas Ustunova¹ , Ismail Meral¹ , Abdurrahim Kocyigit² , Aysu Kilic¹ ,
Oyku Zeybek¹ , Mehmet Uyuklu³ , Sedat Meydan⁴ 

¹Bezmi Alem Vakıf University, School of Medicine, Department of Physiology, Istanbul, Turkey

²Bezmi Alem Vakıf University, School of Medicine, Department of Biochemistry, Istanbul, Turkey

³Siirt University, School of Medicine, Department of Physiology, Siirt, Turkey

⁴Bezmi Alem Vakıf University, School of Medicine, Department of Anatomy, Istanbul, Turkey

ORCID IDs of the authors: S.U. 0000-0003-1870-229X; I.M. 0000-0002-0973-4305; A.K. 0000-0003-2335-412X; A.K. 0000-0002-8593-1415; O.Z. 0000-0002-4554-3995; M.U. 0000-0002-7100-9817; S.M. 0000-0002-1393-3235

Please cite this article as: Ustunova S, Meral I, Kocyigit A, Kilic A, Zeybek O, Uyuklu M, Meydan S. Effects of *Nigella sativa* on Plasma Oxidative Stress, and Some Apoptotic Protein Markers in Cerebrum and Hippocampus in Pentylentetrazol-Induced Kindling Rats. Eur J Biol 2020; 79(2): 124-131. DOI: 10.26650/EurJBiol.2020.0088

ABSTRACT

Objective: This study was designed for investigating the effectiveness of the *Nigella sativa* (*N. sativa*) extract on apoptosis in cerebrum and hippocampus and also plasma oxidative stress, in pentylentetrazol (PTZ)-induced kindling rats.

Materials and Methods: The kindling model was induced by subconvulsive doses (35 mg/kg i.p.) of intraperitoneal PTZ injections in *N. sativa* treated and non-treated PTZ groups (PTZ and PTZ + NS). The PTZ + NS group were also treated with an extract of *N. sativa* (10 mg/kg) 2 h before each PTZ injection. The total oxidant and antioxidant status, oxidative stress index, paraoxonase, arylesterase, catalase (CAT) and total thiol levels were analyzed in plasma. Brain derived neurotrophic factor (BDNF), cyclin-B1 and B-cell lymphoma 2 (Bcl-2) expressions were investigated in the cerebrum and hippocampus.

Results: PTZ decreased the oxidative stress by increasing the activities of CAT, arylesterase, and paraoxonase. *N. sativa* decreased activities of arylesterase, paraoxonase, while increasing the CAT. It also brought the decreased BDNF and Bcl-2 expression levels to their normal levels in the cerebrum but not in the hippocampus.

Conclusion: *N. sativa* treatment improved the PTZ induced-impairments in BDNF and Bcl-2 expressions, resulting in a neuronal apoptosis in the cerebrum, without affecting blood oxidative stress.

Keywords: Apoptosis, epilepsy, cerebrum, hippocampus, *N. sativa*, oxidative stress

INTRODUCTION

Epilepsy is a neurological disease which affects millions of people with different ages worldwide (1). In recent years, many third-generation anti-epileptic drugs have been introduced. However, anti-epileptic drugs have some side effects including nausea, dizziness, and somnolence (2). Due to the fact that anti-epileptic drugs have some side effects and fail to control seizures in some patients, new therapies with lesser side effects

have been investigated by researchers. Plant-origin therapies are especially popular nowadays due to their minimal side effects. Among them, *Nigella sativa* (*N. sativa*) is regarded as a kind of miracle herb since many scientists have revealed its vast spectrum of pharmacological potentials (3). In particular, studies on antiepileptic effects of *N. sativa* or one of its active constituents, thymoquinone, are popular. In many previous studies, the potent anti-epileptic role of *N. sativa* was investigated (4,5).



Corresponding Author: Ismail Meral

E-mail: imeral@bezmialem.edu.tr

Submitted: 13.10.2020 • **Revision Requested:** 07.11.2020 • **Last Revision Received:** 09.11.2020 •

Accepted: 12.11.2020 • **Published Online:** 21.12.2020

© Copyright 2020 by The Istanbul University Faculty of Science • Available online at <http://ejb.istanbul.edu.tr> • DOI: 10.26650/EurJBiol.2020.0088

Kindling is one of the most studied and well-understood chronic animal models of epilepsy, generated either by a chemical or an electrical stimulus which is applied in subconvulsive doses repetitively and finally causes the generation of a chronic epilepsy model. Regular administration of pentylenetetrazol (PTZ) in subconvulsive doses triggers convulsions by causing decreased inhibitory or increased excitatory effects, which is called PTZ kindling (6).

Oxidative stress can trigger remarkable damage in the nervous system. Production of reactive oxygen species (ROS) in particular may cause multiple neuronal injuries that include lipid destruction of the cellular membrane, the cleavage of DNA, cell membrane lipid peroxidation and protein oxidation. In addition to the destruction of cellular integrity, ROS may also interrupt mitochondrial respiration (7). The endogenous antioxidant enzymes, such as catalase (CAT), arylesterase, paraoxonase and thiol are vital for compensating oxidative stress (8-10). Their amounts in serum or tissue are important for elucidating the oxidant-antioxidant balance. It has been shown that *N. sativa*, which contains many antioxidant compounds such as thymoquinone, has a neuroprotective effect on the brain by reducing oxidative stress (11).

Brain derived neurotrophic factor (BDNF) is one of the most important growth factors in the central nervous system (CNS). It has a few different biologically active isoforms, which also interact with different receptor types (12). It is vital for the development of the CNS and for brain plasticity (13). Due to the fact that BDNF plays a crucial role in CNS, it has close relationships with any disease that affects the brain, such as epilepsy. The B-cell lymphoma 2 (Bcl-2) protein family has vital roles in cells, especially in the process of apoptosis. Bcl-2 itself is an anti-apoptotic protein from the Bcl-2 family and its amount is directly proportional to the vitality of the cell. Increment levels in the Bcl-2 protein lead to the survival of the cell via inhibiting apoptosis. Additionally, cyclins and cyclin-dependent kinases, CDKs, are the basic regulators for the cell cycle and their amount regulates cell-cycle events, such as neurogenesis, progression of cell to apoptosis and maintaining the health of CNS and are also shown to take part in many pathophysiological process in CNS including epilepsy (14).

Therefore, this study was planned for investigating the effects of *N. sativa* extract on plasma oxidative stress, and some apoptotic and cell-cycle protein markers in cerebrum and hippocampus in PTZ-induced kindling rats.

MATERIALS AND METHODS

Chemicals

A physiological saline solution was used to dissolve the PTZ (Sigma-Aldrich Co., St. Louis, MO, USA). PTZ was injected intraperitoneally (i.p). *N. sativa* seeds were obtained from a local herbal market. The seeds were ground by a classical grinder (MC 23200, Siemens-Elektrogeräte GmbH, Hamburg, Germany), and its methanolic extract was prepared as described previously (15). Four ml sterile physiological saline solution was used to dissolve 10 mg of lyophilized extract to have a stock solution which then was administered to animals by gastric gavage in adequate volumes.

Animals and Experimental Design

Twenty one male adult Wistar albino rats (230–300 g) were used in our study. The rats were obtained from Bezmalem Vakif University's Experimental Animal Centre and housed under standard temperature (25±1°C), humidity (50–60%), dark-light conditions (12 h light/12 h dark cycle) and fed *ad libitum*. Ethical approval was obtained from the Bezmalem Vakif University Laboratory Animals Ethics Committee. The rats were divided into 3 groups: a control group (C, n=7); PTZ treated (PTZ, n=7) and PTZ + *N. sativa* treated (PTZ + NS, n=7). PTZ-kindling model was achieved for the PTZ and PTZ + NS groups by multiple PTZ injections in a subconvulsive dose of 35 mg/kg on days 1, 3, 5, 8, 10, 12, 15, 17, 19, 22 and 24 of the study. Ten mg/kg methanolic extract of *N. sativa* was administered to the rats in the PTZ + NS group by oral gavage, just 2 hours before PTZ injection. The control group was only treated with 4 ml/kg saline. Seizures were observed after 30 minutes following PTZ administration. After establishment of the kindling model, convulsive doses of PTZ (75 mg/kg) were injected to the PTZ and PTZ + NS groups to induce tonic and clonic seizures on the 26th day of the study. The control group was not injected with PTZ. For the PTZ + NS group, convulsive doses of PTZ were injected 2 hours after *N. sativa* extract (10 mg/kg) administration. For describing the characteristics of the behavioral seizure, a modified scale was used (data not shown) (16). Upon the completion of the experiment, the rats were anesthetized (15 mg/kg xylazine and 50 mg/kg ketamine), decapitated, and the hippocampi and cerebrum were dissected for Western blot and biochemical analysis. The samples were stored at -80°C.

Blood Sampling

The blood was drawn by cardiac puncture into heparinized tubes, and stored at +4 °C. The blood samples were centrifuged at 3.500 x g for 5 minutes. The plasma samples were stored at -80°C until the analysis of paraoxonase, arylesterase and CAT activities, and total thiol, total oxidant and antioxidant status (TOS and TAS) levels.

Analysis of Oxidant Markers

Total Oxidant and Antioxidant Status

The TOS and TAS levels were measured by commercial kits using spectrophotometric methods according to manufacturer instruction (Rel Assay Diagnostics, Gaziantep, Turkey). A 1420 Victor 3 Multilabel Plate Reader was used for the spectrophotometric analysis (PerkinElmer, Waltham, MA, USA). The test results of TOS were demonstrated in terms of µm H₂O₂ Equiv/L, and the test results of TAS were demonstrated in terms of µm Trolox Equiv/L.

Calculation of Oxidative Stress Index (OSI)

Following the measurement of TOS and TAS values, the results were calculated according to the formula below and demonstrated as an arbitrary unit.

$$\text{Oxidative Stress Index (OSI)} = \frac{\text{TOS } (\mu\text{mol. H}_2\text{O}_2 \text{ Equivalent/L})}{\text{TAS } (\mu\text{mol. Trolox. Equivalent/L})} \times 100$$

Paraoxonase and Arylesterase Activities

The activities of paraoxonase and arylesterase were assayed

by a commercial kit (Rel Assay Diagnostics, Gaziantep, Turkey). Two different substrates were used for the paraoxonase-1 activity. Owing to the formation of p-nitrophenol, the paraoxon hydrolysis rate was calculated by recording the increment in absorbance at 412 nm, 25°C. Paraoxonase-1 activity was defined as 1 mmol p-nitrophenol generated per minute under standard conditions and demonstrated as U/L (17). Arylesterase activity was demonstrated in terms of kU/L and it was identified as 1 mmol of phenol generated per minute under standard reaction conditions. No enzyme was added to blanks and they were used to correct the spontaneous hydrolysis of both substrates (18).

Catalase Activity

A gasometric procedure, which measures the amount of oxygen produced by the decomposition of H₂O₂ was performed for assessing CAT activity. The activity of CAT was established by the decrease in H₂O₂ absorbance at 240 nm. A multiplate reader was used for assessment (Varioskan Flash Multimode Reader; Thermo Fisher Scientific, Waltham, MA).

Total Thiol Measurement

Natural thiol and total thiol, as well as disulfide levels, were measured with a new automated method (19). The new method is based on the reduction of disulfide bonds to thiol groups and sulfhydryl groups of proteins, converting them to the reversible disulfide form under oxidative conditions. The final diagnosis was approved by histopathological testing. The findings of the appendectomy sample histopathology were classified as non-perforated or perforated appendicitis.

Western Blotting Assay

The hippocampus and cerebrum regions of the brains were surgically removed and homogenized in a lysis buffer containing pro-

tease inhibitor cocktails (MP FastPrep-24, MP Biomedicals, Irvine, CA USA). Then the homogenates were centrifuged at 14.000 x rpm (Beckman Coulter, Krefeld, Germany) at 4°C for 10 minutes and the cytosolic fraction was separated as the final supernatant. The Bradford assay was used to assess protein concentrations in the supernatants. A 5× loading buffer was added to the above-mentioned supernatant and boiled at 100°C for 15 minutes (19). Protein content was then separated on 8–12% sodium SDS-PAGE, transferred to a membrane made of PVDF, and then incubated with both primary and secondary antibodies conjugated with horseradish peroxidase (Cell Signaling Technology, Denver, MA, USA). Separated protein bands were made visible by Pierce ECL Western blotting substrate (Thermo Fisher Scientific, Waltham, MA, USA) on secondary antibodies for BDNF, cyclin-B1, Bcl-2 and β-tubulin (Santa Cruz, Biotechnology, Dallas, TE, USA).

Statistical Analysis

All data were analyzed statistically using GraphPad Prism 6.0 (GraphPad Prism Software, San Diego, CA, USA), and demonstrated as mean ± standard error of mean (mean ± SEM). One-Way ANOVA and Student's *t*-test were used to analyze results in order to compare groups. The *p*<0.05 value was considered to be statistically significant.

RESULTS

Oxidant Markers

The plasma TAS, TOS and OSI levels of the study groups are shown in Figure 1. The plasma TOS levels of PTZ and PTZ + NS groups were significantly lower (*p*<0.01) than controls (Figure 1B). Although the plasma OSI level was significantly (*p*<0.05) lower in PTZ group, it was not statistically different (*p*>0.05) in PTZ + NS group compared to controls (Figure 1C).

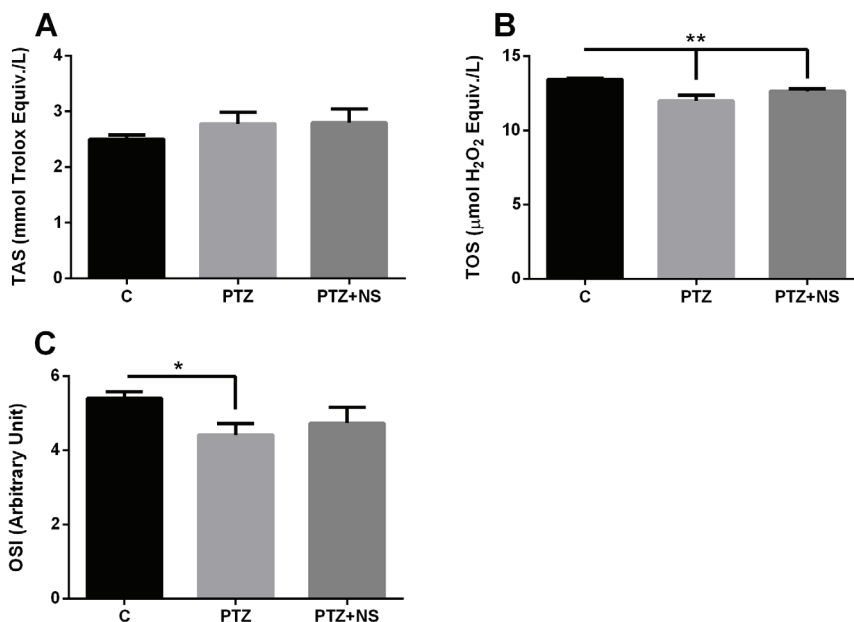


Figure 1. The plasma TAS (A), TOS (B) and OSI (C) levels of the study groups (n=7). Data is presented as mean ± standard error of mean. TOS; Total Oxidant Status, TAS; Total Antioxidant Status, OSI; Oxidative Stress Index. *, *p*<0.05, **, *p*<0.01.

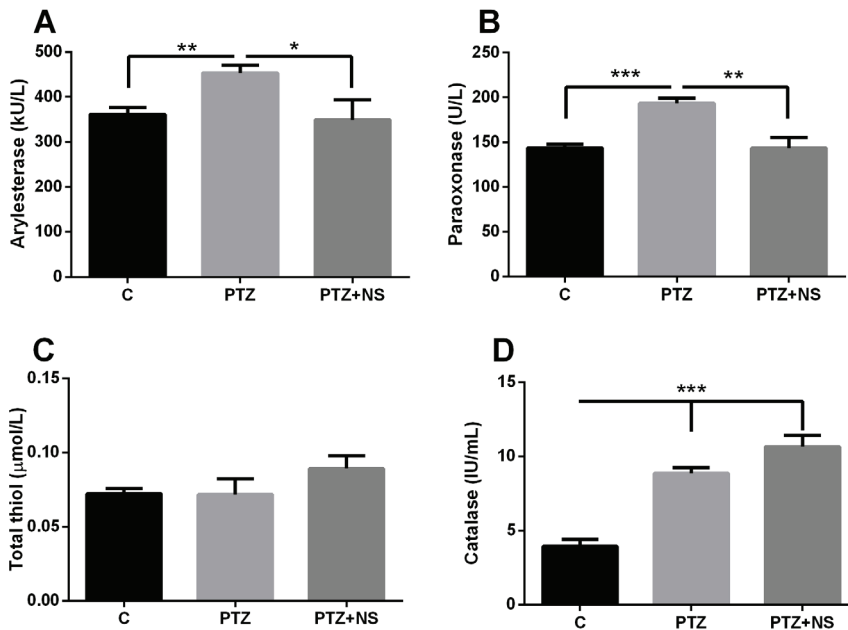


Figure 2. The plasma arylesterase (A), paraoxonase (B), total thiol (C) and CAT (D) levels of groups (n=7). Data is presented as mean ± standard error of mean. CAT; Catalase. *, $p < 0.05$, **, $p < 0.01$, ***, $p < 0.001$.

Antioxidant Markers

The plasma arylesterase, paraoxonase and CAT activities, and total thiol levels of groups are shown in Figure 2. The plasma arylesterase activity significantly ($p < 0.01$) increased in the PTZ group compared to the C group. But it decreased ($p < 0.05$) in PTZ + NS group compared to PTZ group, there was no significant difference ($p > 0.05$) between the C and PTZ + NS groups (Figure 2A). Similar results were also obtained regarding plasma paraoxonase activity. It significantly ($p < 0.001$) increased in

PTZ group compared to the C group. But it decreased ($p < 0.01$) in the PTZ + NS group compared to PTZ group, there was no significant difference ($p > 0.05$) between the C and PTZ + NS groups (Figure 2B). Although the plasma total thiol level tended to increase in the PTZ and PTZ + NS groups compared to the controls, it was not different ($p > 0.05$) among the groups (Figure 2C). However, the plasma CAT activity significantly ($p < 0.001$) increased in both PTZ and PTZ + NS groups compared to the controls (Figure 2D).

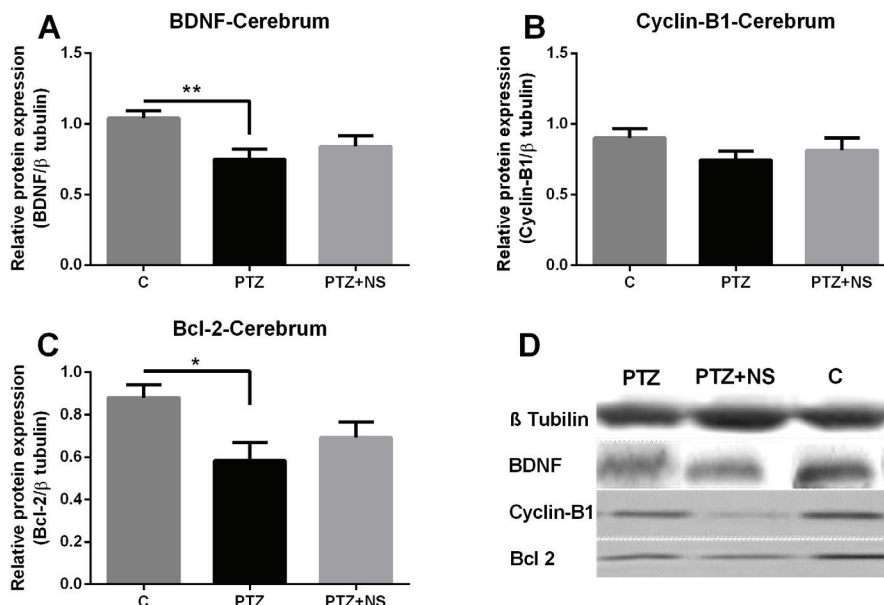


Figure 3. The Western blotting assay results of BDNF (A), Cyclin-B1 (B), Bcl-2 (C) and the image of related bands (D) in cerebrums of groups (n=7). Data is presented as mean ± standard error of mean. BDNF; Brain derived neurotrophic factor, Bcl-2; B-cell lymphoma 2. *, $p < 0.05$, **, $p < 0.01$.

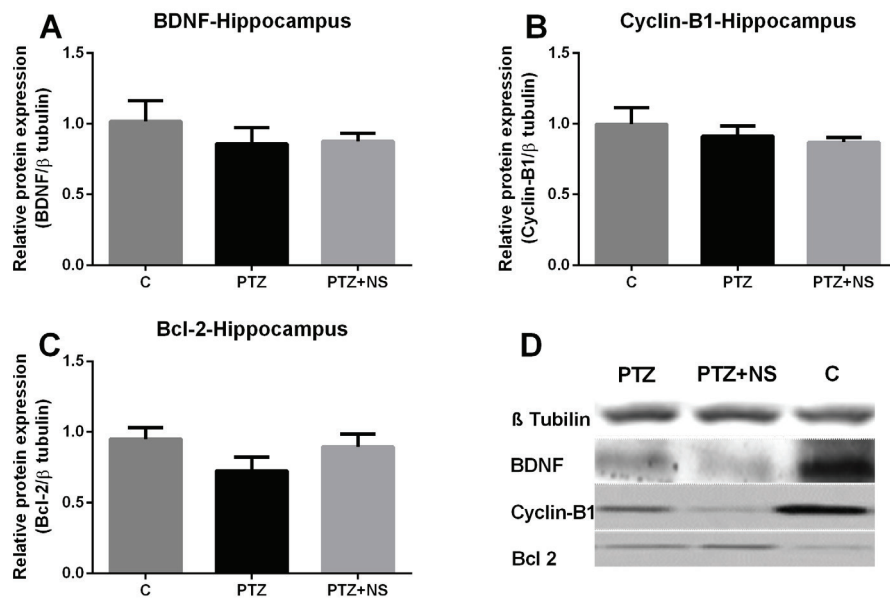


Figure 4. The Western blotting assay results of BDNF (A), Cyclin-B1 (B), Bcl-2 (C) and the image of related bands (D) in hippocampus of groups (n=7). Data is presented as mean \pm standard error of mean. BDNF; Brain derived neurotrophic factor, Bcl-2; B-cell lymphoma 2.

Western Blotting Assay

Western blotting assay results of cerebrum are shown in Figure 3. The protein expression levels of BDNF (Figure 3A) and Bcl-2 (Figure 3C) significantly ($p < 0.01$ and $p < 0.05$, respectively) decreased in the PTZ group compared to the controls. However, there was no significant ($p > 0.05$) difference between C and PTZ + NS groups in terms of BDNF or Bcl-2 protein expression levels. In addition, the level of cyclin-B1 protein expression was not different ($p > 0.05$) among the groups (Figure 3B).

Western blotting assay results of hippocampus are shown in Figure 4. There was no statistical ($p > 0.05$) difference among groups regarding BDNF, cyclin-B1 or Bcl-2 protein expression levels.

DISCUSSION

This study is a part of our previously published study (20) and was designed for investigating the effects of *N. sativa* extract on some plasma oxidant and antioxidant markers in PTZ-induced kindling rats. It was found that the PTZ treatment decreased the plasma oxidative stress by increasing the activities of arylesterase, paraoxonase and CAT. It is well known that oxidative stress has a crucial role in the pathogenesis of epilepsy (21). Some studies indicated that oxidative stress increased in PTZ-induced epilepsy (22,23). However, our findings contrast with the findings of previous studies in the literature. This might be due to high plasma antioxidant arylesterase, paraoxonase and CAT activities that reduced the oxidative stress in the PTZ group. Exogenous antioxidant *N. sativa* treatment, on the other hand, decreased the activities of endogenous antioxidant enzymes arylesterase and paraoxonase. To maintain homeostasis, when animal or human cells are subjected to mild biological stress, they activate cellular and physiological processes (24).

Increased production of endogenous antioxidant enzymes in response to mild biological stress protects the organism from intense oxidative stress produced by heavy metals, toxic substances or pro-oxidant compounds (25). Low doses of various stress producing agents may disturb the physiological parameters of an organism but may not induce severe damage. It may improve the ability of an organism to resist severe stresses by inducing adaptive responses, and has actually a beneficial effect, which is called hormesis (26). Hormetic response is formed when cells or organisms are exposed to mild biological stress, such as caloric restriction, exercise, environmental toxins and inorganic compounds (27). The dose of PTZ used in this experiment for 11 treatments was subconvulsive (35 mg/kg), and only the final (12th treatment) was convulsive (75 mg/kg). Therefore, it might be said that the subconvulsive dose of PTZ produced a hormetic response that increased the antioxidants arylesterase, paraoxonase and CAT activities leading to a reduction in the oxidative stress in PTZ group compared to the controls.

Theoretically, intake of exogenous antioxidants should support the endogenous defence system by decreasing oxidative damage. However, in our study, exogenous antioxidant *N. sativa* treatment decreased the elevated-activities of endogenous antioxidants arylesterase and paraoxonase, with no net change in OSI level. The endogenous antioxidants are produced in the body, and many of them are encoded by the nuclear factor erythroid 2-related factor 2 (Nrf2) - keap1 (kelch-like ECH-associated protein 1) pathway (28,29). It has been commonly suggested that thymoquinone, an active biological form of *N. sativa*, serves antioxidant activity and reduces lipid peroxidation by increasing the production of antioxidant enzymes and the expression of Nrf2 in many tissues (30,31). Hamdan, Al-Gayyar (32) suggested that the exposure of rats' brain tissues to TQ

ameliorated the sodium nitrite-induced oxidative stress, and increased the lowered Nrf2 expression and antioxidant enzymes. However, in our experiment, PTZ treatment did not induce oxidative stress or decrease in the antioxidant enzyme activities. Conversely, it lowered the oxidative stress by increasing the antioxidant enzyme activities. Subsequently, the *N. sativa* treatment decreased the elevated-activities of endogenous antioxidants arylesterase and paraoxonase in PTZ-treated rats. From the results of our present, and also previous studies it might be said that *N. sativa* had dual effects on antioxidant enzyme activities (20). It increases the antioxidant enzyme activity when their activities are low but it decreases the antioxidant enzyme activity when their activities are high. Similar to our finding, it has been reported that exogenous antioxidants may downregulate the endogenous protection, thus causing no net change in antioxidant defences (33).

In this study, the exogenous antioxidant *N. sativa* treatment increased the CAT level further. CAT is a ubiquitous antioxidant enzyme that is present in nearly all living organisms. It is active in the detoxification of H_2O_2 in human erythrocytes (34). Increased CAT activity by *N. sativa* treatment may be an attempt by the body to compensate for the low antioxidant (arylesterase and paraoxonase) effect, or may be a direct effect of *N. sativa* treatment. There are studies indicating that *N. sativa* treatment increased CAT activity (35,36).

The second aim of this study was to examine the effects of *N. sativa* extract on the expression levels of some apoptotic proteins in both cerebrum and hippocampus in PTZ-induced kindling rats. In the cerebrum, the protein expression levels of Bcl-2 and BDNF decreased but cyclin-B1 level did not change in the PTZ group compared to the controls. *N. sativa* extract treatment brought the levels of Bcl-2 and BDNF to normal. BDNF is a small dimeric protein that is responsible for the growth of neurons. Its most common site is the hippocampus and the cerebral cortex. It has a protective effect on neurons and is associated with neuroplasticity (37). Decreased BDNF levels correlate with many neurodegenerative diseases that exhibit neuronal loss (38). A number of studies have shown that both BDNF and its specific receptor tropomyosin receptor kinase B (TrkB) expression increases in epilepsy models (39-43). Current studies suggest that serum BDNF is constantly higher in patients with epilepsy and appears to be associated with the pathology of the disease. Hong et al. indicated that the concentration of the serum BDNF is proportional with the severity of the disease (44). It has been reported that BDNF levels significantly decreased during the interictal period of epilepsy in patients with cerebral autoregulation and autonomic function impairment. Severe and long-term epilepsy may disrupt BDNF signalling, thus causing impaired cerebral autoregulation and autonomic dysfunction in patients with epilepsy. It has been demonstrated that acute administration of BDNF, both in vivo and in vitro, induces the neuronal excitability and facilitates epileptogenesis (45).

Bcl-2 is a cell survival protein whose main role is to inhibit apoptosis by preventing the cytochrome c release and the activation

of caspases (46). The levels, and also interactions of Bcl-2 with other pro-apoptotic proteins are critical for the vitality of a neuron. Under certain cellular stress, Bcl-2/pro-apoptotic protein ratio decreases, leading to apoptosis (47). PTZ is a neurotoxic agent that causes neuronal stress and provokes kindling. Similarly, Shi et al. indicated that PTZ treatment decreased the expression of the Bcl-2 protein (22). The decreased expressions of Bcl-2 and BDNF in the cerebrum of PTZ-treated rats indicated an increased apoptosis. The *N. sativa* treatment reversed the decreased-expression of Bcl-2 and BDNF to normal levels, indicating the prevention of tissue from apoptosis. Hosseini et al. demonstrated that thymoquinone, an active compound of *N. sativa*, may decrease Bax/Bcl-2 ratio, thus reducing the severity of apoptosis under stress conditions, such as ethanol toxicity (48). Ullah et al. demonstrated that PTZ treatment decreased the expression of Bcl-2 and pre-treatment with thymoquinone reversed that decrement by upregulating Bcl-2 and also down-regulating pro-apoptotic Bax (49).

Cyclin-B1 is among the most important core cell-cycle regulators. There is a link between the cell-cycle and neuronal death. Neuronal cell death that was accompanied by cyclin-B1 expression was reported in the hippocampal field of PTZ-kindled rats (50). Although BDNF and Bcl-2 expressions in the cerebrum were affected as indicated before, cyclin-B1 expression was not affected by PTZ-treatment in our study.

We obtained different results in hippocampus than those in the cerebrum, regarding expressions of Bcl-2 and BDNF proteins in PTZ-treated rats. Although their expression levels were not different in groups of hippocampus tissues, they decreased in cerebrum tissues of PTZ-treated rats. This indicated that apoptosis occurred in the cerebrum but did not occur in the hippocampus of PTZ-treated rats. These results are similar to the results of our previous study, which demonstrated that PTZ treatment caused a neuronal loss due to apoptosis in the cerebral cortex, but not in the hippocampus (20). From the results of both studies, it might be said that apoptotic neuron numbers of the cerebrum increases in PTZ-kindling epileptic rats due to the decreased expression of Bcl-2 and BDNF proteins. The *N. sativa* brought the decreased-expression levels of Bcl-2 and BDNF back to normal.

CONCLUSION

It was concluded that the *N. sativa* treatment improved the PTZ-induced impairments in BDNF and Bcl-2 expressions that reflect a neuronal apoptosis in the cerebrum, without affecting blood oxidative stress.

Peer-review: Externally peer-reviewed.

Author Contributions: Conception/Design of study: S.U., I.M.; Data Acquisition: S.U., I.M., A.K., A.K., O.Z., M.U.; Data Analysis/Interpretation: S.U., I.M., A.K., A.K., O.Z., M.U.; Drafting Manuscript: S.U., I.M., A.K., O.Z.; Critical Revision of Manuscript: S.U., I.M., A.K., M.U., S.M.; Final Approval and Accountability: S.U., I.M.; Technical or Material Support: S.U., I.M.; Supervision: S.U., I.M.

Conflict of Interest: The authors declare that they have no conflicts of interest to disclose.

Financial Disclosure: This work was supported by the Research Fund of Bezmialem Vakif University [grant number 6.2013/8].

REFERENCES

1. Stafstrom CE, Carmant L. Seizures and epilepsy: an overview for neuroscientists. *Cold Spring Harbor Perspect Med* 2015; 5(6): a022426.
2. Anderson J, Moor C-C. Anti-epileptic drugs: a guide for the non-neurologist. *Clin Med (Lond)* 2010; 10(1): 54-8.
3. Ahmad A, Husain A, Mujeeb M, Khan SA, Najmi AK, Siddique NA, et al. A review on therapeutic potential of *Nigella sativa*: A miracle herb. *Asian Asian Pac J Trop Biomed* 2013; 3(5): 337-52.
4. Hosseinzadeh H, Parvardeh S, Nassiri-Asl M, Mansouri M-T. Intracerebroventricular administration of thymoquinone, the major constituent of *Nigella sativa* seeds, suppresses epileptic seizures in rats. *Med Sci Monit* 2005; 11(4): BR106-BR110.
5. İlhan A, Gurel A, Armutcu F, Kamisli S, Iraz M. Antiepileptogenic and antioxidant effects of *Nigella sativa* oil against pentylenetetrazol-induced kindling in mice. *Neuropharmacology* 2005; 49(4): 456-64.
6. Dhir A. Pentylenetetrazol (PTZ) kindling model of epilepsy. *Curr Protoc Neurosci* 2012; 58(1): 9-37.
7. Radad K, Rausch W-D, Gille G. Rotenone induces cell death in primary dopaminergic culture by increasing ROS production and inhibiting mitochondrial respiration. *Neurochem Int* 2006; 49(4): 379-86.
8. Chaudière J, Ferrali-liou R. Intracellular antioxidants: from chemical to biochemical mechanisms. *Food Chem Toxicol* 1999; 37(9-10): 949-62.
9. Haley RW, Billecke S, La Du BN. Association of low PON1 type Q (type A) arylesterase activity with neurologic symptom complexes in Gulf War veterans. *Toxicol Appl Pharmacol* 1999; 157(3): 227-33.
10. Hernández AF, Gil F, Lacasaña M, Rodríguez-Barranco M, Gómez-Martin A, Lozano D, et al. Modulation of the endogenous antioxidants paraoxonase-1 and urate by pesticide exposure and genetic variants of xenobiotic-metabolizing enzymes. *Food Chem Toxicol* 2013; 61: 164-70.
11. Hobbenaghi R, Javanbakht J, Sadeghzadeh S, Kheradmand D, Abdi F, Jaberli M, et al. Neuroprotective effects of *Nigella sativa* extract on cell death in hippocampal neurons following experimental global cerebral ischemia-reperfusion injury in rats. *J Neuro Sci* 2014; 337(1-2): 74-9.
12. Lucini C, D'Angelo L, Cacialli P, Palladino A, de Girolamo P. BDNF, brain, and regeneration: Insights from zebrafish. *Int J Mol Sci* 2018; 19(10): 3155.
13. Autry AE, Monteggia LM. Brain-derived neurotrophic factor and neuropsychiatric disorders. *Pharmacol Rev* 2012; 64(2): 238-58.
14. Wolgemuth DJ, Manterola M, Vasileva A. Role of cyclins in controlling progression of mammalian spermatogenesis. *Int J Dev Biol* 2013; 57: 159.
15. Ali BH, Blunden G. Pharmacological and toxicological properties of *Nigella sativa*. *Phytotherapy Research: An international journal devoted to pharmacological and toxicological evaluation of natural product derivatives*. *Phytother Res* 2003; 17(4): 299-305.
16. Eraković V, Župan G, Varljen J, Laginja J, Simonić A. Altered activities of rat brain metabolic enzymes caused by pentylenetetrazol kindling and pentylenetetrazol-induced seizures. *Epilepsy Res* 2001; 43(2): 165-73.
17. Eckerson HW, Wyte CM, La Du B. The human serum paraoxonase/arylesterase polymorphism. *Am J Hum Genet* 1983; 35(6): 1126.
18. Haagen L, Brock A. A new automated method for phenotyping arylesterase (EC 3.1.1.2) based upon inhibition of enzymatic hydrolysis of 4-nitrophenyl acetate by phenyl acetate. *Eur J Clin Chem Clin Biochem* 1992; 30(7): 391-6.
19. Kruger NJ. The Bradford method for protein quantitation. *Methods Mol Biol* 1994; (32): 9-15.
20. Meral I, Esrefoglu M, Dar K, Ustunova S, Aydin M, Demirtas M, et al. Effects of *Nigella sativa* on apoptosis and GABAA receptor density in cerebral cortical and hippocampal neurons in pentylenetetrazol induced kindling in rats. *Biotech Histochem* 2016; 91(8): 493-500.
21. Pearson-Smith J, Patel M. Metabolic dysfunction and oxidative stress in epilepsy. *Int J Mol Sci* 2017; 18(11): 2365.
22. Shi Y, Miao W, Teng J, Zhang L. Ginsenoside Rb1 protects the brain from damage induced by epileptic seizure via Nrf2/ARE signaling. *Cell Physiol Biochem* 2018; 45(1): 212-25.
23. Zhu X, Dong J, Han B, Huang R, Zhang A, Xia Z, et al. Neuronal nitric oxide synthase contributes to PTZ kindling epilepsy-induced hippocampal endoplasmic reticulum stress and oxidative damage. *Front Cell Neurosci* 2017; 11: 377.
24. Calabrese EJ. Overcompensation stimulation: a mechanism for hormetic effects. *Crit Rev Toxicol* 2001; 31(4-5): 425-70.
25. Ungvari Z, Parrado-Fernandez C, Csiszar A, de Cabo R. Mechanisms underlying caloric restriction and lifespan regulation: implications for vascular aging. *Circ Res* 2008; 102(5): 519-28.
26. Calabrese EJ, Mattson MP. How does hormesis impact biology, toxicology, and medicine? *NPJ Aging Mech Dis* 2017; 3(1): 13.
27. Calabrese EJ, Baldwin LA. Hormesis: a generalizable and unifying hypothesis. *Crit Rev Toxicol* 2001; 31(4-5): 353-424.
28. Magesh S, Chen Y, Hu L. Small Molecule Modulators of Keap1-Nrf2-ARE Pathway as Potential Preventive and Therapeutic Agents. *Med Res Rev* 2012; 32(4): 687-726.
29. Ungvari Z, Bagi Z, Feher A, Recchia FA, Sonntag WE, Pearson K, et al. Resveratrol confers endothelial protection via activation of the antioxidant transcription factor Nrf2. *Am J Physiol Heart Circ Physiol* 2010; 299(1): H18-H24.
30. Giudice A, Arra C, Turco MC. Review of molecular mechanisms involved in the activation of the Nrf2-ARE signaling pathway by chemopreventive agents. In: *Transcription factors*. *Methods Mol Biol* 2010; (634): 37-74.
31. Kamble SM, Goyal SN, Patil CR. Multifunctional pentacyclic triterpenoids as adjuvants in cancer chemotherapy: a review. *RSC Advances* 2014; 4(63): 33370-82.
32. Hamdan AM, Al-Gayyar MM, Shams ME, Alshaman US, Prabahar K, Bagalagel A, et al. Thymoquinone therapy remediates elevated brain tissue inflammatory mediators induced by chronic administration of food preservatives. *Sci Rep* 2019; 9(1): 7026.
33. Murphy MP. Antioxidants as therapies: can we improve on nature? *Free Radic Biol Med* 2014; 66: 20-3.
34. Gaetani GF, Galiano S, Canepa L, Ferraris AM, Kirkman HN. Catalase and glutathione peroxidase are equally active in detoxification of hydrogen peroxide in human erythrocytes. *Blood* 1989; 73(1): 334-9.
35. Alam MF, Khan G, Safhi MM, Alshahrani S, Siddiqui R, Sivagurunathan Moni S, et al. Thymoquinone ameliorates doxorubicin-induced cardiotoxicity in swiss albino mice by modulating oxidative damage and cellular inflammation. *Cardiol Res Pract* 2018; 1483041 (6 pages).
36. Asgharzadeh F, Bargi R, Beheshti F, Hosseini M, Farzadnia M, Khasaei M. Thymoquinone Prevents Myocardial and Perivascular Fibrosis Induced by Chronic Lipopolysaccharide Exposure in Male Rats: Thymoquinone and Cardiac Fibrosis. *J Pharmacopuncture* 2018; 21(4): 284.

37. Horch HW, Katz LC. BDNF release from single cells elicits local dendritic growth in nearby neurons. *Nat Neurosci* 2002; 5(11): 1177.
38. Bathina S, Das UN. Brain-derived neurotrophic factor and its clinical implications. *Arch Med Sci* 2015; 11(6): 1164.
39. Altar CA, Whitehead RE, Chen R, Wörtwein G, Madsen TM. Effects of electroconvulsive seizures and antidepressant drugs on brain-derived neurotrophic factor protein in rat brain. *Biol Psychiatry* 2003; 54(7): 703-9.
40. Falcicchia C, Paolone G, Emerich DF, Lovisari F, Bell WJ, Fradet T, et al. Seizure-suppressant and neuroprotective effects of encapsulated BDNF-producing cells in a rat model of temporal lobe epilepsy. *Mol Ther Methods Clin Dev* 2018; 9: 211-24.
41. Porcher C, Medina I, Gaiarsa J-L. Mechanism of BDNF modulation in GABAergic synaptic transmission in healthy and disease brains. *Front Cell Neurosci* 2018; 12: 273.
42. Unsain N, Nunez N, Anastasia A, Mascó D. Status epilepticus induces a TrkB to p75 neurotrophin receptor switch and increases brain-derived neurotrophic factor interaction with p75 neurotrophin receptor: an initial event in neuronal injury induction. *Neuroscience* 2008; 154(3): 978-93.
43. Volosin M, Trotter C, Cragolini A, Kenchappa RS, Light M, Hempstead BL, et al. Induction of proneurotrophins and activation of p75NTR-mediated apoptosis via neurotrophin receptor-interacting factor in hippocampal neurons after seizures. *J Neurosci* 2008; 28(39): 9870-9.
44. Hong Z, Li W, Qu B, Zou X, Chen J, Sander J, et al. Serum brain-derived neurotrophic factor levels in epilepsy. *Eur J Neurol* 2014; 21(1): 57-64.
45. Chen S-F, Jou S-B, Chen NC, Chuang H-Y, Huang C-R, Tsai M-H, et al. Serum Levels of Brain-Derived Neurotrophic Factor and Insulin-Like Growth Factor 1 Are Associated With Autonomic Dysfunction and Impaired Cerebral Autoregulation in Patients With Epilepsy. *Front Neurol* 2018; 9: 969.
46. Cosulich SC, Savory PJ, Clarke PR. Bcl-2 regulates amplification of caspase activation by cytochrome c. *Curr Biol* 1999; 9(3): 147-50.
47. O'Brien MA, Kirby R. Apoptosis: A review of pro-apoptotic and anti-apoptotic pathways and dysregulation in disease. *J Vet Emerg Crit Car* 2008; 18(6): 572-85.
48. Hosseini SM, Taghiabadi E, Abnous K, Hariri AT, Pourbakhsh H, Hosseinzadeh H. Protective effect of thymoquinone, the active constituent of *Nigella sativa* fixed oil, against ethanol toxicity in rats. *Iran J Basic Med Sci* 2017; 20(8): 927.
49. Ullah I, Badshah H, Naseer MI, Lee HY, Kim MO. Thymoquinone and vitamin C attenuates pentylentetrazole-induced seizures via activation of GABA B1 receptor in adult rats cortex and hippocampus. *Neuromolecular Med* 2015; 17(1): 35-46.
50. Pavlova T, Stepanichev M, Gulyaeva N. Pentylentetrazole kindling induces neuronal cyclin B1 expression in rat hippocampus. *Neurosci Lett* 2006; 392(1-2): 154-8.

Numerical Taxonomic Analysis on Some *Lepidium* L. taxa (Brassicaceae) from Turkey

Mehmet Bona¹ 

¹Istanbul University, Science Faculty, Department of Biology, Division of Botany, Istanbul, Turkey

ORCID IDs of the authors: M.B. 0000-0003-1656-2641

Please cite this article as: Bona M. Numerical Taxonomic Analysis on Some *Lepidium* L. taxa (Brassicaceae) from Turkey. Eur J Biol 2020; 79(2): 132-143. DOI: 10.26650/EurJBiol.2020.0020

ABSTRACT

Objective: This study reveals the relationship between *Lepidium campestre*, *L. spinosum*, *L. sativum* ssp. *sativum*, *L. sativum* ssp. *spinescens*, *L. ruderales*, *L. virginicum*, *L. perfoliatum*, *L. vesicarium*, *L. caespitosum*, *L. pumilum*, *L. cartilagineum*, *L. latifolium*, *L. lyratum*, *L. graminifolium*, to determine the effectiveness of the characters used in taxonomic classification, and to help solve taxonomical problems of this large genus at the specific and intraspecific levels by comparing the numerical results with classical taxonomic classification.

Materials and Methods: This numerical taxonomic study is based on morphological data that come from a wide range of herbarium material and material collected in the wild. For the analyses, 14 taxa were studied. A range of characteristics of sepal, petal, stamen, silicle, pedicel, septum, stigma, and sinus that are considered to be taxonomically important in the genus were investigated. Morphological data, 90 character states, which belong to 55 characters scored as the binary state for each taxon were used in unweighted pair-group method using arithmetic averages and principle components analyses.

Results: *L. caespitosum*, *L. pumilum* and *L. cartilagineum* are recognised at species rank, not subspecies or varieties. *L. sativum* ssp. *sativum* and *L. sativum* ssp. *spinescens* should be evaluated as two subspecies not synonyms of *Lepidium sativum*. The most effective characters for the delimitation of the studied taxa are seed length, the habitus of plant, sepal length, septum length, seed wings, the presence of swelling leaf residues on the base of the plant, pedicel length.

Conclusion: Numerical analysis studies based on morphological data on *Lepidium* taxa growing in Turkey are a useful tool for solving the taxonomic problems of taxa belonging to the genus *Lepidium*.

Keywords: Brassicaceae, *Lepidium*, Numerical Taxonomy, PCA, UPGMA

INTRODUCTION

The Brassicaceae is one of the largest families that has major scientific and economic importance (1,2). There are 3660 species and 321 genera in 49 tribes in the family (3). The classification of the Brassicaceae is problematic because the characters traditionally used are variable, even within genera, and may not support natural groups (4).

The first comprehensive taxonomic approach of the Brassicaceae is based on two characteristics: the position of the radicle with cotyledons in the seed and fruit type (5). After almost a century, tribal and

subtribal classification revised mainly based on fruit characters and seed morphology (6). Brassicaceae is represented by 555 species and 91 genera in the Flora of Turkey (6-9). Generic delimitation has been changed according to molecular phylogenetic studies focused on Brassicaceae in the last two decades (10-12). Recent studies show that Turkey is a centre of diversity with 660 taxa belonging to 91 genera, including 571 species, 65 subspecies, and 24 varieties (13).

The genus *Lepidium* L. is primarily distributed in temperate and subtropical regions (14). The genus includes 250 species and one of the largest genera in the Brassicaceae (3). *Cardaria* Desv. was defined as



Corresponding Author: Mehmet Bona

E-mail: mehmetbona@gmail.com

Submitted: 30.04.2020 • **Revision Requested:** 05.05.2020 • **Last Revision Received:** 11.07.2020 •

Accepted: 25.09.2020 • **Published Online:** 22.12.2020

© Copyright 2020 by The Istanbul University Faculty of Science • Available online at <http://ejb.istanbul.edu.tr> • DOI: 10.26650/EurJBiol.2020.0020

a section of *Lepidium* (15), later it was accepted as a separate genus (7,14,16). In light of molecular research not only *Cardaria* but also *Coronopus*, *Stroganowia*, *Winklera* Regel, and *Stubendorffia* Schrenk ex Fisch., C.A. Mey. & Avé-Lall. have been classified within *Lepidium* sensu lato (10,12,17-20).

Cardaria, *Coronopus*, and *Stroganowia* are represented by five species in Turkey: *L. coronopus* (L.) Al-Shehbaz and *L. didymium* L. (formerly *Coronopus*), *L. draba* L. and *L. chalepense* L. (formerly *Cardaria*), *Stroganowia leventii* V.I. Dorofeev (3,21-23)

Lepidium sensu stricto (excluding *Cardaria*, *Coronopus*, and *Stroganovia*) includes 13 species and 2 subspecies in Turkey (7,8,24).

Numerical taxonomy is a grouping method that groups to a taxonomic unit based on their character states using statistical methods (25). In this study, the morphological features of *Lepidium* s.str. taxa distributed in Turkey were examined and their diagnostic characteristics were determined. Detailed measurements based on these characters were used in numerical taxonomic analyses.

This study reveals the relationship between *L. campestre*, *L. spinosum*, *L. sativum* ssp. *sativum*, *L. sativum* ssp. *spinescens*, *L. ruderales*, *L. virginicum*, *L. perfoliatum*, *L. vesicarium*, *L. caespitosum*, *L. pumilum*, *L. cartilagineum*, *L. latifolium*, *L. lyratum*, *L. graminifolium*, to determine the effectiveness of the characters used in taxonomic classification, and to help solve taxonomical problems of this large genus at specific and intraspecific ranks by comparing the numerical results with classical taxonomic classification.

MATERIALS AND METHODS

The flowering and fruiting material of the genus *Lepidium* were collected from different parts of Turkey during the period May-August 2008, 2009 and 2010. Specimens were collected from as many different parts of the distribution area of the genus as possible in order to thoroughly examine variation patterns. The specimens collected were kept at the Istanbul Uni-

versity, Department of Pharmaceutical Botany Herbarium (ISTE) and compared with the collections of ANK, E, GAZI, HUB, ISTF, ISTE, K, and VAN herbaria.

A range of characteristics of sepal, petal, stamen, silicle, pedicel, septum, stigma, and sinus that are considered to be taxonomically important in the genus were investigated. For these investigations, all parts of the specimens were photographed using MOTIC 2000 camera stereo microscope system, and then measured by using Motic Image Plus 2.0-program. These measurements were used for numerical analyses. For the analyses, 14 taxa (Table 1) and 90 character states, which belong to 55 characters, were scored as the binary state for each taxon (Table 2). To investigate the relationships between the studied taxa,

Table 1. Studied taxa list.

OTU1	<i>L. campestre</i>
OTU2	<i>L. spinosum</i>
OTU3	<i>L. sativum</i> ssp. <i>sativum</i>
OTU4	<i>L. sativum</i> ssp. <i>spinescens</i>
OTU5	<i>L. ruderales</i>
OTU6	<i>L. virginicum</i>
OTU7	<i>L. perfoliatum</i>
OTU8	<i>L. vesicarium</i>
OTU9	<i>L. caespitosum</i>
OTU10	<i>L. pumilum</i>
OTU11	<i>L. cartilagineum</i>
OTU12	<i>L. latifolium</i>
OTU13	<i>L. lyratum</i>
OTU14	<i>L. graminifolium</i>

Table 2. Character list.

No	Characters	Character states
C1	Fruit length maximum value	Shorter or longer than 3 mm
C2		Shorter or longer than 4 mm
C3		Shorter or longer than 5 mm
C4	Fruit length minimum value	Shorter or longer than 2 mm
C5		Shorter or longer than 3 mm
C6	Fruit width maximum value	Shorter or longer than 4 mm
C7		Shorter or longer than 3 mm
C8		Shorter or longer than 4 mm

Table 2. Continue		
C9	Fruit width minimum value	Shorter or longer than 2 mm
C10		Shorter or longer than 3 mm
C11	Pedicel length maximum value	Shorter or longer than 4 mm
C12		Shorter or longer than 6 mm
C13	Pedicel length minimum value	Shorter or longer than 2 mm
C14		Shorter or longer than 3 mm
C15	Septum length maximum value	Shorter or longer than 2.5 mm
C16		Shorter or longer than 3.5 mm
C17	Septum length minimum value	Shorter or longer than 2 mm
C18		Shorter or longer than 3 mm
C19	Septum width maximum value	Shorter or longer than 0.7 mm
C20	Septum width minimum value	Shorter or longer than 0.5 mm
C21	Stigma length maximum value	Shorter or longer than 0.3 mm
C22		Shorter or longer than 0.5 mm
C23	Stigma length minimum value	Shorter or longer than 0.25 mm
C24	Stigma width maximum value	Shorter or longer than 0.25 mm
C25		Shorter or longer than 0.35 mm
C26	Stigma width minimum value	Shorter or longer than 0.15 mm
C27		Shorter or longer than 0.25 mm
C28	Sepal length maximum value	Shorter or longer than 1.5 mm
C29	Sepal length minimum value	Shorter or longer than 1 mm
C30	Sepal width maximum value	Shorter or longer than 1 mm
C31	Sepal width minimum value	Shorter or longer than 0.8 mm
C32	Petal length maximum value	Shorter or longer than 2.5 mm
C33	Petal length minimum value	Shorter or longer than 2 mm
C34	Petal width maximum value	Shorter or longer than 1 mm
C35		Shorter or longer than 1.6 mm
C36	Petal width minimum value	Shorter or longer than 0.8 mm
C37	Stamen length maximum value	Shorter or longer than 2 mm
C38	Stamen length minimum value	Shorter or longer than 1.5 mm
C39	Seed length maximum value	Shorter or longer than 2 mm
C40		Shorter or longer than 2.5 mm
C41	Seed length minimum value	Shorter or longer than 1.5 mm
C42		Shorter or longer than 2 mm
C43	Seed width maximum value	Shorter or longer than 1 mm

Table 2. Continue		
C44	Seed width minimum value	Shorter or longer than 1 mm
C45	Basal leaves length minimum value	Shorter or longer than 15 cm
C46	Basal leaves width minimum value	Shorter or longer than 4 cm
C47	Basal leaves pedicel length minimum value	Shorter or longer than 4 cm
C48	Plant length maximum value	Shorter or longer than 50 cm
C49	Life time	Perennial or not
C50	Habitus	Erect or not
C51		Single stemmed or not
C52		Many stemmed or not
C53	Plant surface	Basal part naked or not
C54		Upper part naked or not
C55		Plant waxy or not
C56	Swelling nodes existence	Present or absent
C57	Petiola remains existence	Present or absent
C58	Basal leaves shape	Lyrate basal leaves present or absent
C59		Pinnatisect basal leaves present or absent
C60		2-pinnatisect basal leaves present or absent
C61		3-pinnatisect basal leaves present or absent
C62		Lanceolate basal leaves present or absent
C63		Ovate basal leaves present or absent
C64		Linear basal leaves present or absent
C65		Lanceolate basal leaves present or absent
C66	Cauline leaves shape	Pinnatisect cauline leaves present or absent
C67		2-pinnatisect cauline leaves present or absent
C68		Lanceolate cauline leaves present or absent
C69		Ovate cauline leaves present or absent
C70	Leaves surface	Both surface has trichome or not
C71		Glabrous above has trichome below
C72	Stipul existence	Present or absent
C73	Sepal center color	Purple or yellow
C74	Sepal margin color	White or yellow
C75	Sepal surface	Glabrous or not
C76	Petal color	White or yellow
C77	Stamen position	Equal or not
C78	Stamen number	2 or not

Table 2. Continue

C79		4 or not
C80		6 or not
C81	Pedicle position	Erect or not
C82	Pedicle surface	Glabrous or not
C83	Silicle shape	Ovate or not
C84		Orbicular or not
C85		Oblong or not
C86	Silicle wing existence	Present or absent
C87	Silicle surface	Glabrous or not
C88	Stilus position	Exceeding sinus or not
C89	Seed wing existence	Present or absent
C90	Seed shape	Ovate or not

two types of numerical analyses were performed using NTSYS–pc 2.1 software (26). The first analysis was the Clustering Analysis (CA) and the second analysis was the Principle Components Analysis (PCA).

RESULTS

The result of the CA is the UPGMA (Unweighted Pair–Group Method using Arithmetic Averages) dendrogram (Figure 1).

The UPGMA dendrogram explains the numerical relationships of the taxa studied. According to the results; *L. sativum* ssp. *sativum* and *L. sativum* ssp. *spinescens* are the closest pair of taxa. *L. spinosum* is grouped with these two taxa and *L. campestre* is

the closest species to the group. *L. lyratum* and *L. graminifolium* are the second closest pair of taxa and related to *L. latifolium*. These taxa are grouped with *L. ruderale* and *L. virginicum*. The third closest pair of taxa are *L. caespitosum* and *L. pumilum*, which are grouped with *L. cartilagineum*.

PCA analysis results were coherent with the CA analysis (Figure 2). According to PCA analysis *Lepidium sativum* subsp. *sativum* and *L. sativum* subsp. *spinescens* the closest studied taxa and these taxa were grouped with *L. campestre* and *L. spinosum*. *L. lyratum* and *L. graminifolium* showed a close relation again and these taxa are grouped with *L. ruderale*, *L. virginicum*, *L. latifolium* like they were grouped in UPGMA dendrogram. *L. caespitosum*, *L. pumilum* and *L. cartilagineum* were also grouped. *L. pumilum*

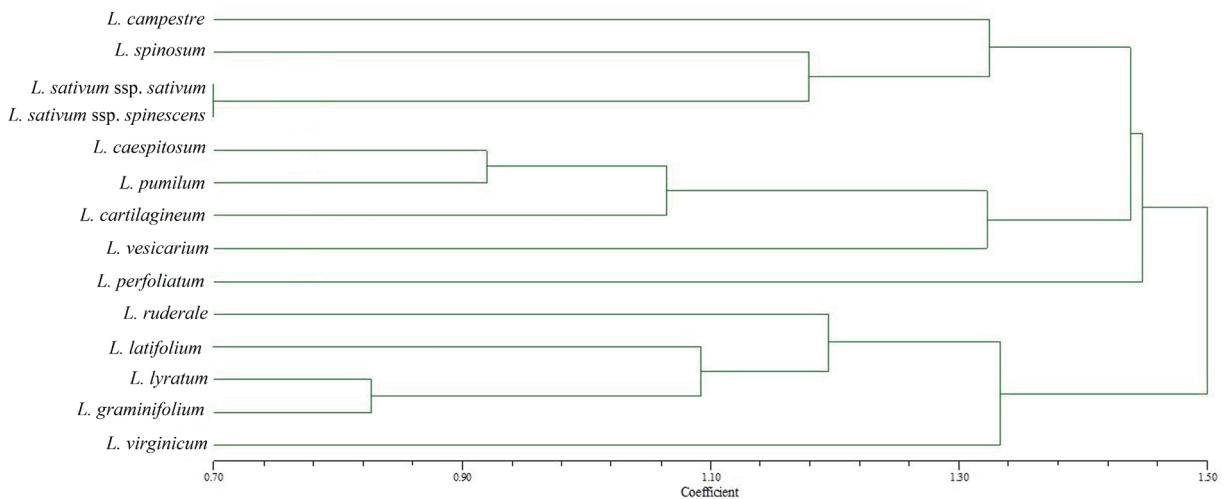


Figure 1. UPGMA Dendrogram.

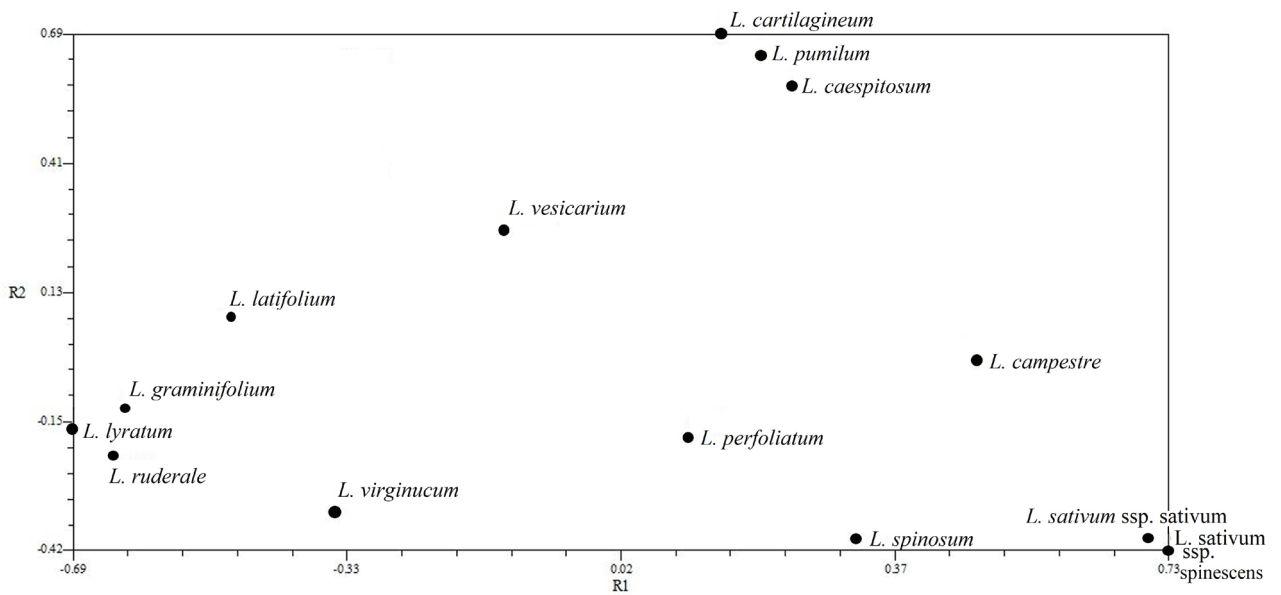


Figure 2. Position of studied taxa on the first two components.

has an equal distance from *L. caespitosum* and *L. cartilagineum*. The pictures of the studied taxa are given in Figures 3-5.

PCA analysis reduces numerous characters to a few number components. Table 3 shows the component's Eigen value and percentage of Eigen value. Eigen vector values of the first 4 components are given in Table 4. The first two components explain 39.61% of the total variation. According to the results of PCA analysis, the first five most effective characters describing the first component are seed length, the habitus of plant, the minimum and maximum length of sepal, and septum length. The first five most effective characters describing the second component are the seeds with or without wings, the presence

of swelling leaf residues on the base of the plant, the length of the pedicel, the presence of the plant with a single stem, and the length of the septum.

DISCUSSION

L. spinosum, *L. sativum* ssp. *sativum* and *L. sativum* ssp. *spinescens* taxa (Figure 3) are clustered in this study and are placed in the section *Lepiacardamon* in classical systematic studies (7). According to the Flora of Turkey (7) *L. campestre*, the only taxon representing the section *Lepia*, is the closest species to the section *Lepiacardamon* (Figure 3). The dendrogram results are compatible with classical taxonomic data in this respect.

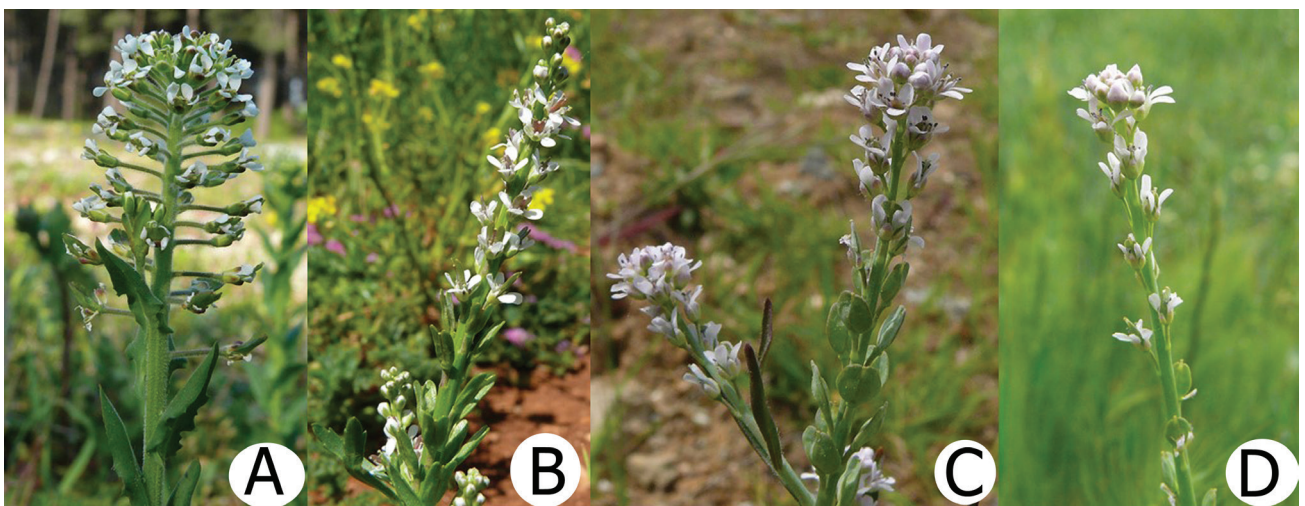


Figure 3. A) *L. campestre*, B) *L. spinosum*, C) *L. sativum* subsp. *sativum*, D) *L. sativum* subsp. *spinescens*.

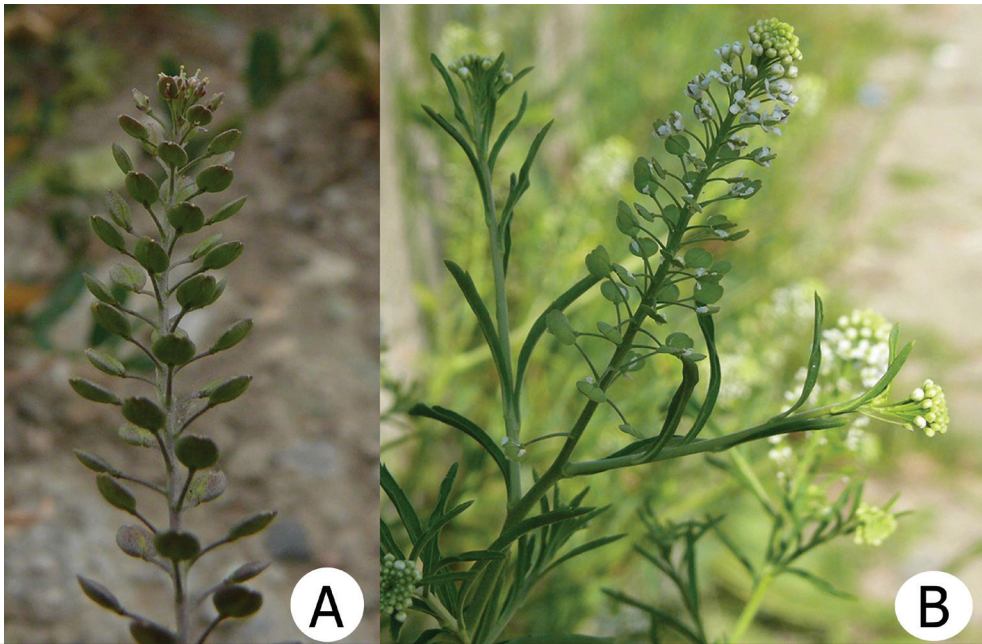


Figure 4. A) *L. ruderale*, B) *L. virginicum*.

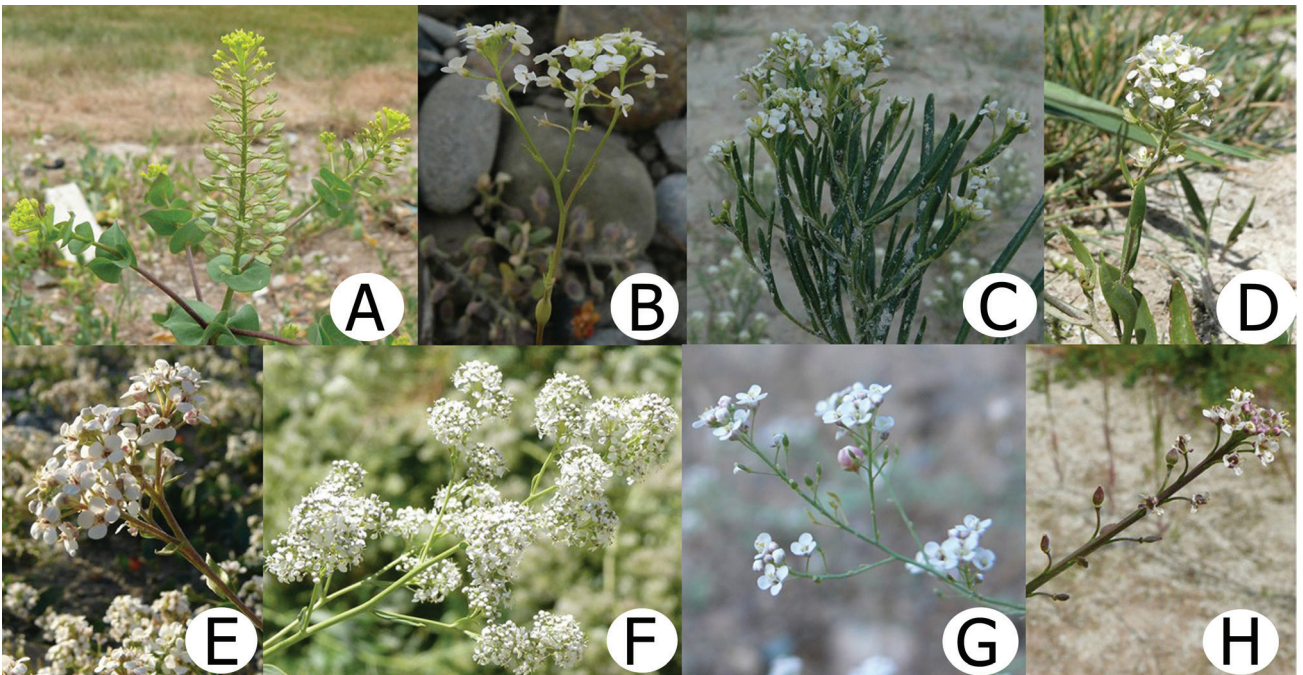


Figure 5. A) *L. perfoliatum*, B) *L. vesicarium*, C) *L. caespitosum*, D) *L. pumilum*, E) *L. cartilagineum*, F) *L. latifolium*, G) *L. lyratum*, H) *L. graminifolium*.

L. sativum is grown as a cultivated plant in many parts of the world. Therefore, it is not easy to draw the boundaries of its geographical distribution. There are different taxonomic approaches in terms of intraspecific classification with the effect of this situation. The species has two subspecies according to the Flora

of Turkey and Flora of Iraq (7,27). In Flora of West Pakistan, the taxonomic level is defined as a variety, not a subspecies (28). According to the revision study conducted in Turkey, because of both the clarity of the morphological differences between the two taxa as well as due to differences in geographical dis-

Table 3. Eigen value and percentage of Eigen value of components.

Components	Eigen Value	Percentage of Eigen Value	Total Percentage Eigen
1	21.6700	24.08	24.08
2	13.9788	15.53	39.61
3	10.8323	12.03	51.65
4	8.3728	9.3	60.95
5	6.4828	7.2	68.16
6	5.7569	6.39	74.55
7	4.9996	5.55	80.11
8	4.4561	4.95	85.06
9	4.1067	4.56	89.62
10	3.7017	4.11	93.74
11	2.5988	2.88	96.62
12	1.7636	1.95	98.58
13	1.2713	1.41	100

Table 4. Component's Eigen vector value.

	B1	B2	B3	B4
C1	8.1577	1.7598	3.3445	7.6318
C2	7.8622	-3.1628	6.4978	-1.6688
C3	7.3615	-5.525	7.1535	-1.4991
C4	8.1577	1.7589	3.3443	7.6318
C5	7.4498	-5.115	-2.5845	-1.7279
C6	7.4498	-5.115	-2.5845	1.7279
C7	8.1067	6.1259	2.8759	-3.1068
C8	7.0984	-1.7069	2.2081	-3.9225
C9	7.2261	-1.0386	2.8368	1.6263
C10	5.1939	-4.874	1.1398	-1.064
C11	-1.3344	4.5014	4.2963	-1.2953
C12	3.1741	7.5122	4.2598	9.0736
C13	-6.4439	5.5676	3.7611	-1.5546
C14	1.3431	8.4926	-1.4174	-9.391
C15	8.1577	1.7589	3.3443	7.6318
C16	8.2272	-5.4576	9.4618	-2.5207
C17	8.3823	-7.2074	5.6088	-1.4323

Table 4. Continue.

C18	7.009	-3.8102	-1.0506	-3.4768
C19	7.528	4.4059	2.6295	2.6688
C20	2.801	-1.0181	1.4588	-5.5078
C21	7.528	4.4059	2.6295	2.6688
C22	7.0941	1.9486	-6.6924	-9.7554
C23	5.9917	5.0211	-8.614	1.0578
C24	1.3428	3.1286	-7.9831	3.6451
C25	-1.408	5.7247	2.2524	3.4448
C26	1.051	2.7864	-7.0197	7.8805
C27	-3.313	2.5432	2.5923	5.3754
C28	8.5043	2.5371	-2.1567	-2.4258
C29	8.5043	2.5371	-2.1567	-2.4258
C30	5.5623	5.869	-1.042	-2.678
C31	1.3188	6.2204	-4.0622	-3.1672
C32	6.9054	4.0033	-4.6847	3.6139
C33	3.789	2.8278	-4.1131	5.3833
C34	1.4221	3.924	-3.8543	-1.9705
C35	1.6754	6.7856	3.7243	-1.549
C36	-3.2513	6.5742	-1.7311	1.1972
C37	6.5701	2.4961	-5.0581	-2.4516
C38	4.3287	1.8748	-4.5252	1.7334
C39	8.7965	2.9907	1.1786	1.425
C40	5.6454	-4.5667	1.7145	3.261
C41	8.1577	1.7589	3.3443	7.6318
C42	7.009	-3.8102	-1.0506	-3.4768
C43	8.1577	1.7589	3.3443	7.6318
C44	5.2255	2.7924	3.5573	-2.0302
C45	4.4301	-1.7607	-5.6159	-5.091
C46	3.8871	-6.922	-5.1692	3.2119
C47	3.5547	-2.0308	-3.6233	-5.4515
C48	-2.3959	-4.1107	-4.2069	-7.7936
C49	4.0749	-7.3958	4.1262	-2.0175
C50	8.6528	5.0179	5.8839	-1.687
C51	-4.0749	7.3958	-4.1262	2.0175
C52	4.7507	-6.8027	1.9056	7.5579

Table 4. Continue.

C53	-1.3428	-3.1286	7.9831	-3.6451
C54	2.3881	5.057	4.4158	-4.327
C55	-2.9336	4.3552	4.4765	-5.122
C56	4.0356	1.1781	2.8518	6.6462
C57	2.1608	8.7231	2.1741	-1.0536
C58	4.4758	2.8737	2.4905	1.7616
C59	-3.9602	5.3022	-3.3933	-2.2854
C60	-1.2301	3.7383	-2.8989	-4.2022
C61	1.0647	-4.7006	-4.6956	-5.4175
C62	2.8898	-5.7685	5.0445	1.737
C63	-4.8731	-3.4476	1.8812	5.6061
C64	-1.1663	-4.6782	1.5965	-4.2597
C65	-1.4111	-4.2019	8.2345	4.1765
C66	-4.7657	2.5251	1.6425	-7.5776
C67	7.7308	-1.9457	-5.1567	-7.1191
C68	-1.6978	-1.2835	3.7654	5.2953
C69	-1.0993	-2.7311	-4.7492	1.0636
C70	2.547	4.2819	-2.3125	4.7474
C71	-4.7657	2.5251	1.6425	-7.5776
C72	-2.6955	-2.2652	-4.9657	4.3641
C73	-2.0825	-3.9243	3.083	4.2735
C74	6.2841	-1.307	5.8645	2.4181
C75	2.1569	-2.6125	2.4595	1.6409
C76	-2.2815	-2.1394	6.5289	3.1386
C77	2.8233	2.3518	-1.0312	6.119
C78	4.2576	3.0021	-4.9163	8.3012
C79	2.0464	2.4789	-3.6733	1.3125
C80	-4.2576	-3.0021	4.9163	-8.3012
C81	-6.4439	5.5676	3.7611	-1.5546
C82	-1.6183	6.0073	4.6361	-6.1571
C83	-2.3005	-3.2699	-3.0227	-5.9666
C84	3.4683	3.9177	6.5477	2.8762
C85	-3.4604	2.2105	1.0309	5.8767
C86	-5.097	-4.4255	-5.8116	-1.3273
C87	-7.2798	-1.711	-5.8173	-3.1014
C88	2.4089	-6.9602	3.6955	7.2506
C89	-5.0479	-9.7737	6.1954	1.0801
C90	-5.9977	-1.4795	2.0557	3.4321

tribution seen between populations, it is stated that the definition should be at the subspecies level. In the Turkey Plant List (Vascular Plants), both subspecies and varieties are listed as a synonym and *L. sativum* is shown as a single species (22). The results of this study support the view that the *L. sativum* species should be better evaluated as two subspecies.

L. latifolium, *L. lyratum*, and *L. graminifolium* (Figure 4) are placed together in section *Lepidium* (7). These species also formed a group in this study and numerical results support the sectional classification. *L. ruderale* and *L. virginicum* (Figure 5), the closest species to the group according to the numerical analysis, are also placed in section *Dileptum* in the Flora of Turkey (7,9).

The last group comprises *L. caespitosum*, *L. pumilum* and *L. crassifolium*. *L. caespitosum* (Figure 5) was evaluated as an endemic species in the Flora of Turkey (7). According to Flora of Turkey (7), *L. pumilum* and *L. crassifolium* were represented as two subspecies; *L. cartilagineum* (J. May.) Thell. subsp. *cartilagineum* and *L. cartilagineum* (J. May.) Thell. ssp. *crassifolium* (Waldst. & Kit.) Thell. Later, Hedge (29) again accepted them as two subspecies but with a new combination. In the Flora of the USSR, they are accepted as separate species (30). These three taxa were listed as subspecies of *L. cartilagineum* by Mutlu (22) while the revision of Turkish *Lepidium* proposed they must be considered as different species (24). Numerical analysis results in this study support the idea of evaluating these three taxa as separate species. It also shows that *L. pumilum* is closer to *L. caespitosum* than to *L. cartilagineum*.

There is a tendency for some of the flower parts to be reduced to the point of absence, and hence flower structure is used in the subgeneric classification in the genus *Lepidium* (31). Flower structure and the characters of vegetative morphology are used in species identification in the genus *Lepidium* (32,33). The results of PCA analysis support the idea that the habitus of plant, the minimum and maximum length of sepal, the presence of swelling leaf residues on the base of the plant, and the presence of the plant with a single stem are important characters.

It has been reported that seed characters tend to have been ignored in *Lepidium*, with the exception of trifold cotyledon of *L. sativum* (31,33). However, the results of the present study showed that seed length, septum length, and the eventual presence and features of the seed wing are diagnostic characteristics for the genus *Lepidium*. This result is coherent with studies using seed characteristics for taxonomic studies in *Lepidium* (31,34,35).

Numerical analysis of *L. sativum* based on 21 morphological traits was performed based on Iranian specimens (36). According to that analysis, the first principal component analysis explained 63.0% of the total variation present in the dataset, besides that, petal length and sepal length and width had the highest positive correlation in PCA analysis (36). The present PCA analysis also shows that the sepal and petal length are two important characteristics that explain the first two components.

CONCLUSION

Numerical analysis studies based on morphological data on *Lepidium* taxa growing in Turkey is a useful tool for solving the taxonomic problems of taxa belonging to the genus *Lepidium*. This study gave significant results as the first step towards more comprehensive studies including more taxa.

Proposed Treatment for Turkish *Lepidium* L. taxa

Section *Lepia* (Desv.) DC.

L. campestre (L.) Aiton, Hort. Kew. ed. 2, 4: 88 (1812).

Section *Lepiocardamon* Thell.

L. spinosum Ard., Animad. Specim. Alt. 2: 34, t. 16 (1764).

L. sativum L., Sp. Pl. 2: 644 (1753). subsp. *sativum*

L. sativum L. subsp. *spinescens* (DC.) Thell. in Vierteljahr. Naturf. Ges. Zürich, 51: 161 (1906)

Section *Dileptium* DC.

L. ruderale L., Sp. Pl. 2: 645 (1753).

L. virginicum L., Sp. Pl. 2: 645 (1753)

Section *Lepidium*

L. perfoliatum L., Sp. Pl. 2: 643 (1753)

L. vesicarium L., Sp. Pl. 2: 643 (1753)

L. caespitosum Desv. in J. Bot. Agric. 3: 165 & 178 (1815)

L. pumilum Boiss. & Bal. in Boiss., Diagn. ser. 2(6): 21 (1859)

L. cartilagineum (J. May.) Thell. in Vierteljahr. Naturf. Ges. Zürich 51: 173 (1906)

L. latifolium L., Sp. Pl. 2: 644 (1753)

L. lyratum L., Sp. Pl. 2: 644 (1753).

L. graminifolium L., Syst. Nat. ed. 10, 2: 1127 (1759)

Peer-review: Externally peer-reviewed.

Authors Contributions: Concept: M.B.; Design: M.B.; Supervision: M.B.; Materials: M.B.; Data Collection and/or Processing: M.B.; Analysis and/or Interpretation: M.B.; Literature Search: M.B.; Writing: M.B.; Critical Reviews: M.B.

Conflict of Interest: The authors declare that they have no conflicts of interest to disclose.

Financial Disclosure: There are no funders to report for this submission.

REFERENCES

1. Koch MA, Mummenhoff K. Editorial: Evolution and phylogeny of the Brassicaceae. *Plant Syst Evol* 2006; 259: 81-3.
2. Roushani A, Miri SM, Hassandokht MR, Moradi P, Abdossi V. Genetic variation within Iranian *Lepidium* species using morphological traits. The First National Congress and International Fair of Medicinal Plants and Strategies for Persian Medicine that Affect Diabetes. 2018 Oct 9; Mashhad, Iran; 2018.
3. Al-Shehbaz IA. A generic and tribal synopsis of the Brassicaceae (Cruciferae). *Taxon* 2012; 61: 931-54.
4. Khalik KA, van der Maesen LJG, Koopman WJM, van den Berg RG. Numerical taxonomic study of some tribes of Brassicaceae from Egypt. *Plant Syst Evol* 2002; 233: 147-275.
5. De Candolle P. *Regni Vegetabilis Systema Naturale*, Volume 2. Paris: Sumptibus Sociorum Treuttel et Würtz; 1821.

6. Schulz OE. Cruciferae. Engler A, Harms H, editors. Die Natürlichen Pflanzenfamilien ed. 2, 17B. Leipzig: Verlag von Wilhelm Engelmann; 1936. p. 227-658.
7. Hedge, I.C. *Lepidium* L. Davis PH, editor. Flora of Turkey and the East Aegean Islands Volume I. Edinburgh: Edinburgh University Press; 1965. p. 279-285.
8. Davis PH, Mill RR, Tan K. Flora of Turkey and the East Aegean Islands Volume X. Edinburgh: Edinburgh University Press; 1988.
9. Güner A, Özhatay N, Ekim T, Başer KHC. Cruciferae. Flora of Turkey and the East Aegean Islands Volume XI. Edinburgh: Edinburgh University Press; 2000.
10. Koch M, Al-Shehbaz IA, Mummenhoff K. Molecular Systematics, Evolution, and Population Biology in The Mustard Family (Brassicaceae). *Ann Mo Bot Gard* 2003; 90: 151-71.
11. Beilstein MA, Al-Shehbaz IA, Kellogg EA. Brassicaceae phylogeny and trichome evolution. *Am J Bot* 2006; 93: 607-19.
12. Al-Shehbaz IA, Beilstein MA, Kellogg EA. Systematics and phylogeny of the Brassicaceae (Cruciferae): an overview. *Plant Syst Evol* 2006; 259: 89-120.
13. Al-Shehbaz IA, Mutlu B, Dönmez AA. The Brassicaceae (Cruciferae) of Turkey, updated. *Turk J Botany* 2007; 31: 327-36.
14. Al-Shehbaz IA. The genera of Lepidieae (Cruciferae; Brassicaceae) in the southeastern United States. *J Arnold Arbor* 1986; 67: 265-311.
15. Thellung A. Die Gattung *Lepidium* (L.) R. Br. Zürich: Verlag von Georg & Co. 1906.
16. Mulligan GA, Frankton C. Taxonomy of the genus *Cardaria* with particular reference to the species introduced into North America. *Can J Bot* 1962; 4: 1411-25.
17. Mummenhoff K. Should *Cardaria draba* (L.) DESV. be classified within the genus *Lepidium* L. (Brassicaceae) Evidence from subunit polypeptide composition of RUBISCO. *Feddes Repert* 1995; 106: 25-8.
18. Al-Shehbaz IA, Mummenhoff K, Appel O. *Cardaria*, *Coronopus*, and *Stroganowia* are united with *Lepidium* (Brassicaceae). *Novon* 2002; 12: 5-11.
19. Bailey CD, Koch MA, Mayer M, Mummenhoff K, O'Kane SL, Warwick SI, Windham MD, Al-Shehbaz IA. Towards a global nrDNA ITS phylogeny of the Brassicaceae. *Mol Biol Evol* 2006; 23: 2142-60.
20. Al-Shehbaz IA, Mummenhoff K. *Stubendorffia* and *Winklera* belong to the expanded *Lepidium* (Brassicaceae). *Edinb J Bot* 2011; 68: 165-70.
21. Dorofeyev VI, Korotyayev BA, Gültekin L. A new species of the genus *Stroganowia* Kar. et Kir. (Cruciferae) from Northeast Turkey and Rhynchophorous beetles (Coleoptera, Curculionoidea) associated with it. *Byull Moskovsk Obshch Isp Prir Otd Biol* 2004; 109: 72-6.
22. Mutlu B. *Lepidium* L. Güner A, Aslan S, Ekim T, Vural M, Babaç MT, editors. Türkiye Bitkileri Listesi (Damarlı Bitkiler). İstanbul: Nezahat Gökyiğit Botanik Bahçesi ve Flora Araştırmaları Derneği Yayını; 2012. p. 284-287.
23. Yüzbaşıoğlu İS, Keskin M. A new record for the flora of Turkey: *Lepidium didymum* L. (Brassicaceae). *Biodicon* 2013; 6: 46-8.
24. Bona M. Taxonomic revision of *Lepidium* L. (Brassicaceae) from Turkey. *J Fac Pharm Ist Univ* 2014; 44: 31-62.
25. Sokal RR, Sneath PHA. Principles of Numerical Taxonomy. USA: W.H. Freeman and Company; 1963.
26. Rohlf FJ. NTSYSpc Numerical Taxonomy and Multivariate Analysis System User Guide. New York: Exeter Software; 1998.
27. Hedge IC, Lamond JM. Brassicaceae. Townsend CC, Guest E, editors. Flora of Iraq Volume IV. Baghdad: Ministry of Agriculture; 1980. p. 827-1199.
28. Jafri SMH. Flora of West Pakistan No: 55 Brassicaceae. Karachi University of Karachi; 1973.
29. Hedge IC. *Lepidium* L. Rechinger KH, editor. Flora Iranica. 57/28. 2, Graz: Akademische Druck- und Verlag-Anst; 1968. p. 63-72.
30. Juss B. *Lepidium* L. Komarov VL. *Flora of the USSR Volume VIII*, Jerusalem: Israel Program for Scientific Translations Ltd.; 1939.
31. Hewson HJ. The genus *Lepidium* L. (Brassicaceae) in Australia. *Brunonia* 1981; 4: 217-308.
32. Bona M. Distribution of *Lepidium* taxa in Turkey. *Boccone* 2012; 24: 221-5.
33. Nasseh Y, Joharchi MR. A new record of *Lepidium* (Brassicaceae) for the flora of Iran. *Nova Biologica Reperta*. 2019; 6: 347-51.
34. Bona M. Seed-coat microsculpturing of Turkish *Lepidium* (Brassicaceae) and its systematic application. *Turk J Botany* 2013; 37: 662-8.
35. Song JH, Moon BC, Choi G, Yang S. Morphological identification of *Lepidium* Seu Descurainiae Semen and adulterant seeds using microscopic analysis. *Applied Sciences* 2018; 8: 2134.
36. Roughani A, Miri SM, Hassandokht MR, Moradi P, Abdossi V. Agro-morphological study on several accessions of garden cress (*Lepidium sativum*-Brassicaceae) in Iran. *Pak J Bot* 2018; 50: 655-60.

The Role of *Aspergillus parasiticus* NRRL:3386 Strain on Petroleum Biodegradation and Biosorption Processes

Sezen Bilen Ozyurek¹ , Nermin Hande Avcioglu¹ 

¹Hacettepe University, Faculty of Science, Department of Biology, Ankara, Turkey

ORCID IDs of the authors: S.B.O. 0000-0002-5056-7051; N.H.A. 0000-0003-2243-5817

Please cite this article as: Bilen Ozyurek S, Avcioglu NH. The Role of *Aspergillus parasiticus* NRRL:3386 Strain on Petroleum Biodegradation and Biosorption Processes. Eur J Biol 2020; 79(2): 144-150. DOI: 10.26650/EurJBiol.2020.0099

ABSTRACT

Objective: Fungi play an important role in the removal of hazardous organic compounds from the environment with their extracellular multiple enzyme systems. In the bioremediation processes, fungi act as a bioreactor by breaking down or are biosorbent by accumulating organic pollutants.

Materials and Methods: The aim of this study was to investigate and to compare the biodegradation and biosorption capacities of different amounts of live and dead biomasses and different concentrations of culture supernatants of *Aspergillus parasiticus* NRRL:3386 with gravimetric, gas chromatography-mass spectrometry (GC/MS) and scanning electron microscope (SEM) analyses.

Results: This study indicated that 1 g of live biomass degraded 80% of petroleum within 4-days of incubation. The cellfree culture supernatant was not as effective as the live biomass in petroleum degradation. The petroleum biosorption was achieved at over 50% by 1 g and 2.5 g; over 70% by 5 g and 7.5 g, and over 80% by 10 g of dead biomasses. The petroleum removal efficiencies of 2 g of live and 10 g of dead biomasses were over 80%. GC/MS analysis demonstrated that C₁₀-C₁₈ n-alkanes (except C₁₁ and C₁₃) and C₁₁, C₁₃, C₁₉-C₂₆ n-alkanes were degraded 47-77% and over 80%, respectively. The most striking result was that C₂₇-C₃₃ n-alkanes were efficiently degraded over 90% in a short incubation period. SEM analysis showed that gaps between fungal hyphae were clear and bright before biosorption of petroleum, whereas gaps between fungal hyphae were closed after biosorption of petroleum.

Conclusion: The results clearly pointed out that *A. parasiticus* will make a significant contribution to advanced mycoremediation studies.

Keywords: *Aspergillus parasiticus* NRRL:3386, petroleum, biosorption, biodegradation, Gas Chromatography-Mass Spectrometry, Scanning Electron Microscope

INTRODUCTION

Petroleum is a non-renewable resource that provides most of the world's energy (1). In addition to being a significant energy source in daily life, petroleum hydrocarbons are an important source of raw materials for industrial chemicals (2). As petroleum is a complex hydrocarbon mixture of saturated hydrocarbons, aromatic hydrocarbons and polar organic compounds, it damages the lungs, kidneys, liver, intestines and other internal organs of living organisms and also causes environmental pollution. Environmental pollution which

is caused by petroleum and petroleum derivatives is one of the most important problems of developing countries (3). Refining, storing and transporting high amounts of petroleum hydrocarbons to fulfill the increase in energy demand, has led to oil spills in large scale areas (4). Remediation of oil spills by chemical and physical remediation methods provide an improvement of 40-50%. However, these methods are quite complex, expensive and time consuming and untreated biodegradable particles are still left in the environment (1,5). In this regard, the most effective approach to the remediation of petroleum contaminated areas



Corresponding Author: Nermin Hande Avcioglu E-mail: hurkmez@hacettepe.edu.tr
Submitted: 30.09.2020 • **Revision Requested:** 27.10.2020 • **Last Revision Received:** 02.11.2020 •
Accepted: 12.11.2020 • **Published Online:** 22.12.2020

© Copyright 2020 by The Istanbul University Faculty of Science • Available online at <http://ejb.istanbul.edu.tr> • DOI: 10.26650/EurJBiol.2020.0099

is the use of biological methods (5). Microbial enhanced oil recovery (MEOR) is a cost-effective and environmentally friendly technique. The primary mechanism in MEOR aims to increase the fluidity and decrease the viscosity of petroleum as a result of biodegradation of long chain saturated hydrocarbons by microbial activity. The biodegradation of petroleum hydrocarbons is carried out by bacteria, fungi and algae with their microbial enzymes. Bacteria have oxygenase and dehydrogenase, while fungi have dehydrogenase and membrane-bound cytochrome P450 as common enzymes. Most microorganisms biodegrade petroleum hydrocarbons via aerobic pathways; however the anaerobic degradation of long chain *n*-alkanes is important for MEOR due to a lack of oxygen in reservoir systems. Additionally, fungal enzymes can degrade *n*-alkanes of petroleum to lower fractions in oxygen-deprived conditions and can be used as an alternative to oxygen-depleting microorganisms with low growth in reservoirs (1,3).

Many microorganisms can use petroleum hydrocarbons as carbon and energy sources and convert them into CO₂, H₂O and nontoxic products (4). While the research in literature is limited to bacterial remediation, the usage of potential fungal strains in remediation processes, is very important in the development of new mycoremediation strategies (5). Fungi are highly capable of degrading complex structures and long chain hydrocarbons and are more resistant to the toxic effects of petroleum hydrocarbons than bacteria (4). In addition to the biodegradation of toxic petroleum hydrocarbons, the surface adsorption and cell absorption of different petroleum hydrocarbons by fungi are noteworthy. It was clearly shown in the literature that the most effective fungi in the bioremediation of petroleum are *Aspergillus* sp., *Penicillium* sp., *Cephalosporium* sp., *Rhizopus* sp., *Fusarium* sp., *Rhodotorula* sp., *Paecilomyces* sp., *Torulopsis* sp., *Pleurotus* sp., *Alternaria* sp., *Mucor* sp., *Talaromyces* sp., *Cladosporium* sp., and *Geotrichum* sp., (6-10). In the bioremediation process, fungi are advantageous compared to bacteria due to potential hydrolytic enzymes and fungal hyphae facilitating penetration. Filamentous fungi can use various substrates with their extracellular hydrolytic enzymes. Thus, they have hydrocarbon biodegradation capabilities as their biodegrading enzyme systems are extracellular and non-specific. In addition, fungal enzymes can be obtained by high efficiency and low-cost methods. Having a short enzymolysis time with the unique biodegradation capabilities of fungi, this process does not require the use of living microorganisms. All these features of fungi make them unique for industrial usage derivatives (1, 3). Although the biodegradation of petroleum hydrocarbons with different bacterial strains, bacterial consortia and fungal strains have been investigated in various studies in Turkey, no similar study has been found on biodegradation and biosorption of petroleum by *Aspergillus parasiticus* NRRL:3386 (11-13). In this context, the study aimed to determine and to compare biodegradation and biosorption capacities of petroleum by different amounts and concentrations of live/dead biomasses and culture supernatants of *A. parasiticus* NRRL:3386 with gravimetric, Gas Chromatography/Mass Spectrometry (GC/MS) and Scanning Electron Microscopy analyses (SEM).

MATERIALS AND METHODS

Sampling

1 L of petroleum sample was collected from an oil field (Diyarbakir, Turkey) and transported to the Environmental Biotechnology Laboratory in Hacettepe University, Beytepe, Ankara, Turkey.

Inoculum Preparation and Storage

The pure culture of *A. parasiticus* NRRL:3386 strain was inoculated onto potato dextrose agar and incubated at 30 °C for a week. The fungal cultures were stored at +4 °C in Hacettepe University Culture Collection Laboratory, Beytepe, Ankara, Turkey.

Preparation of Fungal Biomass

The pure culture of fungal strain was inoculated in potato dextrose broth (PDB) and the incubation process was carried out at 30°C and 150 rpm for 7 days (IKA® KS 4000i, Germany) (14). Following the incubation period, the fungal cultures were filtered using Whatman No: 1 filter paper under sterile conditions. Fungal pellets drying in sterile petri dishes at 30°C in a static incubator (Mipro MCI, Turkey), were used as live biomass. Filter-dried fungal pellets were autoclaved at 121°C for 15 minutes and the pellets were used as dead biomass.

Preparation of Cell-Free Culture Supernatant

The pure culture of fungi was inoculated into Bushnell Haas (BH) (g/L: 0.2 MgSO₄, 0.02 CaCl₂, 1 KH₂PO₄, 1 K₂HPO₄, 1 NH₄NO₃, 0.05 FeCl₃) (Sigma-Aldrich) medium with 1% sterile petroleum and the incubation process was carried out at 30 °C and 150 rpm for 7 days (IKA® KS 4000i, Germany). Following the incubation period, the fungal cultures were filtered using Whatman No: 1 filter paper under sterile conditions. The filtrate was used as the cell-free culture supernatant for petroleum biodegradation assays.

Petroleum Biodegradation and Biosorption

BH medium was used for biodegradation and biosorption of petroleum by *A. parasiticus* NRRL:3386. 0.1% glucose, 0.1% yeast extract and 1% Triton X:100 were added in BH medium as an additional carbon, nitrogen and surfactant sources, respectively. Following the sterilization process and cooling to 45°C of BH medium (121°C for 15 min), 1% of sterilized petroleum (0.22 µm cellulose acetate syringe filter) (Millipore, Sartorius) was also added. The different amounts of live/dead biomasses and concentrations of culture supernatants were inoculated into the medium and the incubation process was carried out at 30°C and 150 rpm for the appropriate period in dark conditions (IKA® KS 4000i, Germany). The experiments were performed in triplicate (15).

Gravimetric Analysis

The biodegradation and biosorption of petroleum were determined by modifying the method recommended by Al-Hawash et al. (4). Following the incubation period, petroleum biodegradation and biosorption were evaluated with gravimetric analysis. The residual petroleum was extracted with dichloromethane (CH₂Cl₂) (1:2) (Sigma-Aldrich) and then the upper phase was also removed. To evaporate the dichloromethane, the flasks were left at 90 °C for half an hour (Memmert, Schwabach, Germany). The degradation of petroleum was calculated as:

$$D (\%) = (p_0 - p_1 - p_2) / p_0 \times 100$$

where p_0 and p_1 indicate the initial and remaining concentrations of petroleum at different incubation periods, p_2 denotes the concentration of abiotic loss.

The specific degradation rate was also calculated as follows:

$$d_x / x_0 \cdot d_t$$

where d_x is the change in concentration of the petroleum, x_0 shows the petroleum concentration and d_t indicates a time interval (10,16).

Degradation Kinetics

The degradation of petroleum follows the first-order reaction kinetics; it can be calculated as:

$$\ln c_t = \ln c_0 - Kt$$

where c_t and c_0 show the residual and initial petroleum concentrations; K indicates first-order reaction speed constant for petroleum biodegradation (day^{-1}), and t is time (day). The half-life period of petroleum can be calculated as follows:

$$t_{1/2} = \ln 2 / k$$

where k is the biodegradation rate constant (day^{-1}) (10, 16).

Effect of the Incubation Period on Biodegradation of Petroleum

1 g of live biomass was inoculated into BH medium and incubation process was carried out at 30 °C and 150 rpm for 7 days (IKA® KS 4000i, Germany). The degradation of petroleum was obtained by gravimetric analysis.

Effect of Different Amounts of Live Biomasses on Biodegradation of Petroleum

0.25, 0.5, 1, 1.5 and 2 g of live biomasses were inoculated into BH medium and the incubation process was carried out at 30 °C and 150 rpm for an appropriate period (IKA® KS 4000i, Germany). The degradation of petroleum was obtained by gravimetric analysis.

Effect of Different Concentrations of Culture Supernatant on Biodegradation of Petroleum

2.5%, 5%, 7.5% and 10% concentrations of culture supernatants were inoculated into BH medium and the incubation process was carried out at 30 °C and 150 rpm for an appropriate period (IKA® KS 4000i, Germany). The degradation of petroleum was obtained by gravimetric analysis.

Effect of Different Amounts of Dead Biomasses on Biosorption of Petroleum

1, 2.5, 5, 7.5 and 10 g of dead biomasses were inoculated into BH medium and the incubation process was carried out at 30 °C and 150 rpm for an appropriate period. The degradation of petroleum was obtained by gravimetric analysis.

SEM Analysis

SEM analysis was carried out by Hacettepe University Advanced Technologies Application and Research Center using with Zeiss

EVO 50 SEM (Germany). The samples were coated with carbon. The biosorption of petroleum by dead biomass of *A. parasiticus* was determined by SEM micrograph.

GC/MS Analysis

GC-MS analysis was performed to determine the removal of *n*-alkane fractions in petroleum with *A. parasiticus* NRRL:3386 strain. GC/MS analysis was carried out by the Petroleum Research Center at Middle East Technical University using TRB-1 GCMS-QP-2020 (Shimadzu, Tokyo, Japan). The procedure was performed according to Ozyurek and Bilkay (16).

RESULTS

The Petroleum Degradation by Different Incubation Periods and Different Amounts of Live Biomasses

In the first step of this study, the incubation periods (1-7 days) and the amounts of live biomasses (0.25, 0.5, 1, 1.5 and 2 g) were investigated to determine the most effective petroleum degradation by live biomass of *A. parasiticus*. As shown in Figure 1, the degradation of petroleum by 1 g of live biomass reached

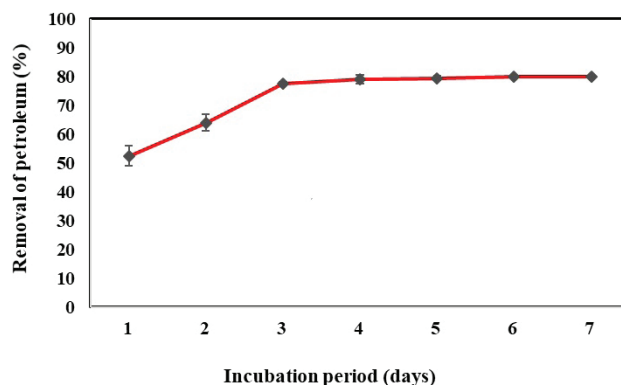


Figure 1. The effect of different incubation periods on biodegradation of petroleum by live biomass of *A. parasiticus*. Growth of *A. parasiticus* strain was carried out at 30 °C and 150 rpm for 7 days. Results are average of three measurements. Standard deviations are shown on graph.

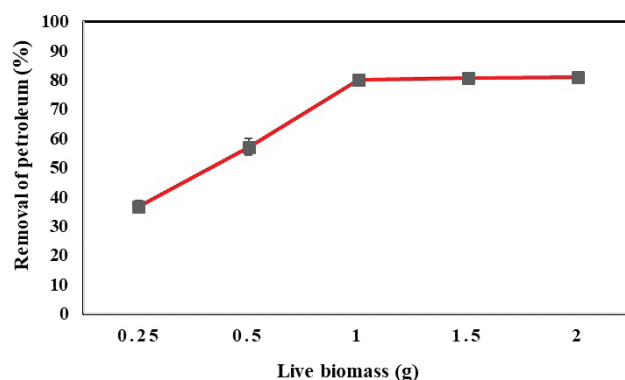


Figure 2. The effect of different amounts of live biomasses on biodegradation of petroleum. Growth of *A. parasiticus* strain was carried out at 30 °C and 150 rpm for 4 days. Results are average of three measurements. Standard deviations are shown on graph.

80% at the 4th day of the incubation period. There was no significant increase in the removal of petroleum after the 4th day. Additionally, Figure 2 also demonstrates that above 1 g of live biomass, there was no dramatic effect on removal of petroleum. According to these results, the specific degradation rate was calculated as 0.200. In the control sample, the specific degradation rate was also calculated as 0.002 day⁻¹ for petroleum. The degradation rate constant and half-life period of live biomass of *A. parasiticus* NRRL:3386 were calculated as 1.609 day⁻¹ and $t_{1/2} = 0.431$. So, it is clearly demonstrated that half-life period was low with high degradation rate constant.

The Petroleum Degradation by Different Concentrations of Cell-Free Culture Supernatants

The effect of different concentrations (2.5%, 5%, 7.5% and 10%) of cell-free culture supernatants on petroleum biodegradation were evaluated. As shown in Figure 3, the culture supernatant containing extracellular enzymes had no significant effect on petroleum biodegradation. Thus, increasing the concentration

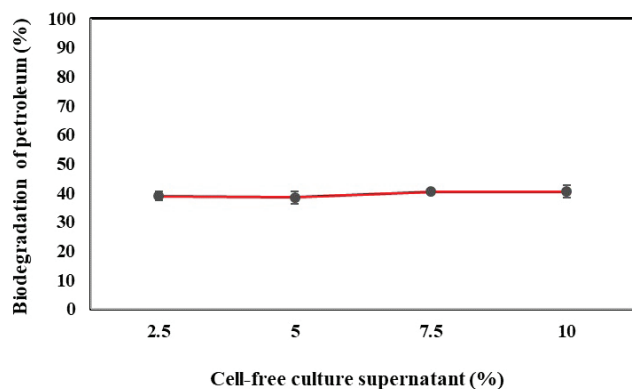


Figure 3. The effect of different concentrations of cell-free culture supernatants on biodegradation of petroleum. Growth of *A. parasiticus* strain was carried out at 30 °C and 150 rpm for 4 days. Results are average of three measurements. Standard deviations are shown on graph.

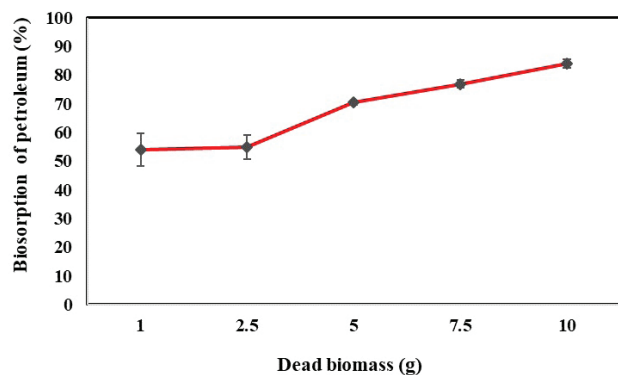


Figure 4. The effect of different amounts of dead biomasses on biosorption of petroleum. Growth of *A. parasiticus* strain was carried out at 30 °C and 150 rpm for 4 days. Results are average of three measurements. Standard deviations are shown on graph.

of culture supernatants did not lead to the expected effect on biodegradation of petroleum.

The Petroleum Biosorption by Different Amounts of Dead Biomasses

The effect of different amounts (1, 2.5, 5, 7.5 and 10 g) of dead biomasses were evaluated for petroleum biosorption. Figure 4 shows that over 50% of petroleum biosorption was observed

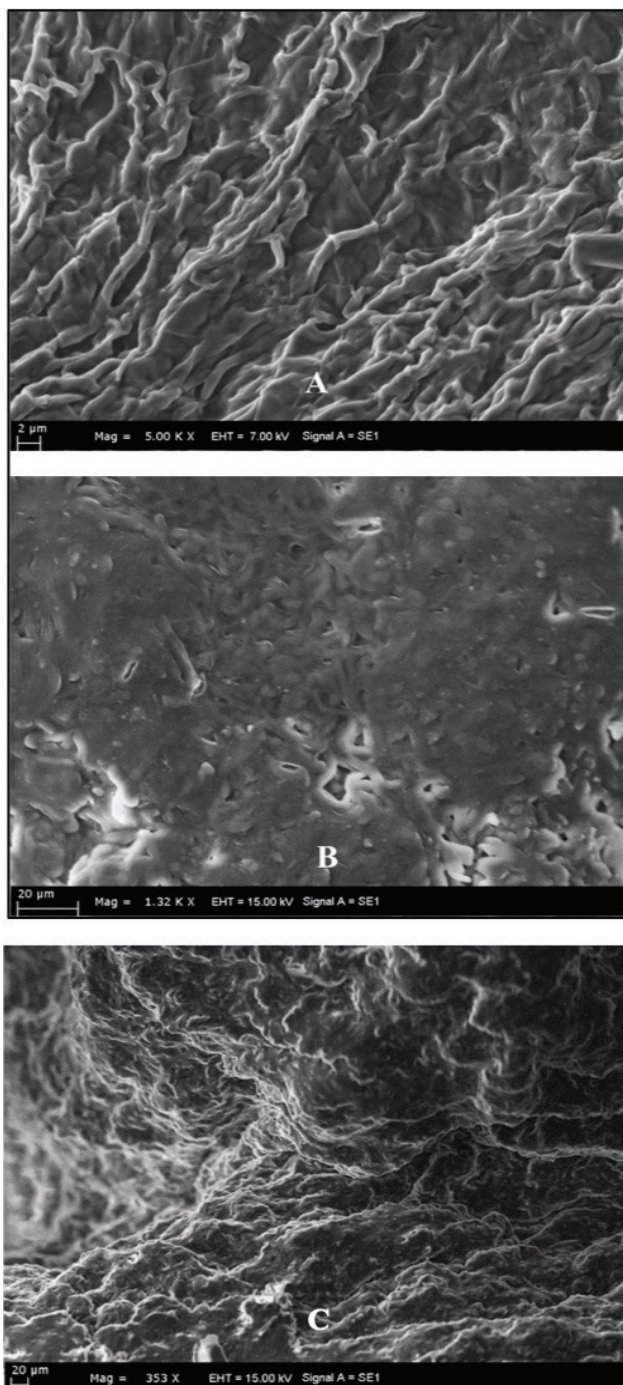


Figure 5. SEM micrograph of dead biomass of *A. parasiticus*: (A) before and (B, C) after biosorption of petroleum.

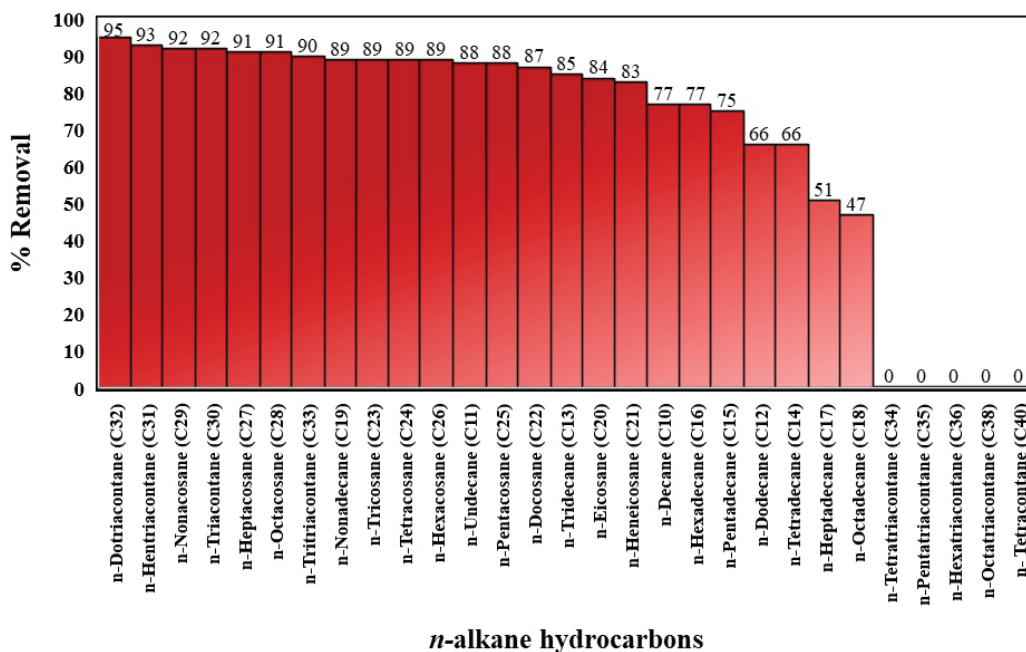


Figure 6. The degradation of n-alkane hydrocarbons by *A. parasiticus*. Growth of *A. parasiticus* strain was carried out at 30 °C and 150 rpm for 4 days.

with 1 and 2.5 g of dead biomasses. Furthermore, over 70%, 70%, and 80% of petroleum biosorption was detected with 5 g, 7.5 g and 10 g of dead biomasses, respectively.

SEM Results

SEM is used to verify the morphological differences between the dead biomass of *A. parasiticus* NRRL:3386 before and after biosorption of petroleum. While the gaps between hyphae of fungi are clear and bright before petroleum biosorption, it has been shown that the gaps between hyphae of fungi are closed due to the accumulation of petroleum. SEM micrographs of dead biomasses of fungi are shown in Figures 5A-C.

GC/MS Results

As shown in Figure 6, C₁₀ - C₁₈ short chain n-alkanes (except C₁₁ and C₁₃) were biodegraded in the range of 47-77% and C₁₁, C₁₃, and C₁₉ - C₂₆ n-alkanes were degraded over 80%. Moreover, long chain n-alkanes in the C₂₇ - C₃₃ range were efficiently degraded over 90% by 1 g of live biomass of *A. parasiticus* NRRL:3386.

DISCUSSION

Petroleum hydrocarbons are used as carbon and energy sources by fungal strains (10,17). *Aspergillus* sp. plays an important role in the biodegradation of a wide range of petroleum hydrocarbons. Accordingly, live biomass of fungi is both degrading and accumulating organic pollutants during the bioremediation process. In this manner, this study focused on the biodegradation and biosorption of petroleum by live/dead biomasses and culture supernatant of *A. parasiticus* NRRL:3386 strain. Because filamentous fungi (*A. parasiticus*) is an important potential agent on removal of petroleum by its ability to rapidly

bind to substrates and being able to grow under environmental conditions, 80% of petroleum degradation was observed by 1 g of live biomass of *A. parasiticus* NRRL:3386 within only 4-days of the incubation period. The degradation rate constant and half-life period of live biomass of *A. parasiticus* NRRL:3386 were 1.609 day⁻¹ and t_{1/2} = 0.431. Similar studies clearly showed that the half-life period was low with a high degradation rate constant (18,19). In the literature, *Aspergillus* sp. and *Rhizopus* sp. were found to be effective in the biodegradation of petroleum and lubricating oil (4, 6, 20). Al-Hawash et al. demonstrated that *Penicillium* sp. RMA1 degraded petroleum at 57% in 14 days (10). Maddela et al. reported that two fungal isolates degraded 79.9% of petroleum in 30 days (17). About 60% of biodegradation of petroleum was performed by different *Aspergillus* strains (*A. flavus*, *A. fumigatus*, *A. versicolor*, *A. terreus*) after 7 days of the incubation period and the biodegradation of petroleum was over 80% after 28 days (5). Although an increase in the incubation period usually led to an increase of petroleum biodegradation in different studies, the increase in incubation period did not lead to a significant increase in the removal of petroleum in this study (Figure 1). With the increase in incubation period, toxic compounds increase with the decrease of nutrients in the culture. So, it is thought that the fungi reached high petroleum biodegradation in a short incubation period.

Fungi with a large enzymatic activity are highly effective in the biodegradation of petroleum hydrocarbons. It is known that fungal enzymes such as hydrocarbon oxidoreductase, laccase and peroxidase play an important role in the bioremediation of sea water, fresh waters and soil (3). The extracellular enzymes produced by *Aspergillus* sp. have a significant effect on the

biodegradation of petroleum (4). However, it was found in this study that the culture supernatant of fungi was not effective in biodegradation of petroleum (Figure 3). Because the live biomass of fungi acts both as a bioreactor by breaking down organic pollutants by their intracellular and extracellular enzymes and biosorbent by accumulating organic pollutants during the bioremediation process, the culture supernatant was not as effective as live biomass on the removal of petroleum (21).

Fungi play an important role in biosorption of petroleum as well as biodegradation (4). Biosorption is a physicochemical process in which chemicals are entrapped in or on the surfaces of biological matrices (21). This passive bioaccumulation process (biosorption) is highly selective and efficient so it can be used in large scale improvements. In addition, no hazardous products are produced in this process (22). Biosorption of hydrocarbons can occur with three basic mechanisms. In the first mechanism, the hydrocarbons dissolved in the aqueous phase are directly absorbed by microbial cells, this mechanism is more suitable for cell uptake of short-chain hydrocarbons. In the second mechanism, small hydrocarbon droplets that are melted or close to melting are absorbed by microbial cells. In the third mechanism, hydrocarbons are transported by active transport or diffusion into the microbial cell by establishing a direct contact. It is known that petroleum hydrocarbons are absorbed by microbial cells by the second and third mechanism (4). In this context, 5, 7.5 and 10 g of dead biomasses achieved over 70%, 70% and 80% of petroleum biosorption, respectively. Because the surface area of the adsorbent plays an important role in the adsorption of petroleum hydrocarbons in aqueous media, the highest biosorption of petroleum was performed by 10 g of dead biomass (Figure 4) (4). SEM analysis emphasized the difference of surface morphology in dead biomass after biosorption of petroleum. Dead biomass of *A. parasiticus* exhibited a uniform interconnected structure with a continuous surface and the gaps between the hyphae of fungi are very clear and bright in Figure 5a. Due to accumulation of petroleum, the gaps between the hyphae of fungi are closed in Figures 5b and 5c.

When the removal efficiencies of live and dead biomasses were compared, over 80% of petroleum removal were achieved using 2 g of live biomass and 10 g of dead biomass of fungi (Figures 2 and 4). So, it can be expressed that the removal of petroleum can be achieved not only by live biomass which is active due to its enzymes but also by dead biomass which acts as a biological material. Because living microorganisms are affected by nutrients, pH and other environmental conditions, the usage of inactivated biological materials is very advantageous in the removal of toxic organic compounds such as petroleum. In a similar study, the biodegradation and biosorption activities of live and dead mycelial pellets of *Penicillium chrysogenum* on different PAHs were investigated. It was determined that the removal of phenanthrene by live and dead mycelial pellets of *P. chrysogenum* were similar. However, the removal of pyrene by dead mycelial pellets was higher than that re-

moved by live mycelial pellets of *P. chrysogenum*. Although the removal of pyrene by the live mycelial pellets was higher than phenanthrene, the removal capacities of live mycelial pellets were also low compared to dead mycelial pellets. Due to the change in permeability of *P. chrysogenum* cells in high-pressure inactivation process, dead mycelial pellets showed high biosorption efficiencies (21).

The GC/MS analysis of *A. parasiticus* also shows that short- and medium-chain *n*-alkanes were degraded in the range of 47 – 89% (Figure 6). Many bioremediation studies have demonstrated that fungi are generally effective on short- and medium-chain *n*-alkanes in the removal process of petroleum. RMA1 and RMA2 fungal strains degraded *n*-alkanes in the range of C_{11} - C_{20} and C_{21} - C_{25} . Aliphatic hydrocarbons such as *n*-undecane, *n*-dodecane, *n*-tridecane, *n*-tetradecane, *n*-pentadecane and *n*-hexane were used by fungal strains (10). Zhang et al. reported that *Geobacillus* sp. degraded only *n*-alkane fractions in the range of C_{12} - C_{21} in crude oil (23). Hadibarata and Tachibana reported that the *Trichoderma* S019 strain was effective on *n*-eicosane (C_{20}) in the presence of glucose as an additional carbon source (24). *Folsomia candida*, isolated from the petroleum contaminated area, degraded 79% of medium- and long-chain aliphatic hydrocarbons (25). The recent studies have clearly indicated that the increase in the density of petroleum hydrocarbons and number of rings in polycyclic aromatic hydrocarbons cause a decrease in the biodegradation process (4). In contrast to the studies in literature, it was quite striking that over 90% of long chain *n*-alkanes were degraded effectively by *A. parasiticus*. The fungi showed a significant effect in the biodegradation of long chain *n*-alkanes, which are more resistant to biodegradation. So, it should be emphasized that *A. parasiticus*, which has a complex enzyme system, is capable of greatly degrading complex structure of long chain hydrocarbons (2).

CONCLUSION

Aspergillus parasiticus NRRL:3386 had a significant effect on biodegradation and biosorption processes of petroleum in a short incubation period. The biodegradation and biosorption capacities of 2 g of live biomass and 10 g of dead biomass were over 80% within 4-days. Furthermore, 1 g of live biomass degraded 80% of petroleum in a short incubation period. While short and medium chain *n*-alkanes were degraded in the range of 47 – 89%, it was quite striking that long chain *n*-alkanes were broken down more than 90% within 4 days. Many bioremediation studies in the literature have shown that fungal strains are generally effective on short- and medium-chain *n*-alkanes in the removal process of petroleum. However, the *A. parasiticus* strain showed a considerable effect on removal of long chain *n*-alkanes compared to short- and medium-chains. The results of this study clearly indicated that biodegradation and the biosorption capacities of *A. parasiticus* were considerably high. It is believed that this study will provide an important contribution to further mycoremediation studies in the literature.

Peer-review: Externally peer-reviewed.

Author Contributions: Conception/Design of study: S.B.O., N.H.A.; Data Acquisition: S.B.O., N.H.A.; Data Analysis/Interpretation: S.B.O., N.H.A.; Drafting Manuscript: S.B.O., N.H.A.; Critical Revision of Manuscript: S.B.O., N.H.A.; Final Approval and Accountability: S.B.O., N.H.A.; Supervision: S.B.O., N.H.A.

Conflict of Interest: The authors declare that they have no conflicts of interest to disclose.

Financial Disclosure: There are no funders to report for this submission.

Acknowledgements: The authors would like to thank all staff in the Hacettepe University Biotechnology Laboratory for supporting and contributing to this work.

REFERENCES

- Zhang JH, Xue QH, Gao H, Ma X, Wang P. Degradation of crude oil by fungal enzyme preparation from *Aspergillus spp.* For potential use in enhanced oil recovery. *J Chem Technol Biotechnol* 2016; 91: 865-75.
- Fan CY, Krishnamurth S. Enzymes for enhancing bioremediation of petroleum-contaminated soils: A brief review. *J Air Waste Manag Assoc* 1995; 45: 453-9.
- Balaji V, Arulazhagan P, Ebenezer P. Enzymatic bioremediation of polyaromatic hydrocarbons by fungal consortia enriched from petroleum contaminated soil and seeds. *J Environ Biol* 2014; 35: 1-9.
- Al-Hawash AB, Zhang X, Ma F. Removal and biodegradation of different petroleum hydrocarbons using filamentous fungus *Aspergillus sp.* RFC-1. *Microbiologyopen* 2018; 8(1): 1-14.
- Islam NF. Bioprospecting fungal diversity from crude oil infiltrate soil of Assam, India's Northeast. *Trop Plant Res* 2017; 4(2): 319-29.
- Al-Nasrawi H. Biodegradation of crude oil by fungi isolated from Gulf of Mexico. *J Bioremediat Biodegrad* 2012; 3(4): 1-6.
- Al-Jawhari IFH. Ability of some soil fungi in biodegradation of petroleum hydrocarbon. *J Appl Environ Microbiol* 2014; 2(2): 46-52.
- Vanishree M, Thatheyu A.J, Ramya D. Biodegradation of petroleum using the fungus *Penicillium sp.* *Forensic Sci Int* 2014; 2(1): 26-31.
- Dawoodi V, Madani M, Tahmourespour A, Golshani Z. The study of heterotrophic and crude oil-utilizing soil fungi in crude oil contaminated regions. *J Bioremediat Biodegrad* 2015; 6(2): 1-5.
- Al-Hawash AB, Alkooorane JT, Abbood HA, Zhang J, Sun, J, Zhang X, Ma F. Isolation and characterization of two crude oil-degrading fungi strains from Rumaila oil field, Iraq *Biotechnol Rep* 2018; 17: 104-9.
- Eraydin Erdogan E, Sahin F, Karaca A. Determination of petroleum-degrading bacteria isolated from crude oil-contaminated soil in Turkey. *Afr J Biotechnol* 2012; 11(21): 4853-9.
- Ustun Kurnaz S, Buyukgungor H. Bioremediation of total petroleum hydrocarbons in crude oil contaminated soils obtained from southeast Anatolia. *Acta Biol Turc* 2016; 29(2): 57-60.
- Bilen Ozyurek S, Seyis Bilkay I. Determination of petroleum biodegradation by bacteria isolated from drilling fluid, waste mud pit and crude oil. *Turk J Biochem* 2017; 42: 609-16.
- Tugrul Yucel, T. Investigation of some parameters affecting methyl orange removal by *Fusarium acuminatum*, *Braz Arch Biol Technol* 2018; 61: e18160237.
- Bilen Ozyurek S, Seyis Bilkay I. Biodegradation of petroleum by *Klebsiella pneumoniae* isolated from drilling fluid. *Int J Environ Sci Technol* 2018; 15: 2107-16.
- Bilen Ozyurek S, Seyis Bilkay I. Comparison of petroleum biodegradation efficiencies of three different bacterial consortia determined in petroleum-contaminated waste mud pit. *SN Applied Sciences* 2020, 272.
- Maddela NR, Scalvenzi L, Perez M, Montero C, Gooty JM. Efficiency of indigenous filamentous fungi for biodegradation of petroleum hydrocarbons in medium and soil: Laboratory study from Ecuador. *Bull Environ Contam Toxicol* 2015; 95: 385-94.
- Yudano B, Said M, Sabaruddin Napoleon A, Fanani Z. Kinetics approach of biodegradation of petroleum contaminated soil by using indigenous isolated bacteria. *J Trop Soils* 2011; 16: 33-8.
- Kachiang'a L, Momba, MNB. Kinetics of petroleum oil biodegradation by consortium of three protozoan isolates (*Aspidisca sp.*, *Trachelophyllum sp.* and *Peranema sp.*). *Biotechnol Rep* 2017; 15: 125-31.
- Thenmozhi R, Arumugam K, Nagasathya A, Thajuddin N, Paneerselvam A. Studies on mycoremediation of used engine oil contaminated soil samples. *Adv Appl Sci Res* 2013; 4(2): 110-18.
- Ding J, Chen BL, Zhu LZ. Biosorption and biodegradation of polycyclic aromatic hydrocarbons by *Phanerochaete chrysosporium* in aqueous solution. *Chin Sci Bull* 2013; 58: 613-21.
- Chergui A, Kerbach R, Junter G-A. Biosorption of hexacyanoferrate (III) complex anion to dead biomass of the basidiomycete *Pleurotus mutilus*: Biosorbent characterization and batch. *Chem Eng J* 2009; 147: 150-60.
- Zhang J, Zhang X, Liu J, Li R, Shen B. Isolation of a thermophilic bacterium *Geobacillus sp.* SH-1, capable of degrading aliphatic hydrocarbons and naphthalene simultaneously, and identification of its naphthalene degrading pathway. *Bioresour Technol* 2012; 124: 83-9.
- Hadibarata T, Tachibana S. Microbial degradation of *n*-eicosane by filamentous fungi. In: *Interdisciplinary studies on environmental chemistry and environmental research in Asia*. (Eds. Y. Obayashi, T. Isobe, A. Subramanian, S. Suzuki and S. Tanabe), Terrapub, Tokyo, 2009; 323-9.
- Covino S, D'Annibale A, Stazi R, Cajthaml T, Čvančarová M, Stella T, Petruccioli M. Assessment of degradation potential of aliphatic hydrocarbons by autochthonous filamentous fungi from a historically polluted clay soil. *Sci Total Environ* 2015; 505: 545-54.

Evaluation of *In Vitro* Wound Healing Activity of Thymoquinone

Murat Pekmez¹ , Nihan Sultan Milat² 

¹Istanbul University, Faculty of Science, Department of Molecular Biology and Genetics, Istanbul, Turkey

²Istanbul University, Institute of Graduate Studies in Sciences, Department of Molecular Biology and Genetics, Istanbul, Turkey

ORCID IDs of the authors: M.P. 0000-0002-6150-8372; N.S.M. 0000-0002-0795-8030

Please cite this article as: Pekmez M, Milat NS. Evaluation of *In Vitro* Wound Healing Activity of Thymoquinone. Eur J Biol 2020; 79(2): 151-156. DOI: 10.26650/EurJBiol.2020.0044

ABSTRACT

Objective: *Nigella sativa* has been extensively investigated as an important potential agent for the healing of wounds and there have been numerous studies regarding its effect. Although thymoquinone (TQ) is a well-known active constituent of *Nigella sativa*, studies in to the usability of TQ on wound healing are still insufficient. In this study, we aimed to evaluate the *in vitro* wound healing potential of TQ.

Materials and Methods: NIH/3T3 mouse embryonic fibroblast cells were used to evaluate the wound healing effect of TQ. Different concentrations of TQ (0.1, 1 and 10 μ M) were applied to the cells and their cytotoxic effect on cells after 24- and 48- hours was measured by MTT assay. Its effect on wound healing after 18- and 24- hours recovery was examined by *in vitro* scratch assay. Also, the level of β -catenin, an effective protein in the process of healing wounds, was determined by Western blot assay.

Results: MTT analysis indicated that 0.1, 1 and 10 μ M doses of TQ had increased the cell numbers. *In vitro* scratch assay data showed that treatment with 1 and 10 μ M TQ resulted in a statistically significant wound closure activity (91.35% and 90.84%, respectively) compared to the control. Additionally, we observed a statistically significant increase in the β -catenin protein level which supported our data.

Conclusion: Our results demonstrated that TQ increases both the viability of NIH/3T3 cells and its wound closure activity *in vitro*, and that it has the effect of increasing crucial protein β -catenin. This study suggests that TQ may be a valuable substance for the healing of wounds and that its usability should be investigated.

Keywords: Thymoquinone, wound healing, NIH/3T3

INTRODUCTION

Wounds are physical injuries that cause disruption to the normal structure and function of the skin (1). Different types of wounds may occur in humans. The most difficult wounds to heal are chronic wounds and delayed acute wounds. Current studies demonstrate that nearly 6 million people in the world have chronic wounds. Annual health care expenditure is extremely high for these types of wounds, at more than \$3 billion (2,3). In addition, it is estimated that 1% of the European population suffers from recurrent and chronic ulceration such as leg and foot ulcers (2,4). Wounds related

to diabetics, burns, and ulcers still have significant impact on the population. Therefore, to develop new strategies is important and recent studies have increasingly focused on natural products to treat wounds.

The current synthetic therapeutics used in wound healing still remains insufficient. They may cause adverse reactions and allergic problems that limit the use of these drugs. In order to eliminate these conditions, the development of wound healing agents taken from sources such as medicinal plants and natural products is highly important. For this reason, numerous medicinal plants have been described in the literature such as *Curcuma*



Corresponding Author: Murat Pekmez

E-mail: mpekmez@istanbul.edu.tr

Submitted: 02.01.2020 • **Revision Requested:** 06.02.2020 • **Last Revision Received:** 24.06.2020 •

Accepted: 30.06.2020 • **Published Online:** 06.10.2020

© Copyright 2020 by The Istanbul University Faculty of Science • Available online at <http://ejb.istanbul.edu.tr> • DOI: 10.26650/EurJBiol.2020.0044

longa, *Moringa oleifera*, *Aegle marmelos*, *Phyllanthus muellerianus* and so on (5). One of these plants is *Nigella sativa*, an herbaceous plant, which belongs to family of the Ranunculaceae (6). It has been used traditionally for the treatment of diseases. It has antimicrobial, antiviral, antifungal, antiparasitic properties (7). *In vitro* and *in vivo* studies have proved that it might be useful for wound healing. In studies performed on *in vivo* burn models, it was demonstrated that *N. sativa* cream and *N. sativa* extract showed significant wound healing effects compared with a commercially available cream (6,8). In the *in vivo* diabetic model, it was shown that the wound area decreased as a result of the treatment of *N. sativa* extract (9). It is also reported that *N. sativa* extract reduces radiation-related delayed wound healing in mice (10). When human gingival fibroblast cells are used as an *in vitro* wound healing model, aqueous extract of *N. sativa* induced fibroblast proliferation and accelerated wound closure activity (1). All these healing effects and properties originate from bioactive compounds of *N. sativa* such as thymoquinone (TQ). It is known that Thymoquinone has antimicrobial (11,12), antiallergic (13), antidiabetic (14), anti-inflammatory (15), and antioxidant (16) properties. These properties make TQ an important potential agent for the healing of wounds. Interestingly, the wound healing potential of TQ has not been clearly investigated. Moreover, most of the studies are based on the *in vivo* models. However, *in vitro* studies are needed to highlight the wound healing mechanism at molecular level.

Thus far, there have been numerous studies on the wound healing effect of *N. sativa*, but studies on TQ are still insufficient. The purpose of this study is to evaluate the role of TQ on the wound healing process and on β -catenin expression in NIH/3T3 fibroblast cell line.

MATERIALS AND METHODS

Experimental Reagents

TQ was purchased from Santa Cruz Biotechnology (Dallas, Texas, USA) and dissolved in dimethyl sulfoxide (DMSO). Tissue culture reagents were obtained from Gibco (Carlsbad, CA, USA). SMART™ BCA Protein Assay Kit was from iNtRON Biotechnology (Seongnam, Gyeonggi, Korea). Polyvinylidene fluoride (PVDF) membrane was obtained from Millipore (Darmstadt, Germany). Mouse anti- β -catenin monoclonal antibody and horseradish peroxidase (HRP)-conjugated goat anti-mouse IgG were obtained from Enzo Life Sciences (Farmingdale, NY, USA). HRP conjugated GAPDH Loading Control Monoclonal Antibody and Pierce™ ECL Western Blotting Substrate was from ThermoFisher Scientific (Kwartsweg, Bleiswijk, Holland). All other chemicals and reagents were from Sigma (St. Louis, MO, USA).

Cell Culture

Mouse embryonic fibroblast cells (NIH/3T3) were kindly provided by Istanbul University Faculty of Science, Department of Biology. NIH/3T3 cells were cultured in Dulbecco's modified Eagle medium (DMEM/F12) which included 1% (v/v) antimycotic-antibiotic solution (100 μ g/mL streptomycin and 0.25 μ g/mL amphotericin B and 100 U/mL penicillin) and 10% (v/v) heat-inac-

tivated fetal bovine serum. The cells were incubated at 37°C in a humidified atmosphere with 5% CO₂. The cells were passaged before they reached full confluence.

Cell Viability Assay

MTT (3-(4,5-dimethylthiazol-2-yl)2,5-diphenyl tetrazolium bromide) cell viability assay was used in order to investigate the proliferative and cytotoxic effect of TQ on NIH/3T3 fibroblast cells. Briefly, the cells were seeded in a 96-well plate at a confluency of 3×10^4 per well. Adherent cells were then treated with increasing concentrations of TQ (0.01-1000 μ M) which was diluted with DMEM/F12. After 24 and 48 h incubation at 37°C, the medium was removed. 30 μ L of MTT (5 mg/ml) was added to the cells. After a 4 h incubation at 37°C, 150 μ L of DMSO was added to solubilize formazan crystals and the absorbance was measured at 540 nm using a microplate reader. Experiments were performed in triplicate.

Thymoquinone Treatment

NIH/3T3 cells were seeded in 24 well-plates at a density of 1.8×10^5 per well for cell treatment with TQ. According to MTT assay results, final TQ concentrations of 0.1, 1 and 10 μ M were applied to the cells incubated for 24 h. Experiments were performed in triplicate.

In vitro Scratch Assay

The capability of TQ on migration of NIH/3T3 cells was determined by *in vitro* scratch assay. The cells were seeded at a confluency of 18×10^4 per well into a 24-well plate containing DMEM/F12 medium and incubated overnight. After incubation, the medium was removed and the adherent cells were scratched with a sterile p1000 pipette tip. The scratched cell layers were washed with phosphate buffered saline (PBS) to remove cell debris. After that, the cells were treated with 0.1, 1, 10 μ M of TQ that was diluted in DMEM/F12. Fresh medium was applied for the control group. Photographs of the scratched area were recorded by inverted light microscope equipped with a camera (Nikon Eclipse Ti-E) under 10X magnification at 0, 18 and 24 h. Data were analyzed with Image J software (NIH, USA) in order to determine the width of the scratch and the rate of migration of cells. Experiments were performed in triplicate.

Immunoblotting Assay

Western blotting assay was performed to analyze samples, as described by Şengelen and Önay-Uçar (17). In short, the cells were trypsinized and centrifugated at 700 \times g for 10 min. Lysis buffer [20 mM Tris-HCl (pH 6.8), 0.04% (w/v) EDTA, 1% (v/v) Triton X-100, and EDTA-free PIC (protease inhibitor cocktail), 1 mM PMSF] was used to resuspend the pellets. The extracts were centrifuged at 20,000 \times g for 20 min at 4°C. Protein concentrations were quantified by bicinchoninic acid protein assay. Thirty μ g of protein was separated by SDS-PAGE gel and transferred onto PVDF membranes. 5% non-fat dry milk in Tris-buffered saline/Tween 20 (TBST) was used to block membranes for 1 h. After that, the membranes were incubated overnight with anti- β -catenin primer antibody (1:1000) at 4°C. The following day, the membranes were washed five times with TBST, and then incu-

bated with IgG-HRP secondary antibody (1:5000) for 2 h at 37°C, and washed with TBST again. Protein bands were visualized using an ECL kit. GAPDH (antibody diluted 1:2000) was used for data normalization. ImageLab 5.2.1 software (Bio-Rad) was used to determine protein expression levels. Experiments were performed in triplicate.

Statistical Analysis

One-way or two-way ANOVA was used to analysis data followed by Tukey post-hoc-test. The statistically significance was taken to be $P < 0.05$. The results were presented as mean \pm standard deviation (SD) and the number of experiments were indicated with n . Statistical analysis and graph generation were carried out in GraphPad Prism Software (San Diego, CA, USA) version 7.0.

RESULTS

Thymoquinone Effects Viability of NIH/3T3 Cells

The effect of increasing concentrations of TQ on cell viability was evaluated in NIH/3T3 after 24 h and 48 h incubation using MTT assay. The data is shown in Figure 1. The cells were treated with 0.01–1000 μM of TQ. MTT results showed that 1 and 10 μM of TQ was able to promote cell viability. However, 50 μM and above of TQ showed decreased cell viability after 24 h incubation. In addition, the data showed that TQ decreased cell viability of NIH/3T3 cells in a dose-dependent manner after 48 h incubation. The half-maximal inhibitory concentration (IC_{50}) was determined 51.43 μM after 24 h and 47.71 μM after 48 h incubation. According to the MTT results, different concentration of TQ was used and selected according to significantly increased cell viability compared to the control. Therefore, the final concentrations of thymoquinone which are 0.1, 1 and 10 μM were used in the experiments.

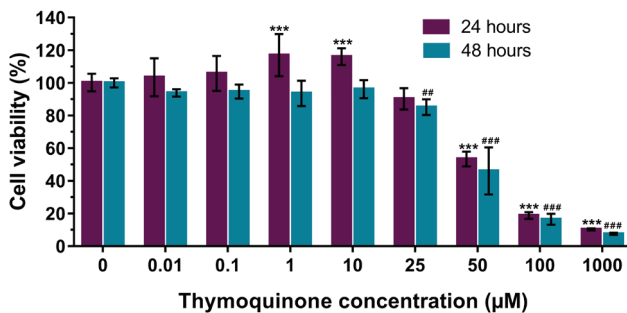


Figure 1. Determination of TQ effect on cell viability after 24 h and 48 h incubation. The graph represents the mean \pm SD of three independent experiments analyzed together ($n=3$). *** $P < 0.001$ compared to control for 24 h, ### $P < 0.001$, ## $P < 0.01$ compared to control for 48 h determined by one-way ANOVA using Tukey post-hoc-test.

The Effect of Thymoquinone on NIH/3T3 Cells Wound Healing

In vitro scratch assay was used to determine wound closure activity of TQ on NIH/3T3 cells after 18 and 24 h recovery. *In vitro* scratch assay data showed that, although there was no statisti-

cally significant difference between 0.1 μM TQ and the control groups, treatment with 1 and 10 μM TQ resulted in a statistically significant recovery in the wound area compared to the control after 18 and 24 h (Figures 2 and 3). The closure of the control was 57.9%, 64.98% for 0.1 μM , 75.38% for 1 μM and 71.82% for 10 μM after 18 h of incubation. After 24 h of incubation, the clo-

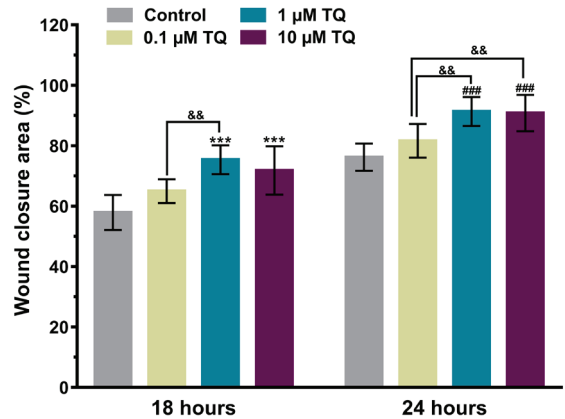


Figure 2. Percentage of wound closure area of NIH/3T3 fibroblast cells treated with TQ determined by *in vitro* scratch assay after 18 hours and 24 h incubation. The graph represents the mean \pm SD of three independent experiments analyzed together ($n=3$). *** $P < 0.001$ compared to control for 18 h, ### $P < 0.001$ for 24 h. && $P < 0.01$ shows multiple comparisons between different groups. P values were determined by one-way ANOVA using Tukey post hoc-test.

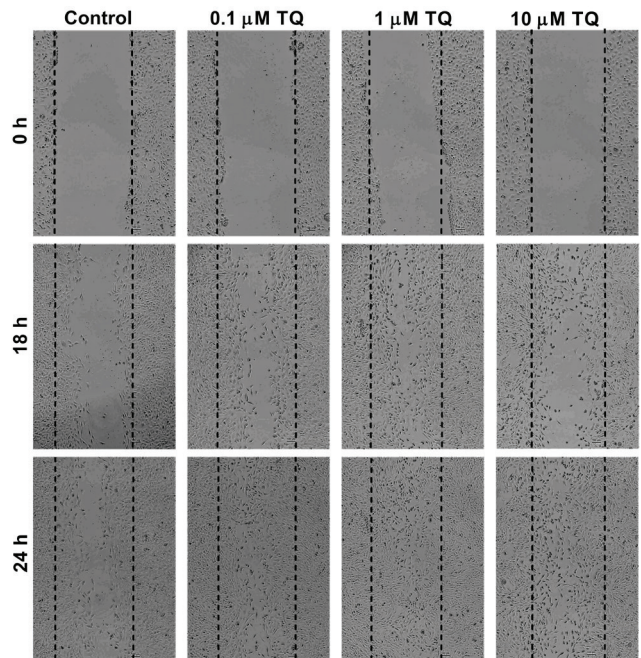


Figure 3. Microscopy images of NIH/3T3 fibroblast cells migration after scratch at 0, 18 and 24th h of 0.1, 1 and 10 μM TQ treatment under 10X magnification.

sure of the control was 76%, 81.64% for 0.1 μM , 91.35% for 1 μM and 90.84% for 10 μM . According to the results, 1 μM of TQ was observed as the most efficient concentration for *in vitro* wound healing activity on NIH/3T3 cells.

Determination of β -catenin Expression in NIH/3T3 Fibroblast Cells

Western blotting assay was performed to analyze the effect of TQ on β -catenin expression in NIH/3T3 fibroblast cells (Figure 4). We observed that 1 μM TQ treatment increased β -catenin expression. No statistically significant difference was observed between 0.1 and 10 μM TQ groups compared to the control ($P>0.05$). 1 μM TQ increased the expression of β -catenin by 35.2%. In contrast, 0.1 μM and 10 μM TQ decreased the level of β -catenin by 12.5% and 4.6% respectively.

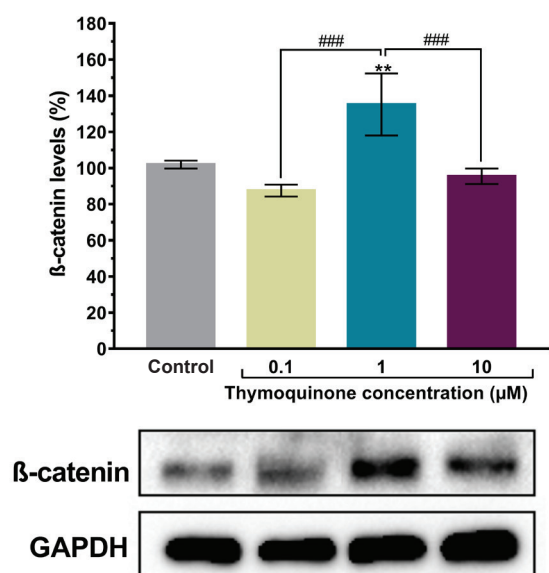


Figure 4. Expression of β -catenin in response to TQ (0.1, 1 and 10 μM) treatments for 24 h. All data were normalized to GAPDH. The graph represents the mean \pm SD (n=3). ** $P<0.01$ versus control group. *** $P<0.001$ shows multiple comparisons between different groups. P values were determined by one-way ANOVA using Tukey post hoc-test.

DISCUSSION

Wounds are still a major global health challenge. Many people suffer from different types of wounds. Although synthetic therapeutics form the basis of wound care, they may cause side effects and allergic problems so the use of these drugs are limited. Current studies have also reported the positive effects of natural products and their bioactive constituents. Many medicinal plants are screened as a wound healing agent and one of these medicinal plants is *N. sativa*. Studies carried out to date have shown the significant wound healing effects of *N. sativa* extracts and oils *in vivo* burn models (6,8), diabetic wound models (9), radiation-related delayed wound models (10) and *in vitro* wound models (1). Although these studies suggest that

N. sativa oil or extract is a wound healing agent, none of them explained which active constituent provides a healing effect on wounds. As is well known, many bioactive compounds are found as a mixture in extracts or oils of medicinal plants. They may cause various side effects such as allergies or irritation. This limits the use of commercially available impure extracts and oils of *N. sativa* as a wound healing agent. In addition, it has been reported that *N. sativa* extract and oil cause irritation or allergic problems (18,19). Therefore, research should focus on active components of *N. sativa*.

Many studies have reported on and evaluated the wound healing effect of natural bioactive components. In diabetic wound healing models, treatment with curcumin provided acceleration of wound healing by its antioxidant effect (20). A study performed on uterine wounds treated with resveratrol showed an increasing activity of antioxidant enzymes and decreasing lipid peroxidation. That resulted in thickness of the uterine wall (21). Furthermore, rosmarinic acid demonstrated anti-inflammatory properties in thermal injury and liver ischaemia-reperfusion rat models (22). TQ is the main biologically active component of essential oil of *N. sativa*, also well known for its pharmacological activities such as antimicrobial (11,12), anti-inflammatory (15), antioxidant (16) effects. According to these known properties, TQ has been thought to have potential as a wound healing agent.

Herein, our results indicated that low concentrations of TQ significantly increased NIH/3T3 cell viability in both a dose and time dependent manner. The highest cell viability was observed after 24 h incubation with 1 and 10 μM TQ, but at high concentrations (>25 μM), cell viability significantly decreased. Additionally, all concentrations of TQ decreased cell viability after 48 h. According to these results, the study was carried out with 24 h of treatment. IC_{50} value of TQ was determined as 51.43 μM . These results suggest that higher doses (>25 μM) of TQ and longtime treatment are more toxic to NIH/3T3 fibroblast cells. Thus, low doses of TQ are more effective for cell viability in healthy fibroblast cells. One study showed that TQ accelerated the rate of wound closure by reducing inflammation and oxidative stress in burn models (23). Another study performed with alloxan-induced diabetic rats resulted in acceleration of wound healing after TQ treatment during the inflammatory phase which arose due to the antioxidant, anti-inflammatory and antimicrobial properties of TQ (24). Our study is consistent with these studies as well as valuable because more thorough investigation is needed *in vitro* with different cell types which act during the phases of wound healing to determine the process at cellular and molecular level and understand the role of TQ. Additionally, the results of treatments with potential agents will be predictable when *in vivo* studies are performed.

In vitro models, wound healing is indicated with migration of cells and explains the rate of wound closure. The *in vitro* scratch assay is an easy method to measure cell migration *in vitro* (25). Accordingly, we used *in vitro* scratch assay to create a wound area and to test TQ treatments *in vitro*. The photographs taken at 0, 18 and 24 h time intervals to observe the closure of the wound

area clearly indicated that all selected doses of TQ (0.1, 1 and 10 μM) have potential wound closure activity due to fibroblast migration. In addition, while 1 and 10 μM TQ showed a statistically significant effect in comparison with the control ($P < 0.001$), the highest wound closure rate was observed in 1 μM TQ treatment. The rate of wound closure is increasingly thought to be related to the idea that TQ may also promote the proliferation of cells.

Following an injury, the wound healing response is controlled by many signaling pathways (26). Studies should be carried out to understand these molecular pathways and their components which are involved in the wound healing process in order to generate potential therapeutic agents and therapies. The canonical Wnt–wingless signaling pathway is well known which regulates many biologic processes by increasing the transcriptional activity and stability of β -catenin (27-29). Additionally, Wnt pathway is important for wound healing because its key mediator β -catenin has a pivotal role on the proliferation phase of wound healing. β -catenin also participates in some phases of wound repair. First the phosphorylation occurs and it accumulates in the cytoplasm and then migrates into the nucleus. In the nucleus the regulation of the target gene transcription occurs and this results in proliferation, migration and accumulation in the collagen of fibroblasts. Our western blot analysis data is showed that 1 μM TQ treatment resulted in an increase by 35.2% in β -catenin expression compared with other selected doses of TQ ($P < 0.001$). It might be thought that TQ plays a role in the activity of β -catenin. To better understand the results of elevated β -catenin protein levels after TQ treatment on wound healing, more parameters should be investigated, and further studies should be performed *in vivo* physiological conditions.

CONCLUSION

Our results show that TQ may promote cell viability, accelerate wound healing and trigger protein levels which are effective in wound healing phases *in vitro*. Our results reveal promising data regarding the possibility of a TQ derived product being used in the treatment of wounds and other dermatological problems. TQ derived products and drugs may be developed combined with other active substances and/or administered topically. Although the study was performed in one of the important cell groups, fibroblasts, on wound healing, further research should be carried out with other cell lines to determine TQ usability on wound healing and understand its effect on the wound healing mechanism.

Peer-review: Externally peer-reviewed.

Author Contributions: Conception/Design of study: M.P., N.S.M.; Data Acquisition: M.P., N.S.M.; Data Analysis/Interpretation: M.P., N.S.M.; Drafting Manuscript: M.P., N.S.M.; Critical Revision of Manuscript: M.P., N.S.M.; Final Approval and Accountability: M.P., N.S.M.; Technical or Material Support: M.P., N.S.M.; Supervision: M.P.

Conflict of Interest: The authors declare that they have no conflicts of interest to disclose.

Financial Disclosure: There are no funders to report for this submission.

REFERENCES

1. Ab Rahman MR, Abdul Razak F, Mohd Bakri M. Evaluation of wound closure activity of *Nigella sativa*, *Melastoma malabathricum*, *Pluchea indica*, and *Piper sarmentosum* extracts on scratched monolayers of human gingival fibroblasts. *J Evid Based Complementary Altern Med* 2014; 1-9.
2. Mathieu D, editor. Handbook on hyperbaric medicine. New York: Springer; 2006.
3. Menke NB, Ward KR, Witten TM, Bonchev DG, Diegelmann RF. Impaired wound healing. *Clin Dermatol* 2007; 25: 19-25.
4. Nelzen O, Bergqvist D, Lindhagen A. The prevalence of chronic lower-limb ulceration has been underestimated: Results of a validated population questionnaire. *Br J Surg* 1996; 83: 255-8.
5. Agyare C, Bekoe EO, Boakye YD, Dapaah SO, Appiah T, Bekoe SO. Medicinal Plants and Natural Products with Demonstrated Wound Healing Properties. *Wound Healing: New insights into Ancient Challenges*. London: InTech; 2016.
6. Sarkhail P, Esmaily H, Baghaei A, Shafiee A, Abdollahi M, Khademi Y, et al. Burn healing potential of *Nigella sativa* seed oil in rats. *Int J Pharm Sci Res* 2011; 2(1): 34-40.
7. Eid AM, Elmarzugi NA, Abu Ayyash LM, Sawafta MN, Daana HI. A Review on the Cosmeceutical and External Applications of *Nigella sativa*. *J Trop Med* 2017; 1-6.
8. Yaman I, Durmus AS, Ceribasi S, Yaman M. Effects of *Nigella sativa* and silver sulfadiazine on burn wound healing in rats. *Vet Med (Praha)* 2010; 55(12): 619-24.
9. Nourbar E, Mirazi N, Yari S, Rafieian-Kopaei M, Nasri H. Effect of hydroethanolic extract of *Nigella sativa* L. on skin wound healing process in diabetic male rats. *Int J Prev Med* 2019; 10:18-24.
10. Jagetia GC, Ravikiran P. Acceleration of wound repair and regeneration by *Nigella sativa* in the deep dermal excision wound of mice whole body exposed to different doses of γ -radiation. *Am Res J Med Surg* 2015; 1(3): 1-17.
11. Kouidhi B, Zmantar T, Jrah H, Souiden Y, Chaieb K, Mahdouani K et al. Antibacterial and resistance-modifying activities of thymoquinone against oral pathogens. *Ann Clin Microbiol Antimicrob* 2011; 10: 29-35.
12. Halawani E. Antibacterial Activity of Thymoquinone and Thymohydroquinone of *Nigella sativa* L. and Their Interaction with Some Antibiotics. *Adv Biol Res* 3. 2009; (5-6): 148-52.
13. Hayat K, Asim MB, Nawaz M, Li M, Zhang L, Sun N. Ameliorative effect of thymoquinone on ovalbumin-induced allergic conjunctivitis in Balb/c mice. *Curr Eye Res* 2011; 36(7): 591-8.
14. Abdelmeguid NE, Fakhoury R, Kamal SM, Al Wafai RJ. Effects of *Nigella sativa* and thymoquinone on biochemical and subcellular changes in pancreatic beta-cells of streptozotocin-induced diabetic rats. *J Diabetes* 2010; 2(4): 256-66.
15. Ali BH, Blunden G. Pharmacological and toxicological properties of *Nigella sativa*. *Phytother Res* 2003; 17(4): 299-305.
16. Hosseinzadeh H, Parvardeh S, Asl MN, Sadeghnia HR, Ziaee T. Effect of thymoquinone and *Nigella sativa* seeds oil on lipid peroxidation level during global cerebral ischemia-reperfusion injury in rat hippocampus. *Phytomedicine* 2007; 14(9): 621-7.
17. Şengelen A, Önay-Uçar E. Rosmarinic acid and siRNA combined therapy represses Hsp27 (HSPB1) expression and induces apoptosis in human glioma cells. *Cell Stress Chaperones* 2018; 23(5): 885-96.
18. Zedlitz S, Kaufmann R, Boehncke WH. Allergic contact dermatitis from black cumin (*Nigella sativa*) oil-containing ointment. *Contact Dermatitis* 2002; 46(3): 188.

19. Gelot P, Bara-Passot C, Gimenez-Arnau E, Beneton N, Maillard H, Celerier P. Éruption Bulleuse À L'Huile De Nigelle. *Ann Dermatol Venereol* 2012; 139(4): 287-91.
20. Kant V, Gopal A, Pathak NN, Kumar P, Tandan SK, Kumar D. Antioxidant and anti-inflammatory potential of curcumin accelerated the cutaneous wound healing in streptozotocin-induced diabetic rats. *Int Immunopharmacol* 2014; 20: 322-30.
21. Sayin O, Micili SC, Goker A, Kamaci G, Ergur BU, Yilmaz O et al. The role of resveratrol on full-Thickness uterine wound healing in rats. *Taiwan J Obstet Gynecol* 2017; 56(5): 657-63.
22. Rocha, J, Eduardo-Figueira M, Barateiro A, Fernandes A, Brites D, Bronze R et al. Anti-inflammatory effect of rosmarinic acid and an extract of *Rosmarinus officinalis* in rat models of local and systemic inflammation. *Basic Clin Pharmacol Toxicol* 2015; 116(5): 398-413.
23. Selçuk CT, Durgun M, Tekin R, Yolbas L, Bozkurt M, Akçay C et al. Evaluation of the effect of thymoquinone treatment on wound healing in a rat burn model. *J Burn Care Res.* 2013; 34(5): 274-81.
24. Yusmin A, Ahmad N. Effect of thymoquinone on wound healing on wound healing in alloxan-induced diabetic rats. *Asian J Pharm Clin Res* 2017; 10(9): 242-5.
25. Liang CC, Park AY, Guan JL. *In vitro* scratch assay: a convenient and inexpensive method for analysis of cell migration *in vitro*. *Nat Protoc* 2007; 2(2): 329-33.
26. Bielefeld Kirsten A, Amini-Nik S, Alman BA. Cutaneous wound healing: recruiting developmental pathways for regeneration. *Cell Mol Life Sci* 2013; 70(12): 2059-81.
27. Polakis P. Wnt signaling and cancer. *Genes Dev* 2000; 14: 1837-51.
28. Taipale J, Beachy PA. The hedgehog and Wnt signalling pathways in cancer. *Nature* 2001; 411: 349-54.
29. Korswagen HC, Clevers HC. Activation and repression of wing-less/Wnt target genes by the TCF/LEF-1 family of transcription factors. *Cold Spring Harb Symp Quant Biol* 1999; 64: 141-7.

Profile of Apoptotic Proteins after Curcumin Treatment by Antibody Array in H69AR Lung Cancer Cells

Süleyman İlhan¹ 

¹Manisa Celal Bayar University, Faculty of Science and Letters, Department of Biology, Manisa, Turkey

ORCID IDs of the authors: S.I. 0000-0002-6584-3979

Please cite this article as: İlhan S. Profile of Apoptotic Proteins after Curcumin Treatment by Antibody Array in H69AR Lung Cancer Cells. Eur J Biol 2020; 79(2): 157-162. DOI: 10.26650/EurJBiol.2020.0015

ABSTRACT

Objective: The aim of the study was to investigate the changes in the expression levels of apoptosis-related proteins after treatment with curcumin (Cur) on multiple drug-resistant H69AR non-small cell lung cancer cells.

Materials and Methods: Viability of H69AR cells after Cur exposure (5-100 µg/mL) was evaluated via MTT assay at 24, 48 and 72 h. Apoptosis was assessed via ELISA assay. Apoptosis related proteins of breast cancer cell lines were analyzed by a Human Apoptosis Antibody Array. Protein-protein interactions were analyzed and visualized by using the STRING database.

Results: Cur inhibited cell viability and induced apoptosis in H69AR cells. The IC50 value of Cur in H69AR cells was 8.75 µg/mL. The array results showed that the protein levels of pro-apoptotic proteins such as Bad, Bax, Caspase-3, TRAIL R1, TRAIL R2, FADD, Fas, SMAC/DIABLO, HMOX2 were significantly increased by 2.4-, 3.1-, 2.6-, 3.1-, 3.4-, 2.4-, 2.1-, 4.1- and 5.5-fold in H69AR cells (p<0.05). Moreover, the protein levels of the anti-apoptotic proteins such as Bcl-2, cIAP-1, CLU and HIF1A were significantly decreased by 4.1-, 3.2-, 2.2- and 2.0-fold, respectively in H69AR cells by Cur exposure (p<0.05).

Conclusion: Findings of this study suggested that Cur induced apoptosis of human H69AR cells via mediating several proteins involved in both extrinsic and intrinsic apoptotic pathways.

Keywords: Curcumin, apoptosis, protein array, protein-protein interactions

INTRODUCTION

Cancer is one of the major public health problems globally. Lung cancer is the most common cancer type and a leading cause of cancer-related deaths. Despite advances in lung cancer therapy, the mortality rate of the disease is extremely high and the 5-year survival rate is approximately 16%. (1). Non-small cell lung cancer (NSCLC) is the most common type, which composes of nearly 85% of all cases. Toxic effects and various side effects limit the efficiency of standard therapy for lung cancer (2). Moreover, drug resistance that leads to tumor recurrence and disease progression is the major problem for therapeutic failure (3). Therefore, there is an urgent need for novel alternative agents to inhibit proliferation and to induce apoptosis of multiple drug-resistant (MDR) lung cancer cells.

Natural plant products are a valuable source of novel bio-active compounds having potential cytotoxic activities. Curcumin (Cur) is a polyphenolic compound originated from the plant *Curcuma longa* L. called turmeric (4) and was extracted from the rhizomes of this plant in a pure crystalline form in 1870 (5,6). Extensive research in the past 50 years has revealed several biological functions of Cur such as anti-proliferative, anti-inflammatory, and antioxidant properties. Recently, Cur has attracted great attention for its anticancer properties on breast, lung, prostate, and brain tumors (7). It is also known that Cur is a potent inducer of apoptotic cell death in several cancer types (8-11).

There are many studies investigating the possible apoptotic effects of Cur on various human cancer cells (7-11), but there is no study on MDR H69AR small cell lung cancer cells. In the current study, potential cyto-



Corresponding Author: Süleyman İlhan

E-mail: suleyman.ilhan@cbu.edu.tr

Submitted: 09.04.2020 • **Revision Requested:** 16.04.2020 • **Last Revision Received:** 29.07.2020 •

Accepted: 21.09.2020 • **Published Online:** 13.12.2020

© Copyright 2020 by The Istanbul University Faculty of Science • Available online at <http://ejb.istanbul.edu.tr> • DOI: 10.26650/EurJBiol.2020.0015

toxic and apoptotic effects of Cur were investigated on MDR H69AR human lung cancer cells. Moreover, the dominant signaling cascades and apoptotic players by Cur-induced cytotoxicity were screened by antibody array analysis.

MATERIALS AND METHODS

Cells and Culture

The human H69AR lung cancer cells utilized in the experiments were obtained from the American Type Culture Collection (ATCC, CRL-11351). H69AR cells were maintained in RPMI 1640 medium (Sigma-Aldrich, UK) with stable L-glutamine (1%) (Sigma-Aldrich, UK), fetal bovine serum (20%) (Sigma-Aldrich, UK) and streptomycin (1%) (Sigma-Aldrich, UK) in 75 cm² flasks (Cellstar, UK). Cells were incubated in a 37 °C incubator during the experiments.

Curcumin Treatment

Cur (Sigma-Aldrich, UK) was prepared as 1 mg/mL ethanol (EtOH) stock solution and stored for experiments at 4 °C. The EtOH concentration in all experimental wells was lower than 0.1% and was not toxic to the cells (Figure 1A-C).

MTT Assay

MTT (3-(4,5-dimethylthiazol-2-yl)-2,5-diphenyltetrazolium bromide) assay (Sigma-Aldrich, UK) was utilized to calculate the viability of cells after Cur exposure. Cells (10⁴/well) were propagated onto 96-well plates in a 200 µL medium. After 24, 48 and 72 h of exposure with increasing concentrations of Cur (5-100 µg/mL), 20 µL MTT was added to each well and incubated for an additional 4 h at 37°C. After the incubation period, wells were drained and existent crystals were dissolved by DMSO (Sigma-Aldrich, UK). Conversion of MTT into formazan by mitochondrial succinate dehydrogenase and other oxidoreductases was detected via spectrophotometer (570 nm, Tecan Infinite 200 PRO, Switzerland) (12). The half-maximal inhibitory concentration (IC₅₀) was evaluated via Graphpad 5.0 software.

Detection of Apoptosis via ELISA Assay

Apoptosis was determined through the Cell Death Detection kit (Sigma Aldrich, UK). This ELISA kit detects DNA fragments in the cytoplasm of apoptotic cells. For this experiment, cells were exposed to Cur (5-100 µg/mL) for 24, 48 and 72 h. After each incubation period, cells were lysed and cytoplasmic fractions were

obtained. Then, 20 µL of the cytoplasmic fractions were put into a streptavidin-coated 96-well. The mixture of “anti-DNA” and “anti-histone” was added to all wells and additionally incubated for 2 h. After washing the plates, diammonium salt was added and optic densities were measured at 405 nm and 490 nm (Tecan Infinite 200 PRO, Switzerland). The fold changes in each treated well were determined as compared to untreated controls.

Protein Array

Apoptosis related proteins of H69AR cells were analyzed by an Apoptosis Antibody Array (R&D Systems, USA). The principle of the array method involves a sandwich immunoassay, which is membrane-based (13). To optimize the exposure time, which allows us the detection of all protein spots, different exposure times were tested for each membrane ranging from 15 s to 15 min. Finally, it was optimized to use for 5 min. The proteins were detected by chemiluminescence methods involving an incubation step with an antibody (biotinylated) for h and, with streptavidin (HP-conjugated) for 1 h. Chemiluminescence imaging was conducted via UVP Biolmaging Systems. Kodaarray® 2.6 software was used to quantitate the pixel intensity in each spot (14).

Analysis of Protein-Protein Interaction

Protein-protein interactions were analyzed and visualized by using the STRING database. (version 11.0; <http://string.embl.de>) (15).

Statistical Analysis

All statistical analyses were done by using Graphpad Prism 5.0 software (USA). For significant values, a one-way analysis of variance test (ANOVA) was utilized (16). Statistically significant data were those with a p value ≤0.05.

RESULTS

Cur Inhibits the Viability of H69AR Human Lung Cancer Cells

The effect of Cur on the viability of H69AR cells was assessed in a concentration- and time-dependent manner. As shown in Figure 1(A-C), the viability of H69AR cells was reduced at 24, 48 and 72 h. Reduction in the viability was also concentration-dependent at all tested time points. There were 1%, 73%, and 96% reductions in the viability of H69AR cells exposed to 5, 25, and 100 µg/mL Cur respectively, as compared to control cells at 24 h (p<0.05). There were 2%, 88%, and 97% reductions in the viability of H69AR cells exposed to 5, 25 and 100 µg/mL Cur respectively, as compared to control cells at

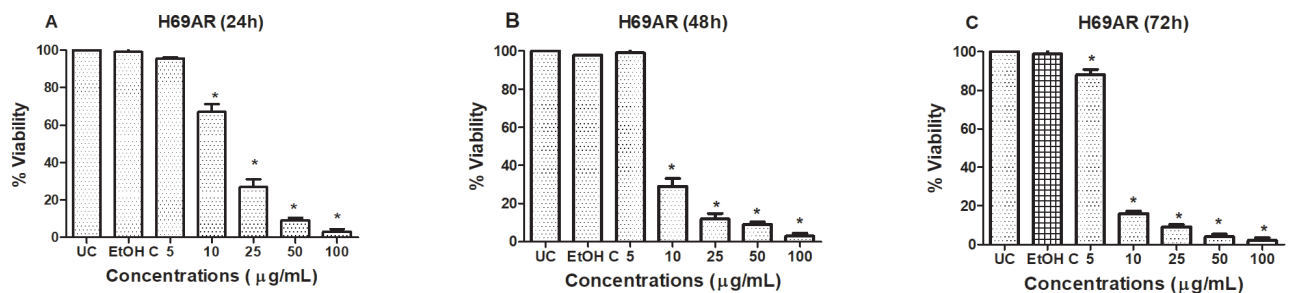


Figure 1. Concentration- and time-dependent inhibition of the viability of H69AR lung cancer cells by Cur. Cell viability was determined by the MTT assay. The results are the mean of 3 different experiments (±SD) (*p<0.05 compared to untreated cells) (UC: Untreated control, EtOH C: Ethanol control).

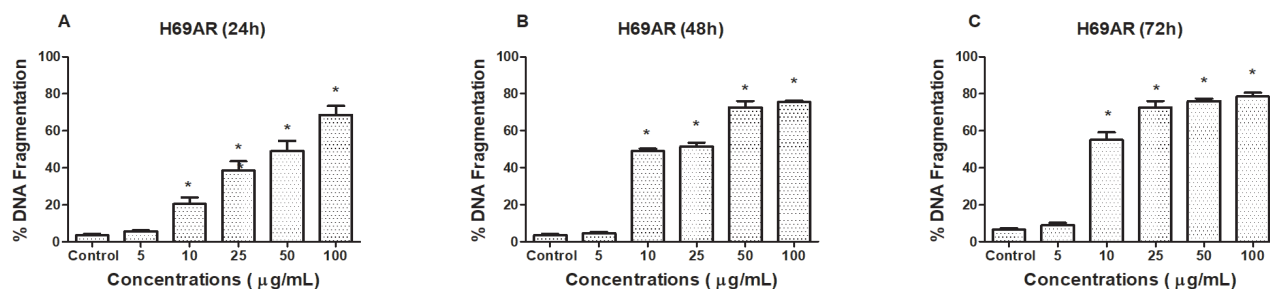


Figure 2. Induction of % of DNA fragmentation in H69AR cells in response to Cur treatment at different time points. (*p<0.05 compared to untreated cells).

48 h (p<0.05). The most effective cytotoxic time point was accepted as 48 h and IC₅₀ value of Cur in H69AR cells was 8.75 µg/mL.

Induction of Apoptotic Cell Death by Cur in H69AR Cells

To assess the induction of apoptosis after exposure to Cur in H69AR cells, increasing concentrations of Cur were applied for 24h, 48 h and 72 h and then apoptotic cell death was evaluated. As shown in Figure 2, Cur exposure increased the DNA fragments concentration dependently in H69AR cells (p<0.05).

Changes in Apoptotic Proteins by Cur in H69AR Cells

Differences in the expression of apoptosis-related proteins were profiled by using apoptosis array in H69AR cells. Table 1 shows the changes in the expression of apoptotic proteins in H69AR cells after Cur exposure. The results revealed that pro-apoptotic proteins such as Bad, Bax, Caspase-3, TRAIL R1, TRAIL R2, FADD, Fas, SMAC/DIABLO, HMOX2 were significantly increased by 2.4-, 3.1-, 2.6-, 3.1-, 3.4-, 2.4-, 2.1-, 4.1- and 5.5-fold in H69AR cells, respectively, as compared to control cells at 48 h (p<0.05). The anti-apoptotic proteins such as Bcl-2, cIAP-1, CLU and HIF1A were significantly decreased by 4.1-, 3.2-, 2.2- and 2.0-fold in H69AR cells, respectively, at 48 h (p<0.05).

Protein-Protein Interaction

To analyze protein-protein interactions, the STRING database was utilized. Figure 3 indicates the protein-protein interaction generated by STRING with an average local clustering coefficient of 0.491.

DISCUSSION

Curcumin, the active component of *C. longa*, has been used traditionally for centuries to treat a variety of impairments and studied on a large scale for its anti-proliferative, anti-inflammatory, and anti-oxidant effects throughout the past few decades (17-19). It has been shown in many studies that Cur has potent antiproliferative effects and exerts activity through multiple signaling mechanisms (20-22). However, in the literature, there is no study investigating the effect of Cur on H69AR small cell lung cancer cells. The H69AR cells are resistant to many chemotherapeutic drugs such as adriamycin, epirubicin, daunomycin, mitoxantrone, etoposide, vincristine and vinblastine. Therefore, H69AR is known as a multi-drug resistant lung cancer cell line (23). The

results revealed that Cur inhibited the viability of H69AR cells in a concentration-dependent manner. In a study by Li et al., similar results were obtained by human lung carcinoma A549 cells (24). Cur exposure significantly inhibited A549 cell proliferation and also induced apoptosis concentration dependently. Yang et

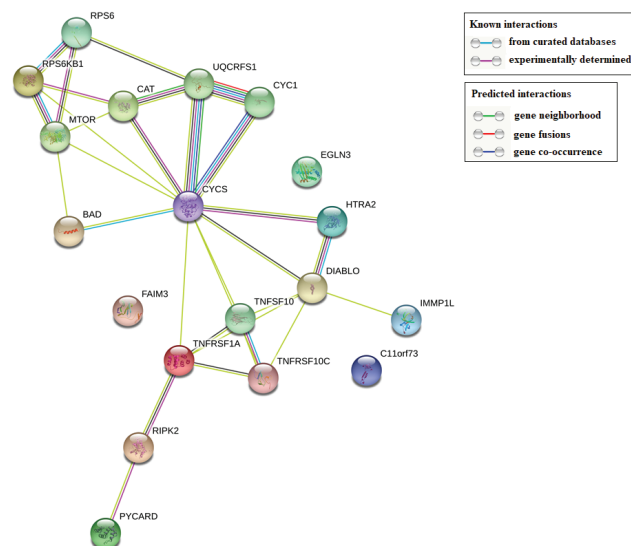


Figure 3. The protein-protein interactions map of the identified proteins. STRING database, version 11 (<http://string.embl.de>) was used to determine the protein-protein interactions of the proteins identified by antibody array analysis (RPS6: 40S Ribosomal Protein S6; RPS6KB1: Ribosomal Protein S6 Kinase B1; MTOR: Mechanistic Target of Rapamycin Kinase; UQCRCF1: Ubiquinol-Cytochrome C Reductase, Rieske Iron-Sulfur Polypeptide 1, CYC1: Cytochrome C1, CYCS: Cytochrome C, EGN3: Egl-9 Family Hypoxia Inducible Factor 3, FAIM3: Fas Apoptotic Inhibitory Molecule 3, HTRA2: HtrA Serine Peptidase 2, DIABLO: Diablo IAP-Binding Mitochondrial Protein, TNFSF10: TNF Superfamily Member 10, TNFRSF1A: TNF Receptor Superfamily Member 1A, TNFRSF10C: TNF Receptor Superfamily Member 10C, RIPK2: Receptor Interacting Serine/Threonine Kinase 2, PYCARD: Caspase Recruitment Domain-Containing Protein 5, IMMP1L: Inner Mitochondrial Membrane Peptidase Subunit 1, C11orf73: Heat Shock Protein Nuclear Import Factor Hikeshi, CLU1: Clusterin Like 1, RFW2: COP1 E3 Ubiquitin Ligase).

Table 1. Changes in apoptosis related proteins in H69AR cells after exposure to curcumin (8.75 µg/mL) for 48 h. The results are the mean of two independent experiments (±SD) (ND: not detectable, Ns: non-significant changes).

H69AR			
Symbol	Protein name	Up/down-regulation	Fold change
Bad	BCL2 Associated Agonist Of Cell Death	↑	2.4±0.2
Bax	BCL2 Associated X Protein	↑	3.1±2.8
Bcl-2	BCL2 Apoptosis Regulator	↓	4.1±2.4
Bcl-x	Bcl-2-Like Protein 1	↔	Ns
Pro-Caspase-3	Pro- apoptosis-Related Cysteine Peptidase	↓	2.0±0.8
Cleaved Caspase-3	Cleaved apoptosis-Related Cysteine Peptidase	↑	2.6±1.2
Cat	Catalase	↑	2.1±2.3
cIAP-1	Apoptosis Inhibitor 1	↓	3.2±0.2
cIAP-2	Apoptosis Inhibitor 2	↔	Ns
CLSPN	Claspin	↔	Ns
CLU	Clusterin	↓	2.2±3.0
CYCS	Cytochrome c	↑	4.2±2.8
TRAIL R1/DR4	Death receptor 4	↑	3.1±2.6
TRAIL R2/DR5	Death receptor 5	↑	3.4±0.8
FADD	Fas Associated via Death Domain	↑	2.4±2.2
Fas/TNFRSF6/CD95	Fas Cell Surface Death Receptor	↑	2.1±0.4
HIF-1A	Hypoxia Inducible Factor 1 Subunit Alpha	↓	2.0±0.2
HO-1/HMOX1/HSP32	Heme Oxygenase 1	↑	2.5±0.8
HO-2/HMOX2	Heme Oxygenase 2	↑	5.2±3.8
HSP27	Heat Shock 27 KDa Protein 1	↑	2.8±0.4
HSP60	Heat Shock 60kDa Protein 1	↔	Ns
HSP70	Heat Shock 70 KDa Protein 4	↑	2.2±0.4
HTRA2/Omi	HtrA Serine Peptidase 2	↑	3.6±2.6
Livin	Baculoviral IAP Repeat Containing 7	↔	Ns
PON2	Paraoxonase 2	↔	Ns
p21/CIP1/CDKN1A	Cyclin Dependent Kinase Inhibitor 1A	↔	ND
p27/Kip1	Cyclin Dependent Kinase Inhibitor 1B	↔	ND
Phospho-p53 (S15)	Tumor Protein P53 (Phospho- Ser15)	↑	3.2±1.2
Phospho-p53 (S46)	Tumor Protein P53 (Phospho- Ser46)	↑	3.6±2.4
Phospho-p53 (S392)	Tumor Protein P53 (Phospho- Ser392)	↑	2.8±1.2
Phospho-Rad17 (S635)	Cell Cycle Checkpoint Protein RAD17 (Phospho-Ser635)	↔	ND
SMAC/Diablo	Diablo IAP-Binding Mitochondrial Protein	↑	4.1±0.8
Survivin	Baculoviral IAP Repeat Containing 5	↔	ND
TNF RI/TNFRSF1A	TNF Receptor Superfamily Member 1A	↔	Ns
XIAP	X-Linked Inhibitor of Apoptosis	↔	Ns

al. also investigated the cytotoxic effect of curcumin on NCI-H446 cells and determined the IC₅₀ value as 15 µM (25). In a study by Jin et al., the apoptotic effect of Cur was investigated on A549 cells at 10-40 µM concentrations at 24 h and showed the apoptotic cell death ascended by the increasing concentrations, as compared to the control cells (26). Further, in the current study, apoptotic effect of Cur was also evaluated in H69AR cells by flow cytometer and found that Cur induced apoptosis at 48 h.

To explore the potential molecular mechanisms responsible for the apoptotic activity, an antibody protein array that provides

the simultaneous evaluation of 35 apoptosis-associated proteins was used. Apoptosis is a programmed cell death characterized by chromatin condensation, phosphatidylserine externalization, DNA fragmentation and apoptotic bodies which can be activated via internal or external signals (27). Apoptosis that has been initiated by external signals such as tumor necrosis factor receptor (TNF), TNF-related apoptosis-inducing ligand receptor 1 (TRAIL) and Fas cell surface death receptor (Fas) is called the extrinsic apoptotic pathway. However, the intrinsic (mitochondrial) apoptotic pathway is initiated internally and includes Bcl-2 family proteins (27-29). The Bcl-2 family proteins containing both

pro-apoptotic and anti-apoptotic members are the main regulators of intrinsic apoptosis. Pro-apoptotic proteins such as Bad and Bak, which are essential for mitochondrial permeabilization, are activators of apoptosis whereas anti-apoptotic members such as Bcl-2, Bcl-xL and Mcl-1 inhibit apoptotic cell death (28). Results revealed an increase in the pro-apoptotic proteins belonging to the intrinsic apoptotic pathways such as Bad, Bax and a decrease in Bcl-2. Zhu et al. showed that protein expression of Bax was induced, while Bcl-2 was reduced indicating the induction of apoptosis by the high dosing groups of Cur in pancreatic cancer cells (30). Yang et al., also demonstrated changes in Bax, Bcl-2 and Bcl-xL proteins in NCI-H446 cells by 15 μ M Cur for 48 h (25). Cytochrome c release from the mitochondria is essential for the activation of caspase-9 and as a result, activation of apoptosis (27). In the same study, authors also stated that Cur induced cytochrome c, caspase-9 and caspase-3 levels. In the current study, array results support the findings of Yang et al. in the case of induction in cytochrome c release and increase in caspase-3 levels (25). However, the array results of the current study do not support some of the findings of Yang et al. They reported that Cur did not cause any change in the expression of FAS and TRAIL apoptotic receptors and stated that Cur did not induce death receptor-mediated pathways (25). In the current study, Cur induced the main death receptors (TRAIL R1, TRAIL R2, FADD and Fas) indicating the induction of death receptor-mediated apoptotic pathway in H69AR cells. Reactive oxygen species (ROS) and mitochondria both play a vital role in the activation of apoptosis. Cytochrome c release is known to be mainly regulated via ROS (29). In many studies, the induction of the ROS-mediated mitochondrial pathway in Cur-treated cells has been demonstrated (31,32). Results of Kuttikrishnan et al. revealed the activation of the intrinsic apoptotic pathway via the generation of ROS in acute lymphoblastic leukemia cells by Cur treatment (33). Similarly, according to array results, Cur induced the proteins involved in ROS-mediated apoptotic pathways such as HIF-1A, HSP27 and HSP70. Here, changes in apoptotic proteins by Cur treatment were investigated by using a protein array method, but this needs to be verified by other methods such as western blotting or qPCR.

To investigate the possible protein-protein interactions of the proteins obtained from array data, bioinformatics STRING analysis was carried out. Combining the protein array data with protein interactome data allows us to investigate the network of proteins that Cur is probably interacting with. The network interaction map revealed complex protein-protein interactions that include direct and indirect functional protein connections. Of these proteins, Ribosomal Protein S6 (RPS6) is a cytoplasmic ribosomal protein and one of the components of the 40S ribosomal subunit. It is the downstream substrate of PI3K/Akt/mTOR/p70S6 kinase pathways and is phosphorylated by several kinases such as Ribosomal Protein S6 Kinase B1 (RPS6KB1) (34). In the literature, it has been shown that Cur inhibits the mTOR pathway via decreasing the phosphorylation of RPS6 leading to blocking the proliferation of human colorectal cancer cells, malignant glioma cells and intestinal epithelial cells (35-37). According to the map, Cur could induce apoptosis in H69AR cells by inhibiting mTOR pathway and phosphorylation of RPS6.

The interaction map also revealed the interaction of TNFSF10 (TRAIL) with Receptor-interacting serine threonine kinase 2 (RIPK2) which is one of the members of the serine/threonine protein kinase family. It acts by binding to the inhibitor of apoptosis proteins (AIPs) such as XIAP, cIAP-1 and cIAP-2. It was shown by the array data that Cur induced both TRAIL R1 and TRAIL R2 and subsequently inhibited cIAP-1, which leads to enhancement of the apoptotic pathway. The STRING data implies the possible interaction of TNFSF10 with RIPK2 and Caspase Recruitment Domain-Containing Protein 5 (PYCARD) after Cur treatment in H69AR cells. PYCARD functions as a key mediator in the activation of the mitochondrial apoptotic pathway and also regulates mitochondrial translocation of BAX and activates initiator caspases, which were found to be increased after Cur treatment in H69AR cells (38).

Although the present findings are notable, there are limitations to the study. The effects of Cur on human MDR small cell lung cancer cells were only detected on H69AR cells. The study should be expanded by using other NSCLC cell lines.

CONCLUSION

Collectively, the novel findings of this study from array data and STRING database suggested that Cur inhibited cell viability and induced apoptotic cell death in human H69AR cells via mediating several proteins involved in both extrinsic and intrinsic apoptotic pathways. By expanding our knowledge of the heterogeneous, biological behavior of the MDR H69AR cells, novel treatment approaches can be developed for the treatment of MDR small cell lung cancer.

Peer-review: Externally peer-reviewed.

Author Contributions: Conception/Design of study: S.I.; Data Acquisition: S.I.; Data Analysis/Interpretation: S.I.; Drafting Manuscript: S.I.; Critical Revision of Manuscript: S.I.; Final Approval and Accountability: S.I.

Conflict of Interest: The authors declare that they have no conflicts of interest to disclose.

Financial Disclosure: There are no funders to report for this submission.

REFERENCES

1. Molina JR, Adjei AA, Jett JR. Advances in chemotherapy of non-small cell lung cancer. *Chest* 2006; 130: 1211-9.
2. Pfister DG, Johnson DH, Azzoli CG, Sause W, Smith TJ, Baker JrS, et al. American Society of Clinical Oncology treatment of unresectable non-small-cell lung cancer guideline: Update 2003. *J Clin Oncol* 2004; 22: 330-53.
3. Sosa Iglesias V, Giuranno L, Dubois LJ, Theys J, Vooijs M. Drug resistance in non-small cell lung cancer: a potential for NOTCH targeting? *Front Oncol* 2018; 8: 267.
4. Alibeiki F, Jafari N, Karimi M, Peeri Dogaheh H. Potent anti-cancer effects of less polar Curcumin analogues on gastric adenocarcinoma and esophageal squamous cell carcinoma cells. *Sci Rep* 2017; 7: 1-9.

5. Aggarwal BB, Surh YJ, Shishodia S. The molecular targets and therapeutic uses of curcumin in health and disease. 1st edition. New York: Springer Science & Business Media; 2007.
6. Priyadarsini Kl. The chemistry of curcumin: From extraction to therapeutic agent. *Molecules* 2014; 19: 20091-12.
7. Anand P, Sundaram C, Jhurani S, Kunnumakkara AB, Aggarwal BB. Curcumin and cancer: An "old-age" disease with an "age-old" solution. *Cancer Lett* 2008; 267: 133-64.
8. Dorai T, Cao YC, Dorai B, Buttyan R, Katz AE. Therapeutic potential of curcumin in human prostate cancer. III. Curcumin inhibits proliferation, induces apoptosis, and inhibits angiogenesis of LNCaP prostate cancer cells *in vivo*. *Prostate* 2001; 47: 293-303.
9. Mukhopadhyay A, Bueso-Ramos C, Chatterjee D, Pantazis P, Aggarwal BB. Curcumin downregulates cell survival mechanisms in human prostate cancer cell lines. *Oncogene* 2001; 20: 7597-7609.
10. Liu Q, Loo WTY, Sze SCW, Tong Y. Curcumin inhibits cell proliferation of MDA-MB-231 and BT-483 breast cancer cells mediated by down-regulation of NFB, cyclinD and MMP-1 transcription. *Phyto-medicine* 2009; 16: 916-22.
11. Moragoda L, Jaszewski R, Majumdar AP. Curcumin induced modulation of cell cycle and apoptosis in gastric and colon cancer cells. *Anticancer Res* 2001; 21: 873-8.
12. Atmaca H, Uzunoglu S. Anti-angiogenic effects of trabectedin (Yondelis; ET-743) on human breast cancer cells. *Eur Cytokine Netw* 2014; 25: 1-7.
13. Karaca B, Kucukzeybek Y, Gorumlu G, Erten C, Gul MK, Cengiz E et al. Profiling of angiogenic cytokines produced by hormone- and drug-refractory prostate cancer cell lines, PC-3 and DU-145 before and after treatment with gossypol. *Eur Cytokine Netw* 2008; 19: 176-84.
14. Erten C, Karaca B, Kucukzeybek Y, Gorumlu G, Cengiz E, Gul MK, et al. Regulation of growth factors in hormone- and drug-resistant prostate cancer cells by synergistic combination of docetaxel and octreotide. *BJU Int* 2009; 104, 107-14.
15. Von Mering C, Jensen LJ, Snel B, Hooper SD, Krupp M, Foglierini M, et al. STRING: known and predicted protein-protein associations, integrated and transferred across organisms. *Nucleic Acids Res* 2005; 33: 433-7.
16. Scheff SW. Fundamental statistical principles for the neurobiologist: A survival guide. 1st edition. New York: Academic Press; 2016.
17. Boroumand N, Samarghandian S, Hashemy SI. Immunomodulatory, anti-inflammatory, and antioxidant effects of curcumin. *J Herbm Pharm* 2018; 7: 211-9.
18. Jurenka JS. Anti-inflammatory properties of curcumin, a major constituent of *Curcuma longa*: a review of preclinical and clinical research. *Altern Med Rev* 2009; 14: 141-53.
19. Hewlings SJ, Kalman DS. Curcumin: a review of its' effects on human health. *Foods* 2017; 6: 92.
20. Tomeh MA, Hadianamrei R, Zhao X. A review of curcumin and its derivatives as anticancer agents. *Int J Mol Sci* 2019; 20: 1033.
21. Allegra A, Innao V, Russo S, Gerace D, Alonci A, Musolino C. Anticancer activity of curcumin and its analogues: preclinical and clinical studies. *Cancer Invest* 2017; 35: 1-22.
22. Vallianou NG, Evangelopoulos A, Schizas N, Kazazis C. Potential anticancer properties and mechanisms of action of curcumin. *Anticancer Res* 2015; 35: 645-51.
23. Mirski SE, Gerlach JH, Cole SP. Multidrug resistance in a human small cell lung cancer cell line selected in adriamycin. *Cancer Res* 1987; 47: 2594-8.
24. Li P, Qin H, Li X. The effect of curcumin on the apoptosis of lung cancer cells by regulating DJ-1-PTEN/PI3K/AKT signaling. *Int J Clin Exp Med* 2019; 12: 8739-45.
25. Yang CL, Ma YG, Xue YX, Liu YY, Xie H, Qiu GR. Curcumin induces small cell lung cancer NCI-H446 cell apoptosis via the reactive oxygen species mediated mitochondrial pathway and not the cell death receptor pathway. *DNA Cell Biol* 2012; 31: 139-50.
26. Jin H, Qiao F, Wang Y, Xu Y, Shang Y. Curcumin inhibits cell proliferation and induces apoptosis of human non-small cell lung cancer cells through the upregulation of miR-192-5p and suppression of PI3K/Akt signaling pathway. *Oncol Rep* 2015; 34: 2782-9.
27. Jin Z, El-Deiry WS. Overview of cell death signaling pathways. *Cancer Biol Ther* 2005; 4: 147-71.
28. Giam M, Huang DCS, Bouillet, P. BH3-only proteins and their roles in programmed cell death. *Oncogene* 2008; 27: 128-36.
29. Zuo L, Zhou T, Pannell BK, Ziegler AC, Best TM. Biological and physiological role of reactive oxygen species—the good, the bad and the ugly. *Acta Physiol* 2015; 214: 329-48.
30. Zhu Y, Bu S. Curcumin induces autophagy, apoptosis, and cell cycle arrest in human pancreatic cancer cells. *Evid Based Complement Altern Med* 2017; 2017.
31. Larasati YA, Yoneda-Kato N, Nakamae I, Yokoyama T, Meiyanto E, Kato JY. Curcumin targets multiple enzymes involved in the ROS metabolic pathway to suppress tumor cell growth. *Sci Rep* 2018; 8: 1-13.
32. Chen Q, Wang Y, Xu K, Lu G, Ying Z, Wu L, et al. Curcumin induces apoptosis in human lung adenocarcinoma A549 cells through a reactive oxygen species-dependent mitochondrial signaling pathway. *Oncol Rep* 2010; 23: 397-403.
33. Kuttikrishnan S, Siveen KS, Prabhu KS, Khan AQ, Ahmed EI, Akhtar S, et al. Curcumin induces apoptotic cell death via inhibition of PI3-Kinase/AKT pathway in B-precursor acute lymphoblastic leukemia. *Front Oncol* 2019; 9.
34. Lu T, Zhu Z, Wu J, She H, Han R, Xu H, et al. DRAM1 regulates autophagy and cell proliferation via inhibition of the phosphoinositide 3-kinase-Akt-mTOR-ribosomal protein S6 pathway. *Cell Commun Signal* 2019; 17: 28.
35. Johnson SM, Gulhati P, Arrieta I, Wang X, Uchida T, Gao T, et al. Curcumin inhibits proliferation of colorectal carcinoma by modulating Akt/mTOR signaling. *Anticancer Res* 2009; 29: 3185-90.
36. Shinjima N, Yokoyama T, Kondo Y, Kondo, S. Roles of the Akt/mTOR/p70S6K and ERK1/2 signaling pathways in curcumin-induced autophagy. *Autophagy* 2007; 3: 635-7.
37. Moreau R, Kaur H. Curcumin and piperine inhibit mTORC1 signaling in intestinal epithelial cells. *The FASEB Journal* 2017; 31: 135-8.
38. Srinivasula SM, Poyet JL, Razmara M, Datta P, Zhang Z, Alnemri ES. The PYRIN-CARD protein ASC is an activating adaptor for caspase-1. *J Biol Chem* 2002; 277: 21119-22.